This PhD dissertation presents an experimental study on Vertical-Cavity Surface-Emitting Lasers (VCSELs) for Optical Frequency Comb (OFC) generation.

OFC systems are typically based on bench top lasers sources, often built with tailored components which make them robust and powerful but complex and difficult to reproduce at the same time. Some of the fields of application of OFCs do not need that bespoke systems but, on the contrary, more straightforward, flexible and compact systems are needed for applications aiming for size, cost and energy efficient set-ups. We address this issue in this work by using Off the Shelf components to obtain suitable combs for applications like THz generation or spectroscopy.

On the other hand, VCSELs are firmly established in the market, which is actually increasing. Their key factors are the circular beam, low threshold current and low energy consumption. VCSELs improve the competence in terms of integrability, compactness, low cost and the possibility of mass production.

VCSEL's evaluation for OFC generation, the expansion of the generated combs and their optimization are the three experimental pillars of this work devoted to research results. For this, techniques like Gain Switching (GS), Electro-Optical (EO) modulation or Optical Injection Locking (OIL) have been implemented as well as components like Highly Nonlinear Fibers (HNLF) or Nonlinear Optical Loop Mirrors (NOLM) or Dispersion Compensation Fibers (DCFs).

In this Thesis, VCSELs under GS have been demonstrated as optimum sources to generate efficient combs when the distance between comb lines is in the few GHz range. The resulting systems are straight-forward, compact and cost effective if we put the VCSEL low size and energy consumption together with the GS technique, which provides high phase coherence and tunability without component count increment. Besides, subsequent comb expansion and optimization has been proved obtaining up to 1THz broad combs.

Universidad Carlos III de Madrid
September 2016

VCSEL-BASED OPTICAL FREQUENCY COMB GENERATION, EXPANSION AND OPTIMIZATION:AN EXPERIMENTAL STUDY

E. PRIOR

VCSEL-BASED OPTICAL FREQUENCY COMB GENERATION, EXPANSION AND OPTIMIZATION: AN EXPERIMENTAL STUDY

Author: ESTEFANÍA PRIOR CANO
Supervisor: CRISTINA DE DIOS FERNÁNDEZ

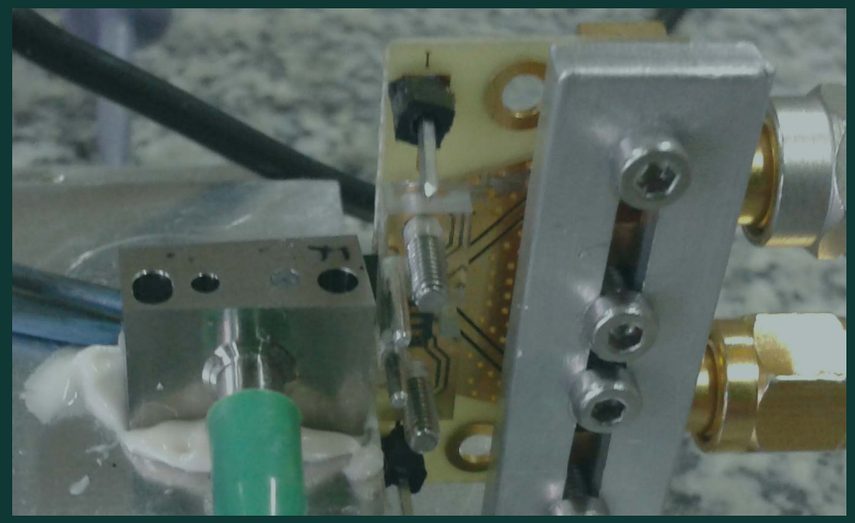

TESIS DOCTORAL

VCSEL-based Optical Frequency Comb Generation, Expansion and Optimization: An experimental study.

Autora: Estefanía Prior Cano

Directora: Cristina de Dios Fernández

Departamento de Tecnología Electrónica

Leganés, septiembre de 2016

TESIS DOCTORAL

VCSEL-based Optical Frequency Comb Generation, Expansion and Optimization: An experimental study.

Autora: Estefanía Prior Cano

Directora: Cristina de Dios Fernández

Firma del Tribunal Calificador:

Firma

Presidente:

Vocal:

Secretaria:

Calificación:

Leganés, de septiembre de 2016

Acknowledgements

A mi padre. A mi madre, mis hermanas, mi hermano y mis abuelas.

A las mujeres ingenieras y científicas y a las personas que cada día nos esforzamos por conseguir un mundo en el que ser mujer no signifique tener que esforzarse más para conseguir lo mismo. *Lo personal es político* dijo Carol Hanisch hace casi 50 años y esta tesis es, para mí, personal y es política. Porque no es fácil hacer una tesis ni investigar cuando te replanteas algunos cánones, y he comprobado que es difícil pero posible, aunque a veces las consecuencias duelan. Es política porque casi todos estos meses he tenido un salario digno en una universidad y en un país que precariza a l@s estudiantes de doctorado y porque es la tesis de una mujer, dirigida por una mujer, en un campo increíblemente ajeno a lo colaborativo y a dejarnos ocupar a las mujeres el 50% que nos corresponde. Toda esta introducción para expresarme y para dar las gracias a las personas que se han ido cruzando en mi camino estos años, con quienes he charlado y aprendido

hasta el punto de ser capaz, aquí y ahora, de poner esto en palabras. A todas las personas que hacemos cosas pequeñas para cambiar el mundo (parafraseando a Galeano) por uno más igualitario y justo.

A todas las personas que estos meses me lo han puesto fácil y a las que me lo han puesto difícil también. Porque con todas vosotras aprendo, apoyándome en los ratos bonitos para ser fuerte en los días menos buenos. A "mis" Cristinas (de Dios, Grimi, Medi, Salís), Ana, Héctor, Alex y a quienes formáis mi *familia madrileña*.

A la gente del grupo y del departamento. Especiales y reiteradas son mis gracias a Cristina porque creo que hemos formado un buen equipo y un bonito vínculo. A Rubén y Pablo que me abrieron las puertas de la universidad y la investigación y se esforzaron por enseñarme. A la gente de Luz por abrirme las puertas de vuestra casa y hacerme sentir en la mía.

To Peter Meissner, it is great having you as reference, seeing your motivation with research and teaching, even after retiring. During our conversations I learn so much that I finish with headache, and that is real fun. To the people in Darmstadt and Göteborg for having me as part of their groups. *To all the people that lights the shadows of my knowledge*.

Por último quiero dejar constancia de la necesidad de mejora de la educación en general en muchos aspectos, la universitaria en particular y, en concreto, la Universidad Carlos III, como he podido comprobar estos años. Como me dijo un compañero "los alumnos pasaron a ser usuarios y ahora ya son clientes". Y todo ese tufillo se respira también en el profesorado, estresado por

compaginar su labor investigadora con la docente y al final ni la una ni la otra, dando lugar a investigaciones que sólo buscan publicar, con calidad o sin ella, y a docencias caducadas con charlas que se perpetúan año tras año sin intención de enseñar. Por otro lado, estamos obviando lo que sucede en los servicios de la universidad donde las renovaciones de las contratas permiten rebajar las condiciones de las personas de cafetería, del gimnasio, de mantenimiento y de limpieza. Esta tesis no habría sido posible sin su presencia en mi día a día, sin ell@s no tendría los edificios limpios y en condiciones, café justo y rico a diario o el cuerpo en forma y listo para volver al laboratorio. A tod@s ell@s y en especial a Juan Carlos, Alberto, Tenti, Rosi, Marisa y Gema.

Para terminar reitero un párrafo que ya escribí en mi tesis de máster en 2014, que envié a la universidad y que nadie nunca contestó: quiero pedir a la Universidad Carlos III y a su equipo rector que no estropee el esfuerzo y el trabajo de estos años para construir unas líneas de investigación y formar unos equipos sólidos. Esta universidad se irá a pique con medidas como la reciente propuesta de Contratos Predoctorales UC3M, que implicarán la pérdida de muchos investigadores y los que se queden lo harán en condiciones realmente precarias. Con un sueldo de 770€ al mes no es fácil vivir en Madrid (y eso sin tener en cuenta que somos personas con formación superior). Estos años he visto como la mayoría trabajamos duro para conseguir compatibilizar docencia, investigación y asignaturas. Me gustaría saber quién va a impartir prácticas y quién va a llenar los laboratorios de investigación cuando nosotros nos hayamos ido. Necesitamos vivir, no sobrevivir"… ¿Será la UC3M un sitio donde poder hacerlo?

"Find your voice. It does not have to be the loud one, but the one that makes you feel comfortable."

Gloria Hoefler

"Do things differently and have fun"

"Tell me that I cannot make it…and I will make it"

Ruth Houbertz

Women in Photonics Silicon Valley Chapter – CLEO Conference, June 2016

Acronyms

OFC:	Optical Frequency Comb
OFCG:	Optical Frequency Comb Generator
LD:	Laser Diode
VCSEL:	Vertical-Cavity Surface-Emitting Laser
DM:	Discrete Mode LD
FP:	Fabry-Perot LD
DFB:	Distributed Feedback LD
ML:	Mode-Locked Laser
EEL:	Edge-Emitting Laser
SEL:	Surface-Emitting Laser
GS:	Gain Switching

OIL:	Optical Injection Locking
CW:	Continuous Wave
RF:	Radio-Frequency
SPM:	Self-Phase Modulation
EDFA:	Erbium Doped Fiber Amplifier
HNLF:	Highly Nonlinear Fiber
DCF:	Dispersion Compensation Fiber
NOLM:	Nonlinear Optical Loop Mirror
SOA:	Semiconductor Optical Amplifier
EO:	Electro-Optic
IM:	EO Intensity Modulator
PM:	EO Phase Modulator
PC:	Polarization Controller
PS:	Polarization Splitter
OC:	Optical Coupler
PD:	Photodiode
TIA:	Transimpedance Amplifier
PCB:	Printed Circuit Board
COTS:	Commercial Off-The-Shelf
OSA:	Optical Spectrum Analyzer

ESA:	Electrical Spectrum Analyzer
PN:	Phase Noise
DANL:	Displayed Average Noise Level
FWHM:	Full Width Half Maximum
TBP:	Time-Bandwidth Product
SMSR:	Side Mode Suppression Ratio
DR:	Dynamic Range

Resumen

Las fuentes ópticas multimodo o peines en frecuencia (Optical Frequency Comb o OFC) han sido y son objeto de investigación en los últimos años dado que ofrecen numerosas posibilidades en diferentes campos como espectroscopía, comunicaciones ópticas, generación de terahercios, generación de señales arbitrarias ópticas, metrología o generación óptica de señales de radiofrecuencia. Los OFC son sistemas típicamente basados en equipos de sobremesa y componentes a medida, obteniendo sistemas robustos y señales de alta calidad pero difíciles de implementar y reproducir al mismo tiempo. Algunas de las aplicaciones de los OFCs tienen como elementos clave la eficiencia en tamaño, coste y consumo, de manera que es importante obtener combs con capacidades más moderadas pero que, a su vez, sean sistemas más flexibles, compactos y fáciles de implementar. Para ello, centramos nuestra atención en sistemas OFCs realizados con componentes comerciales que

sean útiles para aplicaciones como generación de THz o espectroscopía.

Para mantener estos objetivos, hemos elegido la generación de combs directa en diodos láser (laser diodes o LDs), dado que el OFC es creado en el interior de la cavidad láser sin necesidad de añadir componentes extra ni aumentar excesivamente la potencia necesaria por el sistema. Entre los diodos láser, los láseres de emisión superficial y cavidad vertical (Vertical-Cavity Surface-Emitting Lasers o VCSELs) son un tipo de láseres de diodo que han experimentado una gran evolución en los últimos años debido a las características que presentan: los VCSELs son dispositivos de bajo coste y pequeño tamaño, por lo que ofrecen la posibilidad de ser modulados a altas frecuencias con muy poco consumo de potencia.

En este trabajo se estudiará el uso de láseres VCSEL (1550nm 10Gbps VCSELs fabricados por Vertilas GmbH) como elemento base de los OFCs utilizando una técnica de modulación no lineal conocida como Gain Switching (GS). Gracias a la modulación GS, el comb generado hereda el ruido del equipo usado para la modulación, obteniendo así alta correlación de fase entre sus modos. Con el dispositivo VCSEL bajo GS se ha obtenido un comb de hasta 135GHz de ancho en los 20dB superiores del espectro, llamado VCSEL-OFC. Los resultados presentados en esta Tesis demuestran que el uso de VCSELs permite la generación de combs más anchos y planos que con otras tecnologías y record en bajo consumo de energía. El comportamiento del VCSEL bajo GS se comparará con un sistema similar usando otro tipo de fuente láser que ha sido usado con buenos resultados anteriormente, un láser Discrete Mode, también bajo régimen GS.

Sin embargo, el VCSEL-OFC sigue limitando su aplicación en algunos campos de nuestro interés como síntesis de THz o espectroscopía dado que necesitan combs más anchos. Esto fundamentó otro de los aspectos clave de este trabajo: la expansión de los combs, usando el VCSEL-OFC como semilla. Tres técnicas para expandir el VCSEL-OFC han sido implementadas, basándonos en fibras altamente no lineales (Highly Nonlinear Fibers, HNLF), lazos ópticos no lineales (Nonlinear Optical Loop Mirrors, NOLM) y moduladores Electro-Ópticos (EO). Con estos sistemas hemos expandido el comb resultante un factor 3, obteniendo combs de alrededor de 450GHz y manteniendo alta correlación entre modos. Posteriormente, dos de estas etapas de expansión, EO y HNLF, han sido implementadas en cascada para aunar sus efectos y se ha conseguido un comb de 1THz de ancho a 20dB, según nuestro conocimiento, el comb más ancho conseguido usando fuentes VCSELs y tecnologías disponibles comercialmente. Este comb es extraordinariamente ancho pero, sin embargo, necesita ser estudiado con más detalle para mejorar otras de sus características como la igualdad de potencia entre los modos considerados (*flatness*) o el rango dinámico.

Por ello, para profundizar en el conocimiento del VCSEL como fuente para generar combs y así optimizar el VCSEL-OFC y todas sus expansiones implementadas, se ha realizado un estudio más profundo de dicho comb en relación a sus componentes de polarización. Los VCSELs típicamente se consideran fuentes monomodo pero tienen un segundo modo con polarización linear y ortogonal. Este modo es residual y se reduce su efecto durante la fabricación de la cavidad pero hemos comprobado que genera un comb residual, con menor potencia y este comb

juega un papel fundamental si se equilibraran las potencias de ambos modos de polarización. Además, el uso de GS para la generación del comb hace que tanto los modos del comb principal como de este comb residual tienen alta correlación de fase. Para equilibrar las potencias de ambos modos de polarización, hemos incluido en nuestros experimentos la técnica de inyección (Optical Injection Locking, OIL) en la que una luz externa se inyecta en el láser para mejorar la señal a la salida. Jugando con la polarización de la señal inyectada, hemos conseguido equilibrar los combs correspondientes a ambos estados de polarización y también suprimir uno de ellos manteniendo únicamente el otro.

En conclusión, un tipo de diodo laser de emisión vertical, VCSEL, ha sido evaluado para generación de peines ópticos multifrecuenciales. Para ello, se ha estudiado su comportamiento bajo GS, optimizando el ancho del comb generado. Posteriormente, se han implementado distintas técnicas para expandir y optimizar dichos combs. Los resultados han sido significativos, teniendo en cuenta el ancho del comb con respecto a la potencia necesaria y el coste y complejidad de los sistemas. Los combs basados en VCSELs prometen ser dispositivos a tener en cuenta para implementaciones de combs versátiles y compactos de bajo coste y bajo consumo de energía.

Abstract

Optical Frequency Combs (OFCs) are versatile systems and therefore many researchers have been interested in them during the last years as they open possibilities in a large variety of fields like spectroscopy, optical communications, THz generation, optical arbitrary waveform generation, metrology, or microwave photonic. OFCs systems are typically based on bench top lasers sources, often built with tailored components which make them robust and powerful but complex and difficult to reproduce at the same time. Some of the fields of application of OFCs do not need that bespoke systems but, on the contrary, more straightforward, flexible and compact systems are needed for applications aiming for size, cost and energy efficient set-ups. These features can be further enhanced by using only Off the Shelf components obtaining suitable combs for applications like THz generation or spectroscopy. This is the approach in which our attention is centered.

Trying to maintain this idea as the horizon of this work, direct OFC generation in laser diodes (LDs), in which the comb is generated inside the LD cavity, has been the focus of the present work. With such an approach, the component count is not increased and the energy consumption remains low. Among the numerous laser diode technologies available, Vertical-Cavity Surface-Emitting Lasers (VCSELs) are cost effective devices with small size. On top of this, they offer high speed capabilities with a very small amount of injected power. These special features are the reason why, in this work, VCSELs (1550nm 10Gbps VCSELs from Vertilas GmbH) are analyzed as the main source to be used for comb generation based on a well stablished nonlinear radio-frequency modulation technique: Gain Switching (GS). Thanks to the GS regime, an optical comb is generated with a very special feature: its modes inherit the stability of the radio-frequency source used for the laser modulation. Hence, the resulting comb exhibits a very high correlation between its modes. With this, a comb of 135GHz in the 20dB span is generated (VCSEL-OFC). The results presented in this Thesis demonstrate that the use of high performance VCSELs permits the generation of very flat optical combs with enhanced optical span and record energy efficiency. The VCSEL performance to generate OFCs is compared in this study to a different type of LD source: Discrete Mode (DM) laser under GS. The results showed that VCSEL-OFC is significantly broader than the comb obtained with other LD technologies under GS.

However, the overall optical span that VCSEL based combs provide still needs to be increased to match the majority of the applications targeted. Especially for THz generation or dual-comb spectroscopy, two of the applications that launched our

interest in LD combs, this is an important issue. Finding a way to overcome this limitation was the beginning of another of the key studies presented here. The expansion of the VCSEL-OFC, the seed comb. For this purpose, three different expansion techniques were implemented to increment the total span: Highly Nonlinear Fibers (HNLF), Nonlinear Optical Loop Mirrors (NOLM) and Electro-Optic (EO) Modulators. The resulting combs are 3 times broader than the seed VCSEL-OFC, thus combs around 450GHz in the 20dB span have been achieved maintaining high correlation between the comb lines. Subsequently, two of these expansion techniques, the EO and HNLF, have been cascaded to join their expansion effects and a comb of 1THz in the 20dB span has been generated, which is, to our knowledge, the broadest comb achieved using LDs and off the Shelf components. Even when this comb is remarkably broad some other features should be improved: the flatness and the dynamic range. Then, more efforts should be done to study the nature of the VCSEL-OFC.

In order to deepen into the VCSEL knowledge for comb generation, to optimize both the VCSEL-OFC and the expansion stages implemented, polarization dynamics studies on the VCSEL in CW emission and the VCSEL under GS were performed. VCSELs are considered monomode laser sources but they present a residual orthogonally polarized mode whose emission is suppressed during fabrication. However, we observed that this residual mode also generates a comb that could play an important role. Using GS for the generation provides high phase correlation among the teeth in the main comb and also in this orthogonally-polarized residual comb. Trying to achieve a balance between both polarization components, Optical

Injection Locking (OIL) was implemented. Playing with the injected state of polarization, the combs correspondent to the two states of polarization in VSCELs were balanced and the resulting comb was slightly broader and flatter. Also, one of the optical combs could be enhanced suppressing the other state of polarization with OIL.

To conclude, Vertical-Cavity Surface-Emitting Lasers (VCSELs) have been evaluated for optical frequency comb generation. For this, their behavior under GS has been studied, focusing on the optimization of the optical span. Subsequently, different techniques for comb expansion and optimization have been implemented obtaining remarkable results, taking into account the optical span, the energy needs and the complexity of the set-ups. For all this, VCSELs are devices to be used to build versatile, compact, low cost and low energy consumption comb generation systems.

Keywords: Optical Frequency Comb, Vertical-Cavity Surface-Emitting Laser, Discrete Mode Laser, Gain Switching, Phase Modulator, Electro-Optics, Highly Nonlinear Fiber, Nonlinear Optical Loop Mirror, Optical Injection Locking, Polarization Dynamics, Cost Off the Shelf component, Energy efficiency

The present document details the research developed within the scope of this PhD Thesis. The content is divided in five main blocks called sections, each one composed by several chapters. These sections are: Introduction, VCSEL Laser Diodes under Gain Switching for OFC generation, VCSEL-based OFC expansion, VCSEL-based OFC optimization and Conclusions. After these sections, several articles already published (or recently submitted) are shown, covering most of the results presented here. The document is closed with some appendixes and the references used.

Contents

Introduction

This section frames the new results on Optical Frequency Comb (OFC) generation based on Vertical Cavity Surface Emitting diode lasers (VCSELs), which constitute the core of the present doctoral Thesis. In order to do so, this introduction section consists of four chapters: in Chapter 1 we present the **Motivation,** explaining the interest that the present study has for the scientific community. Then, a brief **Background and state of the art** is described in Chapter 2, where we define the main concepts that are relevant for the present research, along with a description of the principal applications and a review of current breakthrough results related to OFC up to our days. In **Methods** (Chapter 3), we describe the main techniques used for the experiments and the measurement approach that we have fulfilled. Lastly, the **Methodology** that has guided the scientific work presented in this document is depicted in Chapter 4.

1. Motivation

Optical Frequency Combs (OFCs) are versatile optical systems that have recently been given special attention by the scientific and the engineering community as they have opened new possibilities in a large variety of fields. Though the exploration of these fields of study began in the seventies, one of the breakthrough events in the history of OFC happened in 2005, when the Nobel Prize in physics was jointly awarded to John L. Hall and Theodor W. Hänsch "for their contributions to the development of laser-based precision spectroscopy, including the optical frequency comb technique" [1]. Ever since that moment, OFC systems have gained significant interest in numerous areas: Spectroscopy [2], optical communications [3], THz generation [4], optical arbitrary waveform generation [5], metrology [6], or microwave photonic devices [7] are some examples of entire disciplines enjoying the benefits that the use of OFC can provide. OFCs have increased their optical spectra and they can be found nowadays covering the range from the ultraviolet to the mid-infrared[8].

OFCs systems are typically based on bench top lasers sources, often built with tailored components which make them robust and powerful but complex and difficult to reproduce at the same time [8], [9]. Some of the fields of application of OFCs do not need that bespoke systems but, on the contrary, more straightforward, flexible and compact systems are needed for applications aiming for size, cost and energy efficient set-ups [10], [11]. These features can be further enhanced by using only Off the Shelf components obtaining suitable combs for applications like THz generation or spectroscopy [12]–[14]. This is the approach in which our attention is centered.

Different methods are currently employed and being studied for optical comb generation, also depending of the targeted application. Femtosecond Ti:Sa lasers [15], Mode-Locked (ML) lasers [16], microresonators [17] or fiber lasers emitting a continuous wave followed by electro-optical modulators [18] are only a few examples of them [19]. They can be divided in two main groups: direct or indirect. The first one includes those where the optical comb generation happens within the laser source itself while the indirect techniques generate the comb including elements that process the light after its emission from the initial optical source, typically a laser device working in continuous wave regime [20]. Direct techniques are considered in the present work as they rely on the use of pulsed laser sources with no extra components needed for the generation. The indirect technique will only be addressed in a specific section (Chapter 8, page 104) for a comparison with the selected direct approach.

In the direct category, we can find high quality OFC, as femtosecond Ti:Sa lasers or Mode-Locking (ML) fiber lasers [9]. However, those applications aiming for compactness and energy and cost efficiency need systems built starting from an optical source that holds these virtues itself: laser diodes (LD) that are commercially available, compact, and have low cost and low energy consumption [21]. Direct generation of optical combs using LDs can be achieved using Mode-Locking LDs (MLLD) devices that offer wide optical combs with high phase relation between modes [22] but they are tailor-made and have limited control of the frequency spacing [23]. Microresonators are another monolithic technology that is coming up as very promising and hot topic [24] as they are really compact and

produce high quality combs [25] but the repetition rate is also fixed during fabrication, typically with values in the hundreds of GHz [19]. However, there is another direct technique that can be applied to any LD, even Commercial Off-The-Shelf (COTS) called Gain Switching (GS) [26]. GS is a straightforward and versatile technique that allows a comb to be generated in most LD devices by only adding a large and fast signal modulation to the laser bias current. Therefore no extra components are needed. It only needs a few miliwatts of power supply to create an optical comb and it will present moderate optical span and high coherence among the comb lines. This technique also offers tunability of the frequency spacing of the OFC [27], a feature that is very limited or not possible in ML diode lasers.

Given the advantages of commercial components and LD devices in terms of cost, size and energy efficiency and the interesting features that GS offers, such as high phase coherence with no need of component count increase, the present thesis has oriented its scientific efforts towards the experimental study and optimization of OFC sources based on these two pillars. This work regarding OFCs comes from our former (and still present) interest in THz generation and it determines the features that will prevail in our focus. Then, the optimization is intended to increase the maximum optical span achieved as main aspect as well as some others (phase noise, flatness, tunability, straight forward set-up, energy consumption...) that are also considered and evaluated, and will be introduced in subsequent chapters.

One kind of LDs, Vertical-Cavity Surface-Emitting Lasers (VCSELs) are firmly established in the market, which is actually increasing: they are the second type of laser in terms of production volume

after Fabry-Perot (FP) LDs [28]. Their key factors are the circular beam, low threshold current and low energy consumption [29]. VCSELs improve the competence in terms of integrability, compactness, low cost and the possibility of mass production [30]. On the contrary, main limits are found in the modulation bandwidth and the emitted power, which are slightly lower compared to other LDs. Some of the VCSELs' fields of application are green photonics [31], [32], spectroscopy [33], optical communications with WDM [34], [35], Optical Coherence Tomography (OCT) imaging [36] and, as described in this Thesis, Optical Frequency Comb generation [20], [27]. All these features, which characterize VCSELs, forecast them to be one of the most appealing LD technologies for compact and efficient comb generation, when the distance between comb lines, limited by the modulation bandwidth, is in the few GHz range. It is important to note that VCSELs under GS have previously been used for short pulse generation [37]. However, our approach is different and we have experimentally evaluated the use of VCSELs as optical sources to generate frequency combs and optimize the optical spectra created in terms of span, flatness and energy consumption.

This is the main objective of the experimental research, performed and detailed along this Thesis: first of all, an evaluation on VCSELs under GS to generate OFCs was done; on the other hand, we deepened our study with the expansion and optimization of these VCSEL-based OFCs to build more powerful systems that are easy to get Out of the Lab and remain compact and efficient. VCSEL's evaluation for OFC generation, the expansion of the generated combs and their optimization are the three experimental pillars of this work devoted to research

results, in correspondence with the three sections included in this Thesis.

As mentioned, our interest in OFCs optimization is a consequence to our previous studies on THz generation as well as current research on spectroscopy and sensing. Moreover, the work presented in this document was supported by a Spanish collaboration program (Retos-Colaboración RTC-2014-2661-7) with the main objective of developing new OFCs to improve the usability and the maximum frequency range of novel THz generators based on photonic techniques. This program encourages the collaboration between academy and the productive sector. For this reason the present research work has been conducted at University Carlos III of Madrid in partnership with the spin-off company Luz Wavelabs S.L. [38] , which focuses on “State-of-the-art THz and photonics products and solutions”. Therefore, some of the experiments detailed here have been implemented and launched together with this company.

2. Background and State of the art

In this section, the main concepts are defined. We present OFCs and VCSELs' current state and the applications in which they are useful. A brief explanation on the components and techniques that we have used for the comb expansion and optimization is also included. With this section we remark the interest on OFC systems based on LDs and, more specifically, on VCSELs as they can provide suitable combs for many applications aiming for versatility and higher efficiency in terms of energy consumption and costs.

I. Optical Frequency Combs (OFC)

Optical frequency combs (OFCs) are optical multi-wavelength signals ideally composed by a train of delta functions in both temporal and frequency domains. In Fig 1, we observe an illustration of it: in the optical spectrum (right part of the picture), we observe that a comb spectrum is, in reality, composed by an definite number of equally spaced and sharp lines, called *comb teeth*. These frequency (or wavelength) lines, back into the time domain, correspond to a train of short pulses if the frequencies are phase correlated, as shown in the left part of Fig 1.

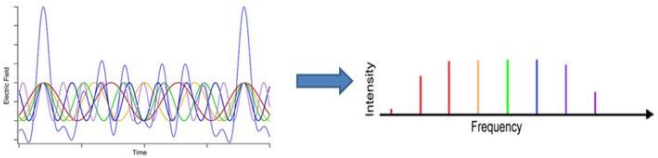

Fig 1. Optical Frequency Comb. Comb's Time and optical illustrations. Extracted from [39]

The Full Width Half Maximum (FWHM) of both the pulse and the comb are related to each other. The temporal duration of the pulse ($\Delta\tau_{FWHM}$) and the optical span (Δf_{FWHM}) are related in the time bandwidth product (TBP) that has a minimum value that depends on the temporal shape of the generated pulses, named *K* [40]:

$$TBP = \Delta\tau_{FWHM} \cdot \Delta f_{FWHM} \geq K \quad (1)$$

On the other hand, the repetition rate (T_{REP}) in time and the repetition frequency (f_{REP}) in the spectra (distance between comb lines) are also related to each other.

$$\cdot_{REP} = \frac{1}{f_{REP}} \quad (2)$$

Therefore, in a real OFC implementation, the width of the time pulse is inversely proportional to the width of the comb and the repetition rate of these pulses is related to the spacing in the comb lines [9]. General information on OFCs is found in books like [9], [41]. These two temporal-frequency relations are shown in Fig 2:

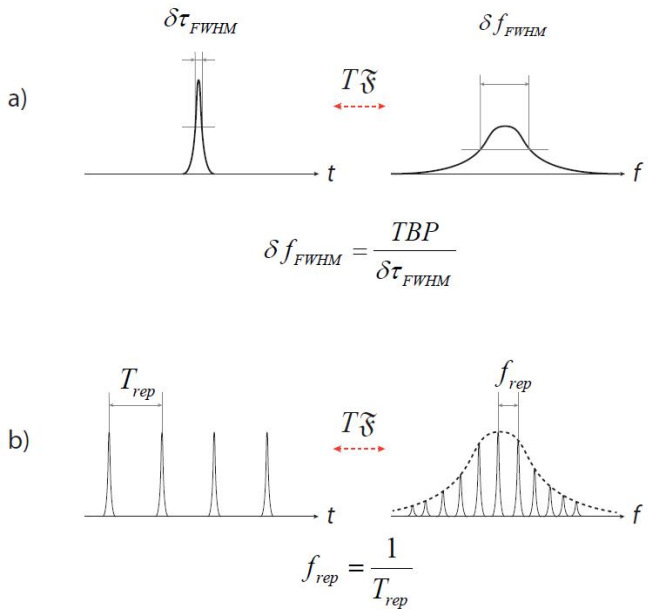

Fig 2. a) Individual temporal pulse and frequency domain representation. b) Temporal pulse train and frequency domain representation. Both the temporal and the frequency signal width and repetition frequency are related to each other. Picture extracted from [42]

As we have already mentioned, OFCs have boosted several fields of application over the last few years, an even more since 2005 [1]. Some of these fields are metrology, spectroscopy, communications, biomedical engineering or microwave photonics. Regarding metrology and optical clocks, they provide a link between the optical and the radiofrequency domain, simplifying enormously the systems needed to count the time cycles. [6], [39], [41], [43]. Powerful OFCs have been generated, even one octave broad allowing self-referencing [44]. This self-

referencing is also useful for other comb applications like low-noise microwave generation. After metrology, other applications benefited rapidly from the OFC technique, like biomedical applications [45] or spectroscopy [46]. This latest field, is currently devoted to dual-comb spectroscopy [2], [47], where the use of combs plunges the measurement time needs obtaining the whole spectra at once and then transferring the information to the RF frequencies by building an interferometer to map the modes of two phase coherent OFCs with close repetition frequencies. Systems including only commercial components have been designed and implemented encouraging the versatility and cost efficiency of dual-comb spectroscopy [13], [48].Recently, a new area of interest has arrived with the demonstration of OFCs in the Mid-infrared area , where gas sensing finds important applications [49]–[52].

Optical Frequency Combs are also of enormous utility for the communications and radiofrequency community. Combs, which might have hundreds of wavelengths using a huge bandwidth of several THz [18], are used for analog or digital wavelength division multiplexing (WDM) [3], [53], [54] and other multiplexing systems with the aim of increasing the capacity of fiber links. Combs are also shaped line-by-line to obtain tailored optical signals [5], [55] (optical arbitrary waveform generation or OAWG)or detect it and generate customized microwave photonic filters [7]. These fields are currently devoted to high repetition-rate optical frequency combs mainly in the range 10-40GHz and will most probably focus their attention on more compact, cheaper and more efficient systems [19].

Microwave photonics include also frequency synthesis in the sub-THZ and THz range where OFCs are an important tool when

using optical downconversion [27], [56]. Combs are multimode sources where the phase coherence among the comb lines (teeth) improves drastically the quality of the generated THz signal. Two of this comb teeth inside certain span can be selected and generate the THz signal using difference frequency generation (DFG). This is one of our expertises and we have published detailed work on the technique improving the state of the art with ultra-narrow linewidth performance, tunability and long term frequency and power stability [4], [12], [23], [57].

The important features to be enhanced in OFCs and their implementation set-ups depend on each application. OFCs systems are typically based on fiber lasers, line-by-line processing and tailored components which make them robust and powerful. With this kind of systems, ultra-broad optical spectra have been achieved in works like [18], where an extremely flat comb of 3.64THz (28nm or 365 teeth) in the 3.5dB optical span was generated. However, these set-ups are complex and difficult to reproduce and some of the fields of application of OFCs do not need that bespoke components. On the contrary, simpler but still useful systems are obtained with Off the Shelf components and LD sources, which are suitable for applications promoting them to be available Out of the Lab and to be manipulated by people not familiar to OFC techniques. These systems are more competitive in cost and versatility but find main constraints in the frequency span, the correlation between modes and the tunability [17], [23]. Set-ups like this have been already implemented in fields like THz generation or spectroscopy [12], [13]. More information on LD-based OFCs using GS will be given later in this chapter.

Direct OFC generation, indirect OFC generation and OFC expansion

Direct and indirect methods for comb generation have already been mentioned: the first one include those where the optical comb generation happens within the laser cavity itself while the indirect techniques generate the comb including elements that process the light after its emission from the initial optical source, typically a laser device working in continuous wave regime [20]. On the other hand, a comb is broadened if we include nonlinear elements that expand the optical spectra. In the following picture we observe the difference in the scheme for the different approaches:

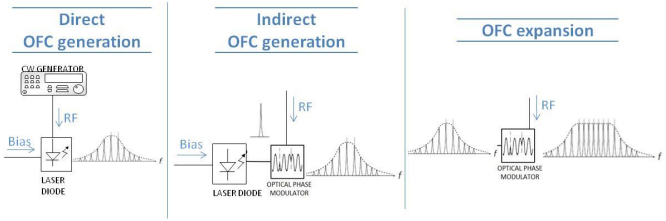

Fig 3. Schemes comparison. Direct generation, indirect generation with phase modulators and comb expansion with modulators. See text for more details

Direct comb generation takes place inside the laser resonator and it is based on the use of pulsed laser sources, like monolithic ML lasers [23], micro-ring resonators [19], or using large signal modulation techniques, GS among them. GS is the modulation technique that has been used to achieve pulse operation and will be explained afterwards, where we see how the pulse is generated by playing with the bias and RF signals injected into the cavity. On the other hand, indirect OFC generation is the

most common approach for OFC generation, leading the laser to emit a continuous signal and modulating the light afterwards using nonlinear elements. Different nonlinear components are used for this, but EO modulators are the most widely used, as shown in the previous figure. The indirect generation using EO modulators will be addressed in this Thesis, in a specific section (Chapter 8, page 104) for a comparison with the GS direct approach. Lastly, once the comb is generated, the nonlinear elements used for indirect generation might also be included for OFC expansion, potentially increasing the optical span is the set-up is properly configured. Different techniques to obtain this expansion will be used in this work, like including EO modulators, Highly Nonlinear Fibers (HNLF) or Nonlinear Optical Loop Mirrors (NOLM). They are explained shortly in this introduction and the work developed is explained in Chapters 8-12.

II. Laser Diodes (LDs)

A laser (from light amplification by stimulated emission of radiation) is a device that emits coherent light thanks to the enhancement of stimulated emission. This phenomenon describes a specific type of light-matter interaction: an incoming photon of light stimulates the decay of an electron that is in an excited state and, under some specific conditions called "population inversion", it might jump to a lower energy level generating a new photon with the same frequency, phase and polarization state as the incoming one who triggered the event. This similarity between photons is the key to some of the main features of the laser light, its extreme spatial and temporal coherence. Then, a laser is a device than boosts this stimulated

emission formed by two main elements: an optical gain medium working under those population inversion conditions (excess of excited electrons), and an optical resonator. Then, the gain medium is enclosed by optical mirrors to build that resonant cavity to make the light travel back and forth inducing this stimulated emission to happen. One specific kind of laser is a laser diode (LD) in which the active medium within the resonant cavity is a PN junction created with semiconductor materials and the electrons are in excited levels thanks to the injection of electrical current. More information on LDs is found in [21], [58], [59].

There exist different types of laser diodes. Regarding the direction of the emission of the light we can classify lasers in two main groups: edge-emitting lasers (EELs) and surface-emitting lasers (SELs). In the first ones the light travels parallel to the PN junction surface while in the latter it propagates perpendicularly [60]. EELs have historically been more popular and for instance, nowadays Fabry-Perot (FP) lasers are widely used for many applications, thanks to their simplicity and low-cost [28].Another approach to the classification of LD is to consider the number of discrete optical modes that constitute its optical emission. In this sense, FP is typically a longitudinal multimode LD technology. However, lasers emitting a single mode are desirable. In this sense, Distributed Feedback Lasers (DFB) is one of the most widespread EELs solutions to provide edge emitted light with a single longitudinal mode.

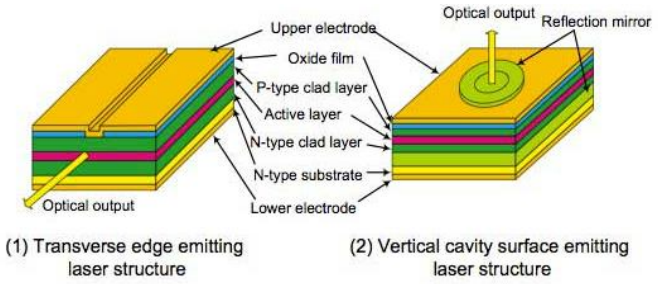

Fig 4. Comparison of semiconductor laser structures. SELs vs. EELs. Extracted from [61]

In our case we will compare a type of SEL called VCSEL to a specific kind of EEL called DM as explained forthwith. Both VCSELs and DMs are longitudinal single-mode devices [62], [63].

Laser Rate Equations

Understanding the dynamics of diode lasers has been a subject of study ever since the first diode laser began to emit. It was a GaAs device that Robert Hall and his team at General Electric made "lase" in 1962 [64]. Among the several approximations to model the behaviour of LDs, the so called Laser Rate Equations are one the simplest yet more accurate and functional models available. A brief description of this formalism is detailed here. This equations offer a means to evaluate the interaction between light (photons, *S*) and matter (electronic carriers, *N*) inside a diode laser. In a very basic form, this equations take the form detailed in (3) and (4) [21], [37]:

$$\frac{dN(t)}{dt} = G_{gen} - R_{spont} - R_{stim} \quad (3)$$

$$\frac{dS_{mode}(t)}{dt} = R_{stim\_mode} - P_{deads} + R_{spont\_mode} \quad (4)$$

The first equation (3) refers to the variation of the carrier density, that depends on the balance between the rate at what carriers are generated due to the current injection (G_{gen}) and the rate at what they recombine, due to spontaneous and stimulated emission mechanisms to produce photons (R_{spont} and R_{stim} respectively). For a given lasing mode, the evolution in time of its photon emission is described in (4). It depends on the rate of stimulated photons R_{spont_mode} and the rate of spontaneous photons R_{stim_mode} coupled to that lasing mode balanced against the "dead ones" (i.e., the rate ones that leave the cavity through the mirrors or the ones scattered or absorbed), P_{deads}. For more information read [21], [58], [59], [65].

Discrete Mode Laser Diode (DM)

DM lasers are a specific and new kind of monomode EELs fabricated and patented by Eblana Photonics [63]. They are known to be high quality ultra-narrow optical linewidth devices. They have also been successfully tested as a cost-efficient source for comb generation, particularly compared to DFB lasers [66]. In DM LDs, single wavelength emission is achieved with the inclusion of index perturbations distributed along the ridge waveguide in the FP cavity enhancing one mode and

suppressing the others as shown in Fig 5 [67]. We have selected LD technology as it presents great characteristics with respect to other horizontal lasers like single wavelength operation (higher SMSR), narrower linewidth and it allows working at higher modulation rates [63]. Some results obtained with GS-DMs to generate OFCs will be shown in this document.

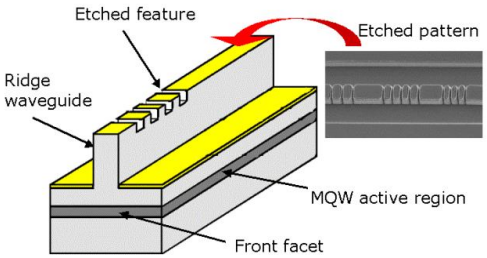

Fig 5. Schematic 1550nm DMLD. Extracted from [68]

Vertical-Cavity Surface-Emitting Laser (VCSEL)

This kind of laser emits perpendicularly to its semiconductor layers. These layers are basically two dielectric mirrors and an active region in between [28]. VERTILAS GmbH is a leader company in the production and distribution of long-wavelength VCSELs. In the following picture we can see a basic scheme of their devices, where we see the different layers and the direction of the emitting light. The VCSELs emitting at 1.5µm from VERTILAS are based in a Buried Tunnel Junction (BJT) to confine the current and waveguide the photons achieving lower threshold currents [69].

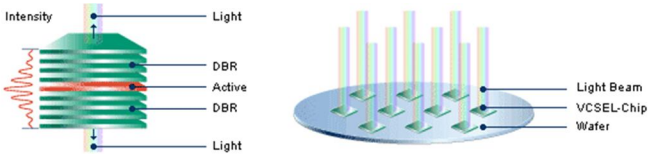

Fig 6. Basic layers of VCSELs and their fabrication in wafers. Extracted from [69]

Horizontal and vertical lasers (and in consequence VCSELs and DMs) have quite different characteristics. VCSELs have a smaller size, a lower threshold current, a circular beam and an easier fabrication process (including on-wafer test) and therefore lower cost in comparison to DMs. On the other hand, their disadvantages are the lower output power and temperature dissipation as it is a small device. VCSEL and DM lasers have also very different physical parameters related to the fabrication process. For more information on VCSELs and their comparison with EELs see [28], [66], [70], [71].

VCSELs are powerful devices that initially found applications in multimode optical networks [72] and optical mice [73] due to their circular beam, low threshold current and low energy consumption. VCSELs improve the competence in terms of integrability, compactness, low cost and the possibility of building arrays, features that boost the possibility of mass production [30]. Actually, they are becoming essential for society as they are the second type of laser in terms of production volume after Fabry-Perot (FP) LDs [28]. Because of their features their market is increasing and new applications will potentially come up besides the current ones. Moreover, variations in the cavity length of VCSELs can be mechanically

performed giving birth to a broadly tunable VCSEL [74] that has increment the possibilities that VCSELs provide to our daily lives: green photonics or spectroscopy [33], optical communications and WDM [34], [35], miniature atomic clocks [75] or Optical Coherence Tomography (OCT) imaging [36]are some of these applications.

The present work is centred on the possibilities that VCSELs offer to generate Optical Frequency Comb [20], [27]. This interest was born in a research environment where VCSELs have successfully been considered for numerous applications. THz generation [57], spectroscopy [76], [77] or Fiber Bragg Grating (FBG) interrogation [78] are some examples. Regarding OFC generation, the results obtained in the frame of this Thesis demonstrate VCSELs to be an important technology to be used in applications that do not need bespoke and expensive set-ups but can afford cost-effective and straightforward schemes using off the Shelf components.

Special attention has been given to the polarization dynamics in VCSELs and how they affect the comb generation. VCSELs are typically considered to be single-longitudinal-mode devices. However, their emission consists of two linearly polarized modes with orthogonal polarizations that, due to the birrefringence in the material, emit at different wavelengths [28], [79], as shown in Fig 7. Manufacturers have developed effective techniques to minimize this duality with polarization pinning processes and present devices that exhibit a side mode suppression ratio above 30dB [80], what makes this device purely monomode for many applications. Our efforts have been made to check if polarization dynamics in VCSELs play an important role in the OFC generation.

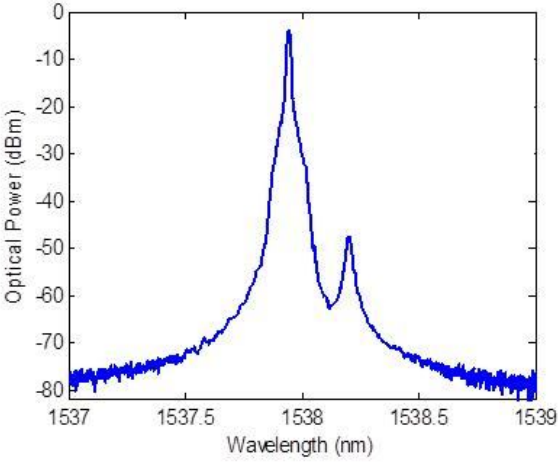

Fig 7. VCSEL CW emission spectra. The dominant main/parallel mode in P at 1537.95nm is more than 40dB above the residual/orthogonal mode shown at 1538.20nm. The birefringence of this VCSEL is 31.21GHz

III. VCSEL Laser Diodes under Gain Switching (GS) for direct OFC generation: VCSEL-OFC

Gain Switching is a straightforward technique to produce optical pulses (i.e., OFCs) that requires "no external cavity and no sophisticated fabrication technology" [58]. It is well known for generating pulses in the picosecond range [81]. GS consists on the radio frequency (RF) nonlinear modulation of the current injected to the diode under certain frequency and power conditions. GS forces the laser to work in nonlinear regime generating short pulses in time and therefore, optical combs in the frequency domain. In GS an RF signal is injected in the laser cavity forcing it to switch quickly from below to above threshold. This fast gain switch makes the light emitted to present relaxation oscillations as it is faster than the time required to

establish a continuous emission of light [82]. The characteristics of this short pulse are related to the physical properties of the laser device as it corresponds to the first spike of the relaxation oscillation.

Therefore GS is a direct technique (the comb is created inside the LD cavity) and can be easily applied to any type of diode lasers, even commercial devices with no extra components. Besides, the distance between modes is set by the RF frequency and therefore the tunability of this technique is continuous and directly achieved, which is the main advantage compared to other direct techniques as it provides a flexibility useful for certain applications . By contrast, main constraints are found in the bandwidth of the laser cavity and the package bandwidth that will limit the comb spacing and the optical span.

In Fig 8 we observe the GS phenomenon related to the PI curve of a laser diode: the LD is biased and modulated with a large signal, which forces it to be switched on and off in each modulation period. If the RF signal is switched off fast enough, then the device is still in the transient response and the first spike of the relaxation oscillation will be the only one excited. Therefore a short pulse is generated, shorter than the half-period of the RF electrical signal injected, due to underdamping [16].

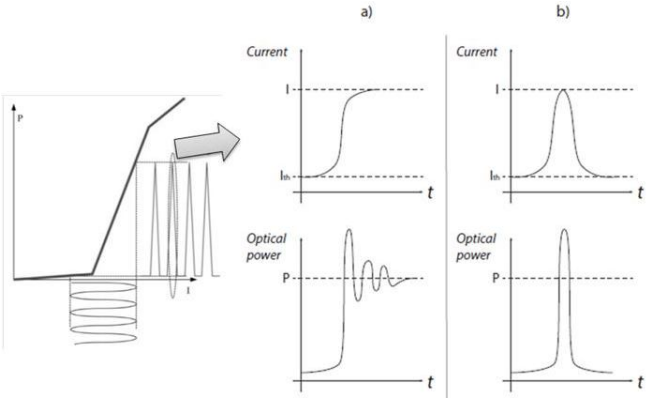

Fig 8. a) Transient response of a LD when switch on. b) Gain switching operation: the current injected in the laser is rapidly switched off so the first spike of the relaxation oscillations of the laser is the only one excited. This is the short pulse emitted by the laser, and this corresponds to a frequency comb when the fast operation is periodically forced. Picture adapted and extracted from [42], [65]

GS for comb generation allows continuous tuning of both the spacing (with the RF frequency) and the central frequency of the comb (with the bias current or temperature), which is important in applications like communication systems to control the channel spacing [83]. Other OFC techniques for comb generation based on LD pulse operation find their main restriction in the channel spacing, which is fixed during the fabrication. On the contrary, GS-LDs for OFC generation find limitations in the maximum spacing limited by the modulation bandwidth allowed by the laser cavity and its RF coupling.

GS has previously been applied to different LD technologies like DFBs [84], [85], DM [66]or FPs [83] to generate combs. With these sources, combs of 60-80GHz in the 3dB bandwidth have

been achieved [12], [83], [84]. They are typically expanded with different techniques as explained subsequently. Also, detailed work has already been done in our group on OFC generation using DM LDs: they show great performance for OFC generation when working under GS regime [4], [12], typically with repetition rates around 10GHz. As mentioned, key factors like high SMSR, narrow linewidth and high modulation bandwidth make this technology appropriate for OFC generation. Actually, in Chapter 5 DMs are modulated to force the GS regime and we will use the resulting combs as a reference to be compared to VCSELs'.

As mentioned, VCSELs enhance the advantages that LDs provide to our OFC GS systems as compared to other LD technologies. They are smaller, more efficient with lower threshold current and available for bulk fabrication, thus cheaper [30]. All these features, which characterize VCSELs, forecast them to be one of the most appealing LD technologies for compact and efficient comb generation, when the distance between comb lines, limited by the modulation bandwidth, is in the few GHz range. Besides, preliminary results have already shown an increase in this bandwidth limit by playing with the birefringence of the material [86].

To our knowledge, VCSELs under GS have previously been used for short pulse generation [37] but have never been used in order to evaluate the optical spectra created. Connecting the growing market of both VCSELs and OFCs, studying VCSEL-based OFCs is the aim of the experimental research detailed along this Thesis. In our opinion, OFCs generated using VCSELs under GS will imply a huge plunge in the system prices and complexity, especially once the VCSEL technology improves its modulation

bandwidth. VCSEL's evaluation for OFC generation, their expansion and their optimization are the objectives of the performed experiments.

VCSEL Rate Equations

The interactions between light and matter in a VCSEL under GS can also be modelled with the Laser Rate Equations introduced in (3)-(4). Different versions of these equations for VCSELs and GS appear in bibliography, but in our work we will use the set of equations (5)-(7), that are extracted from [37]:

$$\frac{dN(t)}{dt} = \frac{I(t)}{qV_{act}} - \frac{N(t)}{\tau_N} - v_G \frac{dG}{dN} \frac{(N(t)-No)}{1+\varepsilon S} S(t) \quad (5)$$

$$\frac{dS(t)}{dt} = v_G \Gamma \frac{dG}{dN} \frac{(N(t)-No)}{1+\varepsilon S} S(t) - \frac{S(t)}{\tau_P} + \beta\Gamma \frac{N(t)}{\tau_N} \quad (6)$$

$$\frac{d\varphi(t)}{dt} = \frac{\alpha}{2}\left(v_G \Gamma \frac{dG}{dN}(N(t)-No) - \frac{1}{\tau_P} \right) \quad (7)$$

In the previous expressions, I is the injected current, N and S are the density of carriers and photons respectively, φ is the optical phase, G the gain in the active area, N_o the carrier density in transparency (gain equals the losses). τ_P and τ_N are the photon and carrier lifetime, ε the nonlinear gain coefficient, β the spontaneous emission coefficient in the lasing mode (part of the total spontaneous emission that is in the lasing mode), Γ the confinement factor (part of the total energy that is in the active

area) and α the linewidth enhancement factor. For more information read [21], [58], [59], [65].

These rate equations have been implemented for VCSELs under GS to get an idea of the correspondence between the simulations and the experiments performed. The results obtained with this numerical study are shown in Appendix 5.

IV. VCSEL-OFC expansion: EO-PM, HNLF and NOLM

The optical span of an OFC is one of the main limiting factors in some applications like THz generation where a comb broad enough to cover the range of frequencies that are to be synthesized is needed [12]. Also, for DWDM enough lines to cover the standards must be generated [87]. To solve this, the OFC research community has made some efforts in the design and implementation of different techniques for optical span expansion [65], [88]. The importance of this expansion is even higher in our case as we are using LDs for comb generation that offer moderate optical span and this comb expansion becomes essential in many applications aiming for combs broader than 100GHz.

The techniques for OFC expansion are based on the generation of new modes in the optical spectra due to different nonlinear effects by including nonlinear elements in the set-up after the generation. They exploit different effects to broaden the initial comb as we saw in Eq.1 (page 37). Most of these nonlinear effects are related to second or third order susceptibilities ($\chi^{(2)}$ and $\chi^{(3)}$) [89]. Three of these expansion techniques have been used in this Thesis to expand the VCSEL-OFC and they are

introduced here: Electro-Optic Phase Modulation, Highly Nonlinear Fibers and Nonlinear Optical Loop Mirrors.

Electro-Optic Phase Modulation (EO-PM)

An Electro-Optic (EO) modulator is an element that can modulate either amplitude, phase or polarization [90]. These devices have an electro-optic crystal inside called Pockels cell, similar to the one in Fig 9, which changes the phase delay of the incident optical signal depending on an injected electric field. The relation of this change is directly proportional to the amplitude of the fields interacting, so it is related to second order susceptibility ($\chi^{(2)}$).

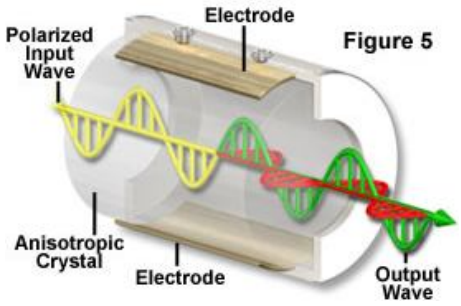

Fig 9. Pockels cell similar to the ones inside the Phase Modulators. Extracted from [91]

In Phase Modulators (PM), when the RF injected field changes in time, a phase modulation is produced in the optical incoming signal and therefore new frequency components appear expanding the incoming optical frequency comb. The equation that describes the phase shift suffered by the signal is the following (8), extracted from [92], where Δφ is the induced

phase shift, r the electro-optic coefficient of the Pockels cell, L the length of the modulator and d the width.

$$\Delta\phi = \frac{\pi}{\lambda} n^3 r V_m \left(\frac{L}{d}\right) = \pi \frac{V_m}{V_\pi} \tag{8}$$

Two important parameters define the phase shift, Vm and Vπ, which are the modulation voltage applied to the modulator and the voltage needed to induce a π phase change, which can be expressed as in (9). As can be observed, Vπ depends on the physical parameters of the modulator and will determine its quality.

$$V_\pi = \frac{\lambda}{n^3 r} \frac{d}{L} \tag{9}$$

The most common indirect technique for comb generation is based on the use of these Electro Optical (EO) modulators. In particular, the technique is specially suitable to generate OFC with repetition rates above the modulation bandwidth of the laser source under use, and has been deeply studied in previous works, using different amount of Phase Modulators (PM) [93]. EO-PMs allow comb generation with tunable teeth spacing below 100GHz [90] independently of the laser source used, typically narrow linewidth bench-top laser sources. Several of these modulators can be cascaded to broaden the comb about two times per modulator, using a common RF signal for their modulation and carefully managing the impedance matching of this RF applied to the different EO elements and the electronic phase [94]. These cascaded schemes generate very flat and tunable combs but, at the same time, the set-up is relatively

complex to adjust especially the RF part. This fact together with the high cost and the energy consumption of the modulators are the main drawbacks of this approximation. With this technique, combs broader than a THz have been obtained in works like [95]. More information can be also found in [96].

Highly Nonlinear Fiber (HNLF)

Typically, optical fibers based on silica, exhibit nonlinear optical behaviour described by a relatively significant third-order nonlinear-optical susceptibility $\chi^{(3)}$, also knows as Kerr-type susceptibility. This means that the refractive index of the material changes with variations in the optical intensity [97], and, when the input power is high enough, the subsequent variation of the nonlinear refractive index leads a modulation in the phase of the incoming signal called Self-Phase Modulation (SPM). This effect can be exploited to increase the optical spectrum of an incoming comb.

HNLFs are specialty fibers that have become essential elements in many set-ups as they exhibit an enhanced nonlinear response, reducing the optical power needed to trigger the nonlinearities. This enhancement is accomplished by the inclusion of micro-structural modifications in the cladding of these fibers [98].[99]. Some examples of these modifications are shown in Fig 10.

The pulse propagation in a passive media, like HNLFs, is described by the Nonlinear Schrodinger Equation (NLSE), derived from the Maxwell Equations [97]. In the following equation (10),extracted from [100], *A* is the envelope of the field, under the slowly varying envelope approximation, α_{loss} are the losses along the fiber, β_2 is the group velocity dispersion

(GVD) and T is the time referenced to a retarded frame. More information on this equation is found in [65], [99], [100].

$$\frac{\partial A}{\partial z} = -i\frac{\beta_2}{2}\frac{\partial^2 A}{\partial T^2} - \frac{\alpha_{loss}}{2}A + i\gamma\left|A\right|^2 A \qquad (10)$$

Lastly, γ is the nonlinear coefficient in the fiber determined with the following equation (11), where A_{eff} is the effective area in the fiber and n_2 the nonlinear refractive index. This parameter in $(W{\cdot}km)^{-1}$ together with the fiber length define the HNLFs used in the experiments.

$$\gamma = \frac{n_2\omega_o}{cA_{eff}} = \frac{2\pi n_2}{\lambda A_{eff}} \qquad (11)$$

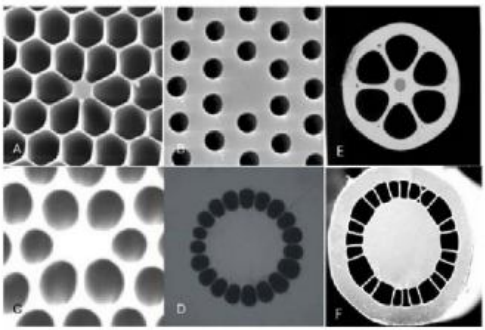

Fig 10. Examples of microstructured fibers. Picture extracted from [99]

HNLFs have been commonly used for comb expansion and broadband signal generation [18], [88], [101]. Some works also refer to this comb expansion technique using HNLFs and

compression elements as parametric mixing [89], [102], [103]. In this work, they are used for comb expansion once comb is generated inside the VCSEL cavity. Prior to this HNLF, the optical pulses should be compressed closer to the TBP limit and then optically amplified to enhance the nonlinear effects into the HNLF.

Nonlinear Optical Loop Mirrors (NOLM)

Nonlinear Optical Loop Mirrors (NOLM) are nonlinear fiber Sagnac interferometers [100]. NOLMs are commonly used for pulse compression and reshaping, comb filtering, and switching or multiplexing optical signals in communication [104]–[106]. Nonlinearities are also related to third order susceptibility effects, $\chi^{(3)}$, and both SPM and Four Wave Mixing (FWM) might be induced.

A loop is implemented with an optical coupler, that can be symmetric (50-50) or asymmetric. Inside the loop, its architecture should include elements that break the nonlinear symmetry of the loop. Then, the optical signals travelling clockwise and counter-clockwise suffer the nonlinear effects differently and both signals interfere with different phases [107]. A typical scheme of an NOLM is shown in Fig 11.

The most basic loop configuration includes only one optical fiber inside [108] with an asymmetric optical coupler, but more complex set-ups include nonlinear elements and dispersion compensation fibers (both DCFs and/or SMFs). In other cases, the nonlinear symmetry breaking element might be an amplifier, i.e. a Semiconductor Optical Amplifier (SOA) [100]. These systems are also called Nonlinear Amplifier Loop Mirror (NALM) [109].

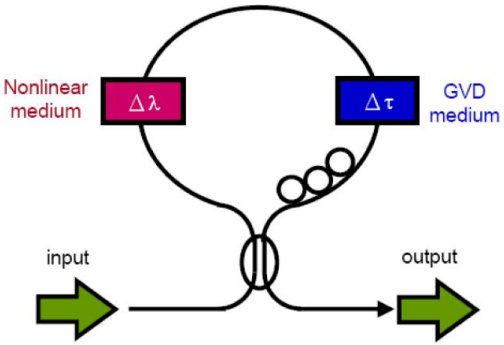

Fig 11. Scheme of an NOLM. A loop is implemented with an optical coupler (symmetric or not) and different elements are placed inside. Typically, there are nonlinear asymmetric elements so that the the pulses travelling clockwise and counter-clockwise suffer differently. See text for more details. Picture extracted from [110]

Passive elements inside the NOLM configuration can also be described with the Non Linear Schrodinger Equation already shown in (11) for the HNLF. Both HNLF and NOLM are often used as building blocks of larger comb generation schemes known as parametric mixers. Parametric mixers have demonstrated ultra-wide and flat optical combs, above 10THz [102]. They are based on the concatenation of numerous nonlinear optical stages to optimize the generation of new frequencies typically based on an initial dual optical source.

In this work, we propose this technique also for comb expansion, focusing therefore in the optical spectra broadening achieved like previously done in [87], [111]. For this, several set-ups have been tested and our final loop will include a SOA as nonlinear element inserted into the loop and a DCF. SOAs

devices are interesting here due to their strong nonlinear operation, low power consumption and small size [112]–[114].

V. VCSEL-OFC optimization: Optical Injection Locking (OIL)

Optical Injection Locking (OIL) in Laser Diodes (LDs) has been extensively used to improve the performance of the emitting light, mainly focused on laser spectral narrowing, frequency chirp reduction, noise reduction and modulation bandwidth enhancement [37], [115]–[117]. This technique consists on the injection of light from an external source, the master laser, into the device under use, called slave laser. Under certain conditions the output light locks the injected light inheriting its frequency and phase [21]. If the locking achieved is stable, this injection improves the performance of the slave laser, providing the master light has enhanced characteristics. Then high performance master locked to a noisier slave yields to low noise output signal [116]. This scheme is shown in Fig 12.

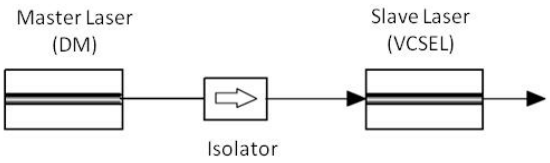

Fig 12. Optical Injection system. In this work a DM will be used as master and a VCSEL as slave laser. Picture adapted from [118]

As shown in the figure, in this thesis a DM as master laser and a VCSEL under GS as the slave laser are used, so we are injecting external light into a laser emitting an OFC. As the active area in VCSELs is much smaller than in edge-emitting LDs, the effect of the external photons going inside the cavity might be significant [118]. VCSELs have also been injected for decades to improve mainly their modulation bandwidth, chirp or low emitted power [119]–[122] in communication applications or some other fields [123]. They have also been modulated and injected to filter comb components [124]. As we have previously mentioned, a VCSEL emits two transversal polarization states and injection can occur in the main polarization state or the orthogonal one. These two injection possibilities are respectively called parallel and orthogonal optical injection. Both have been considered in previously published works [121], [125]–[127].

VCSEL under OIL Rate Equations

The lasing condition for an injected laser is also described using the rate equations previously introduced. The VCSEL rate equations shown in (6)-(8) become now the following equations (13)-(15) if we include the injection locking effects into the VCSEL cavity [128]:

$$\frac{dN(t)}{dt} = \frac{I(t)}{qV_{act}} - \frac{N(t)}{\tau_N} - v_G \frac{dG}{dN} \frac{(N(t) - No)}{1 + \varepsilon S} S(t) \tag{12}$$

$$\frac{dS(t)}{dt} = v_G \Gamma \frac{dG}{dN} \frac{(N(t) - No)}{1 + \varepsilon S} S(t) - \frac{S(t)}{\tau_P} + \beta \Gamma \frac{N(t)}{\tau_N} + \frac{v_G}{L} \sqrt{S(t) S_{inj}} \cos(\vartheta) \tag{13}$$

$$\frac{d\varphi(t)}{dt} = \frac{\alpha}{2}\left(v_G \Gamma \frac{dG}{dN}(N(t) - No) - \frac{1}{\tau_P}\right) - \Delta\omega - \frac{v_G}{2L}\sqrt{\frac{S_{inj}}{S(t)}}\sin(\vartheta) \quad (14)$$

Where the carrier density equation does not change but there are new terms appearing in the photon density and the optical phase equations, due to the external light that is now coupled into the VCSEL cavity. In the previous expressions, I is the injected current, N and S are the density of carriers and photons, φ is the optical phase, G is the gain in the active area, N_o is the carrier density in transparency (gain equals the losses). τ_P and τ_N are the photon and carrier lifetime, ε is the nonlinear gain coefficient, β is the spontaneous emission coefficient in the lasing mode (part of the total spontaneous emission that is in the lasing mode), Γ is the confinement factor (part of the total energy that is in the active area) and α is the linewidth enhancement factor. New factors related to the injection are S_{inj}, that corresponds to the photon density of the injected signal and ϑ that is the phase difference between both optical fields. As mentioned before, Δω is the frequency detuning between master and slave and it is an important parameter to achieve the injection locking. More information in the VCSEL's rate equations under OIL is found in [128].

3. Methods

In this chapter, we include an explanation of the measurement procedures considered to evaluate the main features of the different combs' characterized in this Thesis. Here, we describe the metrics and figures of merit used in this work to evaluate the generated optical combs and compare their features. Along this research, four dimensions of the signals have been explored: optical spectra, temporal pulses, electrical spectra and energy consumption estimation. The values for the resulting combs are seen at a glance in Table I (page 132) where all of them have been collected.

1- Optical Spectrum Measurement

The main source of information along the present work has been the optical spectra of the different generated signals. It gives information of the span of the optical frequency comb, the frequency spacing, its shape and the number of teeth generated. To measure it, we use an Optical Spectrum Analyzer (OSA) with 0.02nm of wavelength resolution. The optical output of each experimental set-up is directly connected to this instrument to obtain the spectral image. From the optical spectrum trace we mainly extract the parameters plotted in Fig 13, which is the measured optical spectra of the VCSEL-OFC and that we will analyse in the corresponding chapter:

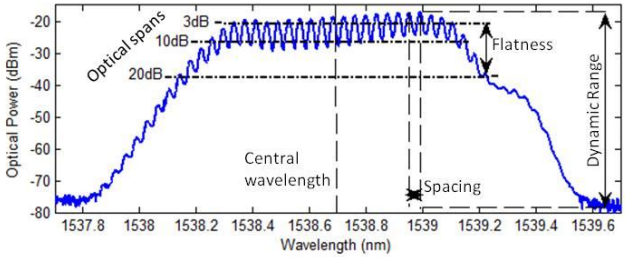

Fig 13. Optical spectra, figures of merit. See text for more details

Optical span: The width of the comb, measured in number of comb teeth or in frequency or wavelength. As we have previously expressed, in this work we define the span as the number of comb lines and/or the spectral width in the uppermost 20dB of the spectra. This is the main parameter in which we focus, and our efforts are centred on increasing the comb span up to or even above 1THz. We use as reference the **20dB span** as the comb teeth in this range are useful for THz photonic generation [12]. Other applications as optical communications have more restrictive span definitions (typically 3-10dB). These metrics are also presented in the table in page 132 but along the work we will mainly focus on the 20dB span as main feature of the different combs.

Another parameter that we extract from the optical span is the **expansion factor**, in the expansion systems (see section: *VCSEL-based OFC expansion*) to check how the comb is expanded due to the addition of these stages. In this work we have defined the expansion factor as the coefficient between

the comb teeth in each comb compared to the comb teeth in the VCSEL-OFC (the VCSEL output under GS).

Flatness: Different comb lines might have different power levels. The term *flatness* is the amplitude deviation in power of the optical teeth in the range of wavelengths considered. The **flatness factor** is defined in this work as the ratio of the 3dB to the 20dB span. The closer this value is to 1, the closer the comb is to exhibit a flat-top shape. This parameter is especially relevant in WDM applications because different user's information will be placed in different wavelengths.

Dynamic range (DR): The inclusion of new elements along the optical path implies some loses in the **dynamic range**, which has been measured in this work as the difference between the peak power in the highest comb tooth and the noise level, in dB. The bigger the DR is, the lower the optical noise floor in the system will be. Then, DR reductions might limit some applications. For instance, in THz generation the noise is translated to the THz synthesize signal lowering its quality and in spectroscopy the optical noise is translated to the RF frequency comb.

Spacing between comb teeth and tunability: The distance between comb lines is related to the repetition frequency of the temporal pulses. Some approaches for comb generation does not allow it to be tuned. However, we are using VCSELs under GS so we can continuously tune this spacing with the **LD RF modulation frequency** (f_{RF}), which is limited by the laser source modulation bandwidth. In this work, the spacing between comb teeth will be the frequency in which the broadest comb is obtained, 5.2-5.4GHz in case of the VCSEL

used. This parameter varies in different applications and, for example, WDM have standards that fixes this parameter to values higher than 10GHz and tunability is not needed, while other applications like spectroscopy require more flexible systems with lower spacing as the trade-off measurement time vs. system resolution will depend on this.

Central wavelength tunability: We are working with long-wavelength VCSELs emitting around 1539nm. This central wavelength can be tuned with the bias and temperature of the laser in a small range (±1nm approximately). However, we will not focus in this parameter and we will select the temperature and bias that provides the widest comb.

Optical Linewidth: In this work, the **optical linewidth** has also been measured. It was included at the end of the experimental work so it is only available for the last set of experiments regarding Optical Injection Locking (see Chapter 14, Fig 48). For this purpose we have used the delayed self-heterodyne interferometric technique [129] and we have obtained the electrical spectra of it, where the optical linewidths are half of the 3dB bandwidth of the plotted lines. The optical linewidth is related to the optical noise in the laser source and to the phase correlation among comb lines, which is important in applications like dual comb spectroscopy (DCS), where it limits the maximum interferometer length. An example of this linewidth measurement is shown with a real measurement in Fig 14.

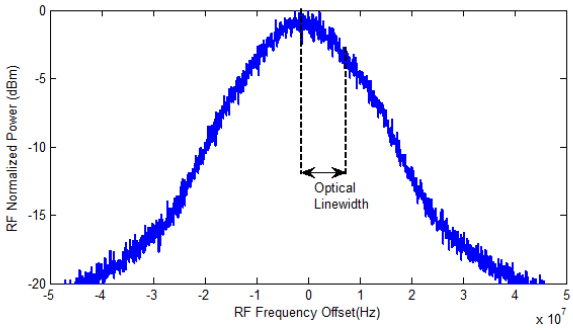

Fig 14. Optical linewidth. See text for more details

2- Temporal Pulses measurement

The autocorrelation is a technique commonly used to measure short optical pulses in the ps or fs ranges. Along this work we use the autocorrelation to extract the temporal information of the correspondent combs, using an Autocorrelator, model PulseCheck from A.P.E GmbH, with a maximum scan range of 150ps. The entrance of this device is directly the optical signal that has previously travelled through an Erbium Doped Fiber Amplifier (EDFA) and a Polarization Controller (PC). The EDFA is important because the power sensibility of this device is around 10dBm. From the autocorrelation trace we obtain its autocorrelation duration with the full width half maximum (FWHM) of the measured trace.

On the other hand, the autocorrelation method is based in Second Harmonic Generation [130] and does not give information of the real pulse shape of the pulses but gives an accurate result of the pulse duration only if the shape of its

temporal profile is known. An example of an autocorrelation trace is shown in Fig 15 where we observe the autocorrelation FWHM that is obtained from this temporal measurement. The plotted trace is the measured autocorrelation trace correspondent to the VCSEL-OFC and, in this case, it presents pedestals at half height. Pedestals are typically present in pulses generated under GS regime because the laser is forced to work under a large signal modulation regime and complex phenomena occur inside its cavity generating asymmetric pulses with trailing sub-oscillations [131].

Pulse duration: From the autocorrelation full width at half the maximum (FWHM) we can compute the real pulse FWHM duration only if we infer it assuming a certain temporal profile. Ideal symmetric pulses, described with Gaussian profiles or sech² shapes are typical of pulsed sources such as mode-locked devices. For example, for a pulse with $sech^2$ temporal shape, there exist an autocorrelation-pulse FWHM relation of $\tau_{ACT\_FWHM}/\tau_{pulse\_FWHM} = 1.543$ [132]. Unfortunately, this is not the case when dealing with GS pulses. Their asymmetric and complex temporal profiles prevent us from extracting the pulse duration only with the information of the autocorrelation [100]. In Fig 15. We observe a measured autocorrelation trace, already processed to extract the FWHM.

In our case, we had access to the autocorrelation and the optical spectra. Using these two sets of information, time-retrieval procedures such as the *Time Information Via Intensity (TIVI) algorithm* or *Gerchberg–Saxton algorithm* helped to find phase information compliant with the measurements to estimate the actual temporal width of the pulses. An example of the results of these procedure is shown in Fig 16. Since this is not the

primary objective of this Thesis, this pulse analysis was based on tools available in the group from the work described in [65].

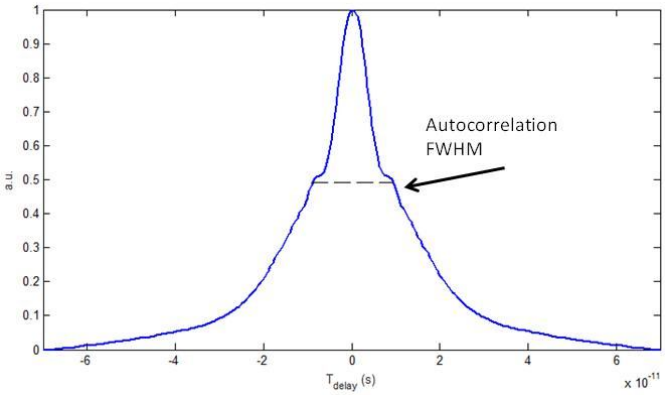

Fig 15. Temporal autocorrelation pulses, figures of merit. See text for more details

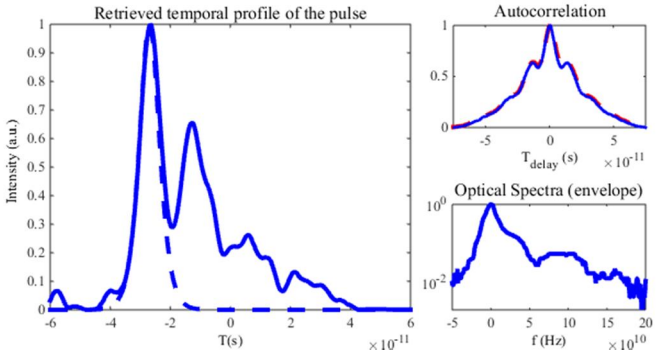

Fig 16. Example of a pulse temporal shape retrieved using TIVI algoritm (left). Figure extracted from [65]

As we mentioned and as Fig 16 shows, the temporal trace of GS pulses is asymmetric and exhibits several subpulses and structures. This is the reason why the evaluation of its FWHM only gives limited information, since the energy associated to the sub-structures may be left unquantified. To answer this problem, we also consider other metrics to evaluate the duration of the optical pulses, or more specifically, how their energy is concentrated in time. Those metrics are the equivalent pulse width τ_e and the *room mean square* pulse width, τ_{rms} defined below [133]:

$$\tau_e \equiv \frac{1}{I_{max}} \int_{-\infty}^{\infty} I(t)\,dt \qquad (15)$$

$$\tau_{rms}^2 = t^2 - t^2, with\, t^n \equiv \int_{-\infty}^{\infty} t^n I(t)\,dt \qquad (16)$$

where t is the time variable and I(t) is the optical intensity. These metrics give an estimation of the pulse width regardless of the shape and permit the comparison of pulses with different and complex structures.

Time Bandwidth Product (TBP): No matter the metric considered to evaluate the pulse duration of the temporal trace associated to an optical comb, the evaluation of the quality of the pulses it contains is incomplete unless the spectral information is also taken into account. Following the uncertainty principle [134]:

$$\tau_{rms} \cdot \omega_{rms} \geq 0.5, where\, \omega_{rms}^2 = \left\langle \omega^2 \right\rangle - \left\langle \omega \right\rangle^2 \qquad (17)$$

where ω_{rms} is the root mean square spectral width of the signal, in our case, the comb under study. Hence, regardless of the shape of the pulse or the profile of its optical spectra, the product defined in (17), called the **Time Bandwidth Product rms** (TBP_{rms}) has a minimum of 0.5. The closer this metric is to this minimum, the less dispersed or phase separated the spectral components are, the less dispersed or *chirped* the pulses are [133]. When the inequality in (17) becomes an equality, the signal exhibits its maximum temporal-spectral quality and is referred to as *Time-Bandwidth Limited, TBL*. Linear pulse compression techniques, such as the use of dispersion compensating optical fibers (DCF) or optical gratings, can reduce the TBP of an optical pulsed signal to its ideal TBL limit of 0.5 [97]. When the FWHM or the equivalent time metrics are used to evaluate the pulse duration and the spectral width of an optical pulsed signal, the TBP has a minimum that depends on the temporal shape of the pulses and is only useful when comparing those with the same profile.

3- Electrical Spectrum measurement

The electrical beat tone signal at f_{RF} generated when the optical comb under study is detected using a high speed photodiode allows us to evaluate the noise in the system and the phase coherence between comb teeth. This phase correlation between comb lines is crucial in many applications as is related to the noise in the system. In this work, the whole comb is directly detected in a 50GHz photodetector, then the signal is amplified with a low noise RF amplifier and the resulting electrical spectra is measured with an Electrical Spectrum Analyzer (ESA) up to 25GHz. Using this experimental approach,

we have obtained up to three measurements from the RF spectra: the spectra from 0 to 6GHz, the phase noise and the electronic linewidth at f_{RF}.

Electrical Spectra 0-6GHz: The Electrical spectra in the range 0-6GHz gives important qualitative information for this work. A clear peak at the RF modulation frequency, which corresponds to the distance between comb teeth, should appear and the rest of the spectrum is close to the noise level. This noise level varies with the noise coming from the set-up. Then, we compare this noise level to the reference noise floor, which is the CW RF signal used for modulation directly connected to the ESA. The difference between the reference and the output of the system will be the noise included by the set-up. This is shown in the following picture:

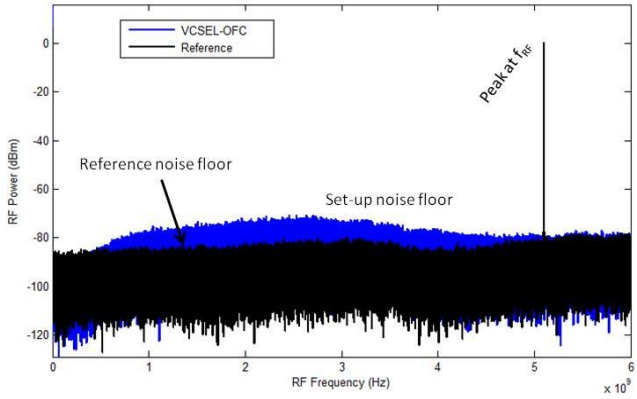

Fig 17. Electrical spectra 0-6GHz, figures of merit. See text for more details

Phase Noise (PN): The **PN of the electrical spectra at the modulation frequency** (f_{RF}) increases when the phase correlation between the teeth in the comb is reduced and/or the noise is increased in the system. This happens because the electrical signal at this frequency is composed by the recombination of all the comb teeth. Therefore, the phase correlation among comb teeth is related to the degradation of the PN along the system.

The PN at f_{RF} is compared for both, the comb under test and the lowest possible limit which is called Reference in the graphs. To measure the PN of the OFC under evaluation is detected in a photodiode and subsequently amplified with an RF amplifier. The amplified RF signal is connected to the ESA already set to measure the PN at f_{RF} and then the decay around this carrier is plotted. It is important, at this point, to observe the carrier power as different PN traces can only be compared with similar power levels. Then, the Reference PN at f_{RF} is obtained by directly connecting the CW generation equipment used for the RF modulation (model Anritsu MG3695A) to the ESA. Attenuation will be included in between the equipment to adjust the carrier power to the OFC obtained level. Lastly, the Displayed Average Noise Level (DANL) is also obtained, which is the noise level of the ESA equipment. This is the lowest level that the ESA is able to measure with this carrier power level. As an example, an actual PN measurement of the VCSEL-OFC is plotted in Fig 18. A zoom in the range 100-1000Hz will be included when considered, as the decay might be relevant in this area and it is not properly visualized in the main plot.

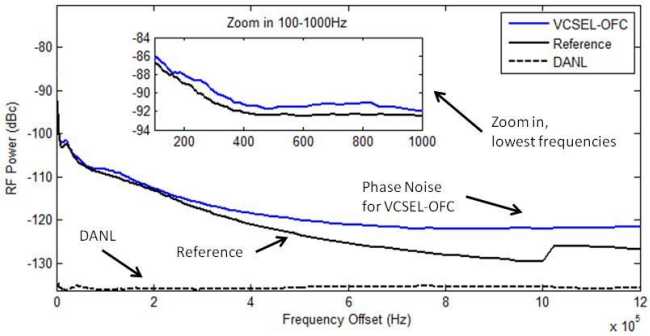

Fig 18. Electrical Phase Noise at f_{RF}. See text for more details

With this representation, we can compare the Reference and the OFC. The difference between the associated PN traces is related to the degradation of the signal along the set-up, due to the electrical to optical conversion in the laser (the OFC generation), the optical to electrical detection in the photodiode and the other components in the set-up. In some cases, we will also compare two or more OFC traces in the same plot to see the difference in the noise among them.

RF Linewidth at 3dB: In this work, the **3dB RF linewidth** of the signal at f_{RF} after the detection of the whole comb in a photodiode is also measured and compared to the reference one (the CW generation equipment used for the RF modulation, model Anritsu MG3695A). This parameter has been recently included in our set of experiments so it is only included in the comparison of the expansion techniques, in Chapter 12 (Fig 41).

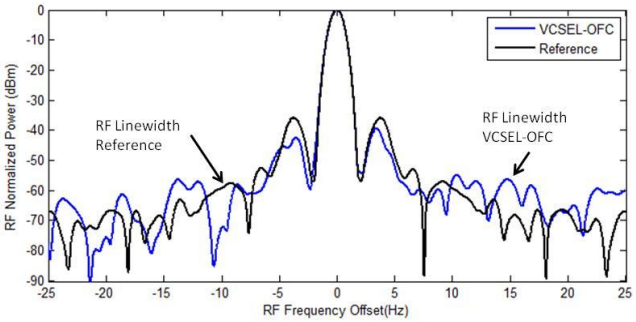

Fig 19. RF Linewidth at f_{RF}. See text for more details

4- Energy consumption estimation

One of the motivations to use VCSEL devices for the generation of optical frequency combs was their energy efficient behavior, and how its inclusion can affect the performance of the overall system. This is why we have made an estimation of the **energy consumption** in Watts of the schemes under study by calculating the electrical power needed by the active elements that are included in each implemented set-up. This is an important parameter when working in fields like green optical communications [13] or incorporating such schemes in actual systems. For this purpose, the experimental supply powers set in the equipment and the datasheets of the components have been used. The power in the EDFA has been computed with the laser current set in the device for each set-up and assuming a typical 980nm pump LD operating at a voltage of 1.7V [33].

4. Methodology

The research described in this Thesis covers an experimental study to evaluate the use of VCSELs as laser sources for optical frequency comb (OFC) generation, and the improvement of the resulting combs using expansion and optimization techniques.

Building OFC systems with off-the Shelf components implementing systems easy to take Out of the Lab is the focus of this research. In this line, previous work on OFC with different LDs was done, but VCSELs came up as a technology that would increase the advantages of LD-OFCs: the energy efficiency is enormously improved compared to other LDs because VCSELs work with less than 20mA of bias and a threshold current around 2mA (see Appendix 1 for detailed characterization of the sources) due to their small sizes. Together with the fact that they emits vertically, this facilitates their fabrication process, offers compactness and a high potential for integration.

The initial plan covered a study of the VCSEL source for OFC generation under GS. After the first VCSEL arrived (VCSEL#1), an RF board was designed and built to match the bias and RF modulation to the VCSEL unit. The first experiment with the VCSEL was promising: a comb of 100GHz was achieved with only 14dBm or RF power and 9mA of bias current. The supply parameters were optimized and the first VCSEL-OFC was obtained, shown in Fig 74. Deeper evaluation on the VCSEL technology under GS was performed, including PI curves, wavelength variations, modulation responses (S11 and S21 parameters), chirp, RIN, etc. All these results are shown in the different appendixes of this Thesis. At that moment, this VCSEL-based comb demonstrated to be the most energy-efficient OFC

with a single-device [27]. This led us to believe that this approach was a promising substitutes for other more complex OFC systems. We also used this initial comb to generate sub-THz radiation, synthesizing an 88.2GHz signal [57]. After this, a second VSCEL was acquired and a detailed evaluation for OFC generation under GS was repeated for this new unit, including an automatization of the measurement procedure, to observe the repeatability of the results. The behaviour of this second sample (VCSEL#2) is slightly better than the first one as its RF coupling is more efficient due to the RF board provided, in this case, by the manufacturer. Then, the work continued using this second sample, VCSEL#2, whose behaviour under GS is detailed in the first section of the body in this Thesis: in "*VCSEL Diodes under Gain Switching",* where the VCSEL is tested and compared to a DM, the previous LD technology that was mainly used in our group for OFC. During this study, the optimum operation point of the VCSEL#2 for OFC generation under GS was obtained after, providing a 135GHz broad comb in the 20dB span (Fig 74).

However, the span was still limited and secondly our efforts were focused on the expansion of this outcome to increase the optical span achieved: even when VCSELs provide broad combs compared to other laser technologies, producing broader combs will increase the possibilities of the system in the fields in which spans below 300GHz are not enough. At the same time, compactness, integrability and energy efficiency are permanent factors taken into account in the systems that we implement. For this purpose, three different nonlinear stages for comb expansion were added after the VCSEL-OFC, used here as seed comb. This set-ups expansion experiments have been included

in a second section of this Thesis, called "*VCSEL-based OFC expansion*".

The main technique, extensively used for both comb generation and/or expansion is the use of one or several EO Modulations, either intensity (IM) or phase (PM) ones. Using two of these devices (PMs), our best results were obtained. Secondly, we used HNLFs for this same purpose, and, in a third approach, dispersion compensation fibres (DCFs) were tested in a specific nonlinear optical loop mirror (NOLM) configuration together with a Semiconductor Optical Amplifier (SOA). With these three different expansion techniques, expansion factors around 3 were obtained and they were compared. Lastly, the two first techniques (EO elements and HNLF fibre) were cascaded in a successful attempt to reach the THz range. All these schemes are deeply analysed following the four characterizations described in Methods and the main results are summarized in Table I (page 132). It collects all the relevant parameters, as each approach has different potentials and drawbacks compared to the others.

Once our understanding of VCSEL-based combs became deeper, our experimental results pointed out that the effect of the residual-suppressed orthogonally polarized mode of the VCSEL was significant for the OFC generation. Then, we decided to focus our attention on it and devoted our efforts to study the polarization components that form the VCSEL-OFC. After observing the polarization dynamics of the VCSEL-OFC, a second work line came out as important for OFC optimization: Optical Injection Locking led us to modify the relation among both polarization components and we evaluated how this affected

the resulting comb. This is presented in the third and last section of the body: "VCSEL-based OFC optimization".

Regarding this document and the upcoming information, the format of each chapter attempts to be straightforward and simple, following a similar structure for an easier reading: the experimental set-up is explained and shown together with the obtained optical spectra. The temporal autocorrelation trace and the electrical spectra will be subsequently presented. Most of this work has already been either published or submitted to different journals or congresses. This is remarked at the end of the chapter in a specific paragraph under the title "*Related publication*" with a link to the correspondent article or abstract. All this published or submitted work is fully available in section "*Publications and related work*". The main goals that have driven the research presented in this doctoral Thesis are collected in this table, together with the chapter and initial page in the document covering the issue:

Objective	Chapter	Page
VCSELs under GS for OFC generation		
DM-OFC Characterization	5	85
VCSEL-OFC Characterization	6	90
DM vs. VCSEL comparison	7	97
VCSEL-OFC expansion		
Using EO Modulators	8	103
Direct vs. indirect generation vs. expansion with Modulators	8.I	104
Using HNLF	9	112
Using NOLM	10	117
1THz broad OFC	11	122
Comparison of expansion techniques	12	125
VCSEL-OFC Optimization		
Polarization Dynamics in VCSEL-OFC	13	139
Optical Injection Locking in VCSEL-OFC	14	145

VCSEL Diodes under Gain Switching for OFC generation

Along this section we focus on the evaluation of Vertical-Cavity Surface-Emitting Lasers (VCSEL) as laser source for Optical Frequency Comb (OFC) generation. For this, we present a detailed research on two different LD technologies: **Discrete Mode (DM) Lasers** in Chapter 5 and **VCSELs** in Chapter 6. DM technology offers good performance under GS among other edge emitting LDs and that is why we use it as reference for comparison. VCSEL technology was used for the first time for OFC generation when these experiments were launched and it is demonstrated that VCSELs under GS provide the most energy efficient single-device OFC with a one-device implementation. This section is closed with a **comparative study of both laser technologies and the generated OFCs** detailed in Chapter 7.

5. Discrete Mode Laser OFCs: DM-OFC

DM laser diodes are state of the technology edge emitting lasers that have been proven to be efficient sources for optical frequency comb generation [66]. In DM lasers, single wavelength emission is achieved with the inclusion of index perturbations distributed along the FP cavity enhancing one mode and suppressing the others [67]. We have selected this device as a reference, as it presents great characteristics with respect to other single wavelength edge emitting lasers. DM lasers exhibit a higher side mode suppression ratio (SMSR), a narrower optical linewidth and they can work at higher modulation rates [63]. DMs have previously been used as the optimum LD source for our OFC systems because they show great performance for OFC generation when working under GS regime in the few GHz modulation range [4], [12]. That is why, in this work, we use them as a reference to see whether our OFC systems are improved with VCSELs. In this chapter we characterize the DM-OFC, which is the broadest comb obtained with this DM sample under GS operation. The resulting DM-OFC and its set-up are shown in Fig 20.

Prior to the achievement of this comb, a detailed characterization was performed. The static and dynamic characterization of the DM laser source are shown in Appendix 1. This appendix shows the DM in a 7-pin butterfly package, adapted for the RF modulation with an SMA connector. The PI curve of the device at 25°C shows that the threshold current of this device is 12mA and the slope efficiency is 0.12 mA/mW, the

wavelength variation with the temperature and bias current are 0.1nm/°C and 0.04nm/mA respectively.

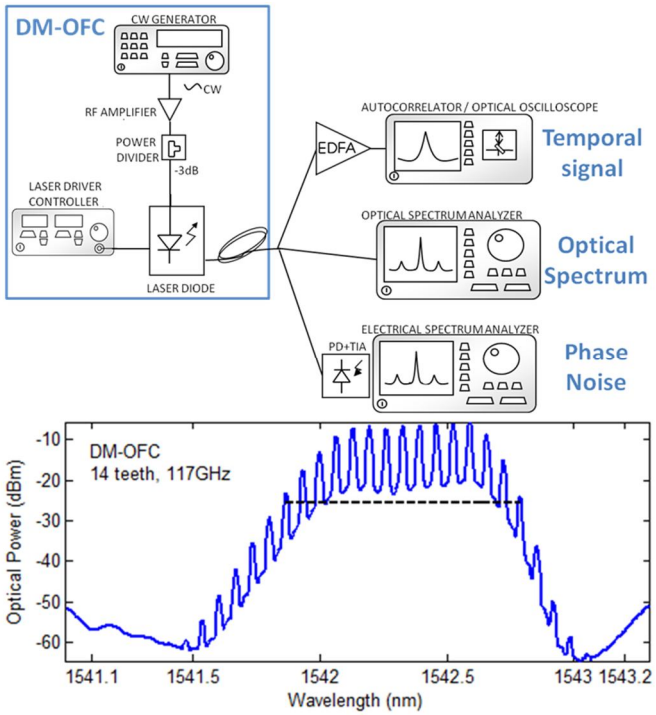

Fig 20. Top: Set-up used for the DM-OFC and measurement equipment. Bottom: DM output under Gain Switching obtained at 25 ºC, 61mA, 8.3GHz, 28dBm. The DM-OFC has 14 teeth in the 20dB span which corresponds to 117GHz. The 20dB span is marked with a dashed black line. See text for more details.

To obtain the DM-OFC shown in Fig 20, the laser is biased at 61mA and temperature stabilized at 25ºC with the use of a Laser Driver Controller. In order to enter the GS regime, very high modulation power is needed so we amplify the 8.3GHz RF signal

with an amplifier and then 28dBm are entered into the DM device. In Fig 20, we show the broadest comb achieved with the DM in terms of its 20dB optical span, which is 117GHz and corresponds to 14 teeth. Besides, the comb obtained presents a flatness of 0.57 in the 3-20dB ratio and a dynamic range of 55dB. More information in the optical span of this comb varying the RF frequency is shown in Appendix 2. The connections with the equipment used for the measurements are also plotted in Fig 20. As was described in Chapter 3, and Optical Spectrum Analyzer (OSA), an Electrical Spectrum Analyzer (ESA) and an Autocorrelator are used for the temporal and spectral characterizations. Before the autocorrelator an EDFA is needed to increase the optical power to values above 10dBm. Before the ESA, we detect the optical signal and amplify the resulting electrical signal using a Photodiode (PD) and a Transimpedance Amplifier (TIA).

The optical autocorrelation trace of this DM-OFC is shown in Fig 21. We see in the figure that the trace is not clean probably due to the limited amount of power entering the autocorrelator. This autocorrelation pulse has a temporal FWHM duration of 46.5ps, so assuming a profile sech^2, our pulse is 22.8ps FWHM long. As we have explained, the pulses generated with GS are chirped and we checked this computing the ideal pulse FWHM related to the optical spectra that is 9.2ps, much lower value than the measured one. The TBP_{rms} is 9.2, far from the fundamental limit (0.5). It is noteworthy that the shape of the GS pulses obtained using the DM device is less complex and closer to an ideal sech^2 shape than the shape obtained using other LD technologies, such as DFB lasers [65]. However, they are particularly chirped as their large TBP_{rms} suggests.

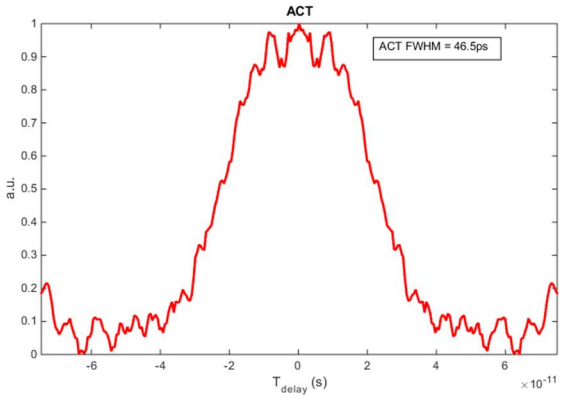

Fig 21. DM-OFC: Temporal autocorrelation pulse

Lastly, we show the phase noise of the electrical signal detected in Fig 22. The DM-OFC PN is shown in the red trace (called GS-OFCG), the Reference CW source is the green line and the DANL is the blue curve. Comparing the traces we observe that the phase noise of both the Reference and the DM-OFC have similar levels in most of the range. From 5KHz, the DM-OFC slightly increases its noise level compared to the Reference and is up to 7dB higher when it reaches 10KHz frequency offset. This similarity between both curves indicates a high phase correlation between the different frequencies that forms the DM-OFC as the noise is not degraded along the system.

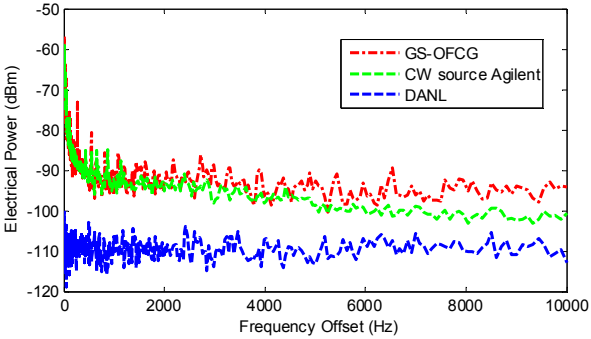

Fig 22. DM-OFC: Phase Noise of the electrical detected signal

As a conclusion DM LDs have nice features for OFC generation as they enter into the GS regime at frequencies close to 10GHz obtaining quite flat combs around 100GHz broad in the 20dB span. We also observe the autocorrelation pulses even when the output is chirped and we extract from the PN measurement that the teeth in the comb are highly phase correlated. For all this, DM LDs have already been used for OFC obtaining attractive results like the ones already referenced ([12], [66]).

6. Vertical-Cavity Surface-Emitting Laser OFCs: VCSEL-OFC

Vertical Cavity Surface Emitting Lasers (VCSELs) are Laser Diodes (LDs) that offer some important features due to their ability to emit the light vertically, perpendicular to their semiconductor layers [28], [135]. VCSELs are cost effective devices, small in size and easy to integrate with high modulation bandwidth and they had not previously been used for OFC generation. Then, they potentially offered broad range of tunability for the Gain Switching (GS) operation, cost efficiency and energy efficiency. VCSELs evaluation for OFCs generation is developed in this chapter. Here we present, the broadest comb obtained using VCSEL technology under GS, which we call VCSEL-OFC. As mentioned, we show the optical spectrum, the temporal optical signal and the phase noise of the electrical detected signal. This result is the seed comb, whose expansion and optimization is detailed in the upcoming chapters of this document.

In order to obtain this optimum comb, shown in Fig 23, an extensive study with two VCSEL samples (VCSEL#1 and VCSEL#2) was previously done, covering their static and dynamic characterization and also their GS behaviour, which are shown in Appendix 1, Appendix 3 and in this chapter. The study has been performed in two different VCSEL devices to check the consistency between samples, as it was their first time working under GS for comb generation. The characterization showed that both samples have similar parameters and the main difference between units is the board for the signal coupling: VCSEL#1 has a board that was designed at the beginning of our research studies (Fig 57) while VCSEL#2 was provided already

connected to a board made by the manufacturer of the device (Fig 58). In any case, we checked that, provided that the actual RF injected power is the same for both samples, the difference was not significant regarding the comb generation. Then, as the S11 and S21 parameters show a better RF performance in VCSEL#2 with a flat response (see Fig 68 to Fig 71), we continued our research using this second sample.

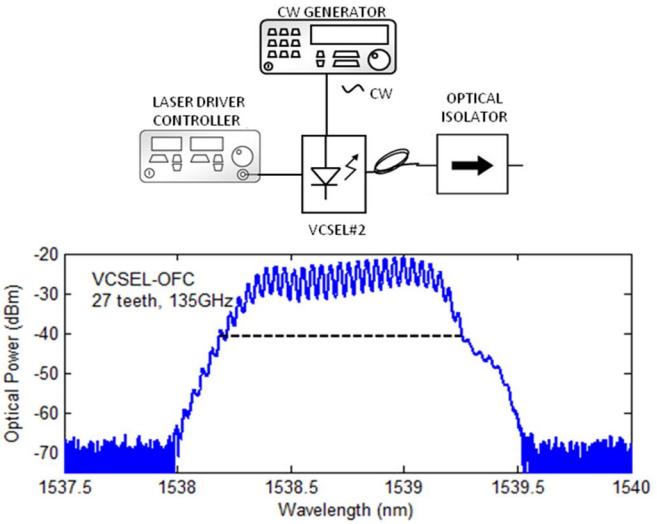

Fig 23. Top: Set-up used for the VCSEL-OFC. Bottom: VCSEL output under Gain Switching obtained at 20 ºC, 11.4mA, 5.2GHz, 16dBm. The VCSEL-OFC has 27 teeth in the 20dB span which corresponds to 135GHz. See text for more details.

This VCSEL#2 has a threshold current of 2.2mA and a slope efficiency of 0.1mW/mA and a modulation bandwidth around 7GHz, as we expected from the datasheets. The behavior of

VCSEL#1 in the GS regime and its chirp characterization is shown in Appendix 3 and the GS behavior of VCSEL#2 corresponds to the VCSEL-OFC presented up in this chapter.

To induce the GS regime that provides the OFC in Fig 23, VCSEL#2 is operated maintaining the bias current at 11.4mA (Ibias/Ith = 5.2) and the temperature stabilized at 20ºC. When the RF power entering the VCSEL is 15dBm (Irf/Ibias = 2.2) at 5.2GHz, we obtain the previously shown comb, which is the broadest and the one that will be used as seed comb in the following chapters, in order to expand it and optimize it. We see that in this set-up (compared to the DM-OFC set-up in Fig 20) the RF amplifier is not needed, because VCSELs needs much lower RF power to enter the nonlinear modulation regime (15dBm vs. 28dBm). The VCSEL-OFC has a 20dB span of 135GHz which corresponds to 27 teeth. Besides, the comb in this case presents a flatness of 0.77 for the 3-20dB ratio which is a high value for a directly generated comb by GS, compared for instance, to the DM-OFC.

The temporal autocorrelation profile of the VCSEL-OFC is presented in Fig 24, measured in the autocorrelator as explained in Chapter 3. These autocorrelation trace corresponds to a pulse FWHM of 14.4ps and a TBP_{rms} of 3. Besides, the VCSEL-OFC autocorrelation trace shows a pedestal at half height as it typically occur in pulses generated with GS due to the complex phenomena inside the VCSEL cavity under this large nonlinear modulation regime [131]:

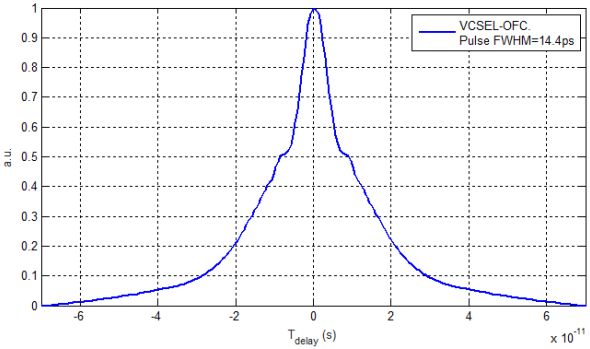

Fig 24. VCSEL-OFC autocorrelation trace. Assuming sech² profile, the pulse width is 14.4ps

Lastly, the phase noise of the electrical detected signal is shown in the following picture. Similarly to the result in the previous chapter, we see that the phase noise of both the Reference (CW source and green line) and the detected signal (VCSEL-OFC and red line, called GS-OFCG in the figure) have the same behaviour at low frequencies. On the other hand, for higher frequency offsets, above 5KHz, the noise floor is slightly higher up to 7dB. As we already observed in the previous chapter with the DM-OFC, both the Reference and the comb curves are very similar which means high phase correlation between modes in the comb created with GS. This means that the stability of the RF source is inherited by the comb lines, which is one of the advantages of using GS for the OFC generation.

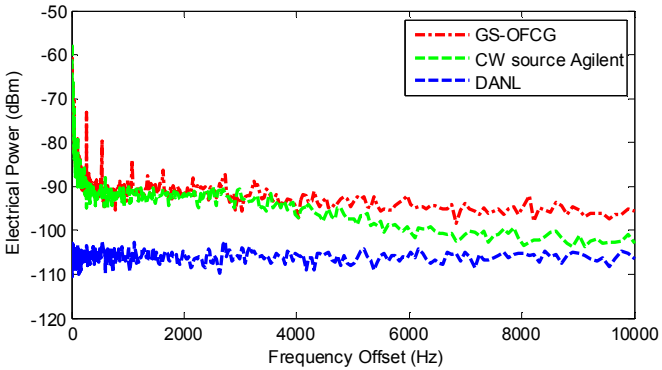

Fig 25. VCSEL-OFC: Phase Noise of the electrical detected signal

To conclude this chapter, it has been checked that VCSELs provide broad optical combs, up to 135GHz with a distance of 5.2GHz between comb teeth. Compared to other LDs, the most remarkable feature is the low energy need, of only 11.4mA bias and 16dBm RF input power. They are also smaller in size and easier to be integrated. All this, together with the fact that the comb is also broader, makes VCSELs a relevant LD source to be used in the implementation of COTS versatile and straightforward OFCs systems with high energy and cost efficiency.

Main disadvantages are found in the power emitted, which is not high but can be solved using amplification and also in the distance between comb lines, which is limited by the modulation bandwidth of the VCSEL. This bandwidth does not reach the 10GHz with optimum performance, so 5.2GHz is the selected frequency for the RF modulation.

On the other hand, the use of GS modulation allows the comb generation with no need of extra components and tunable distance between comb lines, independently of the LD used. It also inherits the phase noise of the reference signal, as the whole comb is generated inside the laser cavity.

As conclusion, these VCSEL-based OFCs generated with GS are versatile systems up to 135GHz broad with low energy and cost needs and high phase correlation between teeth. Some applications of OFCs need broader combs above 300GHz, so our efforts continue trying to increase the optical span of these VCSEL-based OFCs.

Related publication: Paper A

This VCSEL-OFC can be directly applied to high-quality and energy-efficient sub-Terahertz generation up to 120GHz. We published about this issue in Electronics Letters in July 2013. In that work, we show a photonic system to generate an 88.2GHz tone generated by Difference Frequency Generation of two comb teeth that were selected from the VCSEL-OFC. This tone has excellent long-term stability and a linewidth lower than the measurement instrumentation capabilities.

Abstract: In this work we present a simple and energy-efficient photonic system to generate continuously tunable, low phase noise, sub-THz waves based on COTS components. The optical scheme is based on the use of a commercial Vertical Cavity Surface Emitting Laser (VCSEL) under gain switching (GS) modulation that provides a very flat optical frequency comb

generator (OFCG) with 23 modes in a 20 dB bandwidth. The laser only needs 15 dBm Continuous Wave (CW) Radiofrequency (RF) input power and 9 mA of bias current to provide this OFCG. Two Optical Injection Locking (OIL) stages filter and amplify the two desired modes that are detected in a photodiode to produce the desired sub-THz signal at the frequency difference of these two selected modes. As an example, in this work we demonstrated the generation of a very stable 88.2 GHz tone with lower linewidth than 10 Hz using a reference of 4.2 GHz to generate the OFCG.

For more information in this work see Paper A [57].

7. OFCs comparison of laser technologies

In this section, the combs explored in the two previous chapters are compared to see the differences between the technologies related to the optical frequency combs generated. In Table I (page 132), we find a compendium of all the main features in combs for each of the OFCs presented along this document. The two first columns of the table correspond to the DM-OFC and the VCSEL-OFC presented in this section. However, these parameters are repeated here and analysed in the following paragraphs.

The bias current for the optimum GS response is much higher in DMs, 61mA, than in VCSELs, 11.4mA. In both cases the devices are stabilized at 20°C. Also the RF power needed to enter this GS regime is much higher for DMs, 28dBm vs 15dBm in the VCSEL. This is the expected result taking into account the PI curves in the appendixes and it is one of the main advantages of using VCSELs for OFC generation: its energy efficiency is much higher due to its smaller size so we can achieve comparable combs with much lower power. On the other hand, the disadvantage of it is the optical power emitted, that is lower too.

The optimum RF frequency depends on the cavity of the laser and the RF coupling in the mounting board in which the laser is soldered. Concerning the laser technology, the modulation bandwidth depends on the relaxation frequency and the damping parameter [136]. Comparing the optical span, we observe that the results are close to each other in terms of 20dB span even when the optimum frequency in the VCSEL-OFC is

lower, 5.2GHz, than the one in the DM-OFC, 8.3GHz. The 20dB span is 135GHz/27 teeth in case of the VCSEL-OFC and 117GHz/14teeth for the DM-OFC. This means higher nonlinearities with the GS modulation in the VCSEL, causing higher number of teeth that compensates for the shorter distance between them. Moreover, we are obtaining similar bandwidth but a significantly higher number of teeth with much less RF power. This makes VCSELs a really interesting technology to take into account when building efficient OFCs as we are focusing on a broad optical span trying to reduce the energy consumption. The flatness is also significantly improved with the use of the VCSEL source, with a flatness factor of 0.77, in respect to the DM one, of 0.57. Lastly, the DR is similar in both samples but slightly higher (thus, better) in the DM source of 55dB compared to 50dB in the VCSEL-OFC. This difference is associated to the lower power emitted by the VCSEL unit.

Regarding the phase noise measurement we cannot really appreciate any difference between sources. The coherence between teeth is more related to the GS regime itself than the source selected, because we observe the same tendency using both LD sources. Then, GS has been proved to be a nice technique to obtain seed combs with high phase correlation between teeth that will also improve the quality in a potential subsequent comb expansion outcome.

The pulse quality is also improved for the VCSEL-OFC with respect to the DM-OFC. Even when this is not a main aspect in our focus it is important to see the differences. The pulse FWHMs obtained with the autocorrelation measurement are 14.4ps and 22.8ps for the VCSEL and DM combs respectively. The difference becomes higher if we compare the TBP_{rms}, with

factors 3 for the VCSEL-OFC and 9.2 in the DM-OFC. This means that the DM pulses are more dispersed or chirped. Therefore, the pulse quality is significantly improved when working with VCSELs. However, the DM pulses are closer to an ideal shape, without significant pedestals or substructures.

Lastly, the energy consumption is estimated by computing the power needs for both the CW and RF supplies. Naturally, the VCSEL consumption is enormously lower of 0.05W compared to the 0.84W needed to make the DM enter the optimum GS regime.

As conclusion, VCSEL-based OFCs generated with GS are interesting systems to be used as they provide broad span with significantly lower energy consumption and higher pulse quality compared to other LD technologies like DMs. Besides, the phase coherence among comb teeth is high in both cases, due to the GS modulation used for the generation. The maximum achieved span is 135GHz, which is remarkable but still limits the use in some applications that need broader spans. Therefore, it will be interesting to use the VCSEL-OFC as seed comb to be expanded afterwards if the quality and low energy consumption are kept. The next section of this report addresses this issue by adding different nonlinear expansion stages.

VCSEL-based OFC expansion

Previously, the interest of VCSELs for OFC generation was covered as they offer broad and highly coherent combs with a few mW of power supply. However, many applications need broader combs. . This why we focused our efforts in the increase of the optical span of VCSEL-OFCs while maintaining high coherence between comb teeth and high energy efficiency. This study is detailed in this section, VCSEL-based OFC expansion, implementing different comb expansion schemes based on different nonlinear elements like **Electro-optical (EO) Phase Modulators (PM)** in Chapter 8, **High Nonlinear Fibers (HNLF)** in Chapter 9 and **Nonlinear Optical Loop Mirrors (NOLM)** in Chapter 10. They exploit different nonlinear optic effects to accomplish the increment of the initial VCSEL-OFC span. All of them offer expansion ratios close to 3 times. Then, we combine the set-ups based on PMs and HNLF to obtain our record comb in terms of its 20dB optical span, which is **increased up to 1THz broad**, in Chapter 11. Finally, and as a summary, **all these implementations are compared and their parameters are collected** in Chapter 12.

8. Expansion with EO Modulators: EO-OFC

Apart from direct comb generation, like GS regime, where the comb is generated inside the laser cavity, there exist techniques in which the comb is created after the light has been emitted from the laser source working in CW operation, using external devices. As mentioned in page 42, we refer to these schemes as indirect comb generation techniques. The most common indirect technique for comb generation is based on the use of Electro Optical (EO) modulators. However, we mainly use them in this work to expand an incoming signal which is already a comb, the VCSEL-OFC, with two EO Phase Modulators (PMs).

In a first step of this work, three different approaches are compared: direct comb generation (VCSEL under GS and no modulators) already shown in Chapter 6; indirect comb generation (VCSEL continuously emitting and two PMs for the generation); and lastly comb expansion (VCSEL under GS and two PMs for the expansion), also called combined comb in the published article that covers this study [20]. In a second step of this work, two different but more powerful modulators are included to enhance the comb expansion. The main advantages of these devices are the lower Vpi and the higher modulation power capabilities, increasing the optical span up to 3 times the initial seed comb. Only for this last approach, in the second part of this chapter, detailed information on the system is presented.

I. Direct generation, indirect generation and comb expansion with EO modulators

The first approach for comb expansion with EO elements is based in the use of two phase modulators (3dB bandwidth up to 10GHz, Vpi=3V typ) from Thorlabs. The set-up implemented is shown in Fig 26:

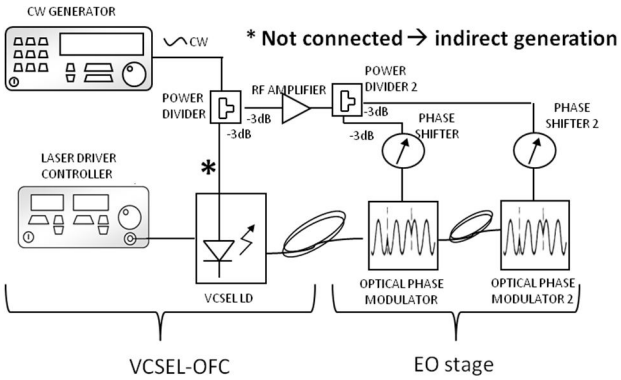

Fig 26. Set-up used for the EO-OFC. It consists of two subsystems. Left: VCSEL-OFC based on a VCSEL source under Gain Switching. Right: EO stage based on two optical Phase Modulators. The EO-OFC connects both subsystems in cascade linking them with the same RF modulating signal. See text for more details.

In this experiment, three different approaches for comb generation are compared: direct generation, indirect generation and combined generation. The latter is also referred as comb expansion because the modulators expand the incoming VCSEL-OFC generated in the direct generation. This experiment is performed with the first VCSEL sample, VCSEL#1 and also with the DM laser, whose results are shown in Appendix 4.

In Fig 26 the set-up developed for the present work is shown. It consists of two different optical subsystems. The first one is the direct Gain Switched VCSEL-OFC. When the GS regime is induced, the injected RF power into the laser is 15dBm at 5.2GHz and the bias current is 11.4mA to offer the best OFC performance. The second subsystem is the EO stage composed of two Electro-Optic phase modulators (PMs).

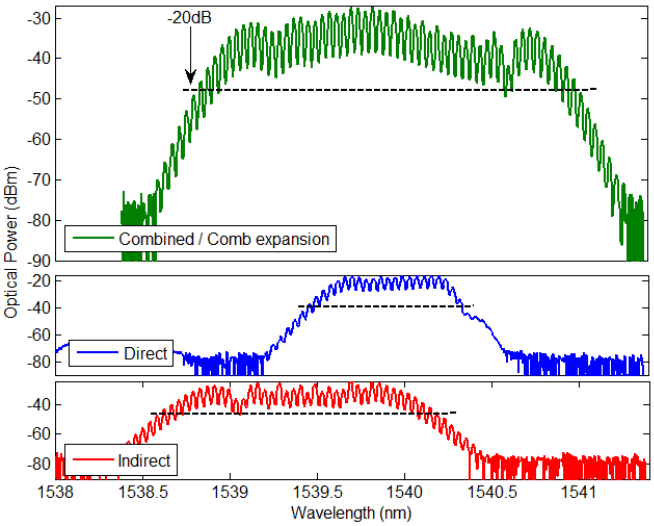

Fig 27. a) Combined set-up in which the VCSEL generates a comb which is expanded in the modulators. It has 53 teeth which corresponds to 272GHz.b) VCSEL-OFC, direct generation with the VCSEL output under Gain Switching. c) Indirect technique where the VCSEL emits in CW and the comb is generated in the PMs. It has 38 teeth in the 20dB span which corresponds to 193GHz. See text for more details

The use of two PMs and no Intensity Modulator (IM) was chosen after evaluating different configurations: while fewer components imply lower expansion, the use of a third

modulating element did not increase the optical span and made the set-up more complex and difficult to adjust in the RF part. On the other hand, the use of an IM did not enhance the flatness significantly in out experiment but implied some losses along the optical path. An RF power of 28dBm is needed for each external modulator to work under optimum conditions (wider span of the resulting comb). Hence, a high power RF amplifier is included. Phase matching between this modulating signals and the optical signal entering the modulators is critical, so a phase shifter is needed before their RF inputs and requires fine tuning to optimize the resulting comb. The simultaneous operation of the two subsystems described before permits the experimental evaluation of the Combined-OFCG technique using VCSELs. The same RF source signal is split to induce the GS regime in the VCSEL with 15dBm and to modulate each modulator with 28dBm, bounding the subsystems together.

In Fig 27 the three resulting combs are compared. The output of the VCSEL in the direct approach has a 20dB span of 106GHz (21 teeth), and with the indirect technique the 20dB span rises up to 193GHz (38 teeth). Finally, the combined approach generates the broadest comb with a 20 dB span of 272GHz (53 teeth).

As a conclusion, the generation of optical combs based on VCSEL diode lasers offers better results when the GS and the EO stages are combined: the advantages of both techniques add up to offer a broader comb. Only the energy efficiency decreases with respect to the GS generation. Also, the advantages of the inclusion of GS to enhance the comb both in the overall number of modes but also in the increase of the phase coherence between comb lines [20].

II. Comb expansion enhancement: EO-OFC

In a second approach to this comb expansion based on EO elements the previously combined configuration is implemented but the modulators are replaced by two more powerful PMs: ultra-Low-Vpi and 10Gb/s phase modulators from the company EOSpace with enhanced RF coupling, we aimed to increase the comb span compared to the previously presented in this chapter. This comb, called EO-OFC, is our best result with EO elements and here we present detailed information on it. The set-up is shown in Fig 28: the output of the laser under GS, the VCSEL-OFC in Fig 23 (20 ºC, 11.4mA, 5.4GHz, 15dBm) enters two PMs with Vpi <3.3V placed in cascade configuration. The RF signals driving them (5.4GHz) are first amplified up to 35dBm and then matched using Phase Shifters (PS) so the expansion is optimized. Finally, the output signal is amplified in the EDFA to increase the signal level to 12.5dBm. It is important to notice that this EDFA is not necessary in the set-up to expand the comb but to increase the signal to a similar power level compared to the subsequent optical combs.

With this technique, that combines GS and high performance EO modulators, the comb is expanded a factor 2.96 which means 80 teeth in the 20dB span, so 427GHz broad taking into account that the RF signal is set at 5.3GHz. This comb is clearly very flat, with a flatness factor of 0.87 and a dynamic range of 28.8dB.

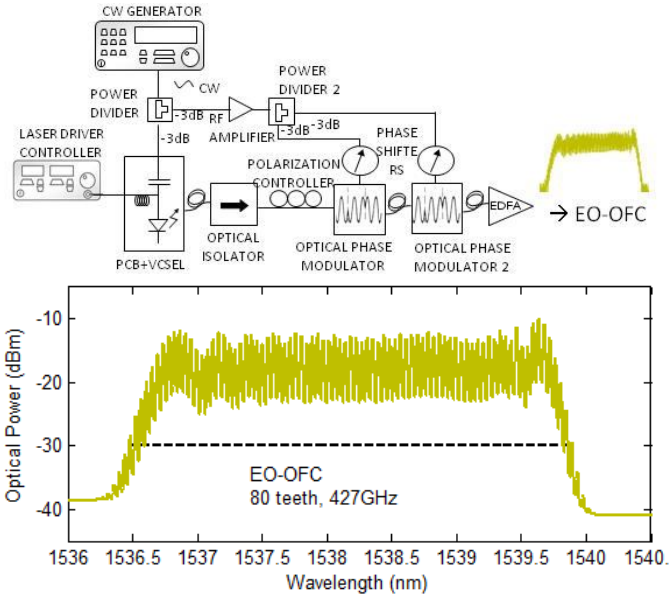

Fig 28. Top: Set-up used for the EO-OFC: The VCSEL-OFC is broadened with two phase modulators in cascade. The RF signal is amplified and matched with the use of one amplifier and two phase shifters. Bottom: The EO-OFC (yellow trace), has 80 teeth in the 20dB span which corresponds to 427GHz. The VCSEL supply parameters are 20 ºC, 11.4mA, 5.4GHz, 15dBm. The RF injected into the modulators is 35dBm and the EDFA has an output power of 12.5dBm. See text for more details.

The temporal autocorrelation of this EO-OFC is shown in Fig 29 and is also compared to the VCSEL-OFC profile. The pulse FWHM durations are 14.4ps for the VCSEL-OFC (already shown in Fig 24) and 11.4ps for this EO-OFC. Even when the pulse is shorter in the EO-OFC system it is important to realize that this does not necessarily mean lower dispersion of the different frequencies that conforms the pulses. On the contrary, the TBP_{rms} are 3 and 7.2 for the VCSEL-OFC and EO-OFC, respectively. This implies

that the EO-OFC scheme broadens the comb but also increases the dispersion in the pulse, induced by the EO modulators. As mentioned, all these parameters are collected in Table I (page 132).

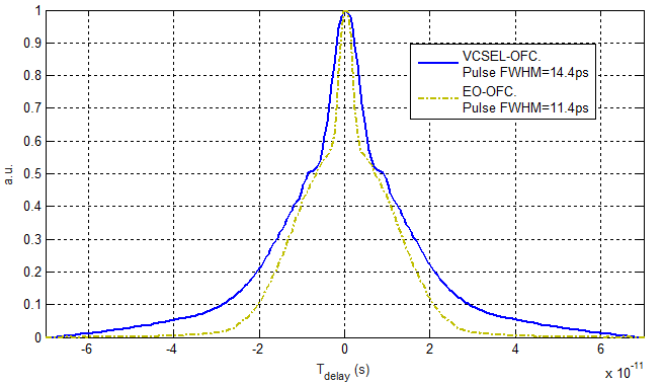

Fig 29. EO-OFC: Temporal autocorrelation pulses. Assuming sech² profile the pulse width is 14.4ps for the VCSEL-OFC (blue trace) and 11.4ps for the EO-OFC (yellow trace). This second pulse is shorter but as the optical spectra is broader this result is related to higher dispersion as we see with the TBP parameter. See text for more details.

Lastly, in Fig 30 we show the phase noise of the electrical detected signal at the modulation frequency (5.4GHz in this scheme) and compare it to the reference (CW source) and to the VCSEL-OFC PN. In the figure, we observe that all these signals have the same decay up to 300KHz but from that frequency the level is a little higher than the reference one. The carrier power when taking this measurement was low and then we observe the traces plotted very close to the DANL, and the curves are noisier than in other measurements of the PN. The EO-OFC is the highest one but the difference among the systems is only

about 2dB. This is consistent with the previous result in which we concluded that the dispersion is increased with the inclusion of the PMs in the set-up, and this dispersion is also related to less phase coherence among the teeth in the comb.

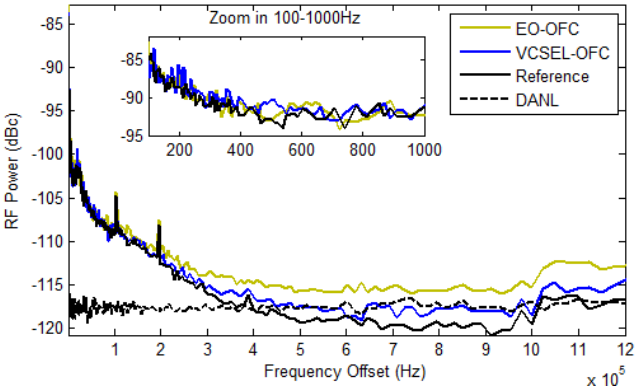

Fig 30. EO-OFC: Phase Noise of the electrical detected signals. EO-OFC (yellow trace), VCSEL-OFC (blue trace), Reference (black trace) and DANL (black dotted trace). The Reference is the CW source signal used for modulation directly detected and the DANL is the equipment noise level. See text for more details.

More information on this result is found in Chapter 12, where we see all the combs presented in this section and compare their main features.

Related publication: Paper B

The comparison of the three techniques (direct, indirect and combined) for VCSEL-based OFCs generation shown in the first section of this Chapter was addressed in an article published in the Photonic Technology Letters in September 2014. With this work we checked that the generation of optical combs based on VCSEL diode lasers offers better results when the GS and the EO techniques are cascaded because the advantages of both techniques add up to offer a 150% wider comb than the sole VCSEL under GS. Besides, the GS modulation links the RF modulating source along the whole set-up presenting higher teeth coherence and stability than the purely indirect approach. At the same time, it is energy efficient thanks to the selection of a VCSEL diode laser that only needs a modulation of 15dBm to generate the comb.

Abstract: In this work we explore the performance of Optical Frequency Comb Generator (OFCG) sources based on Vertical-Cavity Surface-Emitting Lasers (VCSELs) diodes. Direct Gain Switching (GS) technique, indirect Electro-Optical (EO) technique and the combination of both have been experimentally evaluated. We have observed that this later combination gives birth to an enhanced OFCG that offers a tunable improved comb in terms of frequency span, flatness and coherence with respect to the sole EO approach, as it partly inherits the high efficiency qualities of the GS-OFCG while offering a wider span.

To see the full information visit Paper B [20].

9. Expansion with nonlinear fiber: HNLF-OFC

Apart from EO elements there are some other nonlinear components that can be used for comb expansion like those related to third order susceptibility ($\chi^{(3)}$). This includes optical fibers (especially Highly Nonlinear Fibers) and, recently, microresonator devices [17]. These elements are monolithic external resonant cavities that generate wide optical combs at a fixed frequency spacing (tens to hundreds of GHz) and have a strong dependence on the optical input power. The method described in this chapter to expand the VCSEL-OFC consists on the use of a Highly Nonlinear Fiber (HNLF). These schemes mainly exploit the enhanced Self Modulation Effect (SPM) [99] exhibited by HNLF fibers and have been commonly used for comb expansion and broadband signal generation [18], [88], [101]. To control the peak power of our pulses and compensate their initial dispersion, we condition the optical signal including a Dispersion Compensation Fiber (DCF) and an EDFA. With the DCF we linearly compress the pulse from the VCSEL-OFC as they are chirped because of the GS regime [136].

In our implementation, the DCF fiber has a dispersion of -1318ps/nm, a length of 1100m and reduces the optical pulse duration (Full Width Half Maximum, FWHM) thus reducing the dispersion and getting closer to the ideal pulse. Then the EDFA increases the optical power up to 22dBm (mean power) before entering into the HNLF with 200m long and a nonlinear coefficient of γ=11 $(W \cdot km)^{-1}$. The broadest comb is obtained with a VCSEL at 20ºC and with bias current of 13mA, while the

modulation remains at 15dBm at 5.2GHz. This expansion scheme is shown in Fig 31.

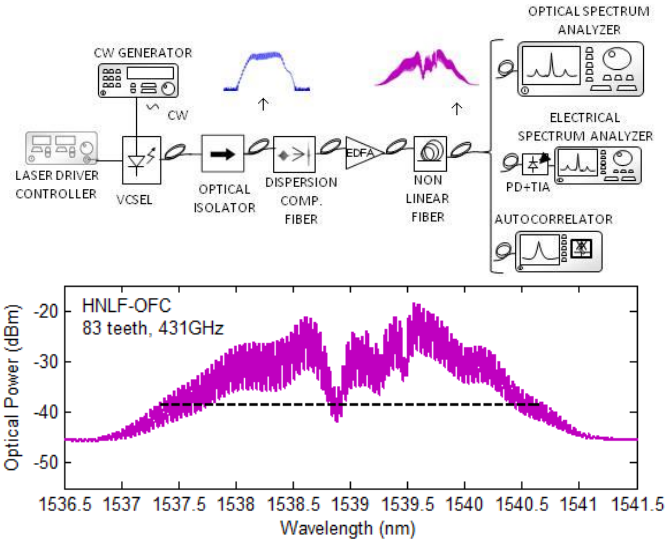

Fig 31.Top: Set-up used for the HNLF-OFC: In the picture we see the VCSEL which is first compressed with a DCF, secondly amplified with an EDFA and then broadened with a HNLF. Bottom: The HNLF-OFC (pink trace), has 83 teeth in the 20dB span which corresponds to 431GHz. See text for more details.

The OFC obtained with this scheme has a 20dB optical span of 431GHz which corresponds to 83teeth in the comb and an expansion factor of 3.07 times the VCSEL-OFC. However, the result is not flat: the flatness factor is only 0.12 in this case. The dynamic range is 25.3dB, so the noise floor is close to the useful optical span.

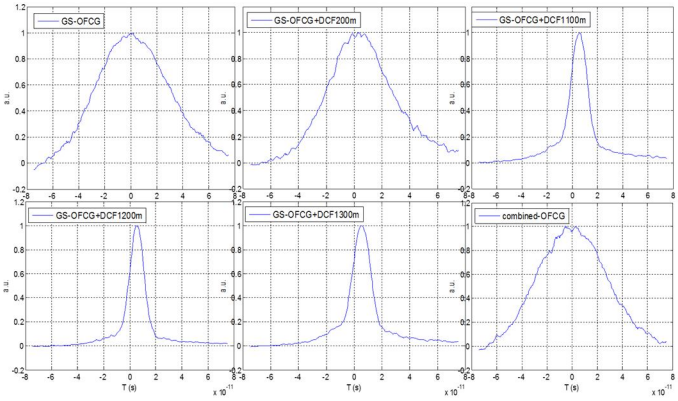

Fig 32. Temporal autocorrelation pulses with and without DCF, for different DCF lengths. The shorter pulse is obtained for a DCF of 1100m long

In Fig 32 we observe why an 1100m long DCF is used as it is the length that most decreases the pulse FWHM, so with 1100m of DCF the pulses are the closest to their TBP limit. The autocorrelation of the pulses correspondent to the VCSEL-OFC in Fig 23 (GS-OFCG), the combined-OFC in Fig 27 (combined-OFCG), and the VCSEL-OFC together with different DCF lengths (200m, 1100m, 1200m and 1300m). Other fiber lengths were also evaluated and the shortest pulse was obtained with an 1100m long DCF (upper right trace).

On the other hand, we have measured the temporal autocorrelation traces of the pulses out of the DCF and the HNLF. They are shown in Fig 33, where they are compared to the trace of the VCSEL-OFC already seen in previous sections.

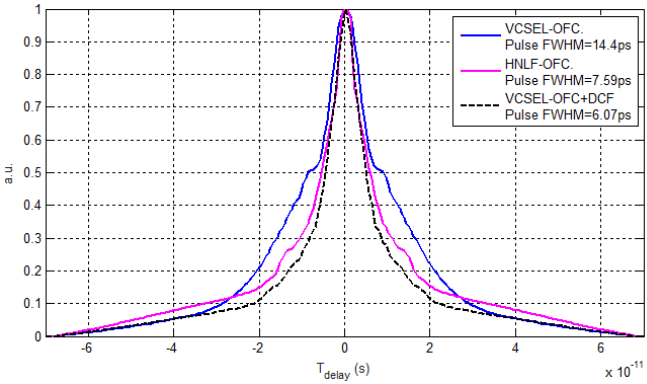

Fig 33. HNLF-OFC: Temporal autocorrelation pulses. Assuming sech² profile the pulse width FWHM are 14.4ps for the VCSEL-OFC (blue trace) and 7.59ps for the HNLF-OFC (pink trace). This second pulse is shorter and present pedestals around 0.25 and not at half height like the VCSEL-OFC. The pulse at the output of the DCF is also shown where we observe that it is the shortest and has no pedestals. See text for more details.

The autocorrelation trace at the output of the DCF is also shown and we can see that the pulse is remarkably compressed along it. We observe how the pulse is compressed also in the HNLF related to the one in the VCSEL's output and also its shape is closer to an ideal $sech^2$. The pedestals at half height are not present but we see some pedestals around the 0.25 area. The pulses after the HNLF are shorter with a FWHM of 7.59ps, but a little higher than the ones at the output of the DCF, of 6.07ps. Even with this shorter pulse, the TBP_{rms} is 10.22, which is significantly higher than the VCSEL-OFC's, 3. This means that the final pulses are highly dispersed.

The PN of the electrical detected signal at 5.2GHz is shown in Fig 34. We see that both curves, the VCSEL-OFC one (blue trace) and the HNLF-OFC (pink trace) follow the same decay. They are

almost the same and a little higher than the reference (black trace). However, if we zoom in (see figure inset) the HNLF-OFC is slightly higher, with less than 2dB difference. We can expect that the phase correlation among the teeth in the comb is similar in the VCSEL-OFC and the HNLF-OFC.

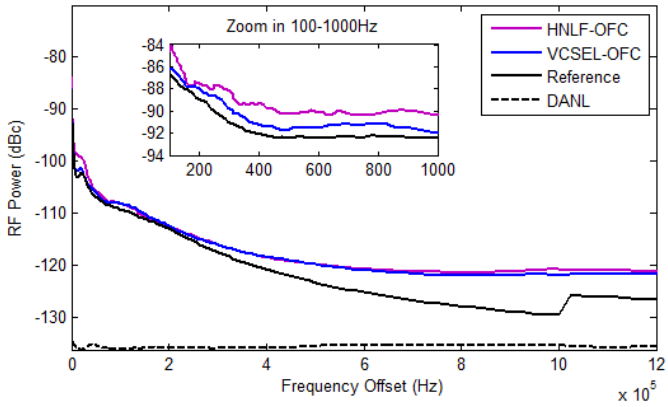

Fig 34. HNLF-OFC: Phase Noise of the electrical detected signals. HNLF-OFC (pink trace), VCSEL-OFC (blue trace), Reference (black trace) and DANL (black dotted trace). The Reference is the CW source signal used for modulation directly detected and the DANL is the equipment noise level. See text for more details.

As conclusion, the HNLF-OFC system allows us to broaden the optical seed comb (VCSEL-OFC) around 3 times in an easy way, by adjusting the fiber lengths and the EDFA as the only active element. The phase coherence in the teeth is close to the initial one and the main parameter which is worsened is the flatness. In the following chapters we will address other expansion techniques and they will all be compared at the end of this section.

10. Expansion with NOLM: NOLM-OFC

Nonlinear Optical Loop Mirrors (NOLM) are optical loops based on fiber Sagnac interferometers to induce Self-Phase Modulation (SPM). Inside the loop, the optical signals travelling clockwise and counter clockwise suffer the nonlinear effects differently and both signals interfere with different phases [107]. NOLMs are commonly used for pulse compression and reshaping, comb filtering, and switching or multiplexing optical signals in communication [100], [104]–[106]. In this section, we propose this technique to expand the comb, focusing therefore on the optical spectral broadening achieved as it was previously done in [87], [111].

Several set-ups have been tested for this work and our final loop includes a Semiconductor Optical Amplifier (SOA) as the main nonlinear element inserted into the loop [100]. These systems are also called Nonlinear Amplifier Loop Mirror (NALM) [109]. SOAs devices are interesting here due to their strong nonlinear operation, low power consumption, and small size [112]–[114]. In this chapter we show the system implemented and the spectral and temporal information of the comb achieved.

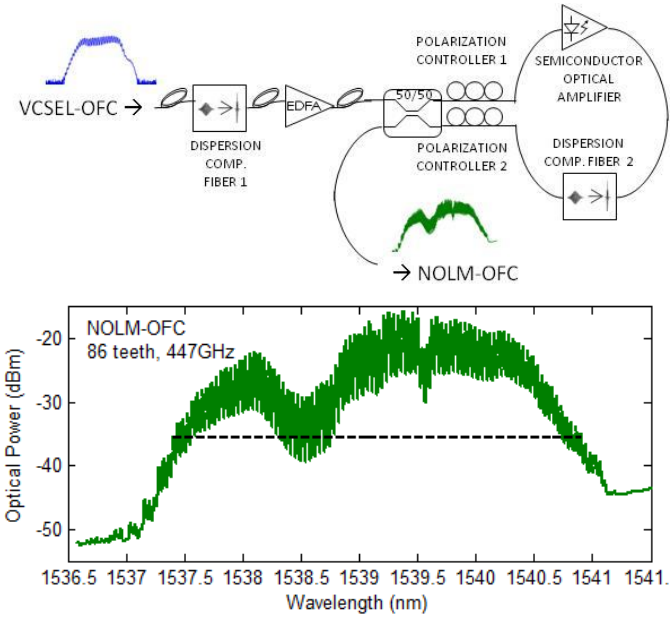

Fig 35. Top:Set-up used for the NOLM-OFC: The VCSEL-OFC is first compressed and then amplified with a DCF and an EDFA. The NOLM "door" is a 50/50 coupler and it has inside a SOA another DCF and two polarization controllers. Bottom: The NOLM-OFC (green trace), has 86 teeth in the 20dB span which corresponds to 447GHz. See text for more details

In Fig 35 we see the set-up used for this comb expansion based on a NOLM. Before the 50/50 coupler, that is the entrance and exit of this loop, the light signal is conformed using a DCF and an EDFA. The DCF is 600m long and it compresses the light pulse right before the EDFA so the peak power at the EDFA output is optimized. The output power of the EDFA in this set-up is 32dBm and higher powers cannot be applied because of operation limits for the SOA. Another DCF fiber with the same

characteristics is placed inside the loop, along with the SOA (QPhotonics QSOA-1550), and the best result has been obtained when this DCF has a length of 500m and the SOA is biased with 396mA. The set-up also includes two polarization controllers to match the clockwise and counter clockwise pulses making them interact in the way that we obtain the highest pulse compression and therefore, the comb broadening is optimized. In order to optimize the NOLM-OFC, the bias current of the VCSEL has been changed to 13mA and the RF frequency is 5.2GHz.

The output comb has a 20dB span of 447GHz which corresponds to 86 teeth and an expansion factor of 3.18. We can see that the noise floor has been increased to -50dBm so the dynamic range at this point is 37 dB and the flatness has been worsened too, presenting a flatness factor of 0.28.

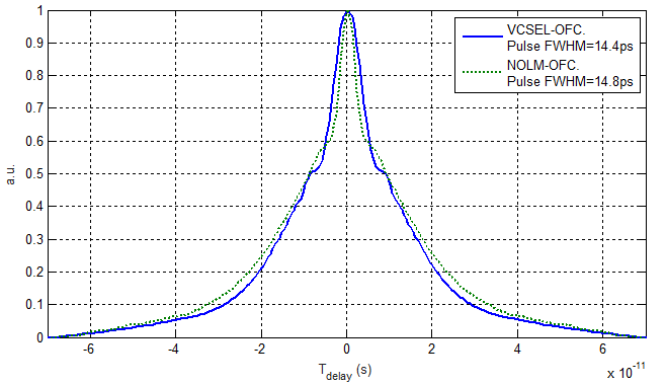

Fig 36. NOLM-OFC: Temporal autocorrelation pulses. Assuming sech² profile the pulse width is 14.4ps for the VCSEL-OFC (blue trace) and 14.8ps for the NOLM-OFC (green trace). Both pulses are very similar with small hips at half height. See text for more details.

On the other hand, we have measured the temporal autocorrelation trace of the pulses in the NOLM-OFC. This trace is shown in Fig 36 and compared to the trace of the VCSEL-OFC, already seen in previous sections. We observe that both traces are really similar, both in pulse duration and in shape. The FWHM is 14.8ps for this NOLM-OFC and 14.4ps for the VCSEL-OFC. Both autocorrelation pulses show small hips at half height which corresponds to pedestals in the pulse, typical shapes coming from GS pulses and NOLMs [131]. The TBP_{rms} associated to this comb and pulse duration is 8.8, which is significantly higher than the VCSEL-OFC's, 3.

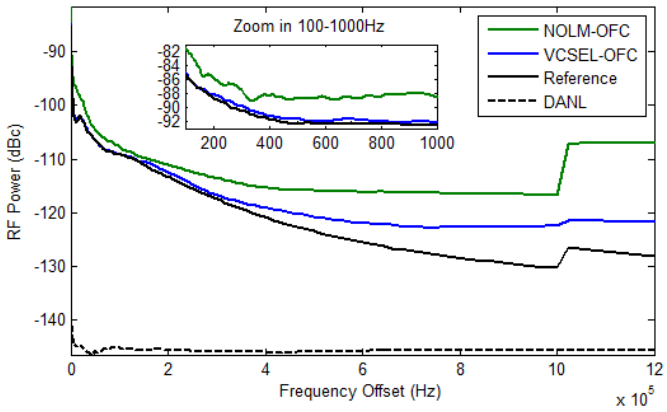

Fig 37. NOLM-OFC: Phase Noise of the electrical detected signals. NOLM-OFC (green trace), VCSEL-OFC (blue trace), Reference (black trace) and DANL (black dotted trace). The Reference is the CW source signal used for modulation directly detected and the DANL is the equipment noise level. In the inset we observe a zoom in the 100Hz to 1KHz range. See text for more details.

The PN of the electrical detected signal at 5.2GHz is shown in Fig 37. We see that the NOLM-OFC (green trace) curve is higher than the VCSEL-OFC one (blue trace) along the whole frequency range and follows a similar decay. However, the NOLM-OFC become constant at -112dBc while the VCSEL-OFC stabilizes at -120dBc both from 400KHz. They are both slightly higher than the Reference (black trace). However, if we zoom in (see figure inset) the NOLM-OFC is about 2-4dB higher than the VCSEL-OFC and the Reference, which decrease similarly up to 300KHz. The phase correlation among the teeth in the comb is, therefore, slightly worsened with the inclusion of this expansion system. We believe this is related to the use of an active device inside the loop, such as the SOA, that adds Amplified Spontaneous Emission (ASE) noise around the beat note.

To conclude, the NOLM-OFC system allows us to broaden the optical seed comb (VCSEL-OFC) around 3 times up to almost 450GHz with a very robust system. The components used are cheap and commercially available and the comb expansion is done by SPM insider a nonlinear Sagnac interferometric structure like a NOLM. The phase coherence in the teeth is slightly worsened and also the flatness. In the following chapters we will address other expansion techniques and they will all be compared at the end of this section.

11. Expansion combining techniques: EO&HNLF-OFC

In this chapter we present our latest results on the expansion of VCSEL-based OFCs using commercially available components. The result is a versatile, and compact comb architecture, that offers cost and energy efficiency. Up to now, the optical frequency span was the main limiting factor when comparing VCSELs with other laser technologies for OFCs, but here we present a breakthrough in this limit: we have obtained the broadest VCSEL-based optical comb, of 1THz (20dB) span, which is a record value to our knowledge. This comb has 193teeth in the 20dB span which corresponds to 9.1nm in wavelength. The distance between comb teeth is 5GHz and the overall power consumption of the components in the set-up is lower than 10W. However, with this configuration, the flatness of the comb and its dynamic range still leave room for improvement.

In our implementation, we have combined two of the previously presented expansion techniques: the EO-OFC and the HNLF-OFC in cascade configuration. We call EO&HNLF-OFC the resulting comb. The optical source starts with a VCSEL set at 20ºC and 11.4mA of bias current. The VCSEL's output is the VCSEL-OFC previously presented when the laser is operating in GS regime using a 16dBm tone at 5.4GHz (blue trace in Fig 38c), and has 27 teeth in the 20dB span that corresponds to 135GHz. This VCSEL-OFC enters the first expansion system with two PMs, obtaining the EO-OFC (yellow trace in Fig 38b), expanding the comb up to 80 teeth in the 20dB span that corresponds to 427GHz. This is the EO-OFC system described in this document in Chapter 8. Finally, the second expansion system is based on a HNLF like the

one described in Chapter 9. As we did in that chapter, before the HNLF we include a DCF to compensate the dispersion and an EDFA in order to increase the peak power of the pulse and enhance the nonlinear effects in the HNLF. In Fig 38 the complete set-up is shown, which is similar to the ones described to expand combs with different laser technologies in [18], [101].

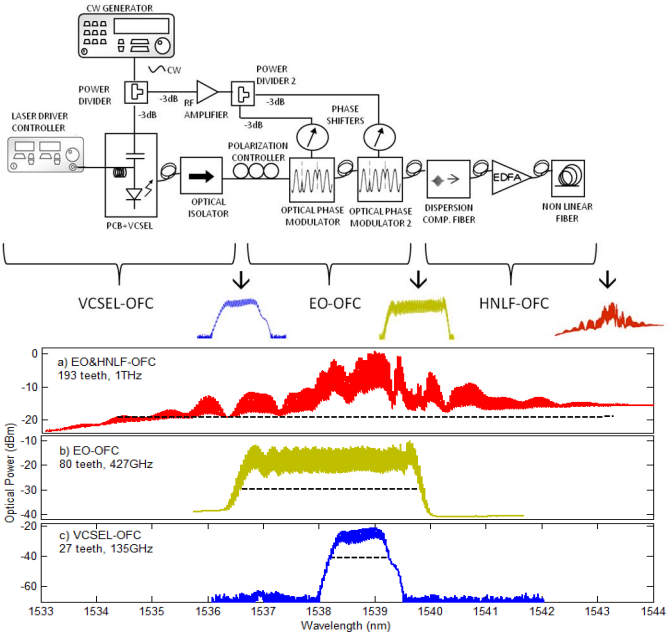

Fig 38. Top: Set-up used for the EO&HNLF-OFC: The VCSEL-OFC is the output of the VCSEL under GS regime. A first expansion stage called EO-OFC is formed by two PMs in cascade configuration. Then, the second expansion stage called HNLF-OFC is formed by a DCF, an EDFA and a HNLF and provides the 1THz broad comb called EO&HNLF-OFC Bottom: Optical Frequency Combs along the set-up: a) EO&HNLF-OFC (red trace) obtained at the output of the set-up, with 1THz (193 teeth) of 20dB span. b) EO-OFC (yellow trace) obtained at the output of the first expansion stage based on PMs, with 427GHz (80 teeth) in the 2dB span. c) VCSEL-OFC (blue trace) obtained at the output of the VCSEL under GS regime, with 135GHz (27 teeth) in the span. The VCSEL supply parameters are 20 ºC, 11.4mA, 5.4GHz, 16dBm. See text for more details.

Future work will be developed to analyze the coherence between the teeth in the comb and obtain the other parameters that we have presented for the previous combs. This is important in order to fully characterize the signal for this remarkable 1THz span comb as it opens a large amount of possibilities in many applications like THz generation or spectroscopy. Then, our efforts continue in order to improve the quality (mainly flatness and dynamic range) of this 1THz broad comb with the goal on improving the quality and energy efficiency of VCSEL-based OFCs, to make them a versatile and low energy and cost effective alternative for many fields of application.

Related publication: Congress B

The analysis of this EO&HNLF-OFCs of 1THz in the 20dB span was presented in the Congress CLEO USA in June 2016. In this oral talk the OFCs obtained with the expansion techniques previously presented were shown as well as the 1THz broad comb generated by cascading the EO stage and the HNLF one.

Abstract: In this work we show, to our knowledge, the broadest VCSEL-based optical comb with 1THz span (20 dB), 193 teeth, obtained by cascading two expansion stages, one with Electro-Optic Modulators and the second based on High Nonlinear Fibers.

To see the full information visit Congress B [137].

12. OFCs comparison of expansion techniques

In this section we have previously detailed the experimental study that have been performed regarding the expansion of a seed OFC generated in a VCSEL working under GS modulation. In former chapters we have shown separately the approaches that we have implemented separately using different nonlinear expansion techniques. These systems increase the comb span around a factor 3 compared to the sole VCSEL under GS regime. However, these schemes have diverse advantages and disadvantages and this might determine their likely or questionable use in certain applications. In this section, different figures of merit of each scheme are compared, analyzing their potentials and weaknesses. All the parameters are mentioned in each paragraph and, besides, they are all included in Table I (pag 132). In Fig 39, the previously shown optical combs with the same ranges of wavelengths are plotted for an easy visual span comparison:

Comb expansion factor: The expansion factor are 3.00, 3.07 and 3.18 for the EO-OFC (the narrowest), the HNLF-OFC and the NOLM-OFC (the broadest) respectively. Doubtlessly, the EO&HNLF-OFC is a combination of techniques that allows us to increment significantly these results, going to the remarkable value of 1THz broad comb. This implies an expansion up to 7.15 times the VCSEL-OFC.

Flatness: The flatness in the VCSEL-OFC is 0.77 which is quite good but is even improved with the EO-OFC set-up with a flatness factor of 0.87. This EO-OFC provides clearly much flatter

combs in comparison to the other methodologies. On the other side, NOLM-OFC has a flatness factor of 0.28 and HNLF-OFC presents quite low flatness, with a factor of 0.12. The combined technique produces an EO&HNLF-OFC whose flatness is only 0.07 with several points in the spectrum that intersect the 20dB line.

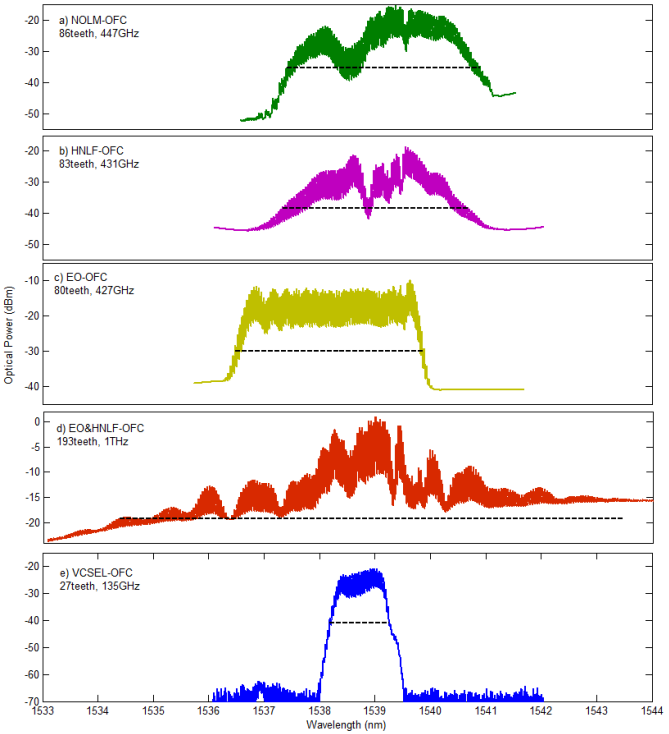

Fig 39. VCSEL-based OFCs comparison. a)NOLM-OFC (green trace) with 86 teeth/447GHz. b)HNLF-OFC (pink trace) with 83 teeth/431GHz. c) EO-OFC (yellow trace) with 80 teeth/427GHz. d) EO&HNLF-OFC (orange trace) with 193teeth/1THz. e) VCSEL-OFC (blue line) with 27 teeth/135GHz. All these OFCs are presented with the same optical wavelength ranges for an easier comparison. The 20dB span is marked with a dotted black line.

Optical dynamic range (DR): In these set-ups the DR is reduced from 50dB in the VCSEL-OFC to 25.3, 28.8, 37 and only 18dB for the HNLF-OFC, EO-OFC, NOLM-OFC and EO&HNLF-OFC respectively. NOLM-OFC is therefore, the most resistant scheme to the noise while the EO&HNLF-OFC worsen the DR substantially, to lower values than the considered span.

Spacing tunability: All these expansion techniques allow tuning of the spacing between comb teeth. For this purpose we first need to shift the RF frequency that modulates the VCSEL to its new value. After this, some adjustments of the set-up are needed depending on the scheme used for the comb expansion. For the HNLF-OFC, no extra adjustment is needed. This is the most direct set-up to change the distance between comb teeth. The NOLM-OFC needs some equalization of the Polarization Controllers (PC) in order to maintain the optical span as high as possible. The most complicated set-up to change the comb spacing is the EO-OFC: it needs optical adjustment of the polarization in the PC placed before the first PM but also some RF readjustment in both Phase Shifters. The same procedure occurs when adjusting the EO&HNLF-OFC.

Pulse quality: The different wavelengths that form the pulse are emitted with slightly different phases and then, the pulses does not have their ideal (and time limited) duration, which is called *chirp*. These chirped pulses of the VCSEL-OFC have 14.4ps at Full Width Half Maximum (FWHM). Neither are they transform limited after the expansion stage. If the actual pulse durations are compared, the scheme with the shortest pulse at the output is the HNLF-OFC with 7.59ps. The FWHM of the pulses is longer with the NOLM-OFC and the EO-OFC, with values of 14.8ps and 11.39ps respectively. However, if we focus

on the TBP_{rms}, then the HNLF offers the highest value. This means that the generated pulses are more dispersed and far from their TBL. All the configurations behave in a similar way and significantly increase the dispersion of the optical pulses compared to the VCSEL-OFC. However, they can be further compressed to their TBP limit using subsequent linear compression techniques.

Electrical spectra: In Fig 40 we show the RF signal after detecting the combs in the range from 0 to 6GHz. As expected it presents a clear peak which corresponds to the RF frequency used for modulation of the VCSEL and also the modulators when included, at 5.4GHz in the EO-OFC and 5.2GHz in the other set-ups. We see that the noise level in the spectra varies significantly among the different set-ups, with a significantly higher level in the NOLM-OFC.

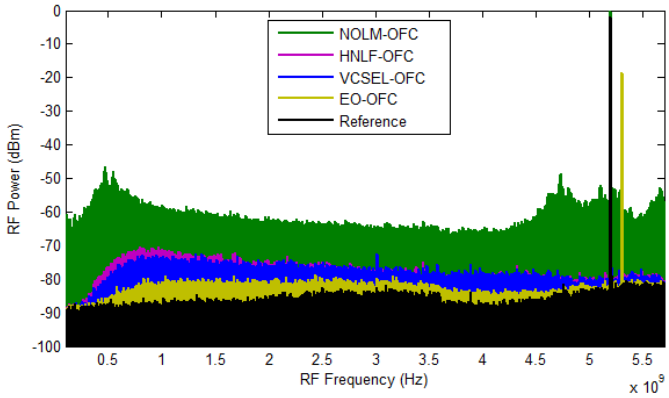

Fig 40. Comparison of the RF Spectra of the electrical detected signal in 0-6GHz

Electrical linewidth: In Fig 41, we see that all the set-ups present a linewidth of 1Hz. This implies that every set-up provide a comb with high coherence between teeth, inherited from the VCSEL-OFC due to the GS modulation, as we are measuring in the limits of the equipment and the obtained values coincide with the reference used.

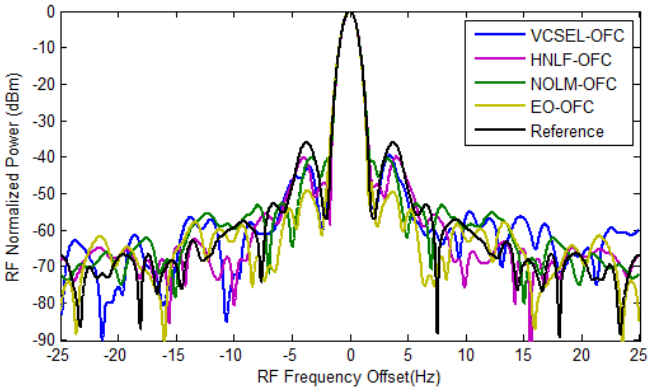

Fig 41. RF Linewidth of the electrical detected signals: VCSEL-OFC (blue line), HNLF-OFC (pink line), LOOP-OFC (green line), EO-OFC (yellow line) and Reference (black line). These measurements are limited by the equipment capabilities; all of them are lower than 1Hz. See text for more details.

Installation and start sequence: Another important fact to select the expansion scheme is the complexity when installing the set-up and the need of readjustments after operation. HNLF-OFC is the simplest scheme and the only parameter to be adjusted during turn-on is the output power in the EDFA. NOLM-OFC needs some other adjustments besides the EDFA output power: the polarization needs to be adjusted with the PCs inside the loop. Lastly, EO-OFC is the most complex

expansion stage to be installed as both, optical and electrical components, need to be tuned: the optical polarization at the entrance of the PM is optimized with the PC but also the RF phase shifters need a careful fine-tuning during installation and switching-on. As this EO stage is present in the EO&HNLF-OFC this system will be the most complex regarding the installation and start sequence.

Component count and cost: HNLF-OFC is the set-up that needs lower number of components in the expansion stage: two fibers (one DCF and one HNLF) and the EDFA. NOLM-OFC is the one with larger (optical) component count as it includes, apart from all these components, another DCF, the coupler, one SOA and two PCs. However, the costliest stage is EO as the electro-optical modulators are very specific and expensive components. Therefore, the EO-OFC and the EO&HNLF-OFC are the costliest set-ups, this second one slightly costlier.

Energy consumption: The NOLM-OFC consumes much more power than the other set-ups. This is mainly due to the high output power needed at the output of the EDFA (32dBm) to achieve maximum expansion in the loop as this component consumes 7.47W by itself and the SOA needs 0.65W in this configuration. The EO-OFC consumes 1.13W in the EDFA and 1.26W in the two PMs, so this set-up has lower energy needs compared to the previous one. The HNLF-OFC, in which the EDFA is the only active component, has the lowest energy needs, with 1.99W. Finally, the EO&HNLF-OFC consumes 3.35W, mainly due to the EO stage and also the EDFA included before the HNLF.

To conclude with this comparison, each comb expansion technique has its strengths and weaknesses depending on the parameters that we focus on. For instance, the EO-OFC is the one that provides the flattest but the most complex and costliest scheme. On the other hand, the HNLF-OFC is the simplest, most energy efficient and cheapest comb but it depends on the laser source and the GS regime and the flatness is low. NOLM-OFC is a balanced option, with high noise resistance and the broadest comb but highly dependent on the laser source, low flatness and much higher energy consumption. A combination of two of them, obtaining the EO&HNLF-OFC provides a comb 1THz broad with is a significant achievement but, the flatness and the dynamic range show the need of some room for improvement.

These differences will make each of these set-ups more or less likely to be used depending on each specific application, as the appropriate selection of the expansion technique will maximize the performance of the whole system that includes an OFC generation sub-system. In the following Table I we see a compilation of most of the previously analysed figures of merit that characterize the OFCs:

Table I. OPTICAL FREQUENCY COMBS MAIN FEATURES

OFC parameter	VCSEL-OFC	DM-OFC	EO-OFC	HNLF-OFC	NOLM-OFC	EO&HNLF-OFC
Laser Temperature (°C)	20	20	20	20	20 (VCSEL) 25 (SOA)	20
Laser Bias Current (mA)	11.4	61	11.4	11.4	13 (VCSEL) 396 (SOA)	11.4
LD RF power (dBm)	15	28	15	15	15	15
LD RF frequency (GHz)	5.2	8.3	5.4	5.2	5.2	5.4
PMs RF supply (dBm)	-	-	35	-	-	35
EDFA supply (mA)	-	-	662	994	3734	1200
EDFA output opt power (dBm)	-	-	12.5	22	32	24
Fiber lengths (m)	-	-	-	HNLF 200 DCF 1100	DCF1 600 DCF2 500	HNLF 200 DCF 600
Optical spectra						
Optical span @20dB	135GHz /27 teeth	117GHz /14teeth	427 GHz /80teeth	431 GHz /83 teeth	447GHz / 86 teeth	1000GHz / 193 teeth

Optical span @10dB	125GHz /24 teeth	91GHz /11teeth	403GHz /76teeth	296GHz /57 teeth	333GHz /64 teeth	140GHz /26teeth
Optical span @3dB	105GHz /21 teeth	66GHz /8teeth	371GHz /70teeth	52GHz /10 teeth	125GHz /24 teeth	76GHz /14 teeth
Optical span @20dB (nm)	1.1	0.92	3.41	3.33	3.5	9
Expansion factor (teeth/teeth)	1	0.52	2.96	3.07	3.18	7.15
Flatness factor (3dB/20dB teeth)	0.77	0.57	0.87	0.12	0.28	0.07
Dynamic range (dB)	50	55	28.8	25.3	37	18
Optical pulses						
Real pulse FWHM (ps)	14.4	22.8	11.39	7.59	14.8	*
Ideal pulse FWHM (ps)	7.7	9.2	1.9	2.3	1.7	*
TBPrms	3	9.2	7.20	10.22	8.80	*
Others						
RF Linewidth (3dB)	<1Hz	<1Hz	<1Hz	<1Hz	<1Hz	*
Energy consumption (W)	0.05W	0.84W	2.44W	2.04W	8.17W	3.35W

* Not measured

Related publication: Paper C

The analysis of the VCSEL-based OFCs detailed in this section and compared in this chapter is fully addressed in an article accepted for publication in the Journal of Lightwave Technology in July 2016.

Abstract: In this work we detail our experimental study on the expansion of Vertical-Cavity Surface-Emitting Laser (VCSEL) Optical Frequency Combs (OFCs) with different nonlinear techniques. For this purpose, we modulate a VCSEL device under Gain Switching (GS) regime to obtain an initial seed comb record in terms of energy efficiency and mode coherence. This seed OFC will be improved adding a nonlinear stage to expand this primary signal. The nonlinear techniques here presented are High Nonlinear Fibers (HNLF), Nonlinear Optical Loop Mirrors (NOLM) and Electro optical (EO) Phase Modulators (PM). In this work, we show the different extended OFCs that these techniques offer and we present a detailed comparison of their characteristics, evaluating the advantages and disadvantages of each technique. We have observed that the obtained OFCs maintain the high coherence offered by the seed VCSEL-OFC. Nevertheless, the optical span, flatness, frequency tunability, dynamic range, energy and cost efficiency or compactness of each expanded OFC significantly vary, depending on the expansion technique used. Our careful evaluation will serve as a reference to evaluate the suitability of each expansion technique depending on the needs or the application.

To see the full information visit Paper C.

VCSEL-based OFC optimization

During our VCSEL-OFC experimental study, the residual orthogonally polarized mode gained significant interest and a deeper study on its effect into the total comb generation was important to analyze for a posterior comb optimization. For this, in Chapter 13 the VCSEL technology and, more specifically, the **polarization dynamics in VCSEL-based OFCs** are studied together to its effect into to the GS behavior and the obtained comb. On the other hand, **Optical Injection Locking** (OIL) in Laser Diodes (LDs) has commonly been used to improve the performance of the emitted light, mainly focused on laser spectral narrowing, frequency chirp and noise reduction and modulation bandwidth enhancement. In this document, experiments regarding OIL in VCSELs are presented in Chapter 14 to evaluate how the optical and electrical spectra of the outcoming VCSEL-based OFCs change with this technique. It is shown that playing with parallel and orthogonal injection (varying the injected states of polarization) varies the resulting comb.

13. Polarization dynamics in VCSEL-based OFCs.

VCSELs are typically considered to be single-longitudinal-mode devices. However, their emission actually consists of two linearly polarized modes with orthogonal polarizations that, due to the birrefringence in the material, emit at different wavelengths [28], [79], as shown in Fig 42. Manufacturers have developed effective techniques to minimize this duality with polarization pinning processes and current devices exhibit a side mode suppression ratio above 30dB [80], what makes this device purely monomode for many applications. However, we have observed that this suppressed mode plays an important role in VCSEL-based OFCs.

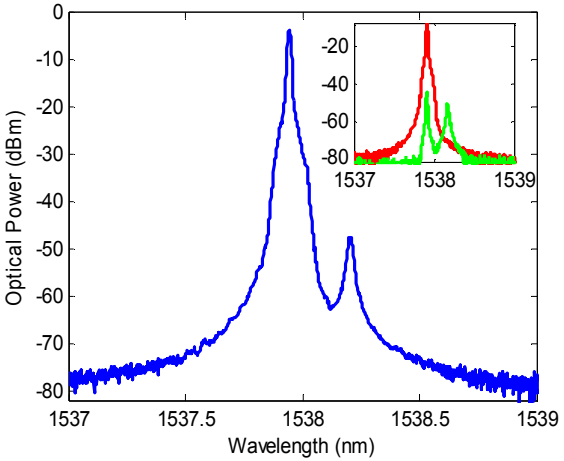

Fig 42. CW emission spectra for P, Px and Py. The dominant main mode in P at 1537.95 nm is more than 40dB above the residual orthogonal mode shown at 1538.20 nm. The birefringence of this VCSEL is 31.21GHz. Both outputs of the polarization splitter selecting Px (red line) and Py (green line) respectively are presented in the figure inset.

The hypothesis was that the hip that is always present in the upper wavelengths in VCSEL-OFCs is generated by the orthogonally polarized mode, typically ignored. Besides that, we wanted to verify if this orthogonally polarized signal generated another comb and which was the link between the parallel/main comb and this orthogonal/residual one. For this purpose, we deepen into the VCSEL technology to study the polarization dynamics of VCSELs and how they shaped the overall comb. The total OFC and the sub-combs obtained by splitting both polarization modes are shown in Fig 43.

To separate the polarization components that form the total comb, VCSEL-OFC or P-OFCG, a polarization controller (PC) and a polarization splitter (PS) are included at the output of the VCSEL. The PC allowed to align the fast axis of the PS with the main or parallel polarization component to obtain the main comb, Px-OFCG and subsequently, the PC was tuned to align the PS fast axis to the orthogonal or residual polarization to measure the orthogonal comb, Py-OFCG.

In Fig 43 we analyze the optical combs generated in the best operation point in terms of optical span and flatness (T = 20°C, I_{BIAS} = 11.4mA, f_{RF} = 5.2GHz, P_{RF} = 16dBm). The total output of the VCSEL, P-OFCG that we show in Fig 43a (upper trace) is the normally called VCSEL-OFC along this work. The 20dB span is measured in the comb with only the main polarization mode, the Px-OFCG shown in Fig 43b (middle line) with also 27 modes and 135GHz. Finally, we see the orthogonal comb, Py-OFCG in Fig 43c (lower line) which is slightly narrower with 26 lines that imply 130GHz in the 20dB span. We observe that the flatness of this comb is significantly worse than the one exhibited by the

total output and Px, and that it has a different shape, shifted in frequency.

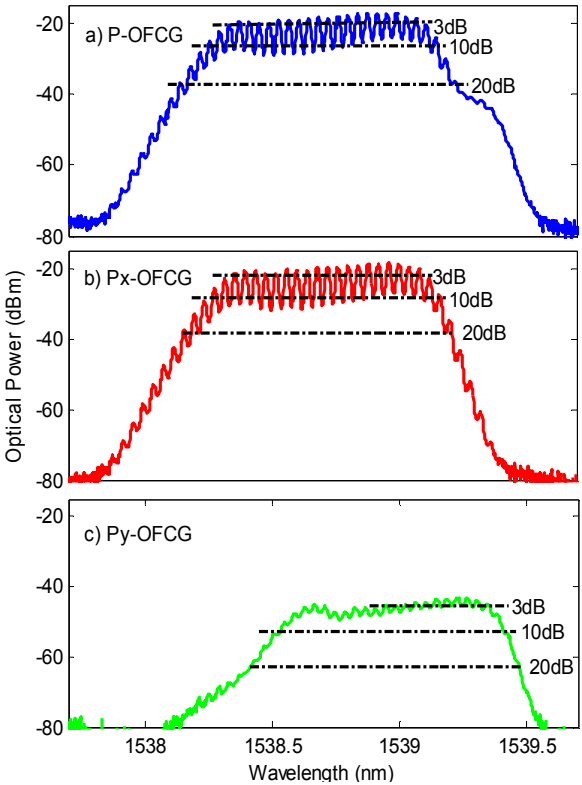

Fig 43. a) The upper line corresponds to the total output of the VCSEL, P-OFCG, with both polarization modes included. This is the VCSEL-OFC already presented in Fig 23. b) The middle line is the comb Px-OFCG, generated only with the parallel polarization signal. c) The lower line is the comb Py-OFCG which has the orthogonal polarization. The combs P-OFCG and Px-OFCG have 27 lines in the 20dB span which corresponds to 135GHz bandwidth. The comb Py-OFCG has one mode less, 26 in total, so the bandwidth in this case is 130GHz. See text for more details

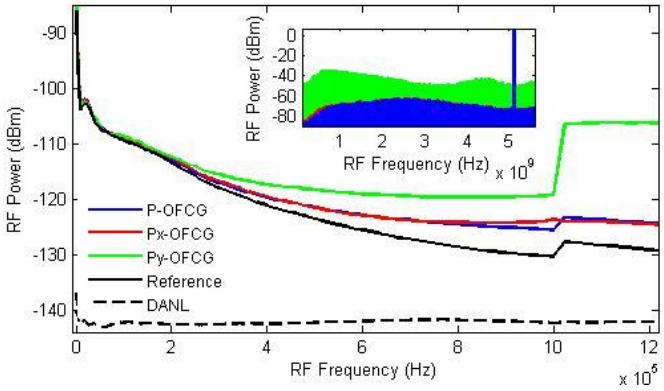

Fig 44. Phase noise (PN) for the combs: P-OFCG (blue line), Px-OFCG (red line) and Py-OFCG (green line). We also plot the PN of reference in the CW source (black line) and the minimum level in the espectrum analyzer used, the DANL (black dashed line). In the inset we plot the RF spectra for these three combs from DC to 5.5GHz. See text for more details.

We have also measured the PN of the electrically detected signal for each of the combs, in Fig 44. Analyzing these PN curves we see that both the total and main comb have similar noise so the coherence between the modes in the comb remains after splitting the polarization components. These lines are very close to the reference one as we were expecting taking into account our previous results with the VCSEL-OFC. This result is not observed in the orthogonal comb which has higher noise values. However, this is probably due to the higher amplification needed in the EDFA to equalize the carrier powers of the three signals. This orthogonal mode has lower power from manufacturing so we are equalizing the powers including more amplification and therefore, injecting more noise in the system. In the inset picture we observe the electrical spectra of the

signals from DC to 6GHz. The total comb and the main comb are very similar, with much lower noise than the Py-OFCG. This confirms that the noise is mainly due to higher amplification, as it is not present in the P-OFCG where the orthogonal comb is included.

Related publications: Paper D and Congress A

This work was fully addressed in an article published in the Journal of Lightwave Technology in September 2015. Additionally it was presented in a poster session in the Congress CLEO Europe 2015. In this article we analyze the evolution of the total comb and each orthogonally polarized sub-comb scanning the supply parameters used to bias and modulate the VCSEL. There we see that the best result occurs under the same conditions and we study the coherence of the teeth in each comb and between sub-combs. We conclude that all the comb teeth are phase correlated due to the GS regime but not completely locked. Therefore VCSELs under GS regime are dual-polarization comb sources that can find applications if we are capable to equalize the optical powers of both polarization modes.

Abstract: In this work we carry out an experimental study on the polarization properties of a Vertical-Cavity Surface-Emitting Laser (VCSEL) working under Gain Switching (GS) regime and the characteristics of the resulting optical frequency comb signal. We have observed that each of the two polarization modes presented in the VCSEL Continuous Wave (CW) emission spectrum generate a separate Optical Frequency Comb (OFC)

whose modes are phase correlated thanks to the GS regime. We study how these combs associated to the main and orthogonal polarization modes respectively vary depending on the input parameters to the VCSEL (bias current and radiofrequency power and frequency). The correlation between both OFCs in the best operation point as defined by the OFC characteristics is also evaluated. Therefore, this work demonstrates that two orthogonally polarized combs are generated that exhibit a high correlation between each other that combine to produce a wider overall optical comb. Hence, we can predict the feasibility of dual-polarization VCSEL-based Optical Frequency Comb Generators (OFCGs) in the few GHz repetition frequency rates, with highly correlated modes and continuously tunable distance between them, in a compact and energy and cost efficient system that can find application in ultrafast laser dynamics studies and or in polarization-division multiplexing optical communications.

To see the full information visit Paper D and Congress A [138].

14. Optical Injection Locking for comb optimization: OIL-OFC

In this chapter we present our latest results regarding our on-going study of VCSEL-based OFCs. We have evaluated the dynamic behaviour of the two orthogonal modes of polarization present in the VCSEL-OFC with and without optical injection. To our knowledge, this is one of the first works on injected VCSELs working under GS focusing on the resulting comb.

This is a research line that came up after the polarization study explained in Chapter 13 because we wanted to determine how the injection affects the VCSEL-OFC and, more specifically, how the injection affects the two sub-combs with orthogonal polarizations that were presented in Fig 43. In that chapter we showed that the VCSEL-OFC is formed by two orthogonally polarized combs, which are strong phase related due to the GS modulation and we suggested that dual-polarization coherent combs could be obtained balancing the power of these orthogonal components with OIL. These results were published and are available in Paper D. For this, the VCSEL is placed as slave laser in the OIL configuration and the master laser is the DM laser in Chapter 5, so its light is coupled into the VCSEL cavity using a circulator. The set-up used in this configuration is shown in Fig 45:

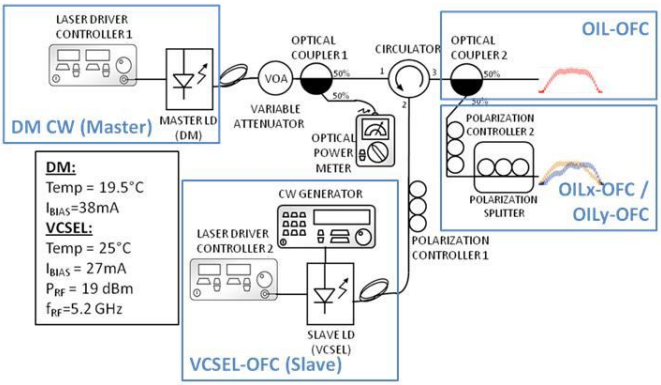

Fig 45. Experimental set-up. The comb is generated inside the VCSEL (25ºC, 27mA, 5.2GHz, 19dBm) which is at the same time optically injected by the DM laser (19.5ºC, 38mA) through a circulator. The injection ratio is -6.6dB. The optical output is first power divided and then one arm is split in two orthogonally polarized sub-combs with a polarization splitter. See text for more details.

The master path starts with the DM laser emitting in Continuous Wave (CW). Then, the signal is attenuated with a Variable Optical Attenuator (VOA) and a 50/50 Optical Coupler (OC) to adjust the appropriate injected power to the slave which will be monitored with the powermeter placed in one of the OC outputs. The second OC output is connected to the port 1 in the circulator, and the incoming signal will exit the circulator through the port 2 connected to the slave optical path. This slave path is formed by the VCSEL and a polarization controller (PC1) to adjust the polarization of the ingoing master light to the light being generated inside the cavity of the VCSEL. This polarization adjustment needs to be carefully done as it is critical for the locking of both signals. The master light coming from the circulator enters the VCSEL and the output signal goes

through the second input in the circulator to the output path. This output path finally arrives to the measurement equipment. In order to check the polarization components of the output comb we have included a second 50/50 coupler to divide the optical output and one of their output branches will be polarization split with a second controller (PC2) and a Polarization Splitter (PS).

The VCSEL used along this experiment as slave is the same device used previously in this document. However, it has been recently deteriorated after years of work so it needs more supply current (in bias and in RF) to achieve an equivalent emission. At the same time, the optical spectrum has been red shifted. However, a comb with the same behaviour and optical span is obtained, now with the following conditions: the device is temperature stabilized at 25°C with a bias current of 27mA and an input RF signal to produce the GS regime of 19dBm at 5.2GHz. The ratio RF-bias current is the same for the initial VCSEL-OFC and the degraded one. The master DM laser will be set at 19°C to fall in the VCSEL-OFC wavelengths and the current will be set around 38mA with some small tuning to achieve the injection.

In Fig 46 we show several significant optical spectra traces. Fig 46a) (blue trace) presents the VCSEL-OFC which is the VCSEL output when there is no external light injected. This comb is similar to the VCSEL-OFC presented in Fig 23 but red-shifted as mentioned in the previous paragraph. It has 25 teeth in the 20dB span which corresponds to 130GHz. The second and green trace in this plot corresponds to the master signal and therefore the injected light. The master DM source is emitting at 1541.63nm to coincide in the VCSEL-OFC teeth that produces the best

optical injection. The injection ratio is -6.6dB and this is controlled measuring the power in the master path and adjusting the VOA.

We know from previous works that this VCSEL-OFC is formed by two sub-combs with orthogonal polarizations, one main comb with parallel polarization (called P_X- OFCG inFig 43) and the residual one with orthogonal polarization and much lower power (P_Y-OFCG in Fig 43). The total comb and both combs' polarization components are shown in Fig 46b). The orthogonal sub-comb is observed in the small hip in the upper wavelengths in the VCSEL-OFC and one of our purposes with the OIL experiment is to power up this residual part with OIL.

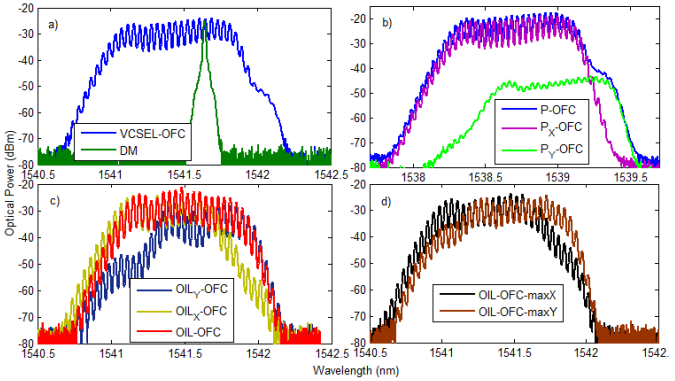

Fig 46. a) VCSEL-OFC (blue trace) with 25 teeth in the 20dB span which corresponds to 130GHz. DM output (green trace), master light being injected into the VCSEL at 1541.63nm. b) P-OFC, Px-OFC and Py-OFC shown in Fig 43, which are the total and split combs when no OIL occurs. c) OIL-OFC (red trace) output signal with OIL adjusting the polarization to equalize both sub-combs. The resulting comb has 27teeth in the 20dB span, which corresponds to 140GHz. OIL_X-OFC (beige trace) and OIL_Y-OFC (dark blue trace) which are the parallel and orthogonal polarization components of the OIL-OFC. This means that with the injection both sub-combs maintain their orthogonal states of polarization. d) OIL-OFCs adjusting the master polarization to maximize either the P_X-OFC (OIL-OFC-maxX or black trace) or the P_Y-OFC (OIL-OFC-maxY or brown trace). See text for details.

The red trace in Fig 46c) is the optical output when an optimum injection is achieved. This OIL-OFC is slightly broader than the previous one, with 27 teeth in the 20dB span which corresponds to 140GHz. It is more symmetric and flatter than the VCSEL-OFC as the polarization of the injected master light has been carefully tuned in PC1 in order to equalize the optical power levels of the parallel and orthogonally polarized sub-combs. It is important to remark that the VCSEL-OFC has instabilities due to temperature variations that imply small shifts in wavelength and the same happens in the master laser due to the resolution in the temperature controllers. At the same time, the detuning is narrow so sometimes the injection might not be stable enough and might be lost.

At this point, the polarization components of the OIL-OFC are checked in order to discriminate whether the injection produces a whole comb with only one state of polarization or both polarization components remain orthogonal. For this purpose, we include the second controller PC2 and the PS after the circulator. Looking at the output, we observe two orthogonally polarized sub-combs and how one mainly include the lower wavelengths, which we call OIL_X-OFC (Fig 46c, beige trace) and the second one, called OIL_Y-OFC (Fig 46c, dark blue trace) corresponds to the upper part of the total comb, the orthogonally polarized one. These OIL_X-OFC and OIL_Y-OFC are, consequently, the correspondent combs to the P_X-OFCG and P_Y-OFCG in Fig 43. This means that including the OIL we balance the power of both sub-combs increasing the presence of the orthogonal state of polarization but the output maintains both orthogonal states of polarization. Therefore, an orthogonally-

polarized dual-polarization VCSEL-based OFC is obtained equalizing both sub-combs with the OIL technique.

Going deeper in our understanding of the resulting OIL-OFC, we aimed to test the possible changes in the resulting comb caused by variations in the injected state of polarization. In order to do so, we altered the polarization in the injected light to achieve polarization switching by injecting close to the suppressed orthogonal linear polarization state of the VSCEL [125]. For this purpose we play with PC1 and we observe the output comb. In Fig 46d), we see that we can obtain an injected comb maximizing either the parallel sub-comb, called OIL-OFC-maxX (Fig 46d, black trace) or the orthogonal one, called OIL-OFC-maxY (Fig 46d, brown trace). The first one is obtained when the polarization in the injected light coincides with the parallel polarization and the second when it matches the polarization of the orthogonal mode in the VCSEL, enhancing this residual mode which turns to be the main one, achieving a polarization switching. These two traces are extreme examples and the OIL-OFC in Fig 46b) will be halfway, obtaining a balance among both states of polarization.

It is important to distinguish the combs in these two latter subfigures: the signals might seem similar but the difference is significant. In Fig 46c) we show the two components that form the OIL-OFC in Fig 46b). On the other hand, Fig 46d) shows the resulting comb after PC1 is adjusted to enhance only one linear state of polarization, and then, suppressing the other one. This implies that we can play with the injected polarization in VCSELs to balance both states of polarization, or to maintain only one (cancelling the other one as a consequence). This polarization effect find applications in ultrafast laser dynamics studies [139]

or in polarization-division multiplexing optical communication [140].

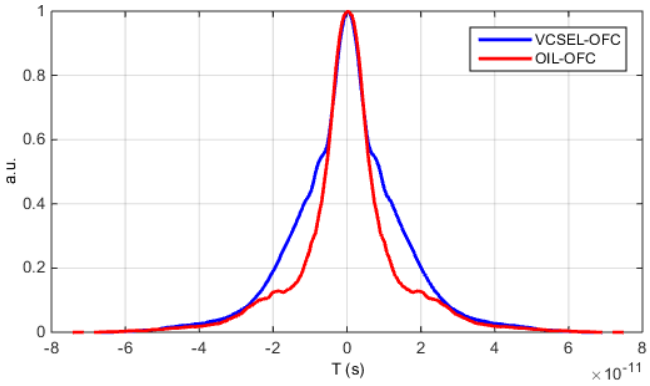

Fig 47. OIL-OFC: Temporal autocorrelation pulses. VCSEL-OFC (blue trace) with 18.3ps FWHM; OIL-OFC (red trace) with 11.8ps FWHM. The OIL technique reduces the width of the ACT traces and changes its shape. See text for more details.

We have also obtained the autocorrelation traces of the temporal pulses generated with and without the OIL scheme. In Fig 47 we observe the autocorrelation trace of the VCSEL-OFC (blue trace) and the OIL-OFC (red trace). The correspondent pulse durations assuming $sech^2$ profile are 18.3ps and 11.8ps. Therefore with the OIL we have achieved the compression of the optical pulse. On the other hand we can also observe in the traces that the upper and lower parts of the pulses are quite similar but they have differences in between, in the 20%-60% area, where the VCSEL-OFC is broader. Lastly, the OIL-OFC presents a pedestal in the 15% area.

Apart from the optical spectra and the temporal autocorrelation we introduce here a measurement not presented in previous results but introduced in Chapter 3: the optical linewidth measured with the delayed self-heterodyne interferometric technique [129]. This measure is related to the optical noise in the laser source and the optical elements along the path and lower linewidth will imply higher spatial and spectral coherence in the OFC. The optical linewidth is supposed to be reduced with the OIL inclusion down to the master source linewidth [141], as DMs present lower linewidths than VCSELs.

After the self-heterodyning interferometer the optical signal is detected and the resulting electrical spectra is shown in Fig 48. The optical linewidths are half the 3dB bandwidth of the plotted lines [129]. In the image, we see the VCSEL's linewidth when it is working in CW emission, which is 1MHz and the VCSEL-OFC linewidth that increases to 4MHz due to the GS regime. After the injection the linewidth obtained is broader, the OIL-OFC has a linewidth of 8MHz. This made us realize that the reason for this is that the DM linewidth was as high as 7MHz, much broader than what we had found in previous characterizations and what was expected from these devices [142]. We believe this sample is degraded after years of work. However, the results are consistent with the expected performance of OIL and, in fact, the linewidth for the OIL-OFC turns to be close to the master linewidth. Future work will be developed in this line with new samples to check if the optical linewidth becomes, then, narrower.

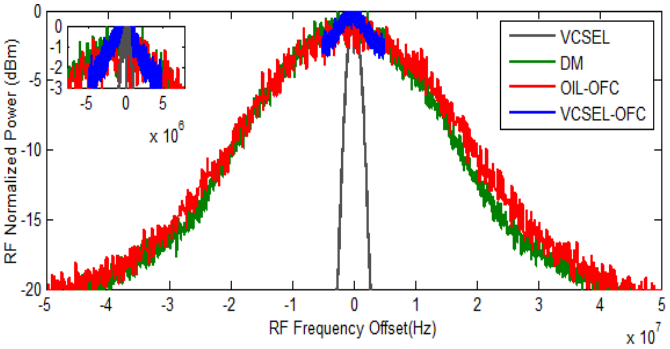

Fig 48. OIL-OFC optical linewidth measurement. The traces are the electrical spectra after self-heterodyning and the optical linewidths are half the 3dB bandwidth shown in these traces. VCSEL in CW (grey trace) which has an optical linewidth of 1MHz, DM in CW (green trace) with 7MHz, VCSEL-OFC (blue trace) with 4MHz, and OIL-OFC (red trace) with 8MHz of optical linewidth. See text for details.

In this section, we have shown our latest results in VCSEL-based OFCs in which we have included optical injection to observe the variations in the output comb depending on the injected light. First, we have injected light into the VCSEL cavity to balance the two orthogonal states of polarizations inherent to VCSELs so we have equalized the power in both sub-combs obtaining a dual-polarization OFC. Besides, we can also tune the injected polarization to cancel one of these sub-combs maintaining the other one in similar power levels obtaining a VCSEL-based comb with only one state of polarization and similar optical span.

Our efforts continue in first place to implement the OIL with a master source with lower linewidth and observe if the output inherits this lower noise [141], which is something that we could not test in this experiment as the DM is degraded. Secondly, our future work also includes deeper understanding in the OIL

technique for VCSEL-based OFCs and the scheme here implemented to check the effects in the noise and the phase coherence among comb teeth. Last but not least, our goal continues in order to achieve VCSEL-to-VCSEL injection to enhance the capabilities of integration and reduce even more the cost and energy consumption of the OFC generation system.

Related publication: Paper E (under revision) and Congress C

The analysis of our optically injected VCSEL-based OFCs detailed in this chapter is fully addressed in an article submitted to Optics Letters in June 2016 and also presented in an invited talk in the VCSEL's day in Darmstadt, June 2016. In this work we present a study of the polarization dynamics of an optically injected OFC based on the VCSEL-OFC. This OFC has two sub-combs associated to the orthogonally polarized modes present in VCSELs and they are phase correlated but not locked (see Chapter 13). In order to lock them, optical injection locking has been done with an external edge-emitting laser with small linewidth as master laser. Carefully adjusting the polarization of this master we obtain an OFC where the two sub-combs with orthogonal polarizations have comparable optical powers. The resulting overall OFC is a dual-polarization comb that maintains the strong phase coherence among its teeth and shows an enhanced optical span with improved flatness.

Abstract: The present experimental work studies the dynamics of dual-polarization optical frequency combs (OFCs) based on Gain Switched (GS) Vertical-Cavity Surface-Emitting Laser

(VCSEL) diodes under optical injection locking (OIL). This study has given two main results. First, we have obtained an overall comb formed by two orthogonally polarized sub-combs with comparable span and power. The overall comb shows enhanced optical span and flatness, and high coherence between its modes. The second result is that we have been able to control the polarization state of the overall comb by tuning the polarization state of the injected light. This produces an overall comb with single polarization, parallel or orthogonal. These are novel findings that open the way to develop efficient and compact OFC based on GS-VCSEL sources with a versatile polarization dynamics.

To see the full information visit Paper E and Congress C.

Conclusions and future work

15. Conclusions

In this document, the research line that started in January 2013 has been described, related to my work with VCSELs for comb generation. This work is part of one of the main research topics in our group focused on broad comb generation and expansion based on COTS components, to implement easily available but still powerful systems that serve as breakthrough in the access to OFCs, typically complex and difficult to implement out of the laboratory. Focusing on different applications like spectroscopy or THz generation this work aims to generate frequency combs and optimize the optical spectra created in terms of span, flatness and energy consumption.

Along this research, we have seen VCSELs under GS as a great opportunity to maintain the quality of our COTS-based OFCs enhancing the system in terms of energy consumption, cost and integrability. Because of their small size, we have increment the optical 20dB span produced compared to other LD technologies, with record energy efficiency [27] as they need lower bias and RF powers: VCSELs under GS provide 135GHz with only 11.4mA bias and 16dBm RF power. This is higher than our reference LD, DMs shown in this document generate 117GHz with 61mA of bias and 28dBm of RF modulation. Besides, using GS for the generation implies high phase correlation among the teeth in the comb and also in the orthogonally-polarized residual comb. This 135GHz comb from the VCSEL under GS, has subsequently been used as a seed comb to be expanded.

The main drawback when using this VCSEL technology is found in the modulation bandwidth that goes up to 7GHz because this limits the spacing between comb teeth. Some applications like

WDM require distances of 25-100GHz. However, some work has already been done by some other groups, trying to raise this bandwidth by playing with the birefringence splitting of the VCSEL's materials obtaining values above 250GHz of this birefringence splitting [86] or by using optical feedback [143].

In a second section of this research, we have included some nonlinear expansion stages after the VCSEL-OFC trying to broaden the comb span. Naturally, the component count, the energy needs and the integrability of the resulting system are diminished, while the optical span is significantly increased. Hence, a compromise appears here. To improve this balance, we have used commercial components and three different approaches based on EO PMs, HNLF and NOLM respectively. All of them increase the optical span about 3 times but other features vary differently, as we have evaluated in the corresponding comparison chapter. Such comparison has offered interesting conclusions, useful for those implementing a specially designed expansion system. It will help to design and adjust the strengths of the expansion stage to the needs of the specific field of application. To finish this section, we have shown a VCSEL-based comb with 1THz span which is a substantial increment compared to previous results, looking beyond the sub-THz range. At the same time, it is costlier and has larger energy needs. Our efforts continue in order to improve this current limitation and/or increase the quality of the obtained combs.

A third block of this Thesis started with deepening in the VCSEL-OFC, to study their polarization dynamics and how the parallel and orthogonal states of polarization interact in the resulting comb under GS. We have demonstrated that each component

generates a comb, and they are both phase correlated. However, the comb corresponding to the residual orthogonal mode has much lower power and our interest in equalizing both components increased. For this, we have inject some external light inside the cavity, using a technique called optical injection locking, OIL. We have seen that we can either neglect one of this states of polarization or equalize both of them producing a dual-polarization VCSEL-based OFC. In order to achieve these different results, we play with the state of polarization of the injected light, which comes from a DM master laser source. VCSELs under OIL has been implemented for the first time, to our knowledge, with the purpose of analysing the optical spectra.

Several lines of work open at this point and most of the aspects covered in this Thesis claim for deeper study in order to expand and optimize VCSEL-based OFCs. The next step would be to directly apply them to each specific application, trying to adjust the system regarding the needed performance and main figures of merit.

To conclude, VCSELs under GS have been demonstrated as optimum sources to generate efficient combs when the distance between comb lines is in the few GHz range. The resulting systems are straight-forward, compact and cost effective if we put the VCSEL low size and energy consumption together with the GS technique, which provides high phase coherence and tunability without component count increment. Besides, subsequent comb expansion and optimization has been proved obtaining up to 1THz broad combs.

16. Future work

The work and experiments here presented are part of an ongoing work that has a projection into the upcoming future. Our efforts will go further in the expansion and optimization of OFCs systems focusing on improving the energy and cost consumption and their usability out of the laboratory. Several lines of future research become important at this point and remain open questions.

The work here developed is purely experimental. This is the moment to start evaluating a different approach to deepen in our knowledge of VCSEL-based OFCs: include simulations that contrast this experimental work against theory. This work will be based on numerical analysis using mathematical models that allow us to simulate the generation of OFCs, their expansion and their behaviour under optical injection to help us understand what we have observed in the laboratory. With this, we will increase our knowledge on OFC generation and expansion by matching the experimental results to the developed models. These studies will help us evaluate the optimum working conditions to generate high quality VCSEL-OFC and implement new experimental designs. Also, we might be able to advance in the state of the art and incorporate new effects in the theory. Initial work has already been done on VCSEL-OFCs evolution with the GS parameters as we can see in Appendix 5 and in the following picture:

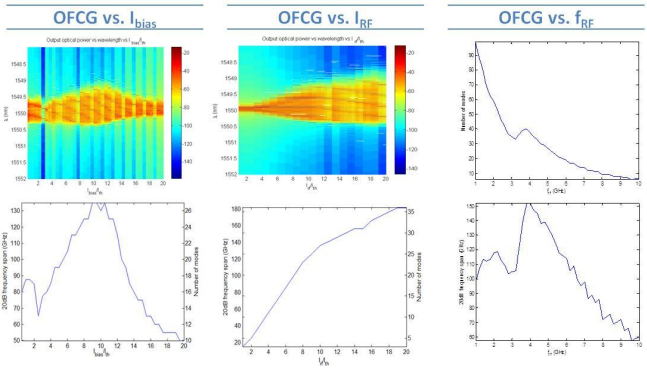

Fig 49. Numerical study that has been done and is continuing in the following months. See Appendix 5 for more details

Of special interest is the inclusion of GS in a Fabry-Perot (FP) LD, which has not previously been tested in our group and is also in the scope of the future work. Its behaviour under this nonlinear regime can be studied as it is a multimode source and GS might lock different small combs each one associated to the different emitting modes. If in this multimode source, GS also phase locks the modes, then a broad spectrum will be generated and this might find important advantages in THz synthesis. Some related works on this aspect are found in publications like [144], [145]. Other techniques here mentioned like self-seeding are also interesting to be studied in the frame of this work for both VCSELs and other LD technologies.

Regarding the OFC expansion in Chapter 11, the EO&HNLF-OFC result calls for further research. We will adjust the fibre components, complete the measurement characterization, and analyse the coherence between the teeth in the comb. We continue working emphasizing in the flatness and the dynamic range of this 1THz broad comb. We also aim to go further into the reduction of the energy consumption of the set-up. These features that should be improved are remarked in the following picture:

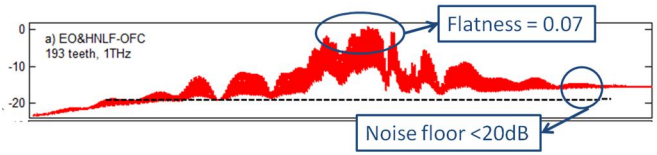

Fig 50. EO&HNLF-OFC in Fig 38 and its characteristics to be improved in future

Even when this is not in the scope of this research , it would be really interesting to check that, after the EO&HNLF-OFC set-up, it is possible to include a system like the one in [57] to generate the 1THz electric signal.

Our efforts continue, and our future work is also oriented to attain a deeper understanding in the OIL technique for VCSEL-based OFCs and the scheme here implemented to check the effects in the noise and the phase coherence among comb teeth. Last but not least, our ultimate objective is to achieve VCSEL-to-VCSEL stable injection.

This work will also be contrasted with theoretical simulations to optimize the experimental procedure. Deeper study in the power injection ratio, frequency detuning and stability maps is planned to be done in both the theoretical simulations and the experimental work.

Publications and related work

The references of the publications cited previously in the different chapters of this document are included below. In the following pages, the whole article/abstract is included too.

Paper A. EL2013

E. Prior, M. Ortsiefer, Á. R. Criado, P. Meissner, C. de Dios, and P. Acedo "Continuous wave sub-THz photonic generation with VCSEL-based optical frequency comb," *Electron. Lett.*, vol. 49, no. 15, pp. 944–945, Jul. 2013. doi:10.1049/el.2013.1896

Continuous wave sub-THz photonic generation with VCSEL-based optical frequency comb

E. Prior, Á.R. Criado, C. de Dios, P. Acedo, M. Ortsiefer and P. Meissner

A simple and energy-efficient photonic system to generate continuously tunable, low phase noise, sub-THz waves based on COTS components is presented. The optical scheme is based on the use of a commercial vertical cavity surface emitting laser under gain switching modulation that provides a very flat optical frequency comb generator (OFCG) with 23 modes in a 20 dB bandwidth. The laser only needs 15 dBm continuous wave radiofrequency input power and 9 mA of bias current to provide this OFCG. Two optical injection locking stages filter and amplify the two desired modes that are detected in a photodiode to produce the desired sub-THz signal at the frequency difference of these two selected modes. As an example, demonstrated is the generation of a very stable 88.2 GHz tone with lower linewidth than 10 Hz using a reference of 4.2 GHz to generate the OFCG.

Introduction: Photonic generation of high-frequency continuous-wave (CW) signals using difference frequency generation (DFG) is a well-established technique in the mm-wave and sub-THz frequency regions [1, 2]. Moreover, some DFG schemes using optical frequency combs generators (OFCG) have successfully demonstrated similar, or even better performance than the electronic counterparts in terms of frequency resolution and phase noise [2]. These OFCG-based schemes rely either on the use of monolithic components, like mode-locking laser diodes [3] with very low, if any, tunability, or on the use of external phase modulators [4], which need radiofrequency (RF) power in the order of 1 W per modulator and several external components, such as RF electronics, highly nonlinear fibres and compensating fibres for proper operation.

In this Letter, described is a simple and energy-efficient photonic system to generate continuously tunable, low phase noise, sub-THz waves using only COTS components. It is based on an architecture similar to our previous works [2, 5], with a newly designed OFCG that dramatically improves the overall cost, compactness and energy consumption of the system. This OFCG is based on a commercial vertical cavity surface emitting laser (VCSEL) under gain switching (GS) modulation that directly provides a very flat single-stage OFCG with 23 modes in a 20 dB bandwidth. It only needs 15 dBm CW RF modulation input power and 9 mA of bias current. We demonstrate with this system the generation of very stable (in terms of frequency), low linewidth (better than 10 Hz) and continuously tunable sub-THz signals.

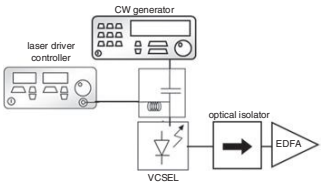

Fig. 1 *VCSEL-based OFCG scheme*

Experimental set-up: In Figs 1 and 2, we can observe the setup that has been used for this experiment. It consists of two different optical subsystems. Fig. 1 shows the OFCG. The core of this first subsystem is a commercial VCSEL (VERTILAS VL-1550-8G-P2-H4) under GS operation using a CW RF generator. The output of this OFCG is shown in Fig. 3 (black trace). A number of 23 lines for 20 dB bandwidth with only 9 mA bias current and 15 dBm RF input ($f_{mod} = 4.2$ GHz) are achieved. The minor asymmetry in the optical spectrum is in good agreement with the expected behaviour under this modulation regime [6]. As we can see in Fig. 1, no external modulators or further components are needed to obtain such a flat and wide spectrum. A standard OFCG based on standard techniques would need more than one order of magnitude more of modulation power and bias current [4].

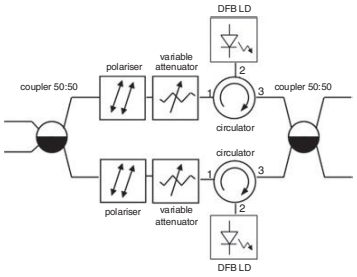

Fig. 2 *Selection of two modes set-up*
Two modes are selected using two-injection locking stages based on COTS DFB lasers

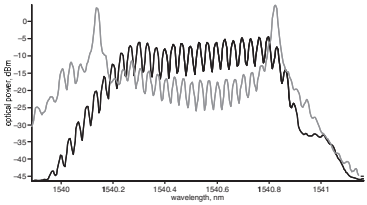

Fig. 3 *Optical spectrum at output of optical frequency comb generator (black trace); and after mode selection stage (grey trace)*

The second optical subsystem, shown in Fig. 2, provides optical mode selection for sub-THz DFG generation. It consists of two identical optical injection locking stages. Two commercial distributed feedback (DFB) lasers are used as slave lasers, in which the OFCG is injected as master signal to select the desired modes. This approach for the optical modes selection allows filtering and amplifying in a single stage and offers much higher performance than selection based on optical filtering [2]. The selection of different lines is achieved by controlling the DFBs' temperatures and bias currents. Continuous tunability of the synthesised frequency is achieved by combining coarse tunability through mode selection and fine tunability through the VCSEL modulation frequency, allowing for continuous coverage of the frequency region covered by the OFCG bandwidth [2].

The output of the mode selection stage after recombination is shown in Fig. 3 (grey trace). In this figure two modes, 21 lines apart, are selected for an 88.2 GHz frequency difference (VCSEL modulation frequency of 4.2 GHz). Besides that, the maximum synthesised frequency can be straightforwardly increased into several hundreds of GHz range using already reported techniques for comb expansion [2].

Experimental result: photonic sub-THz generation: Sub-THz photonic generation in DFG systems is achieved detecting the two optical wavelengths in a photodetector with enough electrical bandwidth. In our case, we have used a commercial photodiode (100 GHz 3-dB bandwidth) directly attached to an electrical spectrum analyser (ESA) that incorporates a subharmonic mixer for the frequency range of interest. The recovered signal is shown in Fig. 4, where we can observe that the expected signal at 88.2 GHz is provided by the system. The tone has a measured 3-dB linewidth in the order of the resolution bandwidth employed (10 Hz, minimum allowed by the ESA). Even though we have 45 dB losses in the subharmonic mixer required for the measurement (these losses have been taken into account to provide the measurement of Fig. 4), the achieved dynamic range is about 40 dB.

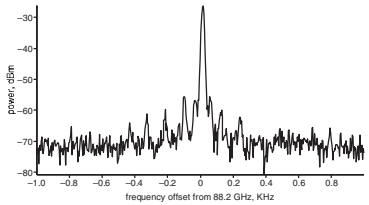

Fig. 4 *Sub-THz generated signal of 88.2 GHz, used span of 2 kHz; x-Axis, frequency offset in Hz (centre frequency 88.2 GHz); y-Axis RF power in dBm*

Finally, we have measured the system's tunability by measuring the sub-THz frequency generated while changing the reference frequency in steps of 1 kHz around 4.2 GHz, i.e. 21 kHz frequency steps in the synthesised sub-THz signal at 88.2 GHz. This characterisation showed an excellent linear behaviour with a coefficient of determination (R^2) to a linear fit of 1.

The signal stability at 88.2 GHz in terms of frequency and amplitude is very high, showing a standard deviation over 1 hour of operation of 25 Hz and 0.9 dB, respectively. It must be noted that the employed resolution bandwidth in this long-term stability analysis is 30 Hz; thus, these standard deviation values are in the measurement instrumentation accuracy and uncertainty limits.

Conclusions: We have developed a system for sub-THz generation using a gain-switched VCSEL-based OFCG. The use of a high-speed VCSEL offers the possibility of low size and high-efficient comb generation systems as we obtain a comb with 23 modes in a 20 dB bandwidth with the GS modulation. No extra components are needed. With this simple scheme, we have synthesised a sub-THz signal at 88.2 GHz with a linewidth lower than 10 Hz and excellent frequency and amplitude long-term stability. Additionally, the frequency tuning characteristic is almost perfectly linear with the reference frequency (f_{REF} is 4.2 GHz in our design). This method is very useful for compact, easy and tunable sub-THz photonic generation systems.

Acknowledgment: The work by Á.R. Criado has been supported by the Spanish Ministry of Science and Technology under the FPI Program, grant no. BES2010-030290.

13 June 2013
doi: 10.1049/el.2013.1896

E. Prior, Á.R. Criado, C. de Dios and P. Acedo (*Electronics Technology Department, Universidad Carlos III de Madrid of Leganes, Madrid 28911, Spain*)

E-mail: eprior@ing.uc3m.es

M. Ortsiefer (*Vertilas GmbH, Garching, Germany*)

P. Meissner (*Technische Universität Darmstadt, Darmstadt, Germany*)

P. Meissner: Also with Electronics Technology Department, Universidad Carlos III de Madrid, Madrid, Spain

References

1 Ho-Jin, S., Shimizu, N., Furuta, T., Suizu, K., Ito, H., Nagatsuma, T., Song, H., and Member, S.: 'Broadband-frequency-tunable sub-terahertz wave generation using an optical comb, AWGs, optical switches, and a uni-traveling carrier photodiode for spectroscopic applications', *J. Lightwave Technol.*, 2008, **26**, (15), pp. 2521–2530

2 Criado, A.R., De Dios, C, Prior, E., Döhler, G.H., Preu, S., Malzer, S., Lu, H., Gossard, A.C., and Acedo, P.: 'Continuous wave sub-THz photonic generation with ultra-narrow linewidth, ultra-high resolution, full frequency range coverage and high long-term frequency stability', *IEEE Trans. Terahertz Sci. Technol.*, 2013, **3**, (4), pp. 461–471

3 Criado, A.R., De Dios, C., Acedo, P., Carpintero, G., and Yvind, K.: 'Comparison of monolithic optical frequency comb generators based on passively mode-locked lasers for continuous wave mm-wave and sub-THz generation', *J. Lightwave Technol.*, 2012, **30**, (19), pp. 3133–3141

4 Wu, R., Torres-Company, V., Leaird, D.E., and Weiner, A.M.: 'Supercontinuum-based 10-GHz flat-topped optical frequency comb generation', *Opt. Express*, 2013, **21**, (5), p. 6045

5 Criado, A.R., De Dios, C., Döhler, G.H., Preu, S., Malzer, S., Bauerschmidt, S., Lu, H., Gossard, A.C., and Acedo, P.: 'Ultra narrow linewidth CW sub-THz generation using GS based OFCG and n-i-pn-i-p superlattice photomixers', *Electron. Lett.*, 2012, **48**, (22), pp. 1425–1426

6 Vasil'ev, P.P., White, I.H., and Gowar, J.: 'Fast phenomena in semiconductor lasers', *Rep. Prog. Phys.*, 2000, **63**, p. 1997

Paper B. PTL2014

E. Prior, C. de Dios, Á. R. Criado, M. Ortsiefer, P. Meissner, and P. Acedo, (2014). “Experimental study of VCSEL-based Optical Frequency Comb Generators,” IEEE Photonics Technol. Lett., vol. 26, no. 21, pp. 1–1, Nov. 2014. doi:10.1109/LPT.2014.2348594

Experimental Study of VCSEL-Based Optical Frequency Comb Generators

Estefanía Prior Cano, Cristina de Dios Fernandez, Ángel Rubén Criado Serrano, Markus Ortsiefer, Peter Meissner, and Pablo Acedo, *Member, IEEE*

***Abstract*— In this letter, we explore the performance of an optical frequency comb generator (OFCG) sources based on vertical-cavity surface-emitting laser diodes. The direct gain switching (GS) technique, the indirect electro-optical (EO) technique, and a combination of both have been experimentally evaluated. We have observed that this later combination gives birth to an enhanced OFCG that offers a tunable improved comb in terms of frequency span, flatness, and coherence with respect to the sole EO approach, as it partly inherits the high-efficiency qualities of the GS-OFCG while offering a wider span.**

***Index Terms*— Optical frequency comb generator, VCSEL, gain switching, phase modulator, electro-optical comb.**

I. Introduction

THE interest Optical Frequency Comb Generators (OFCG) have attracted in the last decade is a consequence of the versatility they cherish. This equally spaced group of optical modes has found application in a large variety of fields. Spectroscopy [1], optical communications [2], THz generation [3], optical arbitrary waveform generation [4], Metrology [5], or microwave photonic filters [6] are some examples of entire disciplines enjoying the solutions that the use of OFCG can provide. To cover such a wide range of fields and expand it an OFCG should offer a tunable, wide and flat optical comb. Its modes should also be highly correlated, since this is an important requirement for applications such as THz generation [3]. An ideal comb should cover these features while taking care of compactness, energy and cost efficiency.

OFCG sources based on lasers diodes (LD) are good candidates to meet the abovementioned requirements, especially if they can use Cost of the Shelf (COTS) devices. The maturity of commercially available LD would benefit the resulting OFCG taking it from the laboratory to the application field in a reliable and cost efficient way. Several techniques have already demonstrated promising results [7], [8]. They can be grouped in direct or indirect techniques.

Manuscript received July 18, 2014; revised August 4, 2014; accepted August 7, 2014. Date of publication August 27, 2014; date of current version September 30, 2014.

E. P. Cano, C. de Dios Fernandez, and P. Acedo are with the Department of Electronics Technology, Universidad Carlos III de Madrid, Madrid 28911, Spain (e-mail: eprior@ing.uc3m.es; cdios@ing.uc3m.es; pag@ing.uc3m.es).

Á. R. C. Serrano is with Luz WaveLabs, Madrid 28919, Spain (e-mail: ruben.criado@luzwavelabs.com).

M. Ortsiefer is with Vertilas GmbH, Munich 85748, Germany (e-mail: ortsiefer@vertilas.com).

P. Meissner is with the Technische Universität Darmstadt, Darmstadt 64289, Germany (e-mail: meissner@imp.tu-darmstadt.de).

Color versions of one or more of the figures in this letter are available online at http://ieeexplore.ieee.org.

Digital Object Identifier 10.1109/LPT.2014.2348594

Direct OFCG techniques are those where the generation of the comb occurs within the diode laser itself when it is operating under pulsed regime. One of the most interesting approaches is Gain Switching (GS). It is based on large signal modulation of the current injected to the LD and can be applied to any COTS device [9]. It offers tunability of the frequency spacing of the comb and a strong phase relation between its modes [3]. Still, optical span and flatness reported so far need to be improved to make GS-OFCG a high quality alternative.

Indirect OFCG techniques process the light after it is emitted using a nonlinear optical element. The most extended approach is the use of external Electro Optical modulators (EO-OFCG) [6], [8]. The resulting comb is tunable and can offer a span in the THz range using a cascade of modulators that requires a careful management of the RF power and the phase of the electrical and the optical signals all along the set-up. This technique typically uses other laser sources but it can also be applied to commercially available LD devices.

There exists a third way to generate optical combs using diode laser sources and it is based on the combination of direct and indirect techniques. A Combined-OFCG source based on GS and EO modulators [3], [10] permits the enhancement of the initial GS comb span and its flatness.

But the characteristics of the final comb are not only determined by the technique. The diode laser technology plays a major role. The use of edge emitting technologies such as Fabry-Perot [10], Distributed Feedback Bragg lasers or Discrete Mode [11] has been recently reported. In this sense, our previous work [7] shows that the use of high performance Vertical Cavity Surface Emitting Lasers (VCSEL) permits the generation of an enhanced comb, record in energy efficiency and optical span. This result drives our interest to study the possibilities of this technology as the core of an OFCG that could meet the requirements detailed before. In the present work, we systematically evaluate the performance of VCSELs for OFCG based on lasers diodes. We have explored the use of direct GS-OFCG, indirect EO-OFCG and Combined-OFCG techniques and compared the resulting combs in terms of span, flatness, frequency tunability, efficiency and coherence.

II. Experimental Set-Up

The core of our experimental scheme is a state of the technology VCSEL diode laser (VERTILAS VL-1550-8G-P2-H4, I_{th}=2.9mA). It is mounted on a pre-commercial prototype developed in collaboration with VERTILAS that includes the

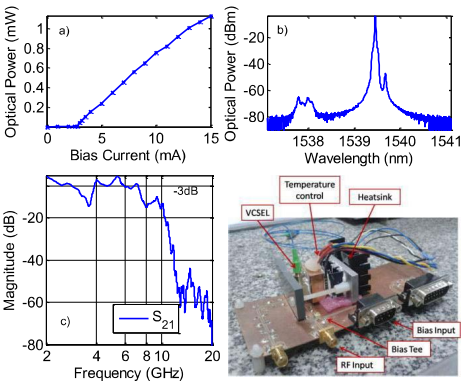

Fig. 1. Static and dynamic characterization of the VCSEL device. a) IP optoelectronic curve. b) Continuous wave optical spectra and c) dynamic small signal response with S21 scattering parameter at $I_{bias} = 11.4$mA. The picture shows the VCSEL device pre-commercial prototype.

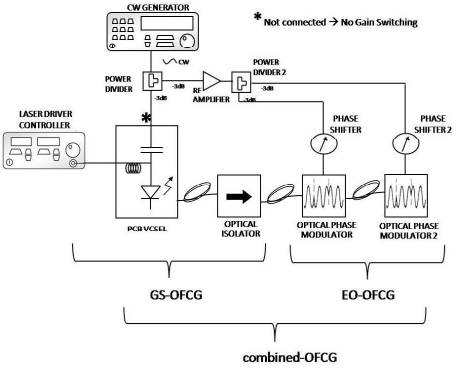

Fig. 2. The experimental set-up consists of two subsystems. Left: GS-OFCG based on a VCSEL source under Gain Switching. Right: EO-OFCG based on two optical Phase Modulators. The complete set-up is the Combined-OFCG that connects both subsystems in cascade linking them with the same RF modulating signal.

VCSEL adapted for radiofrequency (RF) modulation with a specially designed high frequency matching PCB network. An optical isolator is included to avoid optical feedback. Its temperature is stabilized at 25°C. A typical characterization of the device is depicted in Figure 1. At the $I_{bias} = 11.4$mA considered (best GS performance) the electronic 3dB bandwidth of the VCSEL is 7GHz. Nevertheless, the frequency response does not show a perfect flat low pass shape due to impedance mismatches related to the high frequency PCB prototype response (3-4 GHz range).

In Figure 2 we show the set-up developed for the present work. It consists of two different optical subsystems. The first one is the direct Gain Switching Optical Frequency Comb Generator (GS-OFCG). When the GS regime is induced, the injected RF power into the laser is $P_{RF,GS} = 15$dBm and the bias current is $I_{bias} = 11.4$mA at $f_{RF} = 5$GHz. These working conditions were chosen in order to offer the best OFCG performance [7].

The second subsystem is the indirect Electro-Optical generation scheme (EO-OFCG) also shown in Figure 2. It is composed of the VCSEL diode in continuous wave (CW) operation (no RF modulation to the diode laser) and an external Electro-Optic modulation stage. In this letter this stage consists of two standard phase modulators (3dB bandwidth up to 10GHz) in cascade configuration. This scheme is the core of larger architectures that have successfully produced enhanced optical frequency combs [6], [8]. As the bias conditions of the VCSEL do not affect the EO stage, we also use $I_{bias} = 11.4$mA to facilitate the comparison. An RF power of $P_{RF,EO} = 28$dBm is needed for each external modulators to work under optimum conditions (wider span of the resulting comb). Hence, a high power RF amplifier is included. Phase matching between this modulating signals and the optical signal entering the modulators is critical, so a phase shifter is needed before their RF inputs and has to be tuned to optimize the resulting comb.

The simultaneous operation of the two subsystems described before permits the experimental evaluation of the Combined-OFCG technique using VCSELs. The same RF signal is split to induce the GS regime in the direct comb subsystem with $P_{RF,GS} = 15$dBm and to modulate each modulator of the indirect EO-OFCG with $P_{RF,EO} = 28$dBm, bounding the subsystems together.

III. Results

In this section, we compare the optical combs we have obtained based on state of the technology VCSEL device. We have used the three available techniques to develop an OFCG based on a laser diodes: direct GS, indirect EO and the combination of both. We have evaluated the comb span, its flatness, its frequency tunability, the phase relation between its modes and the energy efficiency of the OFCG sources.

A. Optical Frequency Span and Flatness

For applications such as THz photonic generation, the useful optical span can be defined up to 20dB [3]. For optical communications, the flatness of the comb is more critical and the useful modes lie within a 3dB or 10dB bandwidth [11]. This is why we have evaluated the comb span using several metrics. We have also defined the comb flatness as the ratio of the 3dB to the 10dB bandwidth and the 10dB to the 20dB span. The closer these values are to 1, the closer the comb is to exhibit a flat-top shape.

In Figure 3.a we show the VCSEL based GS optical comb with $f_{RF} = 5$GHz. The output of the VCSEL has a 3dB bandwidth of 80GHz (16 modes) and a 20dB bandwidth of 106GHz (21 optical modes). The comb exhibits a remarkable flatness (0.84 and 0.9 in Table I). Figure 3.b shows the comb obtained using the indirect EO-OFCG technique alone with the same $f_{RF} = 5$GHz. The 3dB bandwidth reaches only

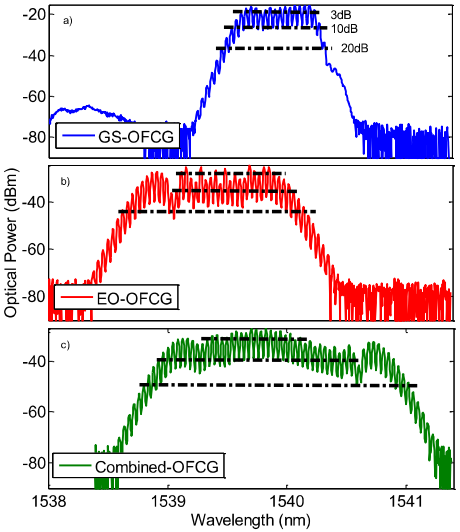

Fig. 3. OFCG techniques with VCSEL diode laser: comparison. a) GS-OFCG technique. b) EO-OFCG. c) Combined-OFCG. The modulation frequency is $f_{RF} = 5$GHz. 3dBm, 10dB and 20dB bandwidths of the combs are indicated. The combined-OFCG has a 20dB span of 272GHz and 53lines.

TABLE I
COMPARISON DIRECT, INDIRECT AND COMBINED OFCG: FREQUENCY SPAN AND FLATNESS@$f_{RF} = 5$GHz

Metric	GS-OFCG	EO-OFCG	Combined-OFCG
Span@3dB	80GHz 16 modes	16GHz 3 modes	100GHz 20 modes
Span@10dB	97GHz 19 modes	126GHz (165) 25 modes (33)	208 GHz (248) 41 modes (49)
Flatness 3dB/10dB, f3dB	16/19 = 0.84	3/25 = 0.12	20/41 = 0.48
Span@20dB	106GHz 21modes	193GHz 38modes	272GHz 53modes
Flatness 10dB/20dB f10dB	19/21 = 0.9	25/38 = 0.66	41/53 = 0.77

16GHz (3 modes), while its 20dB bandwidth rises to 193GHz. The flatness of the EO comb is far from 1 (0.12 and 0.66 Table I). To improve the flatness of this type of comb an extra External Intensity Modulator is typically included. Figure 1.c depicts the Combined-OFCG comb that has a 3dB span of 100GHz (20 modes) and a 20 dB span of 272GHz (53 modes).

We have seen that the VCSEL based comb using GS technique offers the best flatness but a limited optical span. An increased 20dB span can be achieved with the EO scheme, however, the flatness of the comb is compromised and extra external modulating elements need to be included in the system. However, the Combined approach applied to the VCSEL device offers an enhanced optical span for all the metrics (40% wider than the EO-OFCG and 150% wider that the GS at 20dB) and a flatness that is below the direct GS approach but better than the indirect EO without adding additional elements.

TABLE II
COMPARISON DIRECT, INDIRECT AND COMBINED OFCG: TUNABILITY

f_{RF} (GHz)/ Span@20dB	GS-OFCG	EO-OFCG	Combined-OFCG
5	106GHz 21modes	193GHz 38modes	272GHz 53modes
9	58GHz 7modes	179GHz 19modes	206GHz 23modes
12	1mode (No GS)	297GHz 24modes	297GHz 24modes

B. Frequency Tunability

The OFCG techniques considered in this letter have the possibility to offer an optical comb that can change the frequency separation between its modes by changing the frequency of the RF modulating signal, f_{RF}. But, for different f_{RF}, the characteristics of the resulting combs may vary. In Table II we present the comb span and the number of modes at 20dB for different f_{RF}.

When the f_{RF} lies within the electronic bandwidth of the VCSEL device (4 to 7GHz for $I_{bias} = 11.4$mA, see figure 1.c), the GS-OFCG and the Combined-OFCG offer their best performance. When the f_{RF} increases further, the VCSEL does not enter Gain Switching operation and the GS and Combined combs offer spans significantly smaller. For $f_{RF} > 12$GHz, the GS comb is inexistent. Then, the frequency tunability for the GS and combined combs is only possible within the electronic bandwidth of the laser diode. This means that careful choice of the parameters that define the Gain Switching regime (I_{bias}, f_{RF}, $P_{RF,GS}$) has to be carried out in order to manage the optical span and/or the number of modes as f_{RF} changes.

For the EO-OFCG, there exists an optical comb for all the f_{RF} under study, but the available span and/or number of modes also depends on the f_{RF}. The optical span and the number of modes decrease at 9GHz to increase again at 12GHz. If a constant span or number of modes is needed, the $P_{RF,EO}$ modulating the EO devices and the phase matching between the RF and optical signals should also be changed as f_{RF} increases.

C. Coherence of the Modes of the Comb

We have studied the coherence between the modes of the combs obtained evaluating the phase noise of the beat tone generated after mixing its modes. A degradation of the phase noise of this beat tone is associated to an overall loss of coherence among the optical modes. In [7] we found that the phase noise of the VCSEL based GS-OFCG is similar to that of the reference signal. In the present work (Figure 4) we have evaluated EO and Combined techniques.

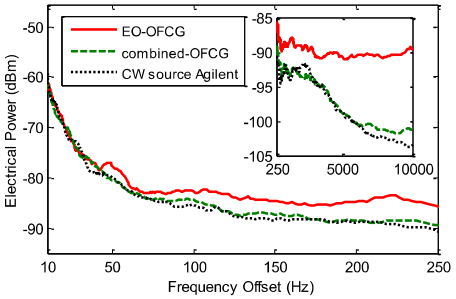

Fig. 4. Phase Noise of the electrical signal detected at the output of the set-up: signal generated after the EO-OFCG (solid), after the Combined-OFCG (dashed) and the signal of the RF source (dotted). The beat-tone obtained from the Combined-OFCG has the same Phase Noise as the source. The signal is degraded with respect to the RF source for the EO-OFCG. The complete signal is shown in the inset while a zoom is in the main picture.

As we can see from this Fig. 4, the phase noise of the VCSEL-based Combined-OFCG and the indirect EO-OFCG remain similar up to 40Hz frequency offset. From this point on, the Combined source exhibits a phase noise that is up to 11dB less that the phase noise of the indirect EO beat tone (at 10KHz offset frequency). Also, the phase noise of the Combined-OFCG remains close to the phase noise of the modulating RF source up to 6.2KHz. From that point on, they slightly diverge and a maximum difference of 2.2dB is observable at 9.7KHz. We have to note here that around 2.2KHz, the phase noise of the RF signal exceeds that of the Combined beat tone in 1.6dB. This can be attributed to instabilities in the radio-frequency generator. In conclusion, the Combined-OFCG offers a comb whose mode coherence and stability are linked to the initial RF modulating source and exceeds that of the EO approach.

D. Energy Efficiency

If we consider the RF power consumption of the different schemes and compare it with the number of generated modes at 20dB, we find that the direct GS approach consumes 15dBm/21modes = 1.5mW/mode. The EO-OFCG needs 33.1mW per mode while the combined approach utilizes 24.4mW/mode. The peak optical power of the generated modes within the 3dB bandwidth is -16dBm for the direct GS comb, -25dBm for the indirect EO and -28dBm for the Combined-OFCG.

IV. Conclusions

After evaluating the results we have presented we can find that the Combined VCSEL-based OFCG offers better results in terms of available optical span, number of modes and coherence of the generate modes. The direct GS VCSEL-based OFCG exhibits also some extra advantages, like the best flatness and the best energy efficiency. The indirect EO-OFGC using VCSEL does not excel in any of the parameters evaluated. Of course its span or flatness could be improved by adding an extra element or choosing EO modulators with better performance, but that would also improve the characteristics of the combined approach, leaving the comparison unchanged. All the techniques are tunable, being the EO the one that offers a higher frequency shift. In all the cases, to generate a stable comb in terms on the number of modes or the span, other parameters that define the working point of the OFCG have to be carefully adjusted as the frequency changes.

Then, the generation of optical combs based on VCSEL diode lasers offers better results when the GS and the EO techniques are combined: the advantages of both techniques add up to offer a better comb in all of the aspects evaluated. Only the energy efficiency decreases with respect to the GS generation. If we compare the EO and Combined techniques in terms of experimental complexity, the combined approach is the most indicated, since its set-up is equivalent to the EO, and the performance of the final comb is clearly enhanced.

If we compare VCSEL based OFCG with sources based on other laser diode technology [10], [11], we find that with equivalent set-ups, VCSELs offer wider combs with better energy efficiency.

Special attention deserves the results describing the coherence of the modes within the generated combs. GS and Combined techniques offer a comb with high stability linked to the CW RF source considered. This is a new remarkable result whose understanding and exploitation will center or future efforts, giving its importance for applications like THz or mid-IR generation.

References

[1] F. Zhu, T. Mohamed, J. Strohaber, A. A. Kolomenskii, T. Udem, and H. A. Schuessler, "Real-time dual frequency comb spectroscopy in the near infrared," *Appl. Phys. Lett.*, vol. 102, no. 12, p. 121116, 2013.

[2] P. J. Delfyett *et al.*, "Optical frequency combs from semiconductor lasers and applications in ultrawideband signal processing and communications," *J. Lightw. Technol.*, vol. 24, no. 7, pp. 2701–2719, Jul. 2006.

[3] A. R. Criado *et al.*, "Continuous-wave sub-THz photonic generation with ultra-narrow linewidth, ultra-high resolution, full frequency range coverage and high long-term frequency stability," *IEEE Trans. Terahertz Sci. Technol.*, vol. 3, no. 4, pp. 461–471, Jul. 2013.

[4] S. T. Cundiff and A. M. Weiner, "Optical arbitrary waveform generation," *Nature Photon.*, vol. 4, no. 11, pp. 760–766, Oct. 2010.

[5] T. Udem, R. Holzwarth, and T. W. Hänsch, "Optical frequency metrology," *Nature*, vol. 416, no. 6877, pp. 233–237, Mar. 2002.

[6] R. Wu, C. M. Long, D. E. Leaird, and A. M. Weiner, "Directly generated Gaussian-shaped optical frequency comb for microwave photonic filtering and picosecond pulse generation," *IEEE Photon. Technol. Lett.*, vol. 24, no. 17, pp. 1484–1486, Sep. 1, 2012.

[7] A. R. C. Serrano, C. de Dios Fernandez, E. P. Cano, M. Ortsiefer, P. Meissner, and P. Acedo, "VCSEL-based optical frequency combs: Toward efficient single-device comb generation," *IEEE Photon. Technol. Lett.*, vol. 25, no. 20, pp. 1981–1984, Oct. 15, 2013.

[8] R. Wu, V. Torres-Company, D. E. Leaird, and A. M. Weiner, "Supercontinuum-based 10-GHz flat-topped optical frequency comb generation," *Opt. Exp.*, vol. 21, no. 5, pp. 6045–6052, Mar. 2013.

[9] C. de Dios and H. Lamela, "Improvements to long-duration low-power gain-switching diode laser pulses using a highly nonlinear optical loop mirror: Theory and experiment," *J. Lightw. Technol.*, vol. 29, no. 5, pp. 700–707, Mar. 1, 2011.

[10] R. Zhou, S. Latkowski, J. O'Carroll, R. Phelan, L. P. Barry, and P. Anandarajah, "40 Nm wavelength tunable gain-switched optical comb source," *Opt. Exp.*, vol. 19, no. 26, pp. B415–B420, Dec. 2011.

[11] P. M. Anandarajah *et al.*, "Generation of coherent multicarrier signals by gain switching of discrete mode lasers," *IEEE Photon. J.*, vol. 3, no. 1, pp. 112–122, Feb. 2011.

Paper C. JLT2016

E. Prior, C. de Dios, Á. R. Criado, M. Ortsiefer, P. Meissner, and P. Acedo, “Expansion of VCSEL-based optical frequency combs in the sub-THz span: comparison of non-linear techniques,” J. Light. Technol, accepted for publishing on July 2016. doi: 10.1109/JLT.2016.2594129

Expansion of VCSEL-based optical frequency combs in the sub-THz span: comparison of non-linear techniques

Estefanía Prior, Cristina de Dios, Á. Rubén Criado, Markus Ortsiefer, Peter Meissner, and Pablo Acedo, *Member, IEEE*

***Abstract*—In this work we detail our experimental study on the expansion of Vertical-Cavity Surface-Emitting Laser (VCSEL) Optical Frequency Combs (OFCs) with different non-linear techniques. For this purpose, we modulate a VCSEL device under Gain Switching (GS) regime to obtain an initial seed comb record in terms of energy efficiency and mode coherence. This seed OFC will be improved adding a non-linear stage to expand this primary signal. The non-linear techniques here presented are High Non Linear Fibers (HNLF), Non Linear Optical Loop Mirrors (NOLM) and Electro optical (EO) Phase Modulators (PM). In this work, we show the different extended OFCs that these techniques offer and we present a detailed comparison of their characteristics, evaluating the advantages and disadvantages of each technique. We have observed that the obtained OFCs maintain the high coherence offered by the seed VCSEL-OFC. Nevertheless, the optical span, flatness, frequency tunability, dynamic range, energy and cost efficiency or compactness of each expanded OFC significantly vary, depending on the expansion technique used. Our careful evaluation will serve as a reference to evaluate the suitability of each expansion technique depending on the needs or the application.**

***Index Terms*— Gain Switching, Laser Diodes, Optical Frequency Comb, Vertical-Cavity Surface-Emitting Laser, Energy Efficiency, Non Linear Optical Loop Mirror, Highly Non Linear Fiber, Electro-Optical Components, Phase Modulator**

I. Introduction

Optical Frequency Combs (OFC) are very attractive and versatile systems that have recently found application in a large variety of disciplines like THz generation, spectroscopy, optical communications, metrology or microwave photonics [1]–[6]. Femtosecond mode-locking lasers or fiber lasers are typical bench-top schemes used to generate high quality wide span optical combs [7]. However, compact systems would be desirable to reduce the complexity, the cost and the energy consumption. An OFC source with these characteristics would widen even further the range of applications and would surely help to bring technologies such as THz generation, dual-comb spectroscopy [4] or optical processing [8] out of the laboratory. In this sense, the implementation of OFC in a single device using Mode-Locking Laser Diodes (MLLD) is one of the possibilities. MLLD have been extensively studied during the last decades [9]. However, they require specially designed structures that still today do not offer repeatability in the manufacturing processes. Another approach is the use of microresonators [10]. These promising devices are able to generate extremely wide OFCs with high repetition frequencies, but are still very new and the excitation of their resonant cavity requires high power and set-ups with several stages.

A straightforward alternative arises here, Gain Switching (GS). Some recent works have recovered this well-known technique to implement multi-GHz OFC for various applications [11] [3]. GS is based on the deep modulation of the gain medium of a semiconductor laser to induce a pulsed regime of operation. Although the resulting OFCs achieve much less optical span than MLLDs or microresonators, GS OFCs offer wide frequency tunability range, high correlation between optical modes, compactness and low-cost, as they can be implemented using any commercial semiconductor laser diode (LD) technology.

One of the LD technologies most appealing for this comb generation are Vertical-Cavity Surface-Emitting Lasers (VCSELs) [12]–[14]. High quality OFCs with record optical span and cost and energy efficiency [10] have been reported using such laser technology and Gain Switching (GS) modulation. However, further research efforts have to be taken in the study of combs based on VCSELs under GS (VCSEL-OFCs), especially on the improvement of their optical span while maintaining the mode coherence and the low power consumption of the system. Such combs will find application in

Manuscript received Feb 24, 2016. The work by E. Prior has been supported by the Spanish Ministry of Economy and Competitiveness under the Retos-Colaboración Program, RTC-2014-2661-7 in collaboration with Luz WaveLabs S. This work was supported by the Spanish Ministry of Economy and Competitiveness under the TEC-2014-52147-R Grant.

E. Prior, C. de Dios, and P. Acedo are with the Electronics Technology Department, Universidad Carlos III de Madrid, Leganés, Madrid 28911 Spain (e-mail: eprior@ing.uc3m.es, cdios@ing.uc3m.es, pag@ing.uc3m.es).

A.R. Criado is with Luz WaveLabs S.L. Av. Gregorio Peces Barba, Leganés, 28919 Spain (email: ruben.criado@luzwavelabs.com).

M. Ortsiefer is with Vertilas GmbH, Munich 85748, Germany (e-mail:ortsiefer@vertilas.com).

P. Meissner is with the Technische Universität Darmstadt, Darmstadt 64289, Germany (e-mail: meissner@imp.tu-darmstadt.de).

Color versions of one or more of the figures in this letter are available online at http://ieeexplore.ieee.org.

Digital Object Identifier xxxxxxxxxxx

fields like THz generation or green optical communications [15], [17].

In this work, we present new results on our study of VCSEL-based GS-OFCs focused on the expansion of the optical span they can offer. We implement and compare different comb expansion schemes based on non-linear elements: Highly Non Linear Optical Fibers (HNLF), Non-linear Optical Loop Mirrors (NOLM) and Electro-optical (EO) Phase Modulators (PM). All these components exploit non-linear optic effects to accomplish the improvement of the initial VCSEL-OFC. HNLF are optical fibers that exhibit a high nonlinear refractive index and help generate new frequencies mainly due to Self Phase Modulation (SPM) and Four Wave Mixing (FWM) when the optical power is high enough [18]. On the other hand NOLMs are optical loops based on fiber Sagnac interferometers. Inside the loop, the optical signals travelling clockwise and counter clockwise suffer differently the nonlinear effects and both signals interfere with different phases [19]. HNLF and NOLM are often used as building blocks of larger comb generation schemes known as parametric mixers. Parametric mixers have demonstrated ultra-wide optical combs (above 10THz) [20]. They are based on the concatenation of numerous nonlinear optical stages to optimize the generation of new frequencies from an initial dual optical source. Finally, the use of EO modulators in cascade configuration is one of the most commonly used technique for comb generation and/or expansion [21], [6], especially for high repetition rates above the modulation bandwidth of the laser source under use. Optical combs that cover above 3THz have been reported with EO modulators. Based on these approaches, we have designed three different schemes to increase the span of an initial VCSEL-OFC while maintaining the coherence between the comb lines. In order to undergo a fair comparison, all of them offer expansion ratios close to 3 times.

In section II, we present each of these expansion techniques and the OFCs experimentally obtained with them. Then, in section III, we present a detailed comparison and the features of the different resulting combs showing the main advantages and disadvantages of each expansion scheme.

II. Experimental Study on Optical Frequency Comb Expansion

In Fig. 1 we can see the initial comb to be expanded using several techniques. This seed comb is the Vertical-Cavity Surface-Emitting Laser (VCSEL) output spectrum under Gain Switching regime. This laser diode is a state of the technology fiber coupled 1550nm manufactured by VCSEL (VERTILAS VL-1550-8G-P2-H4) that is stabilized at 20ºC and biased at Ibias/Ith = 1.04. The VCSEL is modulated at 5.2 GHz with a 16 dBm RF signal (modulation depth of $I_{RF}/I_{bias} = 2.5$). Under these conditions we generate the broadest Optical Frequency Comb (OFC) [10] with 27 teeth in the 20dB span, which corresponds to 135GHz total bandwidth. An optical isolator is placed at the output of the VCSEL to avoid any optical feedback. We have given more details in this VCSEL device and its Continuous Wave (CW) and GS operation [15].

In the following sections we study and compare different expansion techniques taking several measurements of the resulting OFCs: the optical spectra, the RF beating of the OFC and the temporal autocorrelation traces (ACT). It is worth mentioning that an Erbium Dopped Fiber Amplifier (EDFA) is introduced for some RF beating measurements in order to equalize the received electrical power. Regarding the AC traces, as they exhibit a complex structure, typical of the GS technique, they have been analysed using time retrieval algorithms and root-mean square time-bandwidth metrics[22].

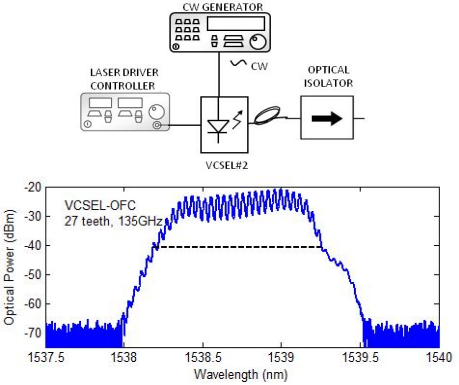

Fig. 1 Top: Setup used for the VCSEL-OFC and the resulting seed comb. Bottom: VCSEL output under Gain Switching obtained at 20 ºC, Ibias/Ith = 1.04, 5GHz, 16dBm. The VCSEL-OFC has 27 teeth in the 20dB span which corresponds to 135GHz. See text for more details.

In the following sections A, B and C, we present the three different schemes to expand this VCSEL-OFC. In order to offer a fair comparison among the techniques under study, we have considered implementations that offer similar output optical 20dB spans. Each expansion stage is formed by all the optical elements found after the output of the initial VCSEL-OFC. For the HNLF and the NOLM configurations, basic initial simulations based on rate equations and nonlinear Schrodinger equation (NLSE) [22] were carried out. This gave an estimation of the linear compression and amplification needs, as well as the configuration of the nonlinear elements to achieve an expansion ratio close to 3. Then, further experimental adjustments led to the final implementations presented here.

A. Comb expansion with non-linear fiber: HNLF-OFC

The first method described in this work to expand the VCSEL-OFC consists in the use of a Highly Non-Linear Fiber (HNLF). This scheme mainly exploits the enhanced Self Phase Modulation Effect (SPM) [23] exhibited by HNLF fibers and has been commonly used for comb expansion and broadband signal generation [6], [24], [25]. The expansion scheme is formed by two sub-stages. Prior to the nonlinear expansion itself, we find the first sub-stage where we condition the optical signal including a Dispersion Compensating Fiber (DCF) and an EDFA. With the DCF we linearly compress the pulses from the VCSEL-OFC as they are chirped because of the GS regime

[26]. This DCF fiber has a dispersion of -1318ps/nm, and a length of 1100m. Then the EDFA increases the optical power up to 22dBm (mean power) before the HNLF which is an optimum trade-off output power vs. noise floor. This sub-stage experimentally reduces the optical pulse duration (Full Width Half Maximum, FWHM) from 14.4ps to 6.07ps but does not influence the optical spectra. Finally, the HNLF is a 200m patch with a non-linear coefficient of $\gamma = 11$ $(W \cdot km)^{-1}$. The broadest comb has been obtained with the VCSEL biased at $I_{bias}/I_{th} = 1.2$, while the rest of the parameters are the values previously mentioned. This expansion scheme is shown in Fig. 2.

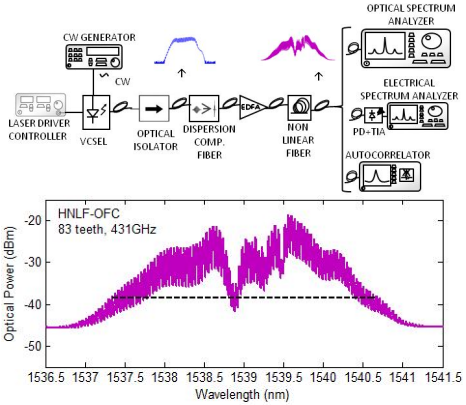

Fig. 2 Top: Setup used for the HNLF-OFC and the resulting comb. In the picture we can see the VCSEL which is first compressed with a DCF, secondly amplified with an EDFA and then broadened with a HNLF. The HNLF-OFC (pink trace), has 83 teeth in the 20dB span which corresponds to 431GHz. See text for more details.

This technique expands the VCSEL-OFC from 27 to 83 teeth, which corresponds to an expansion factor of 3.07 and 431GHz (20dB span). The resulting HNLF-OFC is not flat, especially in the area between 1538.5nm and 1539.5nm with a flatness factor is 0.12 (more details in Section III). The optical noise level has now increased to -45dBm having a dynamic range of 25.3dB. We believe that this degradation is likely to be related to the amplified spontaneous emission noise (ASE) of the EDFA amplifier. We experimentally found that any further increase in the optical gain of the EDFA would cause a dramatic growth of the noise floor without any further expansion of the OFC. However, this is a simple way to obtain broad combs with moderate energy consumption.

B. Comb expansion with NOLM: NOLM-OFC

Non-linear Optical Loop Mirrors (NOLM) are commonly used for pulse compression and reshaping, comb filtering, switching or multiplexing optical signals [22], [27], [28]. In this section, we propose this technique to expand the comb, therefore focusing on the spectral broadening achieved. These systems are basically nonlinear fiber Sagnac interferometers based on SPM [19]. Several set-ups have been tested for this work and our final loop includes a Semiconductor Optical Amplifier (SOA) as non-linear element inserted into the loop [22]. These systems are also called Non-linear Amplifier Loop Mirrors (NALM) [29]. SOAs devices are interesting here due to their strong non-linear operation, low power consumption and small size [18], [30].

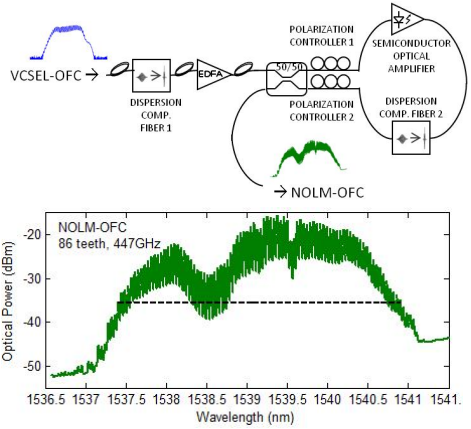

Fig. 3 Top: Setup used for the NOLM-OFC and the resulting comb. The VCSEL-OFC is first compressed and then amplified with a DCF and an EDFA. The NOLM "door" is a 50/50 coupler and it has inside a SOA another DCF and two polarization controllers. Bottom: The NOLM-OFC (green trace), has 86 teeth in the 20dB span which corresponds to 447GHz. See text for more details

The set-up used for this comb expansion based on a NOLM is depicted in Fig. 3. In order to maximize its performance, we included a sub-stage before the 50/50 coupler, at the entrance of the loop. At this sub-stage, the light signal is conformed using a DCF and an EDFA. The DCF is 600m long and it compresses the light pulse right before the EDFA (14.4ps to 6.07ps FWHM) so the peak power at the EDFA output is optimized. The output power of the EDFA in this set-up is 32dBm. Higher powers cannot be applied because of operational limits for the SOA. Another DCF fiber with the same characteristics is placed inside the loop with the SOA (QPhotonics QSOA-1550), and the best result has been obtained when this DCF has a length of 500m and the SOA is biased with 396mA. The set-up also includes two polarization controllers to match the clockwise and counter clockwise pulses making them interact in the way that we obtain the highest pulse compression and therefore, the comb broadening is optimized. In order to improve the NOLM-OFC, the bias current of the VCSEL has been changed to $I_{bias}/I_{th} = 1.2$ and the RF frequency is 5.2GHz.

The output comb has a 20dB span of 447GHz which corresponds to 86 teeth and an expansion factor of 3.18. We can see that the noise floor has been increased to -45dBm so the dynamic range at this point is 32dB and the flatness has been worsened too, presenting a flatness factor of 0.28. However, a significant amount of power is needed from the EDFA to

achieve an expansion factor close to 3.

C. Comb expansion with EO Modulators: EO-OFC

Apart from direct comb generation, like GS regime, in which the comb is generated inside the laser cavity, there exist indirect techniques in which the comb is generated with the laser working in CW operation and using external non-linear elements, typically Electro Optical (EO) modulators. This is the most common technique for comb generation and expansion, and has been deeply studied in previous works, using different amount of both Intensity Modulators (IM) and Phase Modulators (PM) [6], [21], [25]. EO modulators allow comb generation with high and tunable teeth spacing independently of the laser source used. Several of these modulators can be cascaded to broaden the comb about two times per modulator. These schemes generate very flat and tunable combs but, at the same time, the set-up is relatively complex to adjust specially the RF part. This fact together with the high cost and the energy consumption of the modulators are the main drawbacks of this technique.

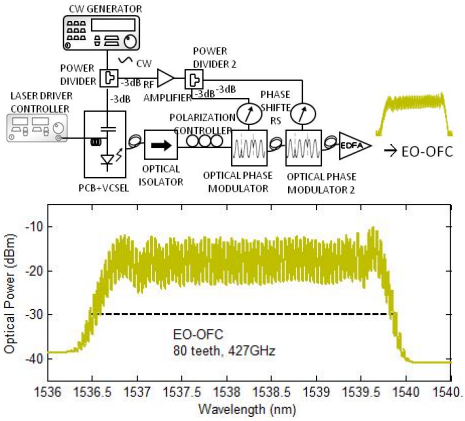

Fig. 4 Top: set-up used for the EO-OFC and the resulting comb. The VCSEL-OFC is broadened with two phase modulators in cascade. The RF signal is amplified and matched with the use of one amplifier and two phase shifters. Bottom: the EO-OFC (yellow trace), has 80 teeth in the 20dB span which corresponds to 427GHz. The VCSEL supply parameters are 20 ºC, 11.4mA, 5.3GHz, 16dBm. The RF injected into the modulators is 35dBm and the EDFA has an output power of 12.5dBm.

In one of our previous works [31], we have combined both the direct GS modulation to generate the comb and the indirect EO modulators (two PMs in cascade) to expand it afterwards obtaining a comb of 272GHz (53 teeth) in the 20dB span. Now we are using a similar set-up with modulators showing higher performance. They have ultra-low V_{pi} and wider modulation bandwidth. The output of the laser under GS (VCSEL-OFC in Fig. 1) enters two PMs with V_{pi} <3.3V placed in cascade configuration. The RF signals driving them are first amplified and after that, phase matched using Phase Shifters (PS) so the expansion is optimized. Finally, the output signal is amplified in the EDFA to increase the signal level to 12.5dBm. It is important to notice that this EDFA is not necessary in the set-up to expand the comb like in the previous schemes, but to increase the signal to a similar power level compared to the previous optical combs. This set-up is shown in Fig. 4. EO schemes typically include intensity modulators (IM) to improve the flatness of the resulting comb. However, when the GS technique is used, the flatness is optimum and no extra modulator is needed, reducing the cost and size of the OFC.

With this technique that combines GS and high performance EO modulators we have expanded the comb a factor 2.96 which means 80 teeth in the 20dB span, so 427GHz broad taking into account that the RF signal is set at 5.3GHz. This comb exhibits a high flatness factor of 0.87; and a dynamic range of 28.8dB. This value was measured after the levelling EDFA. Without it, the dynamic range slightly increases to 31dB. On the other hand, this set-up is the costliest of the ones presented here and requires more complicated adjustments (more details in Section III).

III. Optical Frequency Combs Comparison

In the previous sections we have presented different configurations for comb expansion based on different non-linear processing techniques. All of them allow us to increase the comb span about three times compared to the bandwidth obtained with the sole VCSEL under GS regime. However, each of these schemes has different potentials and weaknesses and this might determine their use in certain applications. In this section we are comparing different features of the resulting combs and each set-up, analyzing their advantages and disadvantage. The factors here analyzed are summarized in TABLE I. In Fig. 5 we can see a comparison of the different combs with the same ranges of wavelengths and optical powers.

Comb expansion factor: Along this work we use the 20dB span to measure the broadness of the comb, as we have done in our previous works because it is the useful span in applications like photonic THz generation [3]. NOLM-OFC provides the broadest comb. In this work we have defined the expansion factor as the coefficient between the comb teeth in the output comb and the comb teeth in the VCSEL-OFC. This factor is, as we see in TABLE I 3.00, 3.07 and 3.18 for the EO-OFC (the narrowest), the HNLF-OFC and the NOLM-OFC (the broadest) respectively.

Flatness: The flatness is an important parameter for many applications. In this work we have defined the flatness factor as the coefficient between the comb teeth in the 3dB and the 20dB spans. The flatness in VCSEL-OFC is 0.77 which is quite good but is even improved with the EO-OFC set-up with a flatness factor of 0.87. This EO-OFC provides much flatter combs in comparison to the other methodologies. On the other hand, NOLM-OFC has a flatness factor of 0.28 and HNLF-OFC presents the lowest flatness, with a factor of 0.12.

Pulse quality: We have also evaluated the properties of the temporal pulses associated to each expansion configuration measuring their background-free autocorrelation traces (ACT). The resulting traces (Fig. 6) are complex and exhibit different shapes with pedestals. This is typical of the GS technique and such traces have to be analysed using time retrieval algorithms

[22] and evaluated using metrics such as the root mean square (*rms*) Time Bandwidth Product: $TBP_{rms} = \omega_{rms}\,\tau_{rms}$, where ω_{rms} is the *rms* width of the optical spectra and τ_{rms} is the *rms* pulse width. Regardless of the pulse shape or spectral structure, the fundamental limit of TBP_{rms} is 0.5 [32]. The use of the *rms* metric permits the comparison among pulses and spectra that do not exhibit the same profile. The results are shown in TABLE I and summarized in figure 6. The EO-OFC configuration is the one offering pulses with slightly better characteristics (TBP_{rms} = 7.2). However, all the configurations behave in a similar way and significantly increase the dispersion of the initial optical pulses. These dispersed pulses could be further compressed to their TBP_{rms} limit using linear compression techniques.

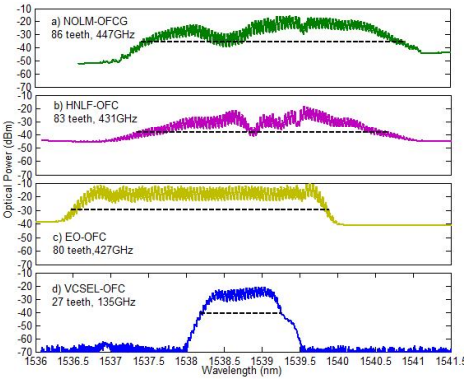

Fig. 5 Optical Spectra comparison. a)NOLM-OFC (green trace) with 86 teeth/447GHz. b)HNLF-OFC (pink trace) with 83 teeth/431GHz. c) EO-OFC (yellow trace) with 80 teeth/427GHz. d) VCSEL-OFC (blue line) with 27 teeth/135GHz. All these OFCs are presented with the same optical power and wavelenght ranges for an easier comparison. The 20dB span is marked with a dotted black line.

Frequency spacing tunability: All these expansion techniques admit the tuning of the spacing between comb teeth. For this purpose, we first need to adjust to its new value the RF frequency that modulates the VCSEL. After this, some adjustments of the set-up are needed depending on the scheme used for the comb expansion. For the HNLF-OFC, no extra adjustment is needed. This is the most direct set-up to change the distance between comb teeth. The NOLM-OFC needs some equalization of the optical paths inside the loop and therefore the Polarization Controllers (PC) in order to maintain the optical span as high as possible. The most complicated set-up to change the comb spacing is the EO-OFC: it needs optical adjustment of the polarization in the PC placed before the first PM but also RF readjustment in both Phase Shifters. Regarding the VCSEL-OFC, a change in the frequency spacing slightly affects the optical span and the flatness as long as it remains within the VCSEL electronic modulation bandwidth (more details in [33]).

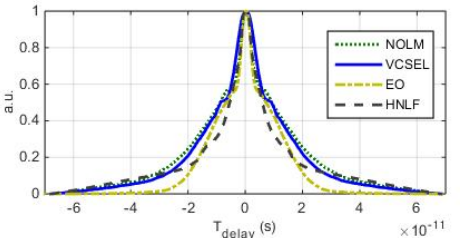

Fig. 6 Autocorrelation traces (ACTs). Solid: VCSEL-OFC ACT with TBPrms = 3. Slash: HNLF-OFC ACT with TBPrms = 10. Dot: NOLM-OFC ACT with TBPrms = 8.8. Slash/Dot: EO-OFC trace with TBPrms = 7.2

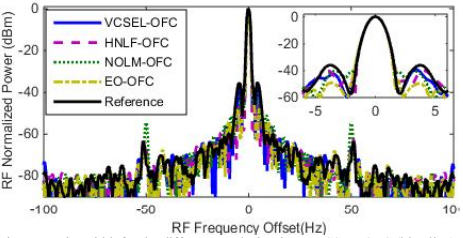

Fig. 7 RF Linewidth for the different combs in Fig. 5: VCSEL-OFC (blue line), HNLF-OFC (pink line), NOLM-OFC (green line), EO-OFC (yellow line) and Reference: linewidth of the RF CW signal used to induce GS (black line). In the inset we plot a zoom obtained with the lower Resolution Bandwidth available in the ESA used. Resolution bandwidth and video bandwidth were set to 1Hz. These measurements are limited by the equipment capabilities. See text for more details. Side-peaks at 50Hz are spurious coming from the Reference.

Optical dynamic range (DR): The inclusion of new elements along the path implies some losses in the DR, which has been measured in this work as the difference between the peak power in the highest comb tooth and the noise level. In our set-ups the DR is reduced from 50dB in the VCSEL-OFC to 25.3, 28.8 and 32dB for the HNLF-OFC, EO-OFC and NOLM-OFC respectively. NOLM-OFC is therefore, the most resistant scheme to the noise. This is consistent with the nonlinear interferometric nature of the NOLM, that filters out low power signal components and hence, reduces noise [34].

Electrical linewidth: The electrical beat tone signal at f_{RF} allows us to evaluate the phase coherence between comb teeth. In this work, we measure the 3dB linewidth of that signal at f_{RF} after the detection of the whole comb in a fast photodiode and compare it to the linewidth of the reference, which is the RF source that modulates the VCSEL-OFC under GS. The measurements were performed using a resolution bandwidth of 1Hz, the minimum offered by the ESA. In Fig. 7, we see that all the comb expansion schemes present an electrical beat tone with a linewidth equal to 1Hz, the resolution limit of the equipment. This implies that every set-up provides a comb with an extremely high coherence between teeth, inherited from the VCSEL-OFC due to GS modulation.

Installation and start sequence: Another important aspect to consider when selecting the expansion scheme is the complexity when installing the set-up and the need of

readjustments after operation. HNLF-OFC is the simplest scheme and the only parameter to be adjusted during turn-on is the output power in the EDFA. NOLM-OFC needs some other adjustments besides the EDFA output power: the polarization needs to be adjusted with the PCs inside the loop. This optical path needs some fine-tuning also each time the set-up is ignited. Lastly, EO-OFC is the most complex set-up to be installed as both, optical and electrical components, need to be tuned: the optical polarization at the entrance of the PM is optimized with the PC but also the RF phase shifters need a careful fine-tuning during installation and switching-on.

TABLE I
OPTICAL FREQUENCY COMBS MAIN FEATURES

	VCSEL-OFC	HNLF-OFC	NOLM-OFC	EO-OFC
Optical span @20dB	135GHz /27 teeth	431 GHz / 83 teeth	447GHz / 86 teeth	427 GHz / 80 teeth
Optical span @10dB	125GHz /24 teeth	296GHz /57 teeth	333GHz /64 teeth	403GHz /76 teeth
Optical span @3dB	105GHz /21 teeth	52GHz /10 teeth	125GHz /24 teeth	371GHz /70 teeth
Optical span @20dB (nm)	1.1	3.33	3.5	3.41
Expansion factor	1	3.07	3.18	2.96
TBPrms	3	10	8.8	7.2
Flatness factor	0.77	0.12	0.28	0.87
Dynamic range (dB)	50	25.3	37	28.8
Linewidth RF (3dB)	<1Hz	<1Hz	<1Hz	<1Hz
Energy consumption (W)	-	1.99W	8.12W	2.39W

Energy consumption: We have made an estimation of the energy consumption of each expansion technique by calculating the electrical power needed in the active elements that are included after the VCSEL-OFC. This is an important parameter when working in fields like green optical communications [17] or incorporating such schemes in actual systems. These elements are the EDFA in all the set-ups, the SOA in the NOLM-OFC and both PMs in the EO-OFC. The power in the EDFA has been computed with the laser current set in the device for each set-up and assuming a typical 980nm pump LD with a diode operating voltage of 1.7V [35]. The results are shown in TABLE I where we see that the NOLM-OFC consumes much more power than the other set-ups. This is mainly due to the high optical power needed at the output of the EDFA (32dBm) to achieve maximum expansion in the loop as this component consumes 7.47W by itself and the SOA needs 0.65W in this configuration. The EO-OFC consumes 1.13W in the EDFA and 1.26W in the two PMs, so this set-up has lower energy needs compared to the previous one. Finally the HNLF-OFC, in which the EDFA is the only active component, has the lowest energy needs, with 1.99W.

Component count and cost: HNLF-OFC is the set-up that needs lower number of components in the expansion stage, two fibers (one DCF and one HNLF) and the EDFA. NOLM-OFC is the one with larger (optical) component count as it includes, apart from all these components, another DCF, the coupler, one SOA and two PCs. However, the costliest set-up is EO-OFC as the electro-optical modulators are very specific and expensive components.

IV. Conclusions

In this work, we have presented out latest results in Optical Frequency Combs (OFCs) based on Vertical-Cavity Surface-Emitting Lasers (VCSELs) under Gain Switching (GS) regime. We have shown different expansion techniques that produce results of combs around 430GHz in the 20dB span, and them all maintain the high coherence offered by the seed VCSEL-OFC. All our set-ups have been implemented with off the shelf components and Laser Diodes (LDs) which allow us to obtain effective, efficient in cost and energy, and compact OFC systems. The use of VCSELs enhanced these factors and provides even wider combs while GS modulation allows us to tune the comb easily with no need of extra components obtaining a system that can be tailored for different applications. For all this reasons we find our VCSEL-based OFCs of significance, and that is why we focus our efforts in improving their capabilities.

Besides, in this work we have presented a thorough comparison of different expansion techniques applied to VCSEL-based OFCs showing that they stand out in different aspects. Therefore, we conclude that the expansion scheme needs to be tailored depending on each particular comb application if we want to optimize the result. For instance, the EO-OFC is the one that provides the flattest but the most complex and costliest scheme. On the other hand, the HNLF-OFC is the simplest, most energy efficient and cheapest comb but it depends on the laser source and the GS regime and the flatness is low. NOLM-OFC is a balanced option, with a high noise rejection and the broadest comb but depends on the source, exhibits low flatness and has a higher energy consumption. These differences will make each of these set-ups more or less interesting depending on each specific application, so the appropriate selection of the expansion technique will maximize the performance of a system that includes an OFC generation stage in it.

Our efforts continue in order to improve the broadness of the resulting combs and reach the 1THz 20dB span while maintaining the simplicity, compactness and energy consumption VCSEL-based combs offer.

V. Acknowledgments

The authors would like to thank VERTILAS for providing the VCSELs, Luz Wavelabs S.L. for their technical support and the Spanish Ministry of Economy and Competitiveness who supports the project under the RTC-2014-2661-7 and TEC-2014-52147-R.

REFERENCES

[1] P. J. Delfyett, I. Ozdur, N. Hoghooghi, M. Akbulut, J. Davila-Rodriguez, and S. Bhooplapur, "Advanced Ultrafast Technologies Based on Optical Frequency Combs," *IEEE J. Sel. Top. Quantum Electron.*, vol. 18, no. 1, pp. 258–274, Jan. 2012.

[2] C. Chen, C. Zhang, D. Liu, K. Qiu, and S. Liu, "Tunable optical frequency comb enabled scalable and cost-effective multiuser orthogonal frequency-division multiple access passive optical network with source-free optical network units," *Optics Letters*, vol. 37. p. 3954, 2012.

[3] A. R. Criado, C. de Dios, E. Prior, G. H. Dohler, S. Preu, S. Malzer, H. Lu, A. C. Gossard, and P. Acedo, "Continuous-Wave Sub-THz Photonic Generation With Ultra-Narrow Linewidth, Ultra-High Resolution, Full Frequency Range Coverage and High Long-Term Frequency Stability," *IEEE Trans. Terahertz Sci. Technol.*, vol. 3, no. 4, pp. 461–471, Jul. 2013.

[4] P. Martin-Mateos, M. Ruiz-Llata, J. Posada-Roman, and P. Acedo, "Dual-Comb Architecture for Fast Spectroscopic Measurements and Spectral Characterization," *IEEE Photonics Technol. Lett.*, vol. 27, no. 12, pp. 1309–1312, Jun. 2015.

[5] T. Udem, R. Holzwarth, and T. W. Hänsch, "Optical frequency metrology.," *Nature*, vol. 416, no. 6877, pp. 233–7, Mar. 2002.

[6] R. Wu, V. Torres-Company, D. E. Leaird, and A. M. Weiner, "Supercontinuum-based 10-GHz flat-topped optical frequency comb generation," *Opt. Express*, vol. 21, no. 5, p. 6045, Mar. 2013.

[7] S. B. Bernfeld, "Stabilization of a Femtosecond Laser Frequency Comb," 2009.

[8] T. P. McKenna, J. H. Kalkavage, M. D. Sharp, and T. R. Clark, "Wideband Photonic Compressive Sampling System," *J. Light. Technol.*, vol. 34, no. 11, pp. 2848–2855, Jun. 2016.

[9] X. Zhang, M. Williams, S. T. Cundiff, and J. N. Kutz, "Semiconductor Diode Laser Mode-Locking by a Waveguide Array," *IEEE J. Sel. Top. Quantum Electron.*, vol. 22, no. 2, pp. 34–39, Mar. 2016.

[10] T. J. Kippenberg, R. Holzwarth, and S. A. Diddams, "Microresonator-Based Optical Frequency Combs ," *Sci.* , vol. 332 , no. 6029 , pp. 555–559, Apr. 2011.

[11] P. M. Anandarajah, S. P. O. Duill, R. Rui Zhou, and L. P. Barry, "Enhanced Optical Comb Generation by Gain-Switching a Single-Mode Semiconductor Laser Close to Its Relaxation Oscillation Frequency," *IEEE J. Sel. Top. Quantum Electron.*, vol. 21, no. 6, pp. 592–600, Nov. 2015.

[12] R. Michalzik, *VCSELs*, vol. 166. Springer Berlin Heidelberg, 2013.

[13] H. E. Li and K. Iga, *Vertical-Cavity Surface-Emitting Laser Devices*, vol. 6. Springer Berlin Heidelberg, 2003.

[14] E. Kapon and A. Sirbu, "Long-wavelength VCSELs: Power-efficient answer," *Nat. Photonics*, vol. 3, no. 1, pp. 27–29, Jan. 2009.

[15] A. R. Criado, C. de Dios, E. Prior, M. Ortsiefer, P. Meissner, and P. Acedo, "VCSEL-Based Optical Frequency Combs: Toward Efficient Single-Device Comb Generation," *IEEE Photonics Technol. Lett.*, vol. 25, no. 20, pp. 1981–1984, Oct. 2013.

[16] A. Consoli Barone, "Short pulse generation from semiconductor lasers: characterization, modeling and applications," E.T.S.I. Telecomunicación (UPM), 2011.

[17] R. S. Tucker, "Green Optical Communications—Part I: Energy Limitations in Transport," *IEEE J. Sel. Top. Quantum Electron.*, vol. 17, no. 2, pp. 245–260, Mar. 2011.

[18] G. P. Agrawal, *Nonlinear Fiber Optics*. Academic Press, 2012.

[19] N. J. Doran and D. Wood, "Nonlinear-Optical Loop Mirror," *Opt. Lett.*, vol. 13, no. 1, pp. 56–58, 1988.

[20] V. Ataie, E. Myslivets, B. P.-P. Kuo, N. Alic, and S. Radic, "Spectrally Equalized Frequency Comb Generation in Multistage Parametric Mixer With Nonlinear Pulse Shaping," *J. Light. Technol.*, vol. 32, no. 4, pp. 840–846, Feb. 2014.

[21] S. Ozharar, F. Quinlan, I. Ozdur, S. Gee, and P. J. Delfyett, "Ultraflat Optical Comb Generation by Phase-Only Modulation of Continuous-Wave Light," *IEEE Photonics Technol. Lett.*, vol. 20, no. 1, pp. 36–38, Jan. 2008.

[22] C. de Dios and H. Lamela, "Improvements to Long-Duration Low-Power Gain-Switching Diode Laser Pulses Using a Highly Nonlinear Optical Loop Mirror: Theory and Experiment," *J. Light. Technol.*, vol. 29, no. 5, pp. 700–707, Mar. 2011.

[23] G. P. Agrawal, "Highly Nonlinear Fibers," in *Applications of Nonlinear Fiber Optics (Second Edition)*, P. A. Govind, Ed. Burlington: Academic Press, 2008, pp. 397–446.

[24] A. Cerqueira Sodre, J. M. Chavez Boggio, A. A. Rieznik, H. E. Hernandez-Figueroa, H. L. Fragnito, and J. C. Knight, "Highly efficient generation of broadband cascaded four-wave mixing products," *Opt. Express*, vol. 16, no. 4, p. 2816, Feb. 2008.

[25] T. Yang, J. Dong, S. Liao, D. Huang, and X. Zhang, "Comparison analysis of optical frequency comb generation with nonlinear effects in highly nonlinear fibers," *Opt. Express*, vol. 21, no. 7, p. 8508, Apr. 2013.

[26] C. Peucheret, "Direct Current Modulation of Semiconductor Lasers." 2011.

[27] K. L. Lee, M. P. Fok, S. M. Wan, and C. Shu, "Optically controlled Sagnac loop comb filter," *Opt. Express*, vol. 12, no. 25, p. 6335, Dec. 2004.

[28] O. Pottiez, R. Paez-Aguirre, H. Santiago-Hernandez, M. Duran-Sanchez, B. Ibarra-Escamilla, E. A. Kuzin, and A. Gonzalez-Garcia, "Characterizing the Statistics of a Bunch of Optical Pulses Using a Nonlinear Optical Loop Mirror," *Math. Probl. Eng.*, vol. 2015, pp. 1–10, 2015.

[29] M. E. Fermann, F. Haberl, M. Hofer, and H. Hochreiter, "Nonlinear Amplifying Loop Mirror," *Opt. Lett.*, vol. 15, no. 13, pp. 752–754, 1990.

[30] Y. S. and H. Rezig, *Advances in Optical Amplifiers*. InTech, 2011.

[31] E. P. Cano, C. de Dios Fernandez, A. R. C. Serrano, M. Ortsiefer, P. Meissner, and P. Acedo, "Experimental Study of VCSEL-Based Optical Frequency Comb Generators," *IEEE Photonics Technol. Lett.*, vol. 26, no. 21, pp. 2118–2121, Nov. 2014.

[32] R. Trebino, *Frequency-Resolved Optical Gating: The Measurement of Ultrashort Laser Pulses*. Boston, MA: Springer US, 2000.

[33] E. Prior, C. De Dios, M. Ortsiefer, P. Meissner, and P. Acedo, "Understanding VCSEL-Based Gain Switching Optical Frequency Combs: Experimental Study of Polarization Dynamics," *J. Light. Technol.*, vol. 33, no. 22, pp. 4572–4579, Nov. 2015.

[34] C. de Dios and H. Lamela, "Noise influence in nonlinear optical loop mirror compression performance," in *Semiconductor Lasers and Laser Dynamics II*, 2006, 1st ed., vol. 6184, pp. 618425–618428.

[35] "Product Specifications 980nm Single-Mode Laser Diodes - Axcel Photonics." .

Paper D. JLT2015

E. Prior, C. De Dios, M. Ortsiefer, P. Meissner, and P. Acedo, "Understanding VCSEL-Based Gain Switching Optical Frequency Combs: Experimental Study of Polarization Dynamics," J. Light. Technol., vol. 33, no. 22, pp. 4572–4579, Nov. 2015. doi: 10.1109/JLT.2015.2476956

Understanding VCSEL-Based Gain Switching Optical Frequency Combs: Experimental Study of Polarization Dynamics

Estefanía Prior, Cristina De Dios, Markus Ortsiefer, Peter Meissner, *Member, IEEE*, and Pablo Acedo, *Member, IEEE*

***Abstract*—In this paper, we carry out an experimental study on the polarization properties of a vertical-cavity surface-emitting laser (VCSEL) working under gain switching (GS) regime and the characteristics of the resulting optical frequency comb signal. We have observed that each of the two polarization modes presented in the VCSEL continuous wave emission spectrum generate a separate optical frequency comb (OFC) whose modes are phase correlated thanks to the GS regime. We study how these combs associated with the main and orthogonal polarization modes, respectively, vary depending on the input parameters to the VCSEL (bias current and radio-frequency power and frequency). The correlation between both OFCs in the best operation point as defined by the OFC characteristics is also evaluated. Therefore, this study demonstrates that two orthogonally polarized combs are generated that exhibit a high correlation between each other that combine to produce a wider overall optical comb. Hence, we can predict the feasibility of dual-polarization VCSEL-based OFC generators in the few gigahertz repetition frequency rates, with highly correlated modes and continuously tunable distance between them, in a compact and energy- and cost-efficient system that can find application in ultrafast laser dynamics studies and or in polarization-division multiplexing optical communications.**

***Index Terms*—Energy efficiency, gain switching (GS), laser diodes (LDs), optical frequency comb generator (OFCG), orthogonal mode, polarization switching, vertical-cavity surface-emitting laser (VCSEL).**

I. Introduction

OPTICAL frequency comb generators (OFCG) are versatile systems that find application in many disciplines like spectroscopy [1], optical communications [2], THz generation [3], optical arbitrary waveform generation, metrology, or microwave photonic [4]. Among OFCGs, those based on cost of the shelf (COTS) laser diodes (LDs) are interesting systems since they offer compactness and cost efficiency.

There are numerous diode laser technologies. One of the most interesting ones is vertical-cavity surface-emitting laser (VCSEL) devices [2], [5], [6]. Previous studies have demonstrated that VCSEL diode lasers under gain switching (GS) regime [7] produce record combs in terms of energy efficiency and mode coherence. The interest of such combs could be extended if wider optical spans could be achieved while maintaining its high quality capabilities. In this sense, the use of external comb extension techniques, like electro-optical modulators could be detrimental as they are costlier components and have higher energy needs [8]. A deeper understanding of the dynamics of VCSEL under GS to generate optical combs could help us comprehend how to obtain wider combs using a single stage OFCG. This is the main focus of this experimental work, where we will center our attention in the polarization dynamics of VCSEL devices under GS operation to produce optical frequency combs. VCSELs are typically considered to be single-longitudinal-mode devices. However, their emission consists of two linearly polarized modes with orthogonal polarizations that, due to anisotropies in the materials, emit at different wavelengths [2], [9]. Manufacturers have developed effective techniques to minimize this duality and present devices that exhibit a side mode suppression ratio above 30 dB, what makes this device purely monomode for many applications. However, we believe that this suppressed mode can play an important role in VCSEL-based OFCG.

In this work we present new results on our study of VCSEL-based GS-OFCGs. We evaluate the dynamic behaviour of these two orthogonal modes of polarization present in a VCSEL under GS and how this affects the overall OFCG. We have observed that each polarization mode generates a separate optical comb and we have analysed the evolution of each of them with the input parameters that determine the GS operation of a VCSEL device (bias and RF modulation). On the other hand, and more importantly, we have seen how these orthogonally polarized combs that appear are related in phase and collaborate to produce a wider overall total comb. This is remarkable if we take into account that the two modes present high anticorrelation if no modulation is applied as it is stated in [10], [11]. Therefore, this will imply that the phase correlation is caused by the GS regime. This result suggests that an enhancement of the emission of the secondary mode, through fabrication or external injection techniques, would help overcome one of the disadvantages of

Manuscript received June 10, 2015; revised July 30, 2015; accepted August 10, 2015. Date of publication September 6, 2015; date of current version September 30, 2015. The work of E. Prior was supported by the Spanish Ministry of Economy and Competition under the Retos-Colaboración Program, RTC-2014-2661-7 in collaboration with Luz WaveLabs S.L. This work was supported by the Spanish Ministry of Economy and Competitiveness under RTC-2014-2661-7 and TEC-2014-52147-R Grants.

E. Prior, C. De Dios, and P. Acedo are with the Electronics Technology Department, Universidad Carlos III de Madrid, Leganés, Madrid 28911, Spain (e-mail: eprior@ing.uc3m.es; cdios@ing.uc3m.es; pag@ing.uc3m.es).

M. Ortsiefer is with Vertilas GmbH, Munich 85748, Germany (e-mail: ortsiefer@vertilas.com).

P. Meissner is with the Technische Universität Darmstadt, Darmstadt 64289, Germany (e-mail: meissner@imp.tu-darmstadt.de).

Color versions of one or more of the figures in this paper are available online at http://ieeexplore.ieee.org.

Digital Object Identifier 10.1109/JLT.2015.2476956

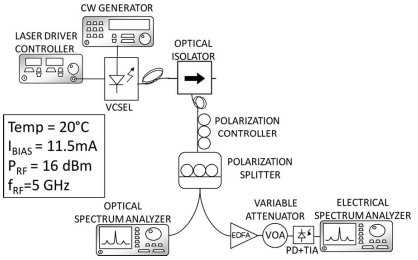

Fig. 1. Experimental set-up. The comb is generated inside the VCSEL and both polarization components are split and presented at each output of the PS. The optical and electrical spectra are measured in the OSA and ESA respectively. See text for details.

this OFCG, which is the limited optical span, if compared to more complicated sources. Another advantage is that the availability of two coherent combs with orthogonal polarizations can find applications in ultrafast laser dynamics studies [12] or in polarization-division multiplexing optical communications [13].

II. Experimental Study

Fig. 1 details the experimental set-up we have used for the present work. The VCSEL diode laser device under study is a state of the technology device (VERTILAS VL-1550-8G-P2-H4) provided together with a specific board for radiofrequency (RF) operation within the laser bandwidth. The comb is generated inside the VCSEL cavity using the non-linear GS regime. Under GS operation, a large RF signal is injected in the laser cavity forcing its pulsed operation. Therefore an optical comb is created in the frequency domain. In our experiments, we will mainly use the VCSEL temperature stabilized at 20 °C with a bias current of 11.5 mA and an input RF signal of 16 dBm at 5 GHz (Fig. 1). Any change on these parameters will be noted in the text. This is the working point where we found the best optical comb characteristics, as it will be explained in the next section.

After the VCSEL, an optical isolator is placed to avoid any optical feedback. The output of the VCSEL is composed of two modes orthogonally polarized that are split with a polarization controller (PC) and a fiber polarization splitter (PS) from Thorlabs (PBC1550PM-APC). We will measure the optical spectra in an optical spectrum analyzer (OSA) with 0.002 nm resolution and the electrical spectra in an electrical spectrum analyzer (ESA) using an ultrafast 50 GHz photodetector. Before the photodetector, an erbium-doped fiber amplifier and a variable optical attenuator are used to equalize the carrier power when needed.

In this work, *P* or *total signal* is the total output power of the VCSEL, including the main mode *Px,* with parallel polarization, and the suppressed side mode *Py,* with orthogonal polarization.

In Fig. 2 we show the PI curves of the two modes with orthogonal polarizations: *Px* and *Py* in dBm. These optical powers have been measured placing a powermeter after each output of the PS and tuning carefully the PC to maximize the contribution of the mode of interest (*Px* or *Py*).

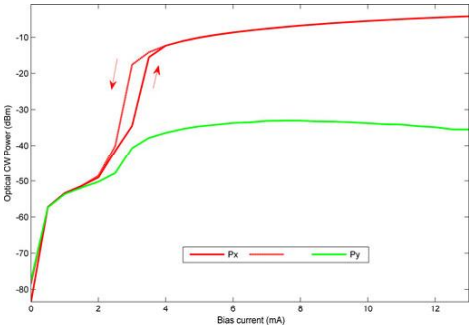

Fig. 2. PI Curves for *Px* and *Py*. The main polarization mode, *Px*, emits most of the power at the output of the VCSEL and the orthogonal mode power is > 40 dB below the main mode.

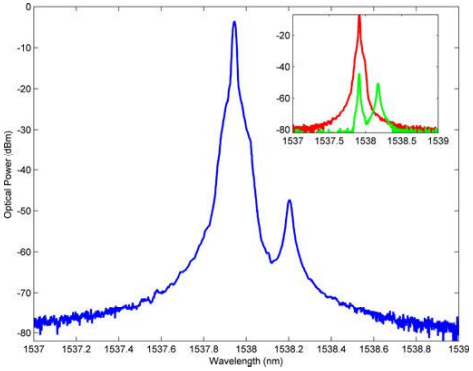

Fig. 3. CW emission spectra for *P*, *Px* and *Py*. The dominant main mode in *P* at 1537.95 nm is more than 40 dB above the residual orthogonal mode shown at 1538.20 nm. The birefringence of this VCSEL is 31.21 GHz. Both outputs of the PS selecting *Px* (red line) and *Py* (green line) respectively are presented in the figure inset.

Below and around threshold ($I_{\mathrm{BIAS}} = 2.5$ mA) both components have similar power levels. Above threshold, *Px* and *Py* are always present but the main mode, *Px*, emits most of the total power (*Px*/*Py* > 40 dB). However, the orthogonal mode shows an increase in emission >10 dB when crossing the threshold, what means it can be considered a lasing mode. We also observe hysteresis around threshold in the PI curves in both modes that shows a parallel evolution with respect to each other. From these results we conclude that the device under study exhibits a stable emission without polarization switching bistable regions. Following the classification of [14], this VCSEL is type c because both modes lase at the same time.

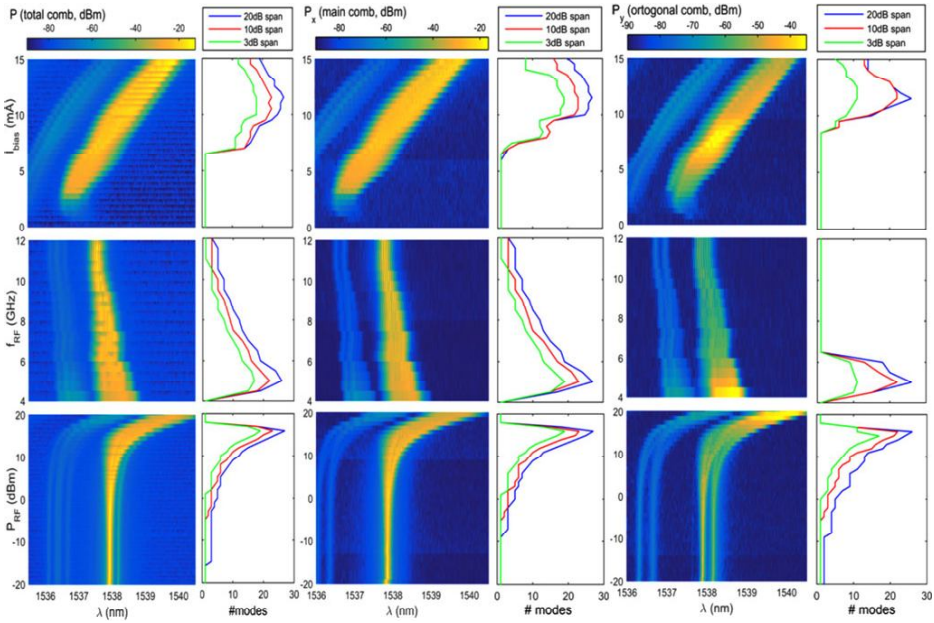

Fig. 4. Left: total comb (*P*-OFCG): maps with its evolution with bias current, RF frequency and RF power respectively and curves detailing the number of modes at 3, 10, and 20 dB spans. Center: Main comb (*Px*-OFCG) maps with its evolution with bias current, RF frequency and RF power respectively, and curves detailing the number of modes. Right: Orthogonal comb (*Py*-OFCG) maps with its evolution with bias current, RF frequency and RF power respectively, and curves detailing the number of modes. The broadest comb for the three signals under study—*P*, *Px* and *Py*—occurs at T = 20 °C, $I_{\rm bias} = 11.5$ mA, $f_{\rm RF} = 5$ GHz and $P_{\rm RF} = 16$ dBm.

In Fig. 3 we can see that at 11.5 mA the VCSEL presents a clear main *Px* mode at 1537.95 nm with −4.2 dBm peak power and an orthogonal *Py* mode at 1538.20 nm with −47.3 dBm. Then, there is a 43.1 dB power ratio between the *Px* and *Py* signals and the frequency difference of the modes with orthogonal state of polarisation due to the birefringence of the laser amounts to 31.21 GHz, what is consistent with the manufacturer's specifications.

The signals at each output of the PS, *Px* and *Py* are also shown (inset Fig. 3). When the *Py* signal is selected (light with orthogonal polarization), a residual part of the main *Px* mode is still detectable even if the PS component reduces its contribution more than 30 dB. Using several PS elements in cascade to improve the polarization selectivity gives the same result as in Fig. 3, so it does not improve the selectivity as, at the output of the first component the polarization in both wavelengths is now the same. Then, from now on, *Px signal* is the light at the output of the VCSEL with parallel polarization, which coincides with the main lasing mode and *Py signal* is constituted by all the light with orthogonal polarization, including the secondary mode and a residual part (minimized but still detectable) of the light of the main mode.

A. Optical Frequency Comb Generation and Characteristics

Under GS operation, the VCSEL generates different optical combs depending on the amount of RF power injected to modulate the laser ($P_{\rm RF}$), its frequency ($f_{\rm RF}$), and the bias current applied ($I_{\rm BIAS}$). In Fig. 4 we depict the maps detailing the evolution of the total comb of the VCSEL *P*-OFCG (left), the *Px*-OFCG (centre) and the *Py*- OFCG (right) when each of these parameters change with respect to the reference values mentioned above. For each comb we show three maps and three figures. The figures correspond to the number of modes exhibited by the comb under study when each of the parameters controlling the GS regime changes. The number of modes is evaluated considering 3 dB, 10 dB and 20 dB optical bandwidths. For applications such as THz photonic generation, the useful optical span can be defined up to 20 dB [15]. For optical communications, the flatness of the comb is more critical and the useful modes lie within a 3 or 10 dB bandwidth [16]. This is why we have evaluated the comb span using several metrics.

In Fig. 4(left) we observe that the total *P*-OFCG redshifts when $I_{\rm BIAS}$ increases. The broadest comb is obtained at 11.5 mA. The RF frequency affects the comb differently and its width decreases with the frequency when we try to drive

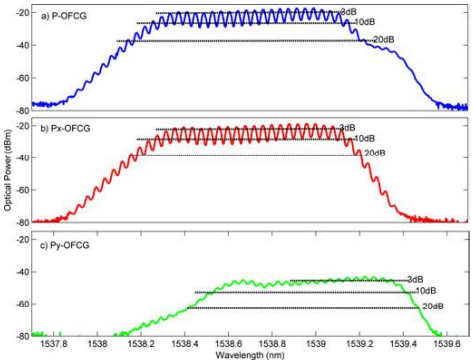

Fig. 5. Best point combs obtained at 20 °C, 11.5 mA, 5 GHz, 16 dBm. (a) The upper line corresponds to the total output of the VCSEL, P-OFCG, with both polarization modes included. (b) The middle line is the comb *Px*-OFCG, generated only with the parallel polarization signal. (c) The lower line is the comb *Py*-OFCG which has the orthogonal polarization. The combs *P*-OFCG and *Px*-OFCG have 27 lines in the 20 dB span which corresponds to 135 GHz bandwidth. The comb *Py*-OFCG has one mode less, 26 in total, so the bandwidth in this case is 130 GHz.

the device above the modulation bandwidth of the laser (around 5 GHz), what weakens the GS regime. The broadest comb in this case, appears at 5 GHz. Finally, the comb evolution with the RF power shows how the comb broadens with the injection of power, as the GS regime accentuates. However, above 17 dBm, the device enters into period doubling operation and the total comb does not broaden any further. We are not interested in this nonlinear regime of the VCSEL as our focus now is a tunable comb with a directly controllable repetition frequency equal to f_{RF}. Therefore, the broadest comb takes place for 11.5 mA, 5 GHz and 16 dBm. In Fig. 4(left) (upper figure, blue line) we show this comb, which has a total of 27 lines which corresponds to 135 GHz considering 20 dB span.

The same evolution study has been done for *Px* and *Py*. It is very interesting to note that the characteristics of these subcombs are similar to the ones presented by the total *P*-comb: we observe the red-shift associated to the increase of the bias current and the opposite happens with the RF frequency due to the modulation bandwidth of the VCSEL. For both *Px* and *Py*, the optimum comb in terms of span occurs at $I_{\mathrm{BIAS}} = 11.5$ mA, $f_{\mathrm{RF}} = 5$ GHz and $P_{\mathrm{RF}} = 16$ dBm. Varying these parameters will imply either a narrower comb or the appearance of period doubling operation. Of course, the orthogonal mode exhibits an optical comb with lower optical power and a slightly higher central wavelength. However, the power ratio between the *Px* and *Py* optical combs is now only 26 dB, when it reached 43.1 dB under CW operation. This is one of the most important results of our study as the GS regime enhances the power associated to the orthogonally polarized signal *Py*.

In Fig. 5 we analyse the optical combs generated in the best operation point in terms of optical span and flatness described before ($T = 20$ °C, $I_{\mathrm{BIAS}} = 11.5$ mA, $f_{\mathrm{RF}} = 5$ GHz, $P_{\mathrm{RF}} = 16$ dBm). For this study, we have defined the comb flatness as the ratio of the 3 dB to the 10 dB optical span and the 10 to the 20 dB optical span. The closer these values are to 1, the closer the comb is to exhibit a flat-top shape, more desirable for applications such as optical communications. The main results for this analysis of the OFCs generated are summarized in Table I. The total output of the VCSEL, *P*-OFCG that we show in Fig. 5(a) (upper trace) has 27 lines in the 20 dB span what corresponds to a bandwidth of 135 GHz and a flatness of 0.88 and 0.89 respectively (see Table I). The same 20 dB span is measured in the comb with only the main polarization mode, the *Px*-OFCG shown in Fig. 5(b) (middle line) of 27 modes and 135 GHz. The 3 and 10 dB spans are 19 and 23 modes respectively so the flatness is 0.83 and 0.85 in each case. Finally, we see the orthogonal comb, *Py*-OFCG in Fig. 5(c) (lower line) which is slightly narrower with 26 lines that imply 130 GHz in the 20 dB span. In this case the 3 and 10 dB spans are 11 and 22 modes and the flatness is 0.5 and 0.85 respectively. Then, the flatness of this comb is significantly worse than the one exhibited by *P* and *Px*, and it has a different shape, shifted in frequency, as the initial secondary mode was.

TABLE I
COMPARISON TOTAL MAIN AND ORTHOGONAL OFCG

	Total-OFCG *P*	Main-OFCG *Px*	Orthogonal-OFCG *Py*
Span@3 dB	10 5 GHz/21 modes	95 GHz/19 modes	55 GHz/11 modes
Span@10 dB	120 GHz/24 modes	115 GHz/23 modes	110 GHz/22 modes
Flatness: f3 dB = 3 dB/10 dB	21/24 = 0.88	19/23 = 0.83	11/22 = 0.5
Span@20 dB	135 GHz/27 modes	135 GHz/27 modes	130 GHz/26 modes
Flatness f10 dB = 10 dB/20 dB	24/27 = 0.89	23/27 = 0.85	22/26 = 0.85

Comparing these three combs we can distinguish each polarization sub-comb in the total one. The part of the total comb above the 20 dB line is mainly formed by the energy with the parallel polarization and we can see that their shapes match perfectly in this central part. However, if we focus on the right decay slope of the total comb (longer wavelengths around 1539.3 nm) we observe that a small hip appears whose shape corresponds to the right part of the orthogonally polarized OFCG, the *Py*-OFCG which has much lower power. There we also see that the *Px*-OFCG is more symmetric than the total comb because these orthogonally polarized components are not present. If the optical power associated to the orthogonal mode could be enhanced, a total optical comb with wider span could be achieved with VCSEL-based OFCG schemes.

Special attention deserves the evolution of the *Py*-OFCG with the radiofrequency modulation power P_{RF}, since this is the parameter that more clearly influences the formation of optical combs under GS regime. The map of such evolution was presented in Figs. 4, and in Fig. 6 we show the evolution of the shape of the *Py* comb more in detail. When the RF modulation power is below -10 dBm, the optical spectra of the orthogonally polarized light is formed by the secondary mode, with a peak power of -50 dBm and a residual emission coming from the main mode with a peak power of -43 dBm. These two orthogonally polarized components of the output of the laser evolve as

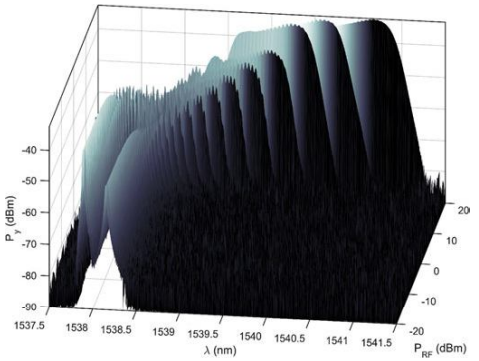

Fig. 6. Evolution of the optical comb with ortogonal polarization, *Py* when P_{RF} increases. Initially, two separate comb-like structures are obsevable, that eventaully melt to produce the final ortogonal comb *Py*.

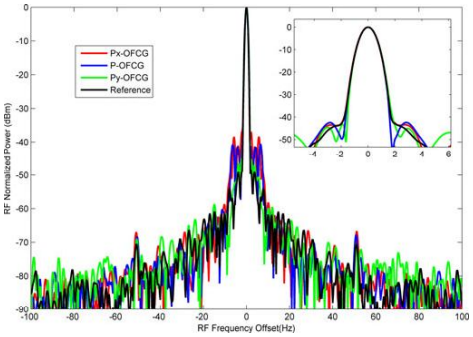

Fig. 7. RF Linewidth for the combs in Fig. 5: *P*-OFCG (blue line), *Px*-OFCG (red line), *Py*-OFCG (green line) and Reference (black line). In the inset we plot a zoom of these signals obtained with the lower Resolution Bandwidth available in the ESA used Therefore in all cases the linewidth is limited by the equipment capabilities. See text for more details.

the GS regime is established. Initially, two separated comb-like spectral shapes appear associated to each of these components, being the one associated to the secondary mode the one whose peak power and optical span evolves faster. When P_{RF} is increased further, the two comb-like structures melt in a single optical comb with orthogonal polarization. After the study of the dynamics of the formation of this orthogonal comb, it is important to evaluate whether this two initial structures end up forming a coherent unique comb and how this *Py* comb is related to the main *Px* comb with parallel polarization. Results on this matter are presented in the next section.

In order to summarize this optical frequency comb generation section, we would like to remark the fundamental conclusions obtained: a) the three combs evolve similarly with the supply parameters and they all offer the best performance at 20 °C of VCSEL temperature, 11.5 mA of bias current, 5 GHz and 16 dBm as modulation signal; b) the power difference between the parallel and orthogonal mode respectively decreases significantly with the GS regime, from 43.1 dB of difference in the CW operation to 26 dB when the modulation in included; and c) both combs seems to be related to each other and they both generate the total comb. Further work is presented in the following section in order to extract whether the total comb is formed by two coherent combs with perpendicular polarizations or they are two independent signals and there is no phase relation between them.

B. Coherence of the Modes of the Comb

In this section we are paying attention to the coherence of the modes that form the combs. We evaluate this coherence by measuring the electrical beat tone signal at f_{RF} that is generated when directly detected in an ultrafast photodiode the signal of each of the combs under study: the ones associated to *P*, *Px* and *Py* signals. Hence, we evaluate mixing all the modes of each comb under study and analyse the electrical spectra and the linewidth of the line at f_{RF}. An increase of the linewidth of this tone or a degradation of the noise present in the spectra is directly related to a decrease in the coherence between the modes and a degradation in the quality of the comb. In previous works, we have already seen the high coherence in the modes of the total comb generated with GS (*P*-OFCG in this article) with a beat note signal with noise level equal the one in the reference signal (the CW source) [7] and how this result is also valid if we add other elements like Electro-Optical Modulators maintaining the initial GS regime in the VCSEL [8]. This implies that the use of a GS technique improves the coherence relation between the different modes in the final comb. Now we want to study if this coherence is maintained among these sub-combs with orthogonal polarization states. Moreover we also want to check with the electrical spectra, the phase coherence between both orthogonally polarized combs to test if they are two independent combs or they are somehow related to each other.

Thus, to evaluate the coherence of the modes in each subcomb we compare the linewidth of the reference signal (the RF CW source used to induce the GS regime) at f_{RF} and the linewidth of the beat tone signals at f_{RF} for each of the combs. In Fig. 7 we present the curves for the total comb *P*-OFCG (blue line), the main comb *Px*-OFCG (red line), the orthogonal comb *Py*-OFCG (green line) and the reference signal which is the radiofrequency CW source at 5 GHz (black line). In the figure we see that all the combs present the same decay slope which is slightly broader than the reference one at around -40 dB from the carrier peak, where we find a broadening of the three combs in respect to the reference. In all these traces the floor is found at -80 dBm. On the other hand, we show in the inset a zoom of the beat tone where we can see that the 3 dB linewidth is, for every signal, around 1 Hz. This means that is in the equipment limit as the minimum resolution bandwidth is this value, 1 Hz.

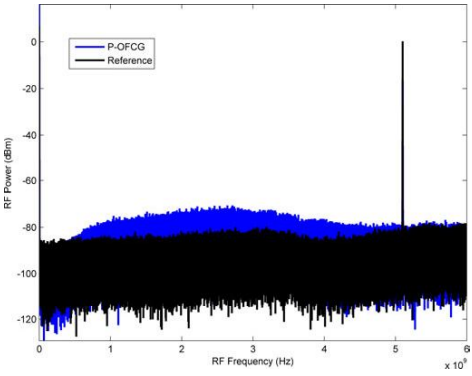

Fig. 8. RF Spectra for the total combs *P*-OFCG (blue line) and Reference (black line). We see that the noise level increases in the *P*-OFCG in respect to the reference curve but still is a remarkable low noise with the RF frequency as the only frequency component. This imply high correlation between the modes in the different combs. See text for more details.

With this figure we deduce that each comb has high coherence in their modes and we have high quality combs as the beat tone signal is always in the order of the reference equipment used for modulation.

On the other hand, we want to evaluate the coherence between modes that belong to different sub-combs. For this purpose, we compare the differences in the electrical spectra of each comb with higher span than the used in the previous image, from DC to some MHz above the RF injected frequency. We want to see if new frequency components appear in the RF spectra (different from 5 GHz) and then both combs are completely independent or not. In the latter case, the main and the orthogonal combs would be phase related and might be locked. In Fig. 8 we show the electrical spectra curve for the total comb *P*-OFCG (blue line) and the electrical spectrum of the reference signal, directly at the output of the CW source (black line).

The total comb curve presents a clear peak at the RF frequency of 5 GHz and no other frequency components appear. This implies that both sub-combs, *Px*-OFCG and *Py*-OFCG, are phase correlated and not free running in respect to each other. Besides, the noise floor in the *P*-OFCG curve is close to the reference one and then the total comb is a signal with high coherence between all its modes as we were expecting taking into account our previous results [7]. This high coherence is driven by the GS regime because the polarization modes of a VCSEL are in CW operation anti-correlated regarding [10], [11].

III. Conclusion

In this work, we have presented a study of the polarization dynamics of VCSELs under GS regime, and how these polarizations contribute in the OFCGs with COTS components. OFCGs are interesting systems for many applications and LDs will allow these systems to become more efficient in cost and energy and more compact at the same time. Inside LDs technologies, VCSELs increment the impact in these three factors, they are easy to integrate and produces at the same time wider combs in comparison to other LDs technologies. GS modulation for generating these OFCGs is a versatile technique that yields to easy generation with tunable mode distance and no need of extra components in the set-up.

Analyzing the VCSEL-based GS-OFCG we observe that both polarization components form two different OFCGs, each of them with orthogonal polarization in respect to each other and they are correlated to each other. This correlation is a consequence of the GS regime as both polarization modes are, in CW operation, anti-correlated. Along this work, we have studied the quality of this OFCG in terms of optical span and flatness and also RF linewidth of the detected beat note of each comb and noise after being detected. For this purpose, here we have analyzed the VCSEL-based OFCG and the properties of the two orthogonally polarized combs that form this optical signal. First we have analyzed the optical spectra of the whole signal and the two different combs, each one with orthogonal polarizations. We have seen that they all evolve with the same pattern depending on the supply characteristics and they all have the best performance at 20 °C of VCSEL temperature, 11.5 mA of bias current, 5 GHz of modulation frequency and 16 dBm as modulation power. We have seen that one of the modes, with an orthogonal polarization, has much lower output power because of the birefringence of the material and a fabrication pinning process but it still produces an optical comb and in this comb the difference in power between both modes is reduced with GS regime compared to the power difference in CW operation. Apart of this optical study, we have presented a RF study where we have checked that each of the sub-combs present high correlation between their modes as the beat tone signal presents a linewidth comparable to the reference and in the limit of the equipment used for measure. We have also seen that both sub-combs are phase correlated to each other and not free running.

Future work will be developed in several lines: on one hand we are interested in repeat these measurements with VCSELs with less orthogonal mode suppression in order to directly compare both sub-combs and go further in the analysis of the polarization components of VCSELs and their influence in comb generation. On the other hand, we would like to check if we can obtain, with Optical Injection Locking, two correlated and completely locked combs with similar properties in which we can play with the polarization with techniques like the ones observed in [17]. We will also work in order to increase the optical power in the orthogonal comb by including Optical Injection Locking of each one of the combs, the *Px*-OFCG and the *Py*-OFCG respectively and how this affects the total comb, *P*-OFCG. Another future line consists in changing the birefringence of the VCSEL sample, varying the distance in the central wavelength of both sub-combs and increasing also the modulation frequency range available. Experiments like this have been previously done in works like [18].

To conclude, our VCSEL-based GS-OFCG offers, in the few GHz repetition frequency rates, dual-polarization combs with tunable distance and high correlation in their modes in an easy, energy efficient and easy to integrate system, with applications in ultrafast laser dynamics studies or in polarization-division multiplexing optical communications. All these features make VCSEL-based GS-OFCGs promising systems to produce low cost and high quality OFCGrs which is a tendency nowadays. However, the optical span and the flatness are still limiting factors in comparison to other non LDs comb generation techniques. Our work continues in order to improve the generated signal and more deeply understand the dynamics of our LD source.

ACKNOWLEDGMENT

The authors would like to thank VERTILAS for providing the VCSELs.

REFERENCES

[1] F. Zhu, T. Mohamed, J. Strohaber, A. A. Kolomenskii, T. Udem, and H. A. Schuessler, "Real-time dual frequency comb spectroscopy in the near infrared," *Appl. Phys. Lett.*, vol. 102, no. 12, p. 121116, 2013.

[2] R. Michalzik, *VCSELs*, vol. 166. Berlin, Germany: Springer, 2013.

[3] A. R. Criado, C. De Dios, G. H. Döhler, S. Preu, S. Malzer, S. Bauerschmidt, H. Lu, A. C. Gossard, and P. Acedo, "Ultra-narrow linewidth CW sub-THz generation using GS based OFCG and n-i-pn-i-p superlattice photomixers," *Electron. Lett.*, vol. 48, pp. 1425–1426, 2012.

[4] R. Wu, C. M. Long, D. E. Leaird, and A. M. Weiner, "Directly generated Gaussian-shaped optical frequency comb for microwave photonic filtering and picosecond pulse generation," *IEEE Photon. Technol. Lett.*, vol. 24, no. 17, pp. 1484–1486, Sep. 2012.

[5] H. E. Li and K. Iga, *Vertical-Cavity Surface-Emitting Laser Devices*, vol. 6. Berlin, Germany: Springer, 2003.

[6] K. Iga, "Surface-emitting laser-its birth and generation of new optoelectronics field," *IEEE J. Sel. Topics Quantum Electron.*, vol. 6, no. 6, pp. 1201–1215, Nov. 2000.

[7] A. R. Criado, C. De Dios, E. Prior, M. Ortsiefer, P. Meissner, and P. Acedo, "VCSEL-based optical frequency combs: Toward efficient single-device comb generation," *IEEE Photon. Technol. Lett.*, vol. 25, no. 20, pp. 1981–1984, Oct. 2013.

[8] E. Prior, C. De Dios, A. R. Criado, M. Ortsiefer, P. Meissner, and P. Acedo, "Experimental study of VCSEL-based optical frequency comb generators," *IEEE Photon. Technol. Lett.*, vol. 26, no. 21, pp. 2118–2121, Nov. 2014.

[9] J. Danckaert, B. Nagler, J. Albert, K. Panajotov, I. Veretennicoff, and T. Erneux, "Minimal rate equations describing polarization switching in vertical-cavity surface-emitting lasers," *Opt. Commun.*, vol. 201, nos. 1–3, pp. 129–137, Jan. 2002.

[10] J.-L. Vey, C. Degen, K. Auen, and W. Elsäßer, "Quantum noise and polarization properties of vertical-cavity surface-emitting lasers," *Phys. Rev. A*, vol. 60, no. 4, pp. 3284–3295, Oct. 1999.

[11] D. Shelly, T. Garrison, M. K. Beck, and D. Christensen, "Polarization correlations in pulsed, vertical cavity, surface-emitting lasers," *Opt. Exp.*, vol. 7, no. 7, p. 249, Sep. 2000.

[12] M. Brunel, J. Thévenin, and M. Vallet, "Dual-polarization frequency comb from a diode-pumped solid-state laser," presented at the Proc. : 2013Conf. Lasers Electro-Opt., San Jose, CA, USA, 2013, Paper CF1G.5.

[13] A. D. Shiner, M. Reimer, A. Borowiec, S. O. Gharan, J. Gaudette, P. Mehta, D. Charlton, K. Roberts, and M. O'Sullivan, "Demonstration of an 8-dimensional modulation format with reduced inter-channel nonlinearities in a polarization multiplexed coherent system," *Opt. Exp.*, vol. 22, no. 17, pp. 20366–20374, Aug. 2014.

[14] J. Albert, G. Van Der Sande, B. Nagler, K. Panajotov, I. Veretennicoff, J. Danckaert, and T. Erneux, "The effects of nonlinear gain on the stability of semi-degenerate two-mode semiconductor lasers: A case study on VCSELs," *Opt. Commun.*, vol. 248, nos. 4–6, pp. 527–534, Apr. 2005.

[15] A. R. Criado, C. De Dios, E. Prior, G. H. Dohler, S. Preu, S. Malzer, H. Lu, A. C. Gossard, and P. Acedo, "Continuous-wave sub-THz photonic generation with ultra-narrow linewidth, ultra-high resolution, full frequency range coverage and high long-term frequency stability," *IEEE Trans. Terahertz Sci. Technol.*, vol. 3, no. 4, pp. 461–471, Jul. 2013.

[16] P. M. Anandarajah, R. Maher, Y. Q. Xu, S. Latkowski, J. O'Carroll, S. G. Murdoch, R. Phelan, J. O'Gorman, and L. P. Barry, "Generation of coherent multicarrier signals by gain switching of discrete mode lasers," *IEEE Photon. J.*, vol. 3, no. 1, pp. 112–122, Feb. 2011.

[17] A. Quirce, P. Perez, H. Lin, A. Valle, L. Pesquera, K. Panajotov, and H. Thienpont, "Polarization switching regions of optically injected long-wavelength VCSELs," *IEEE J. Quantum Electron.*, vol. 50, no. 11, pp. 921–928, Nov. 2014.

[18] K. Panajotov, B. Nagler, G. Verschaffelt, A. Georgievski, H. Thienpont, J. Danckaert, and I. Veretennicoff, "Impact of in-plane anisotropic strain on the polarization behavior of vertical-cavity surface-emitting lasers," *Appl. Phys. Lett.*, vol. 77, no. 11, p. 1590, Sep. 2000.

Estefanía Prior received the B.Sc. and M.Sc. degrees in telecommunication engineering from the Universidad Carlos III de Madrid, Madrid, Spain, in 2012, and the M.Res. in electronics engineering in 2014. She is currently working toward the Ph.D. degree at the Carlos III University of Madrid. In 2012, she was involved in research and development tasks related to microwave photonics and radio over fiber, in both transmission and receiver systems. Since 2013, her work has been focusing on pulsed operation (gain switching) on semiconductor lasers and, more specifically, on vertical-cavity surface-emitting lasers for optical frequency comb generation.

Cristina de Dios received the M.Sc. degree in applied physics and electronics from the Universidad Complutense of Madrid, Madrid, Spain. Then, she joined the private sector as a Technical Consultant for Hewlett-Packard. Since 2002, she has been a Member of the Optoelectronics and Laser Technology Group, Universidad Carlos III de Madrid, Madrid, where she received the M.Res. in 2004 and the Doctorate degree in 2010 for her work in ultrafast pulsed diode lasers and nonlinear pulse compression. She is currently an Assistant Professor at the Electronics Technology Department, Universidad Carlos III de Madrid. She is also cofounder of the spin-off company Luzwavelabs (www.luzwavelabs.com) that provides hardware solutions for generation and detection in the THz range using photonic techniques. Her research interests include high-speed optical communications, pulsed semiconductor laser sources, nonlinear optical phenomena, and subterahertz and millimeter wave photonic signal synthesis and detection and optical frequency comb generation.

Markus Ortsiefer received the University degree in physics and the doctoral degree from the Technical University of Munich, Munich, Denmark, in 1997 and 2001, respectively. During his Ph.D. work, he was involved in research on InP-based lasers and related materials. He is the Co-Founder of VERTILAS GmbH, Garching, Germany, where he was the Managing Director from 2001 to 2003, and since 2003, he has been the Chief Technical Officer. He is responsible for the company's production and research activities. He has authored or coauthored more than 130 publications in scientific journals, conference proceedings, and books and filed several patents on optoelectronic devices. He is a Member of the German Physical Society.

Peter Meissner (M'94) was born in Adelsdorf, Germany, on November 1943. He received the Dip.-Ing. and Dr.-Ing. degrees in electrical engineering from the Technical University, Berlin, Germany, in 1971 and 1977, respectively. In 1971, he was with the Heinrich Hertz Institut für Nachrichtentechnik, Berlin, where he was involved in the field of navigation systems and adaptive echo control. From 1985 to 1994, he was involved in the field of optical communications, where his main interests were theory of semiconductor lasers, coherent optical communications, and wavelength division multiplexing (WDM) systems and networks. Since 1995, he has been a Professor of optical communications with the Technische Universität Darmstadt, Darmstadt, Germany. His main research topics are tunable micromachined components for WDM systems and high-speed optical communications, polarization mode dispersion compensation techniques, and optical terahertz generation.

Pablo Acedo (M'00) received the Bachelor's degree in telecommunication engineering from the Universidad Politécnica de Madrid, Madrid, Spain, in 1993, and the Doctorate (Hons.) degree from the Universidad Carlos III de Madrid, Madrid, in 2000 for his work on heterodyne two color laser interferometry for fusion plasma diagnostics. His doctoral work included the development of the first two color laser system based on Mid-IR sources for a Stellarator Fusion Device (Stellarator TJ-II, Laboratorio Nacional de Fusión, CIEMAT, Madrid) and the first two-color Nd:YAG system for a Fusion Device (Tokamak C-Mod Plasma Science and Fusion Centre, Massachusetts Institute of Technology—MIT), the later during several doctoral visits to MIT during 1996–1999.

In 2002, he became an Assistant Professor at the Universidad Carlos III de Madrid, where he continued with the development of scientific instrumentation systems for fusion plasma diagnostics and biomedical applications, leading national projects and contracts on these fields. Also, since his incorporation to the UC3M, he has been involved in research with the Optoelectronics and Laser Technology Group, participating in different national and EU funded research projects (Fp4, Fp5, Fp6, and FP7) on semiconductor laser devices and photonic architectures for microwave, millimeter-wave, and terahertz generation and processing. Starting 2009, his research interests in this line focused on the development of multimode laser sources (optical frequency combs) and their applications in photonic signal synthesis with the development of several architectures for the generation, detection and processing of terahertz signals, leading several research projects and contracts in this field. He has also been very active in technology transfer through R&D contracts with different companies (INDRA Sistemas S.A., AIRBUS Defence and Space) as well as with the creation of the spin-off company Luzwavelabs (www.luzwavelabs.com) that provides hardware solutions for generation and detection in the terahertz range using photonic techniques. Nowadays, his research interests still involve the development of optical frequency combs and their use in fields such as bioengineering, environmental applications, and nondestructive testing. He has published more than 80 contributions in journals and international conferences, including invited conferences and seminars.

Paper E. OL2016 (Submitted)

E. Prior, C. de Dios, Á. R. Criado, M. Ortsiefer, P. Meissner, and P. Acedo, "Dynamics of Dual-polarization VCSEL-based Optical Frequency Combs under Optical Injection Locking," Photonics Technology Letters, submitted June 2016

Polarization dynamics in optically injected VCSEL-based Optical Frequency Combs

E. Prior,[1,*] C. de Dios,[1] R. Criado,[2] M. Ortsiefer,[3] P. Meissner,[4] P. Acedo[1]

[1]Electronics Technology Department, Universidad Carlos III de Madrid, Leganés, 28911 Spain
[2]Luz Wave Labs S.L. Av. Gregorio Peces Barba, Leganés, 28919 Spain
[3]Vertilas GmbH. Garching, Germany
[4]Technische Universität Darmstadt, Darmstadt, Germany
*Corresponding author: eprior@ing.uc3m.es

Received 23 March 2016; revised XX Month, XXXX; accepted XX Month XXXX; posted XX Month XXXX (Doc. ID XXXXX); published XX Month XXXX

In this work we present a study of the polarization dynamics of an optically injected Optical Frequency Comb (OFC) based on a Vertical-Cavity Surface-Emitting Laser (VCSEL). The comb is generated with a VCSEL under Gain Switching modulation. This OFC has two sub-combs associated to the orthogonally polarized modes present in VCSELs and they are phase correlated but not locked. In order to lock them, optical injection locking has been done with an external edge-emitting laser with small linewidth. By playing with the master laser and the polarization we obtain a dual-polarization VCSEL-based optical frequency comb powering up the orthogonal comb to the main comb level and maintaining the phase coherence among their teeth.

OCIS codes: *(250.7260) Vertical cavity surface emitting lasers; (230.0250) Optoelectronics, (260.5430) Polarization, (140.3520) Lasers, injection-locked*

http://dx.doi.org/10.1364/OL.99.xxxxx

Optical Injection Locking (OIL) in Laser Diodes (LDs) has been commonly used to improve the performance of the emitting light, mainly focused on laser spectral narrowing, frequency chirp reduction, noise reduction and modulation bandwidth enhancement [1]–[4]. This technique consists on the injection of light from an external source, the master laser, into the device under use, called slave laser. Under certain conditions the output light locks the injected light inheriting its frequency and phase [5]. If the locking achieved is stable, this injection improves the performance of the slave laser, as the output light locks the master light inheriting its frequency and phase. Then high performance master locked to a noisier slave yields to low noise output signal [2].

In our case, we are using a Vertical-Cavity Surface-Emitting Laser (VCSEL) as the slave laser. Besides, this VCSEL is directly modulated with Gain Switching (GS) to generate an Optical Frequency Comb (OFC) [6]. As the active area in VCSELs is much smaller than in edge-emitting LDs, the effect of the external photons going inside the cavity might be significant [7]. VCSELs have also been injected for decades to improve mainly their modulation bandwidth, chirp or low emitted power [8]–[11] in communication applications or some other fields [12]. They have also been modulated and injected to filter comb components [13]. However, not much work on injected VCSELs working under GS has been done focusing on the resulting comb, to our knowledge, which is the scope of this work.

For the last years, OFCs have found a large variety of fields of application [14]–[19]. Besides, OFCs based on LDs offer suitable combs for some of them with more competitive cost. Going deeper, our work with VCSELs show that they improve this competence in terms of integrability and compactness, low cost, low energy consumption and the possibility of mass production [20].

In this work we present new results on our on-going study of VCSEL-based OFCs. We have evaluated the dynamic behaviour of the two orthogonal modes of polarization present in a VCSEL output under GS for OFC with and without injection. We want to determine how the injection affects the comb generated with the VCSEL, called VCSEL-OFC and, more specifically, how the injection affects the two sub-combs with orthogonal polarizations that form the VCSEL-OFC. The analysis of the polarization dynamics in our VCSEL-OFC without injection were previously detailed in our works [21], [22] and this continues one of the future work there highlighted. In that previous work we showed that the VCSEL-OFC is formed by two orthogonally polarized combs, which are strong phase related due to the GS modulation and we suggested that dual-polarization coherent combs could be obtained balancing the power of these orthogonal components with OIL. That is proved in this work. This dual-polarization OFC will find applications in ultrafast laser dynamics studies [23] or in polarization-division multiplexing optical communication [24].

The VCSEL used in this work is a state of the technology device (VERTILAS model VL-1550-BG-P2-H4) lasing at 1.55um already adapted for the RF modulation in the laser bandwidth with a specific board provided with the laser. However, after years of

work this device is deteriorated so it needs more supply current (in bias and in RF) to achieve an equivalent emission. At the same time the optical spectrum has been red shifted. However, it is the same sample used in works like [6], [21], [25]. An equivalent comb, called VCSEL-OFC, is obtained, now with the following conditions: the device is temperature stabilized at 25°C with a bias current of 27mA and an input RF signal to produce the GS regime of 19dBm at 5GHz. This VCSEL-OFC is shown in Fig. 2a). The slave VCSEL will be injected using a Discrete Mode (DM) laser as master laser, as they are LD with narrow linewidth emission [26] which have been used previously in our group with good results [16]. The DM laser will be set at 19°C to fall in the VCSEL-OFC wavelengths and the current will be set around 38mA with some small tuning to achieve the injection. The VCSEL comb under injection locking will be called along this work OIL-OFC and this comb is shown in Fig. 2b).

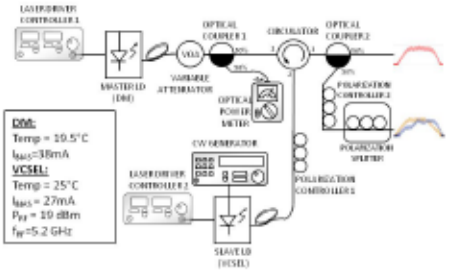

Fig. 1. Experimental set-up. The comb is generated inside the VCSEL (25ºC, 27mA, 5.2GHz, 19dBm) which is at the same time optically injected by the DM laser (19.5ºC, 38mA) through a circulator. The injection ratio is -6.6dB. The optical output is first power divided and then one arm is split in two orthogonally polarized sub-combs with a polarization splitter. See text for more details.

In Fig. 1 we present the experimental set-up used in the work here described. The master path starts with the DM laser emitting in Continuous Wave (CW). Then, the signal is attenuated with a Variable Optical Attenuator (VOA) and a 50/50 Optical Coupler (OC) to adjust the appropriate injected power to the slave which will be monitored with the powermeter placed in one of the OC outputs. The second OC output will enter de circulator and exit in the slave optical path.

The slave path is formed by the VCSEL and a polarization controller (PC1) to adjust the polarization of the ingoing master light to the light being generated inside the cavity of the VCSEL. This polarization adjustment needs to be carefully done as it is critical for the locking of both signals. The master light coming from the circulator enters the VCSEL and the output signal goes through the second input in the circulator to the output path. This output path goes to the measurement equipment. We will measure the optical spectra in an optical spectrum analyzer (OSA) with 0.002nm resolution and the electrical spectra after the linewidth set-up in an electrical spectrum analyzer (ESA) using an ultrafast 50GHz photodetector. The temporal trace will be measured in an autocorrelator which has an Erbium-Doped Fiber Amplifier (EDFA) and a PC in its entrance.

In order to check the polarization components of the output comb we have included a second 50/50 coupler to divide the optical output and one of their output branches will be polarization split with a second controller (PC2) and a Polarization Splitter (PS). With this set-up we obtain the traces in Fig. 2c).

In Fig. 2 we show the already mentioned OFCs and some other significant optical traces. Fig. 2a) (blue trace) presents the VCSEL-OFC which is the VCSEL output when there are no external light injected. This comb has 25 teeth in the 20dB span which corresponds to 130GHz. We know from previous works, that this VCSEL-OFC is formed by two sub-combs with orthogonal polarizations, one main comb with parallel polarization (called P_X-OFCG in [21]) and the residual one with orthogonal polarization and much lower power (P_Y-OFCG in [21]). This sub-comb is observed in the small hip in the upper wavelengths in the VCSEL-OFC and one of our purposes in this work is to power up this residual part with OIL.

The master CW light is traced in this same plot (green line). The master DM source is emitting at 1541.63nm to coincide in the VCSEL-OFC teeth that produces the best optical injection. The injection ratio is -6.6dB and this is controlled measuring the power in the master path and adjusting the VOA.

The red trace in Fig. 2b) is the optical output when the injection is achieved. This OIL-OFC is a little broader than the previous one, with 27 teeth in the 20dB span which corresponds to 140GHz. It is more symmetric and flatter than the VCSEL-OFC as the polarization of the injected master light has been carefully tuned in PC1 in order to equalize the optical power levels of the parallel and orthogonally polarized sub-combs.

As we have mentioned before, VCSEL-OFC is composed by two combs with orthogonal polarizations, one of them with much lower power as it belongs to the residual linear polarization present in VCSELs [21]. At this point, we want to check the polarization components of the OIL-OFC to discriminate whether with the injection both polarizations have produced a whole comb with only one state of polarization or both orthogonal components remains after the injection. For this purpose we include the second controller PC2 and the PS. At its outputs we observe two orthogonally polarized sub-combs and how one mainly include the lower wavelengths, which we call OIL_X-OFC (Fig. 2c, beige trace) and the second one, called OIL_Y-OFC (Fig. 2c, dark blue trace) corresponds to the upper part of the total comb, the orthogonally polarized one. These OIL_X-OFC and OIL_Y-OFC are, consequently, the correspondent combs to the P_X-OFCG and P_Y-OFCG in [21]. This means that including the OIL we balance the power of both sub-combs increasing the effect of the orthogonal state of polarization but the output maintains both orthogonal polarizations. Therefore, an orthogonally-polarized dual-polarization VCSEL-based OFC is obtained equalizing both sub-combs with the OIL technique.

On the other hand, we aim to test the possible OIL-OFCs that are generated by varying the state of polarization in the injected light. We want to alter the injected state of polarization to achieve polarization switching by injecting close to the suppressed orthogonal linear polarization state of the VSCEL [27]. For this purpose we play with PC1 and we observe the output comb. In Fig. 2d), we see that we can obtain an injected comb maximizing either the parallel sub-comb, called OIL-OFC-maxX (Fig. 2d, black trace) or the orthogonal one, called OIL-OFC-maxY (Fig. 2d, brown trace).

The first one is obtained when the polarization in the injected light coincides with the parallel polarization and the second when it agrees to the polarization of the orthogonal mode in the VCSEL, enhancing this residual mode which turns to be the main one, achieving this polarization switching. These two traces are polar examples and the OIL-OFC in Fig. 2b) will be halfway, obtaining a balance among both polarization states.

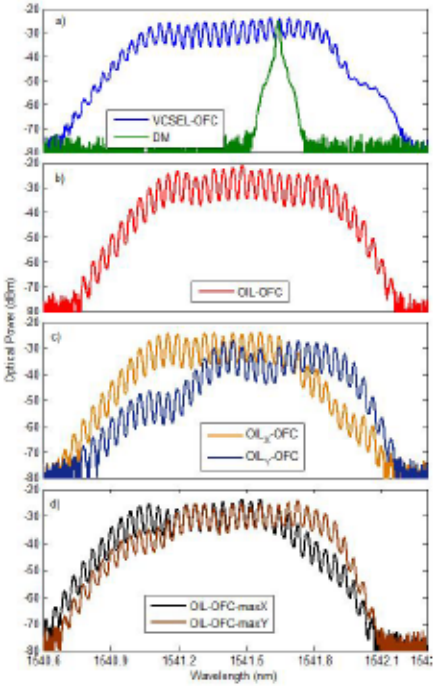

Fig. 2. a) VCSEL-OFC (blue trace), output of the VCSEL with GS. This is a comb with 25 teeth in the 20dB span which corresponds to 130GHz. DM output (green trace) which is the master light being injected into the VCSEL at 1541.63nm. b) OIL-OFC (red trace) output signal with optical injection locking adjusting the polarization to equalize both sub-combs. The resulting comb has 27teeth in the 20dB span, which corresponds to 140GHz. c) OILx-OFC (beige trace) and OILy-OFC (dark blue trace) which are the parallel and orthogonal polarization components of the OIL-OFC. This means that with the injection both sub-combs maintain their orthogonal polarizations. d) OIL-OFCs adjusting the master polarization to maximize either the P_X-OFC (OIL-OFC-maxX or black trace) or the P_Y-OFC (OIL-OFC-maxY or brown trace). See text for details.

It is important to remark the difference between the combs in these two latter subfigures: In Fig. 2c) we show the two components that form the OIL-OFC in Fig. 2b). On the other hand, in Fig. 2d), we adjust the polarization to enhance only one linear state of polarization so suppressing the other one. This implies that we can play with the injected polarization in VCSELs to balance both states of polarization, or to maintain one of them cancelling the other one.

Apart from the optical spectra we have measured the optical linewidth of the different signals previously shown so deeper understanding of the OIL-OFC is achieved. At first, we expected the narrowing of the optical linewidth of the signal down to the master source linewidth [28] when the master has a narrower linewidth.

For this purpose we have used the delayed self-heterodyne interferometric technique [29] and we have obtained the electrical spectra shown in Fig. 3, where the optical linewidths are half the 3dB bandwidth of the plotted lines. In the image we see the VCSEL's linewidth when it is working in CW emission, which is 1MHz and the VCSEL-OFC linewidth that increases to 4MHz due to the GS regime. On the contrary than the expected, after the injection the linewidth obtained is broader, the OIL-OFC has a linewidth of 8MHz. The reason for this is the DM linewidth that is 7MHz regarding our measurement. This is much broader than expected in this sample, probably because it is degraded after years of work and this explains the linewidth for the OIL-OFC which turns to be in the order of the master linewidth. Future work will be developed in this issue, observing the optical linewidth after injection with lasers with narrower values.

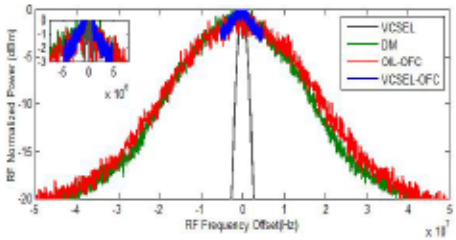

Fig. 3. Electrical spectra after self-herodyning. The linewidths are half the 3dB bandwidth shown in the traces. VCSEL in CW (grey trace) which has an optical linewidth of 1MHz, DM in CW (green trace) with 7MHz, VCSEL-OFC with 4MHz, and OIL-OFC with 8MHz of optical Linewidth. See text for details.

Lastly, we have also obtained the autocorrelation traces of the temporal pulses generated with and without the OIL scheme. The autocorrelator traces are directly measured and we infer the pulse durations computing the Full Width Half Maximum (FWHM) assuming that they follow a sech² profile. This means that we assume a relation between the autocorrelation FWHM and the pulse FWHM of 1.543. In Fig. 4 we observe the autocorrelation trace of the VCSEL-OFC (blue trace) and the OIL-OFC (red trace). The correspondent pulse durations assuming sech² profile are 11.77ps and 7.59ps. Therefore with the OIL we have achieved a light pulse compression. On the other hand we can also observe in the traces that the upper and lower parts of the pulses are quite similar but they have differences in between, in the 20%-60% area. The VCSEL-OFC is broader in this region than the OIL-OFC and more symmetric at the same time. On the other hand, the OIL-

OFC presents a pedestal in the right part of it, which is typically observed in pulses generated with GS modulation [30].

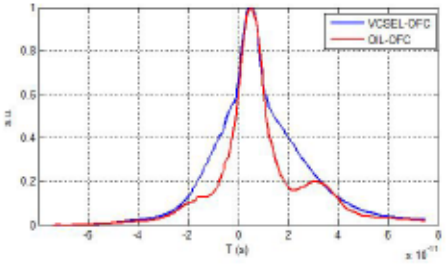

Fig. 4. Autocorrelation traces. VCSEL-OFC (blue trace) with pulse FWHM of 11.77ps, and OIL-OFC (red trace) with pulse duration of 7.59ps. We are measuring the autocorrelation traces and obtaining the pulse durations assuming they follow a sech² profile. See text for details.

As conclusion, we have shown our latest results in VCSEL-based OFCs in which we have included optical injection to observe the variations in the output comb. We have checked that we can play with the injected polarization and then balance the two orthogonal states of polarizations inherent to VCSELs to to equalize the power in both sub-combs obtaining a dual-polarization OFC. Besides, we can also tune the injected polarization to cancel one of these sub-combs maintaining the other one in similar power levels.

Our efforts continue in first place to implement the OIL with a master source with lower linewidth and observe if the output inherits this lower noise [28]. Future work also includes deeper understanding in the OIL technique for VCSEL-based OFCs and the scheme here implemented to check the effects in the noise and the phase coherence among comb teeth. Last but not least, we would like to go further implementing VCSEL-to-VCSEL injection to enhance the capabilities of integration and reduce even more the cost and energy consumption of the OFC generation system.

Funding. Spanish Ministry of Economy and Competitiveness (RTC-2014-2661-7, TEC-2014-52147-R).

References

1. A. Consoli, A. Vallo, L. Pesquera, I. Esquivias, and F. J. Lopez-Hernandez, in Conference on Lasers and Electro-Optics/International Quantum Electronics Conference, 2009, p. JThE11.
2. L. Chrostowski and C. J. Chang-Hasnain, in IEEE J. Sel. Top. Quantum Electron., vol. 9, no. 5, pp. 1386, Sep. 2003.
3. E. K. Lau and M. C. Wu, in IEEE J. Sel. Top. Quantum Electron., vol. 15, no. 3, pp. 618, 2009.
4. A. Consoli and I. Esquivias, in Opt. Express, vol. 20, no. 20, pp. 22481, Sep. 2012.
5. L. A. Coldren and S. W. Corzine, Diode lasers and photonic integrated circuits. Wiley, 1995.
6. A. R. Criado, C. de Dios, E. Prior, M. Ortsiefer, P. Meissner, and P. Acedo, in IEEE Photonics Technol. Lett., vol. 25, no. 20, pp. 1981, Oct. 2013.
7. J. Ohtsubo, Semiconductor Lasers, vol. 111. Berlin, Heidelberg: Springer Berlin Heidelberg, 2013.
8. D. Pareikh, "Optical Injection Locking of Vertical Cavity Surface-Emitting Lasers Digital and Analog Applications," 2012.
9. P. J. Delfyett, S. Bhooplapur, N. Hoghooghi, and E. Sarailou, in IEEE Photonics Conference 2012, 2012, pp. 368.
10. M. Torre, A. Hurtado, A. Quirce, A. Valle, L. Pesquera, and M. Adams, in IEEE J. Quantum Electron., vol. 47, no. 1, pp. 92–99, Jan. 2011.
11. A. Gatto, A. Bolotti, P. Boffi, and M. Martinelli, in Opt. Express, vol. 17, no. 24, pp. 21748, Nov. 2009.
12. A. Hurtado, I. D. Henning, and M. J. Adams, in Opt. Express, vol. 18, no. 24, pp. 25170, Nov. 2010.
13. M. Akbulut, S. Bhooplapur, I. Ozdur, J. Davila-Rodriguez, and P. J. Delfyett, in Opt. Express, vol. 18, no. 17, pp. 18284, Aug. 2010.
14. P. J. Delfyett, I. Ozdur, N. Hoghooghi, M. Akbulut, J. Davila-Rodriguez, and S. Bhooplapur, in IEEE J. Sel. Top. Quantum Electron., vol. 18, no. 1, pp. 258, Jan. 2012.
15. C. Chen, C. Zhang, D. Liu, K. Qiu, and S. Liu, in Optics Letters, vol. 37. p. 3954, 2012.
16. A. R. Criado, C. de Dios, E. Prior, G. H. Dohler, S. Preu, S. Malzer, H. Lu, A. C. Gossard, and P. Acedo, in IEEE Trans. Terahertz Sci. Technol., vol. 3, no. 4, pp. 461, Jul. 2013.
17. P. Martin-Mateos, M. Ruiz-Llata, J. Posada-Roman, and P. Acedo, in IEEE Photonics Technol. Lett., vol. 27, no. 12, pp. 1309, Jun. 2015.
18. T. Udem, R. Holzwarth, and T. W. Hänsch, in Nature, vol. 416, no. 6877, pp. 233, Mar. 2002.
19. R. Wu, C. M. Long, D. E. Loaird, and A. M. Weiner, in IEEE Photonics Technol. Lett., vol. 24, no. 17, pp. 1484, Sep. 2012
20. E. Kapon and A. Sirbu, "Long-wavelength VCSELs: Power-efficient answer," Nat. Photonics, vol. 3, no. 1, pp. 27–29, Jan. 2009.
21. E. Prior, C. De Dios, M. Ortsiefer, P. Meissner, and P. Acedo, in J. Light. Technol., vol. 33, no. 22, pp. 4572, Nov. 2015.
22. E. Prior, C. de Dios, M. Ortsiefer, P. Meissner, and P. Acedo, in CLEO, 2015, p. CB_P_11.
23. M. Brunel, J. Thévenin, M. Vallet, J. Thevenin, and M. Vallet, in CLEO: 2013, pp. 1.
24. A. D. Shiner, M. Reimer, A. Borowiec, S. O. Gharan, J. Gaudette, P. Mehta, D. Charlton, K. Roberts, and M. O'Sullivan, in Opt. Express, vol. 22, no. 17, pp. 20366, Aug. 2014.
25. E. Prior, C. de Dios, A. R. Criado, M. Ortsiefer, P. Meissner, and P. Acedo, in IEEE Photonics Technol. Lett., vol. 26, no. 21, pp. 1, Nov. 2014.
26. B. Kelly, R. Phelan, D. Jones, C. Herbert, J. O'Carroll, M. Rensing, J. Wondelboe, C. B. Watts, A. Kaszubowska-Anandarajah, P. Perry, C. Guignard, L. P. Barry, and J. O'Gorman, in Electron. Lett., vol. 43, no. 23, p. 1282, 2007.
27. A. Quirce, P. Perez, H. Lin, A. Valle, L. Pesquera, K. Panajotov, and H. Thienpont, in IEEE J. Quantum Electron., vol. 50, no. 11, pp. 921, Nov. 2014.
28. S. Ulvin, S. Keyvaninia, F. Lelarge, G.-H. Duan, B. Kuyken, and G. Roelkens, in Opt. Express, vol. 24, no. 5, p. 5277, Mar. 2016
29. T. Okoshi, K. Kikuchi, and A. Nakayama, in Electron. Lett., vol. 16, no. 16, p. 630, Jul. 1980.
30. C. de Dios and H. Lamela, in *IEEE Photonics Technol. Lett.*, vol. 22, no. 6, pp. 377, Mar. 2010

Full References

[1] A. Consoli, A. Valle, L. Pesquera, I. Esquivias, and F. J. Lopez-Hernandez, "Optical Injection-Induced Timing Jitter Reduction in Gain-Switched Single-Mode 1550 nm-VCSELs," in *Conference on Lasers and Electro-Optics/International Quantum Electronics Conference*, 2009, p. JThE11.

[2] L. Chrostowski and C. J. Chang-Hasnain, "Injection locking of VCSELs," *IEEE J. Sel. Top. Quantum Electron.*, vol. 9, no. 5, pp. 1386–1393, Sep. 2003.

[3] E. K. Lau and M. C. Wu, "Enhanced Modulation Characteristics of Optical Injection-Locked Lasers: A Tutorial," *IEEE J. Sel. Top. Quantum Electron.*, vol. 15, no. 3, pp. 618–633, 2009.

[4] A. Consoli and I. Esquivias, "Pulse shortening of gain switched single mode semiconductor lasers using a variable delay interferometer.," *Opt. Express*, vol. 20, no. 20, pp. 22481–9, Sep. 2012.

[5] L. A. Coldren and S. W. Corzine, *Diode lasers and photonic integrated circuits*. Wiley, 1995.

[6] A. R. Criado, C. de Dios, E. Prior, M. Ortsiefer, P. Meissner, and P. Acedo, "VCSEL-Based Optical Frequency Combs: Toward Efficient Single-Device Comb Generation," *IEEE Photonics Technol. Lett.*, vol. 25, no. 20, pp. 1981–1984, Oct. 2013.

[7] J. Ohtsubo, *Semiconductor Lasers*, vol. 111. Berlin, Heidelberg: Springer Berlin Heidelberg, 2013.

[8] D. Parekh, "Optical Injection Locking of Vertical Cavity Surface-Emitting Lasers Digital and Analog Applications," 2012.

[9] P. J. Delfyett, S. Bhooplapur, N. Hoghooghi, and E. Sarailou, "Injection locked VCSELs for microwave photonic applications in analog RF links and real time arbitrary waveform generation," in *IEEE Photonics Conference 2012*, 2012, pp. 368–369.

[10] M. Torre, A. Hurtado, A. Quirce, A. Valle, L. Pesquera, and M. Adams, "Polarization Switching in Long-Wavelength VCSELs Subject to Orthogonal Optical Injection," *IEEE J. Quantum Electron.*, vol. 47, no. 1, pp. 92–99, Jan. 2011.

[11] A. Gatto, A. Boletti, P. Boffi, and M. Martinelli, "Adjustable-chirp VCSEL-to-VCSEL injection locking for 10-Gb/s transmission at 1.55 micron.," *Opt. Express*, vol. 17, no. 24, pp. 21748–53, Nov. 2009.

[12] A. Hurtado, I. D. Henning, and M. J. Adams, "Optical neuron using polarisation switching in a 1550nm-VCSEL.," *Opt. Express*, vol. 18, no. 24, pp. 25170–6, Nov. 2010.

[13] M. Akbulut, S. Bhooplapur, I. Ozdur, J. Davila-Rodriguez, and P. J. Delfyett, "Dynamic line-by-line pulse shaping with GHz update rate.," *Opt. Express*, vol. 18, no. 17, pp. 18284–91, Aug. 2010.

[14] P. J. Delfyett, I. Ozdur, N. Hoghooghi, M. Akbulut, J. Davila-Rodriguez, and S. Bhooplapur, "Advanced Ultrafast Technologies Based on Optical Frequency Combs," *IEEE J. Sel. Top. Quantum Electron.*, vol. 18, no. 1, pp. 258–274, Jan. 2012.

[15] C. Chen, C. Zhang, D. Liu, K. Qiu, and S. Liu, "Tunable optical frequency comb enabled scalable and cost-effective multiuser orthogonal frequency-division multiple access passive optical network with source-free optical network units," *Optics Letters*, vol. 37. p. 3954, 2012.

[16] A. R. Criado, C. de Dios, E. Prior, G. H. Dohler, S. Preu, S. Malzer, H. Lu, A. C. Gossard, and P. Acedo, "Continuous-Wave Sub-THz Photonic Generation With Ultra-Narrow Linewidth, Ultra-High Resolution, Full Frequency Range Coverage and High Long-Term Frequency Stability," *IEEE Trans. Terahertz Sci. Technol.*, vol. 3, no. 4, pp. 461–471, Jul. 2013.

[17] P. Martin-Mateos, M. Ruiz-Llata, J. Posada-Roman, and P. Acedo, "Dual-Comb Architecture for Fast Spectroscopic Measurements and Spectral Characterization," *IEEE Photonics Technol. Lett.*, vol. 27, no. 12, pp. 1309–1312, Jun. 2015.

[18] T. Udem, R. Holzwarth, and T. W. Hänsch, "Optical frequency metrology.," *Nature*, vol. 416, no. 6877, pp. 233–7, Mar. 2002.

[19] R. Wu, C. M. Long, D. E. Leaird, and A. M. Weiner, "Directly Generated Gaussian-Shaped Optical Frequency Comb for Microwave Photonic Filtering and Picosecond Pulse Generation," *IEEE Photonics Technol. Lett.*, vol. 24, no. 17, pp. 1484–1486, Sep. 2012.

[20] E. Kapon and A. Sirbu, "Long-wavelength VCSELs: Power-efficient answer," *Nat. Photonics*, vol. 3, no. 1, pp. 27–29, Jan. 2009.

[21] E. Prior, C. De Dios, M. Ortsiefer, P. Meissner, and P. Acedo, "Understanding VCSEL-Based Gain Switching Optical Frequency Combs: Experimental Study of Polarization Dynamics," *J. Light. Technol.*, vol. 33, no. 22, pp. 4572–4579, Nov. 2015.

[22] E. Prior, C. de Dios, M. Ortsiefer, P. Meissner, and P. Acedo, "Dual-polarization VCSEL-based optical frequency comb generation," in *The European Conference on Lasers and Electro-Optics*, 2015, p. CB_P_11.

[23] M. Brunel, J. Thévenin, M. Vallet, J. Thevenin, and M. Vallet, "Dual-polarization frequency comb from a diode-pumped solid-state laser," in *CLEO: 2013*, 2013, pp. 1–2.

[24] A. D. Shiner, M. Reimer, A. Borowiec, S. O. Gharan, J. Gaudette, P. Mehta, D. Charlton, K. Roberts, and M. O'Sullivan, "Demonstration of an 8-dimensional modulation format with reduced inter-channel nonlinearities in a polarization multiplexed coherent system.," *Opt. Express*, vol. 22, no. 17, pp. 20366–74, Aug. 2014.

[25] E. Prior, C. de Dios, A. R. Criado, M. Ortsiefer, P. Meissner, and P. Acedo, "Experimental study of VCSEL-based Optical Frequency Comb Generators," *IEEE Photonics Technol. Lett.*, vol. 26, no. 21, pp. 1–1, Nov. 2014.

[26] B. Kelly, R. Phelan, D. Jones, C. Herbert, J. O'Carroll, M. Rensing, J. Wendelboe, C. B. Watts, A. Kaszubowska-Anandarajah, P. Perry, C. Guignard, L. P. Barry, and J. O'Gorman, "Discrete mode laser diodes with very narrow linewidth emission," *Electron. Lett.*, vol. 43, no. 23, p. 1282, 2007.

[27] A. Quirce, P. Perez, H. Lin, A. Valle, L. Pesquera, K. Panajotov, and H. Thienpont, "Polarization Switching Regions of Optically Injected Long-Wavelength VCSELs," *IEEE J. Quantum Electron.*, vol. 50, no. 11, pp. 921–928, Nov. 2014.

[28] S. Uvin, S. Keyvaninia, F. Lelarge, G.-H. Duan, B. Kuyken, and G. Roelkens, "Narrow line width frequency comb source based on an injection-locked III–V-on-silicon mode-locked laser," *Opt. Express*, vol. 24, no. 5, p. 5277, Mar. 2016.

[29] T. Okoshi, K. Kikuchi, and A. Nakayama, "Novel method for high resolution measurement of laser output spectrum," *Electron. Lett.*, vol. 16, no. 16, p. 630, Jul. 1980.

[30] C. de Dios and H. Lamela, "Compression and Reshaping of Gain-Switching Low-Quality Pulses Using a Highly Nonlinear Optical Loop Mirror," *IEEE Photonics Technol. Lett.*, vol. 22, no. 6, pp. 377–379, Mar. 2010.

Congress A. CLEO Europe 2015 (poster)

E. Prior, C. de Dios, M. Ortsiefer, P. Meissner, and P. Acedo, “Dual-polarization VCSEL-based optical frequency comb generation,” in The European Conference on Lasers and Electro-Optics, 2015, p. CB_P_11

Dual-polarization VCSEL-based optical frequency comb generation

E. Prior[1], C. de Dios[1], M. Ortsiefer[2], P. Meissner[3], P. Acedo[1], *Member*, IEEE
1. Electronics Technology Department, Universidad Carlos III de Madrid, Leganés, 28911 Spain
2. Vertilas GmbH. Garching, Germany
3. Technische Universität Darmstadt, Darmstadt, Germany

Optical Frequency Comb Generators (OFCG) based on Cost of the Shelf (COTS) laser diodes (LDs) are interesting systems for many applications as they offer compactness and cost efficiency. However, the optical frequency span and the coherence of the modes is still a limiting factor when comparing to combs based on other laser technologies. Among LDs, Vertical-Cavity Surface-Emitting Lasers (VCSELs) under Gain Switching (GS) regime [1] produce record combs in terms of energy efficiency and mode coherence. GS is a well-known nonlinear technique to directly generate OFCGs from LDs.

In this work we present new results on our on-going study of VCSEL-based GS-OFCGs. We have evaluated the dynamic behaviour of the two orthogonal modes of polarization present in a VCSEL output under GS for OFCG. We have observed that each mode generates a separate optical comb. The orthogonal mode, usually suppressed during fabrication, contributes to the total VCSEL-based OFCG obtaining a broader span.

Fig. 1b) shows that the VCSEL-based OFCG total output, P (blue), with an optical frequency comb with a 20dB span of 132GHz, is formed by two different combs: one associated to the main transversal mode, P_y (red) and the other one to the orthogonal mode, P_x (green). In order to evaluate the phase relation of these orthogonal polarized combs and how they combine to produce the total comb output, we compare the Phase Noise (PN) of the RF detected signal at $f_{comb} = \Delta f = f_{N+1} - f_N = f_{RF} = 5$GHz, the frequency spacing of the lines of the combs, for the three cases of Fig 1 b (Fig. 1c). All the measurements show almost the same PN level. This means that the coherence of the optical modes associated to the combs for P_y and P_x are very similar and equal to the coherence of the total comb. These findings suggest that the modes in the overall comb share a stable phase relation independently of their state of polarization. Further work will be developed to understand if these observations are related to the fact that these two modes are degenerate states of the same spatial mode or this is a hint of a possible mutual injection locking mechanism between the P_x and P_y combs.

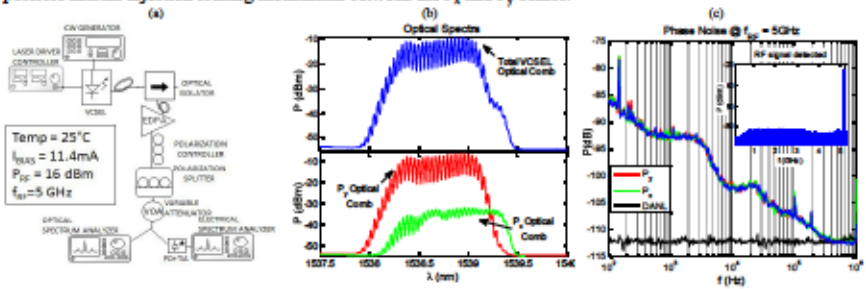

Fig. 1 a) Experimental set-up with a VCSEL test device provided by VERTILAS GmbH. b) OFCGs comparison: total OFCG (blue), OFCG generated by the main polarization mode Py (red) and OFCG generated by the orthogonal polarization mode Px (green). c) Phase Noise of the electrical signal detected with the total OFCG (blue), the main polarization comb Py (red) and the orthogonal polarization comb Px (green). The Noise Floor of the electrical spectrum analyzer (black) is also plotted. The inset shows the detected signal from DC to 5.4GHz where no other frequency components appear.

These results point out that VCSELs with the orthogonal mode not suppressed, would be able to generate a broader dual-polarization comb with a similar amount of energy injected and offering a very good phase relation between its modes. The availability of two coherent combs with separate polarization find applications in ultrafast laser dynamics studies [2] or in polarization-division multiplexing optical communication [3]. Our efforts continue in order to determine how each mode influences the total comb and how both combs are correlated with each other.

References

[1] E. Prior, C. de Dios, A. R. Criado, M. Ortsiefer, P. Meissner, and P. Acedo, *Photonics Technol. Lett.*, vol. PP, no. 99, pp. 1–1, 2014.
[2] M. Brunel, J. Thévenin, and M. Vallet, *CLEO: 2013*, 2013, p. CF1G.5.
[3] A. D. Shiner, M. Reimer, A. Borowiec, S. O. Gharan, J. Gaudette, P. Mehta, D. Charlton, K. Roberts, and M. O'Sullivan, *Opt. Express*, vol. 22, no. 17, pp. 20366–74, Aug. 2014.

Congress B. CLEO USA 2016 (oral talk)

E. Prior, C. de Dios, Á. R. Criado, M. Ortsiefer, P. Meissner, and P. Acedo, "1THz span optical frequency comb using VCSELs and off the Shelf expansion techniques," in The Conference on Lasers and Electro-Optics, June 2016. doi:10.1364/CLEO_SI.2016.SF2O.3

1THz span optical frequency comb using VCSELs and off the Shelf expansion techniques

E. Prior[1], C. de Dios[1], R. Criado[2], M. Ortsiefer[3], P. Meissner[4], P. Acedo[1], *Member*, IEEE
1. Electronics Technology Department, Universidad Carlos III de Madrid, Leganés, 28911 Spain
2. Luz WaveLabs S.L. Av. Gregorio Peces Barba, Leganés, 28919 Spain
3. Vertilas GmbH Garching, Germany
4. Technische Universitat Darmstadt, Darmstadt, Germany
eprior@ing.uc3m.es

Abstract: We show, to our knowledge, the broadest VCSEL-based optical comb with 1THz span (20 dB), 193 teeth, obtained by cascading two expansion stages, one with Electro-Optic Modulators and the second based on High Non-Linear Fibers.
OCIS codes: 250.7260 Vertical cavity surface emitting lasers; 230.0250 Optoelectronics; 060.4370 Nonlinear optics, fibers;

In this work, we present our latest results on VCSEL-based Optical Frequency Comb (OFC) generation and expansion using commercially available components. The result is a versatile, and compact comb architecture, that offers cost and energy efficiency. Our OFCs are based on Vertical-Cavity Surface-Emitting Lasers (VCSELs) under Gain Switching (GS) regime that provide record combs in energy efficiency and mode coherence compared to other laser diodes (LD) technologies [1]–[3]. Among others, these systems are useful in fields of application like spectroscopy, THz generation or green optical communications [4]–[8].

Up to now, the optical frequency span was the main limiting factor when comparing VCSELs with other laser technologies for OFCs, but here we present a breakthrough in this limit: we have obtained the broadest VCSEL-based optical comb, of 1THz (20dB) span, which is a record value to our knowledge. This comb has 193teeth in the 20dB span which corresponds to 9.1nm in wavelength. The distance between comb teeth is 5GHz and the overall power consumption of the components in the set-up is lower than 10W. However, with this configuration, the flatness of the comb and its dynamic range still leave room for improvement.

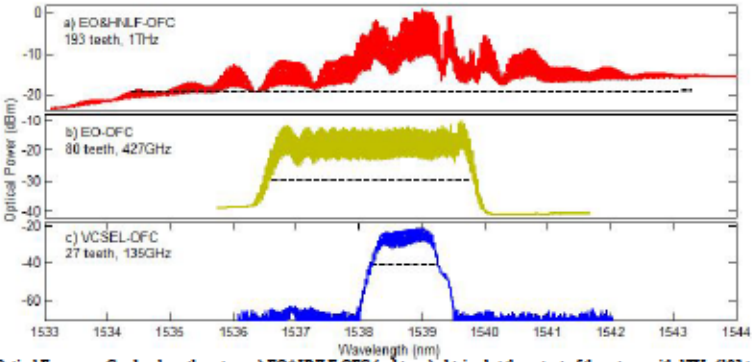

Fig. 1 Optical Frequency Combs along the set-up. a) EO&HNLF-OFC (red trace) obtained at the output of the set-up, with 1THz (193 teeth) of 20dB span. b) EO-OFC (yellow trace) obtained at the output of the first expansion stage based on PMs, with 427GHz (80 teeth) in the 2dB span. c) VCSEL-OFC (blue trace) obtained at the output of the VCSEL under GS regime, with 135GHz (27 teeth) in the span. The VCSEL supply parameters are 20 °C, 11.4mA, 5.4GHz, 16dBm.

In Fig. 1a, we observe the reported 1THz comb, called EO&HNLF-OFC (red line) and its 20dB span (black dotted line). The dynamic range of this spectrum is lower than 20dB in the upper wavelengths so the 20dB line covers the span where the teeth are at least 0.5dB above the noise level (the OSA used has 0.002nm resolution). In order to obtain this spectrum we have implemented a set-up that combines two different expansion techniques as explained in the following paragraph.

The optical source starts with a VCSEL set at 20ºC and 11.4mA of bias current. The VCSEL is operating in GS regime using a 16dBm tone at 5.4GHz. The obtained comb, called VCSEL-OFC (blue trace in Fig. 1c), has 27 teeth in the 20dB span that corresponds to 135GHz (previously presented in [1], [2], [9]). This VCSEL-OFC enters the first expansion stage, with two Electro Optical (EO) Phase Modulators (PM). Cascading several EO modulators is one of the most common techniques for comb generation and expansion [10]. The obtained comb EO-OFC (yellow trace in Fig. 1b), has 80 teeth in the 20dB span that corresponds to 427GHz. Finally, the second expansion stage is based on Highly Non-Linear Fiber (HNLF). Before this element, we include a Dispersion Compensating Fiber (DCF) to compensate the dispersion and an Erbium Dopped Fiber Amplifier (EDFA) in order to increase the peak power of the pulse and enhance the non-linear effects in the HNLF. In Fig. 2 the complete set-up is shown, which is similar to the ones described to expand combs with different laser technologies in [10], [11].

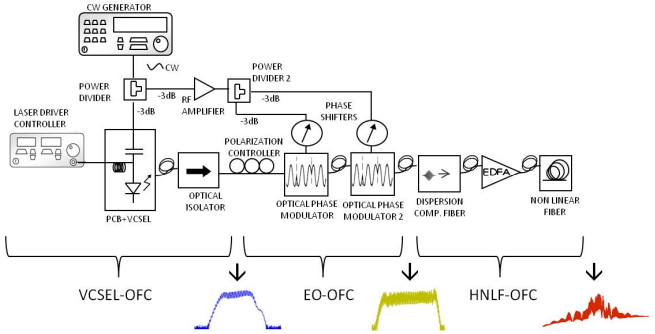

Fig. 2 Set-up used for the EO&HNLF-OFC. VCSEL-OFC (blue trace) is the output of the VCSEL under GS regime. A first expansion stage called EO-OFC is formed by two PMs and provides an output comb of 427GHz in the 20dB span (yellow trace). Then, the second expansion stage called HNLF-OFC is formed by a DCF, an EDFA and a HNLF and provides an output comb called EO&HNLF-OFC (red trace), which is the 1THz broad optical frequency comb. See text for more details.

This is a remarkable result and our efforts continue in order to improve the flatness and the dynamic range of this 1THz broad comb. We will also continue analyzing the coherence between the teeth in the comb and other features that characterizes a comb spectra and a comb system. At the end we focus on the improvement of the quality and energy efficiency of these VCSEL-based OFCs.

References

[1] E. Prior, C. de Dios, A. R. Criado, M. Ortsiefer, P. Meissner, and P. Acedo, "Experimental study of VCSEL-based Optical Frequency Comb Generators," *IEEE Photonics Technol. Lett.*, vol. 26, no. 21, pp. 1–1, Nov. 2014.

[2] E. Prior, C. de Dios, M. Ortsiefer, P. Meissner, and P. Acedo, "Dual-polarization VCSEL-based optical frequency comb generation," in *The European Conference on Lasers and Electro-Optics*, 2015, p. CB_P_11.

[3] E. Prior, C. De Dios, M. Ortsiefer, P. Meissner, and P. Acedo, "Understanding VCSEL-Based Gain Switching Optical Frequency Combs: Experimental Study of Polarization Dynamics," *J. Light. Technol.*, vol. 33, no. 22, pp. 4572–4579, Nov. 2015.

[4] P. J. Delfyett, I. Ozdur, N. Hoghooghi, M. Akbulut, J. Davila-Rodriguez, and S. Bhooplapur, "Advanced Ultrafast Technologies Based on Optical Frequency Combs," *IEEE J. Sel. Top. Quantum Electron.*, vol. 18, no. 1, pp. 258–274, Jan. 2012.

[5] C. Chen, C. Zhang, D. Liu, K. Qiu, and S. Liu, "Tunable optical frequency comb enabled scalable and cost-effective multiuser orthogonal frequency-division multiple access passive optical network with source-free optical network units," *Optics Letters*, vol. 37. p. 3954, 2012.

[6] A. R. Criado, C. de Dios, E. Prior, G. H. Dohler, S. Preu, S. Malzer, H. Lu, A. C. Gossard, and P. Acedo, "Continuous-Wave Sub-THz Photonic Generation With Ultra-Narrow Linewidth, Ultra-High Resolution, Full Frequency Range Coverage and High Long-Term Frequency Stability," *IEEE Trans. Terahertz Sci. Technol.*, vol. 3, no. 4, pp. 461–471, Jul. 2013.

[7] P. Martin-Mateos, M. Ruiz-Llata, J. Posada-Roman, and P. Acedo, "Dual-Comb Architecture for Fast Spectroscopic Measurements and Spectral Characterization," *IEEE Photonics Technol. Lett.*, vol. 27, no. 12, pp. 1309–1312, Jun. 2015.

[8] R. Wu, C. M. Long, D. E. Leaird, and A. M. Weiner, "Directly Generated Gaussian-Shaped Optical Frequency Comb for Microwave Photonic Filtering and Picosecond Pulse Generation," *IEEE Photonics Technol. Lett.*, vol. 24, no. 17, pp. 1484–1486, Sep. 2012.

[9] A. R. Criado, C. de Dios, E. Prior, M. Ortsiefer, P. Meissner, and P. Acedo, "VCSEL-Based Optical Frequency Combs: Toward Efficient Single-Device Comb Generation," *IEEE Photonics Technol. Lett.*, vol. 25, no. 20, pp. 1981–1984, Oct. 2013.

[10] R. Wu, V. Torres-Company, D. E. Leaird, and A. M. Weiner, "Supercontinuum-based 10-GHz flat-topped optical frequency comb generation," *Opt. Express*, vol. 21, no. 5, p. 6045, Mar. 2013.

[11] T. Yang, J. Dong, S. Liao, D. Huang, and X. Zhang, "Comparison analysis of optical frequency comb generation with nonlinear effects in highly nonlinear fibers.," *Opt. Express*, vol. 21, no. 7, pp. 8508–20, Apr. 2013.

Congress C. VCSEL's DAY 2016 (invited talk)

E. Prior, C. de Dios, Á. R. Criado, M. Ortsiefer, P. Meissner, and P. Acedo, "Dynamics of Dual-polarization VCSEL-based Optical Frequency Combs including Optical Injection Locking," in VCSEL's day, 2016

Dynamics of Dual-polarization VCSEL-based Optical Frequency Combs including Optical Injection Locking

E. Prior,[1,*] C. de Dios,[1] R. Criado,[2] M. Ortsiefer,[3] P. Meissner,[4] P. Acedo[1]

[1]*Electronics Technology Department, Universidad Carlos III de Madrid, Leganés, 28911 Spain*
[2]*Luz WaveLabs S.L. Av. Gregorio Peces Barba, Leganés, 28919 Spain*
[3]*Vertilas GmbH. Garching, Germany*
[4]*Technische Universität Darmstadt, Darmstadt, Germany*

Vertical-Cavity Surface-Emitting Laser (VCSEL) Optical Frequency Combs (OFC) generated using a large signal modulation technique called Gain Switching (GS) are interesting systems for many applications: they produce record combs in terms of energy efficiency and mode coherence and offer compactness, integrability and cost efficiency [1]. In this work we present new results on our on-going study of VCSEL-based GS-OFCs. Firstly, we have evaluated the dynamic behaviour of the two orthogonal modes of polarization present in a VCSEL output under GS. We have observed that each mode generates a separate optical comb and the orthogonal mode, usually suppressed during fabrication, contributes to the total VCSEL-OFC [2]. Secondly, we have included Optical Injection Locking (OIL) to modify and adjust both polarization contributions. We have observed that the control of the polarization of the injected light clearly influences the overall optical comb and the sub-combs it is formed of. We have been able to balance and equalize the power associated to those sub-combs obtaining an enhanced dual-polarization OFC. Besides, we have also tuned the injected polarization to cancel one of these sub-combs maintaining the other one in similar power levels inducing a polarization switching along all the modes of the overall comb. This means that we can control the polarization state of the final comb as we prefer, which is quite a remarkable result.

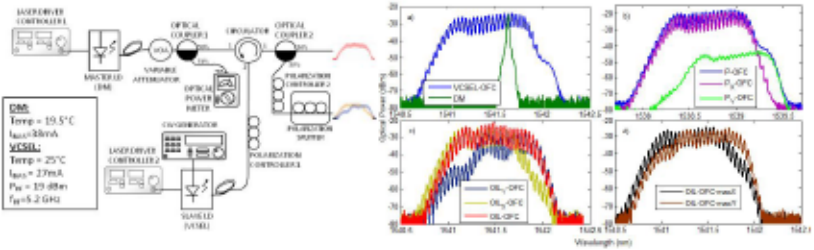

Fig. 1 (left) Experimental set-up. The comb is generated inside the VCSEL (25ºC, 27mA, 5.2GHz, 19dBm) which is at the same time optically injected by the DM laser (19.5ºC, 38mA) through a circulator. The injection ratio is -6.6dB. The optical output is first power divided and then one arm is split in two orthogonally polarized sub-combs with a polarization splitter. (right) a) VCSEL-OFC (blue trace) with 25 teeth in the 20dB span which corresponds to 130GHz. DM output (green trace), master light being injected into the VCSEL at 1541.63nm. b) VCSEL-OFC (blue trace) and its polarization components: Px-OFC (purple trace) and Py-OFC (green trace). c) OIL-OFC (red trace) output signal with OIL adjusting the polarization to equalize both sub-combs. The resulting comb has 27teeth in the 20dB span, which corresponds to 140GHz. The polarization components of the OIL-OFC are OILx-OFC (yellow trace) and OILy-OFC (dark blue trace). This means that with the injection both sub-combs maintain their orthogonal states of polarization. d) OIL-OFCs adjusting the master polarization to maximize either the P_X-OFC (OIL-OFC-maxX or black trace) or the P_Y-OFC (OIL-OFC-maxY or brown trace).

The availability of two coherent combs with separate polarization find applications in ultrafast laser dynamics studies [3] or in polarization-division multiplexing optical communication [4]. Our efforts continue to implement the OIL using a VCSEL as master. Future work will also be oriented to a deeper understanding in the OIL technique for VCSEL-based OFCs facing these results with theory.

References

[1] A. R. Criado, C. de Dios, E. Prior, M. Ortsiefer, P. Meissner, and P. Acedo, "VCSEL-Based Optical Frequency Combs: Toward Efficient Single-Device Comb Generation," *IEEE Photonics Technol. Lett.*, vol. 25, no. 20, pp. 1981–1984, Oct. 2013.

[2] E. Prior, C. De Dios, M. Ortsiefer, P. Meissner, and P. Acedo, "Understanding VCSEL-Based Gain Switching Optical Frequency Combs: Experimental Study of Polarization Dynamics," *J. Light. Technol.*, vol. 33, no. 22, pp. 4572–4579, Nov. 2015.

[3] M. Brunel, J. Thévenin, M. Vallet, J. Thevenin, and M. Vallet, "Dual-polarization frequency comb from a diode-pumped solid-state laser," in *CLEO: 2013*, 2013, pp. 1–2.

[4] A. D. Shiner, M. Reimer, A. Borowiec, S. O. Gharan, J. Gaudette, P. Mehta, D. Charlton, K. Roberts, and M. O'Sullivan, "Demonstration of an 8-dimensional modulation format with reduced inter-channel nonlinearities in a polarization multiplexed coherent system," *Opt. Express*, vol. 22, no. 17, pp. 20366–74, Aug. 2014.

Related work

Besides the previously included publications, that have communicated the core results of this Thesis, other relevant results have also been disseminated. These publications and other international collaborations are detailed below.

Manuscripts in Journals

Jerez, B., Martín-Mateos, P., **Prior, E**., de Dios, C., & Acedo, P, "Gain-Switching Injection-Locked Dual Optical Frequency Combs: Characterization and Optimization," in **Optics Letters**, submitted July 2016.

Jerez, B., Martín-Mateos, P., **Prior, E**., de Dios, C., & Acedo, P, "Dual optical frequency comb architecture with capabilities from visible to mid-infrared," in **Optics Express**, 24(13), 14986, Jun 2016. doi:10.1364/OE.24.014986

Criado, A. R., de Dios, C., **Prior, E**., Dohler, G. H., Preu, S., Malzer, S., … Acedo, P. (**2013**). "Continuous-Wave Sub-THz Photonic Generation With Ultra-Narrow Linewidth, Ultra-High Resolution, Full Frequency Range Coverage and High Long-Term Frequency Stability," ***IEEE Transactions on Terahertz Science and Technology***, *3*(4), 461–471. doi:10.1109/TTHZ.2013.2260374

A. R. Criado, C. de Dios, **E. Prior**, M. Ortsiefer, P. Meissner, and P. Acedo, "VCSEL-Based Optical Frequency Combs: Toward Efficient Single-Device Comb Generation," ***IEEE Photonics Technol. Lett.***, vol. 25, no. 20, pp. 1981–1984, Oct. **2013**. doi:10.1109/LPT.2013.2280700

De Dios, C., Criado, A. R., **Prior, E**., & Acedo, P. (**2013**). "Enhancing the Performance of Electro-Optical Heterodyne Receivers Using Gain Switched Photonic Local Oscillator," ***Journal of Lightwave Technology***, *31*(8), 1331–1336. doi:10.1109/JLT.2013.2248121

Congresses

P. Martín-Mateos, B. Jerez, **E. Prior**, C. de Dios, and P. Acedo, "Optical Communication Components Characterization using Electro-Optic Dual-Combs," in **The Conference on Lasers and Electro-Optics, 2016**

Criado, A. R., de Dios, C., **Prior, E**., Acedo, P., Ortsiefer, M., & Meissner, P. (**2013**). "Photonic generation of CW sub-THz and THz waves using an efficient Gain-Switching based VCSEL optical frequency comb," In *2013* ***38th International Conference on Infrared, Millimeter, and Terahertz Waves (IRMMW-THz)*** (pp. 1–1). IEEE. doi:10.1109/IRMMW-THz.2013.6665842

International Collaborations

07/2015: Universidad Carlos III, Madrid. **Organization and participation** in the 25rd International travelling **Summer School** on Microwaves and Lightwaves (ITSS).

11/2014: Institute of Electron Technology, Warsaw, Poland. Participant in the **STSM Workshop** organized by the MPNS COST Action MP1204 Tera-Mir Radiation.

06/2014: Chalmers University of Technology, Sweden. **Visitor researcher** as master student in the Photonics Laboratory in the Microtechnology and Nanoscience Department. Temporal pulses characterization of VCSEL-OFC and research on other nonlinear techniques for its expansion.

06/2013-07/2013: Technische Universität Darmstadt, Germany. **Visitor researcher** as master student in the Institut für Mikrowellentechnik und Photonik (IMP). Chirp and RIN characterization of VCSEL#1- OFC.

07/2013: Warsaw University of Technology, Poland. Participant in the 23rd International travelling **Summer School** on Microwaves and Lightwaves (ITSS).

Dissemination

The work described in this thesis is a product of our research since January 2013 in nonlinear optical techniques and components and their application to VCSEL-based optical frequency comb generation, expansion and optimization. Along this time, I have been in collaborations with other universities and we have published and submitted some manuscripts in which I am either author or co-author.

This work line started at the end of 2012, when Prof. Dr.-Ing. Peter Meissner came to our group for an international collaboration. His expertise on VCSELs appeared in the appropriate moment and the group decided to embrace them as laser source to explore the possibilities of this technology for comb and terahertz generation.

After the first VCSEL arrived, thanks to our collaboration with Vertilas, the results rapidly materialized: we increased the optical span with much lower energy consumption [27] and generate THz signals around 100GHz [57]. Since then, the work regarding VCSELs has evolved as explained along this dissertation yielding several publications and related work in international journals most of them in the first quartile (Journal of Lightwave Technology, Optics Letters, Electronics Letters), and important international Congresses like The Conference on Lasers and Electro-Optics, CLEO. The acceptance of our work in the CLEO conference has given me the opportunity attend this event in both the European conference (2015) and the US conference (2016) chapters. In 2015, I presented a poster while two oral talks were given in 2016. Also, an invited talk during the VCSEL's day organized by the Technische Universität Darmstadt was given in June 2016 regarding our latest results.

Apart from the published work, this research has given special attention to international collaborations. In 2013, two months were I working in the Technische Universität Darmstadt, in Darmstadt, Germany. There, I had the opportunity to deepen into our knowledge

of the chirp and RIN measurement of VCSELs. By that time, I also attended to the 23rd International travelling Summer School on Microwaves and Lightwaves (ITSS2013) that took place in Warsaw. Two years after, in 2015, I had the opportunity of both attending and organizing this same Summer School, as Prof. Pablo Acedo hosted in our university the 25th edition of this ITSS.

It was in Chalmers University of Technology (Göteborg, Sweden) where my second international pre-doctoral visit took place during my master research. I was there for three weeks in June 2014 performing experiments on the characterization of temporal pulses generated with VCSEL-OFC using a fast optical scope and also on other nonlinear techniques for comb expansion. This visit was funded by the COST Action MP1204 Tera-Mir Radiation, so I presented the outcome of this visit in the STSM workshop of that year in Warsaw, in November 2014.

This research line continues and, in a few weeks, we are expecting to host Dr. Ana Quirce, who is expert in VCSEL simulations and experiments regarding polarization switching of VCSELs under optical injection [125], [146]. Her work has been an important reference during our investigation on VCSEL polarization dynamics and now she will join our group for some months to collaborate joining our lines of work.

Appendices

Appendix 1. Static and dynamic characterization of the laser diodes

The static characterization is a set of measurements in which no modulation (RF power) is present in the laser cavity. Therefore, it is emitting constant power, what is also called continuous wave regime (CW). In the static characterization we include the optoelectronic Power to bias current (PI) curve at 25°C and the variation in the emitted wavelength with temperature and with bias current. The PI curve represents the relation between the bias current and the optical power. We only present the curve at 25°C as it is the only temperature in which we work for the OFC, since there is laser temperature stabilization. On the other hand, we will see how the wavelength of the lasers varies depending on the temperature in which we are working and the bias current that we are injecting.

After the static characterization we show the dynamic performance of a laser that is the behaviour when a modulation signal is applied. In this chapter we show the dynamic linear regime, in which the laser is always working above the threshold current and under small signal conditions. For this purpose, a photodetector with transimpedance amplifier (model Discovery DSC-R402DC) is placed after the laser and the S21 and S11 parameters are presented. The S21 parameter shows the relation between the amount of radiofrequency power at the output (after the photodiode) and the amount of power injected in the laser at this same frequency. It is a measurement of the transmitted power in the system. In contrast, the S11 is the amount of power reflected in the input port in respect to

the power injected in this same port. Then, this second S-parameter shows the reflected power in the system.

I. Discrete Mode (DM)

The DM component used along this work is the model EP 1550-DM-HAA from Eblana Photonics. It is a DM laser in a 7-pin Butterfly package and includes an SMA connector and an impedance matched radiofrequency line for injecting the RF signal.

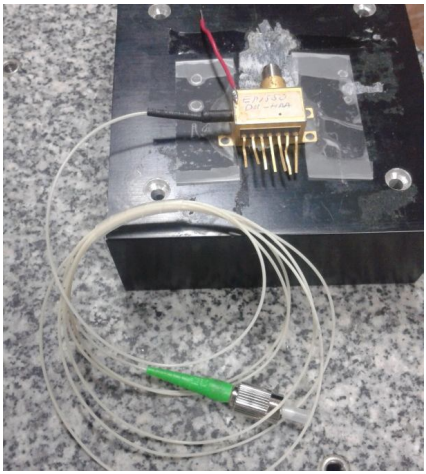

Fig 51. Picture of the DM source

Static performance

1- PI curve at 25°C

In the following picture we represent the PI curve of the DM source. The threshold current of this device is 12mA and the slope efficiency is 0.12 mA/mW. We will see later that our working bias current will be 61mA for the GS modulation.

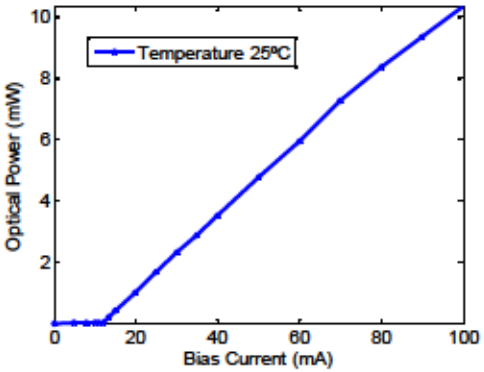

Fig 52. PI curve for the DM source at 25°C

2- Wavelength variation with temperature

In the following picture we can see the different wavelengths in which the DM laser emits depending on the working temperature that we establish. As we can see in the image below, the emitting wavelength changes 1nm (from 1542 to 1543nm) with a variation of 10 degrees in the temperature, that is 0.1nm/°C, when keeping the bias current at 61mA.

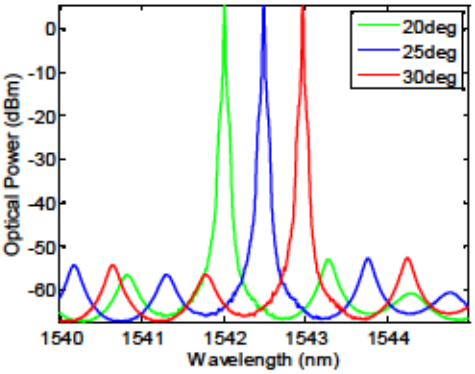

Fig 53. Optical power vs emitting wavelength for different temperatures

3- Wavelength variation with bias current

The wavelength also changes with the variation of the bias current that we apply in the device. Now the variation is 0.04nm/mA when maintaining the temperature fixed at 25°C.

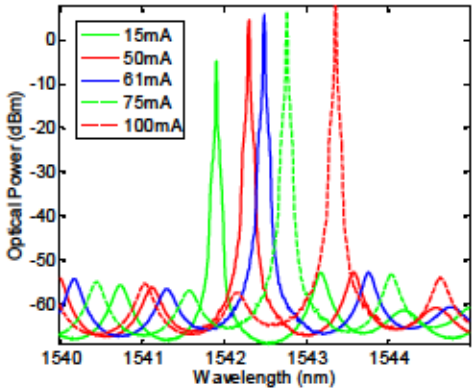

Fig 54. Optical power vs emitting wavelength for different temperatures

Dynamic performance

1- S21 parameter

In the following image we can observe the radiofrequency response of the DM laser and the Discovery photodetector.

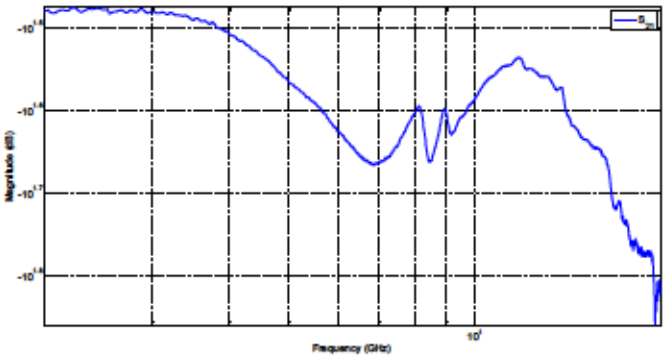

Fig 55. S21 parameter DM+Discovery

2- S11 parameter

The S11 parameter is presented in this picture:

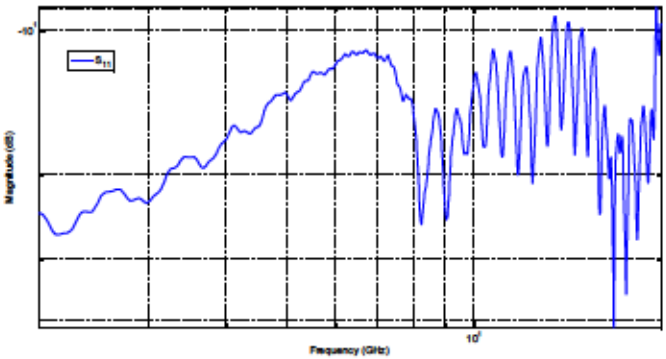

Fig 56. S11 parameter DM+Discovery

II. Vertical-Cavity Surface-Emitting Laser (VCSEL)

The VCSEL sources used along this work are two samples of a prototype of the model VL-1550-8G-P2-H4 provided by VERTILAS. This component is provided in a package with 5 pins, similar to the TO one. For the first sample we designed a specific PCB for the temperature control and bias and RF injection. This PCB was fabricated in the radiofrequency group in this university. The design and fabrication of the PCB was not easy to do as we are working in high frequencies and we would like to have broad bandwidth in the GHz range. Designing and building the set-up was therefore a time consuming task. From now, we call this sample VCSEL#1. The group VCSEL and PCB is shown in the following picture:

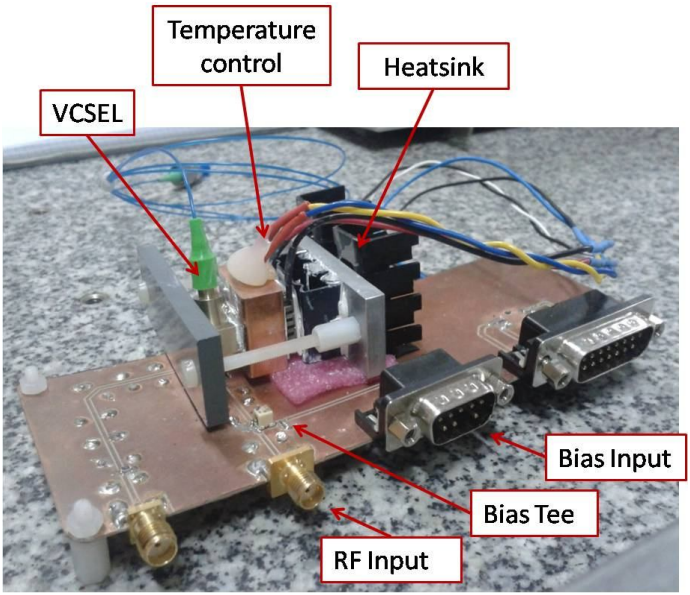

Fig 57. Picture of VCSEL#1 and its set-up

The second VCSEL, called VCSEL#2 in this document, is the same model than the previous one but this time it is provided with a PCB made by the supplier company, VERTILAS. In the following picture we can see a picture of this device and its set-up:

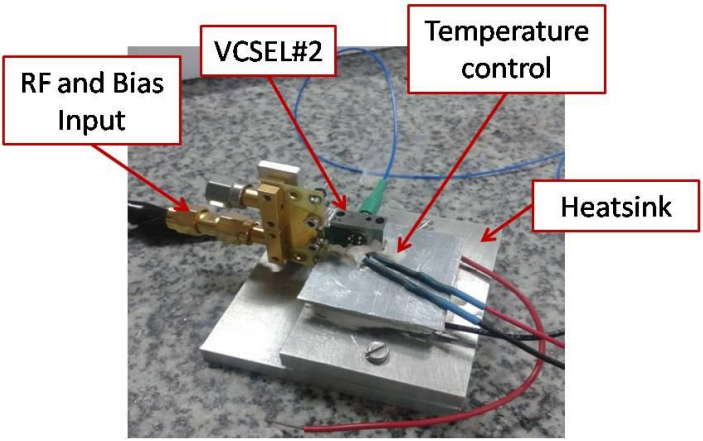

Fig 58. Picture of VCSEL#2 and its set-up.

Static performance VCSEL#1

Following the same procedure as before, we show the static characteristics that are useful in order to modulate the VCSEL in the Gain Switching technique for the OFCG (GS-OFCG). Besides, with this device we include another static measurement that was taken only for VCSEL#1 source during my stay in Darmstadt: the RIN measurement.

1- *PI curve at 25°C*

In the picture we see that the threshold current of this device is 2.9mA and the slope efficiency is 0.1 mA/mW. We will see later that our working bias current will be 11.4mA for the GS-OFCG.

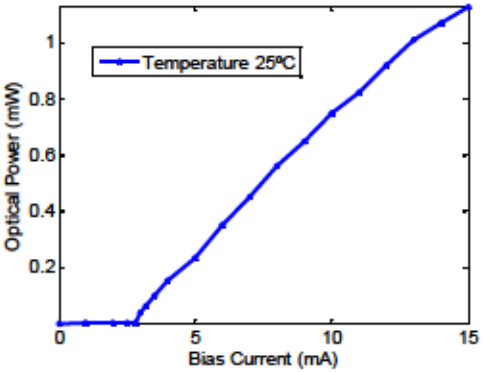

Fig 59. PI curve for VCSEL#1 source at 25°C

2- *Wavelength variation with temperature*

In the following picture we see the different wavelengths in which the VCSEL emits depending on the working temperature that we establish. The emitting wavelength changes 2nm with a variation of 20 degrees in the temperature that is 0.1nm/° C, when keeping the bias current at 11.4mA.

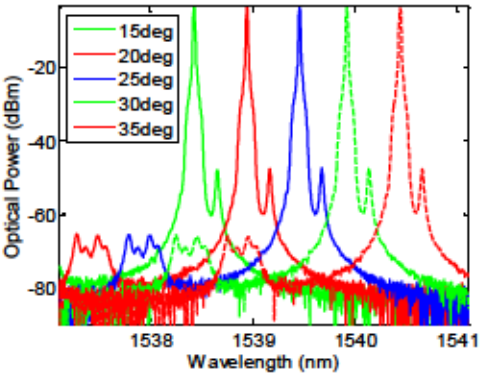

Fig 60. Optical power vs emitting wavelength for different temperatures

3- *Wavelength variation with bias current*

In the following picture we see a variation of 0.25nm/mA in the wavelength, because of a change of 2nm varying the bias current 8mA. The temperature has been fixed at 25°C.

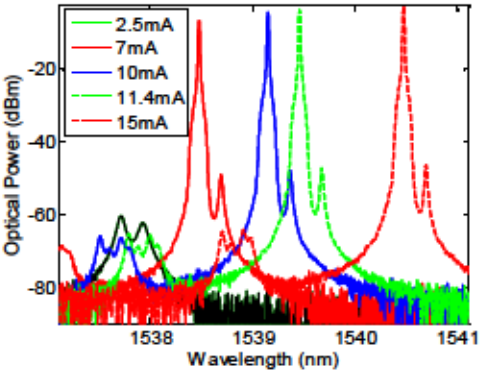

Fig 61. Optical power vs emitting wavelength for different bias currents

4- *RIN measurement*

We see in Fig 62 (left picture) that keeping the temperature and the bias current constant, the output optical power is theoretically supposed to be constant. However, the real case in Fig 62 (right) shows that there are power fluctuations due to an intensity variation called intensity noise [147]. This variation is caused by the spontaneous emission that is added to the stimulated emission in the wavelength and that is usually neglected when computing with the rate equations and it is called Relative Intensity Noise (RIN). The formula for the RIN will be the following:

$$RIN_{LIN} = \frac{\left\langle \delta P(t)^2 \right\rangle}{Po^2 \Delta f} \quad [1/Hz]$$

These optical power variations also imply fluctuations in the electrical signal received in a photodetector when no modulation is applied generating a noise that is added to the total electrical noise and can be measured in an Electrical Spectrum Analyzer (ESA). It is usually measured with normalized bandwidth (dB/Hz).

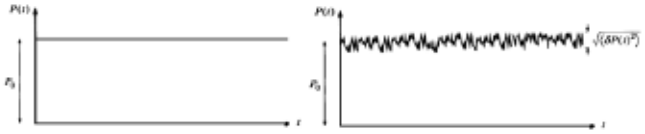

Fig 62. Ideal (left) and real (right) output power of a laser with fixed temperature and bias current [147]

Taking into account that we measure noise fluctuations, the RIN is not easy to obtain. We need to keep constant the temperature and bias current and have a low noise detector and an ESA with low noise floor. RIN in VCSELs is usually below -125dB/Hz [148]. Typically the RIN spectrum is related with the frequency response of the device and therefore it presents a peak at the relaxation oscillation frequency of the laser. Then, we get the maximum intrinsic modulation frequency for the laser.

This measurement was really important in our case for the following reason: the PCB specially designed for the VCSELs that we use is interfering in the S21 measurement and we cannot extract the resonant frequency with it. Then, with this RIN measurement we could observe the relaxation oscillation frequency and how it is increased with the increment in the bias current.

As we see in the picture, the RIN decreases for higher bias currents. On the other hand, we observe a peak that corresponds with the relaxation oscillation frequency and how it moves towards higher frequencies with the increase in the bias current. This is the normal result for a RIN measurement. The selection of the equipment and the resolution and video bandwidths in the ESA is critical, as we are measuring a signal below -130dB/Hz. For this reason we have based our set-up in the one described in [149].

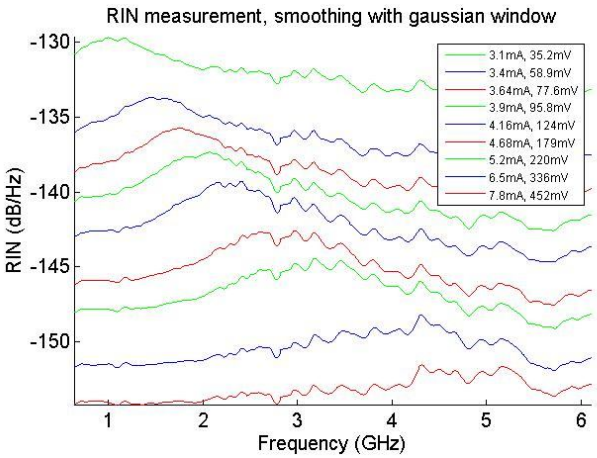

Fig 63. RIN measurement for the VCSEL source for different bias currents

The following graphics are obtained from the data in Fig 63. In them we observe the linear relations between some parameters that are typical in lasers and VCSELs [150], [151]. We check that the RIN level decreases linearly with the increase in the bias current because the mean power emitted is higher (see RIN formula). On the other hand, we show that the resonant frequency increases linearly with the square root of the increase in the bias current.

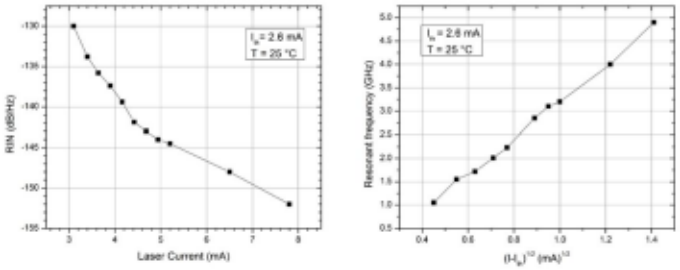

Fig 64. RIN level and resonant frequency variation in respect to the laser bias current

This RIN measurement was taken during my stay in Darmstadt with their set-up and was only taken for this sample (neither for the DM source nor VCSEL #2). For more information about it see [147], [149].

Static performance VCSEL#2

1- PI curve at 25°C

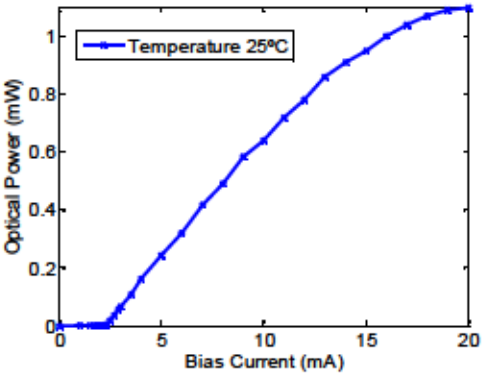

Fig 65. PI curve for the VCSEL#2 source at 25°C

In the picture we see that the threshold current of this device is 2.2mA and the slope efficiency is 0.1 mA/mW. We will see later that our working bias current will be 12mA for the GS-OFCG.

2- *Wavelength variation with temperature*

In the following picture we check that the emitting wavelength in VCSEL#2 varies 2nm in 20°C when keeping the bias current at 12mA that corresponds to 0.1nm/°C. Then, we have obtained the same temperature variation in both VCSELs samples.

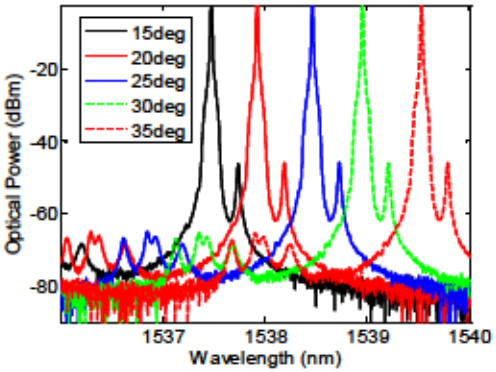

Fig 66. Optical power vs emitting wavelength for different temperatures

3- *Wavelength variation with bias current*

In the following picture we see the wavelength variation with the bias current in this sample, VCSEL#2. There is a variation of 3nm in 12.5mA, so 0.24nm/mA.

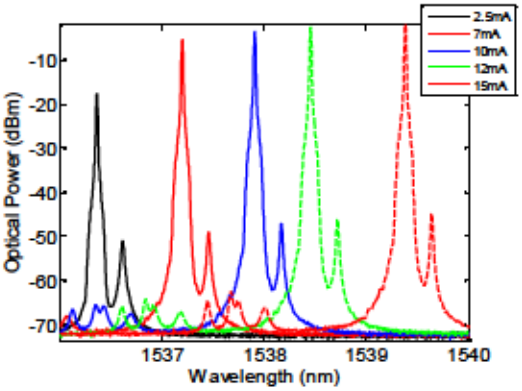

Fig 67. Optical power vs emitting wavelength for different bias currents

Dynamic performance VCSEL#1

1- S21 parameter

In the following image we can observe the radiofrequency response of VCSEL#1 and the Discovery photodetector. We see that the following S21 parameter is not the typical S21 curve for a laser (second order response with a peak at the resonant frequency). Then, we can guess that the PCB is hiding the real response of the laser and consequently our dynamic response is also determined by the PCB and not only by the laser.

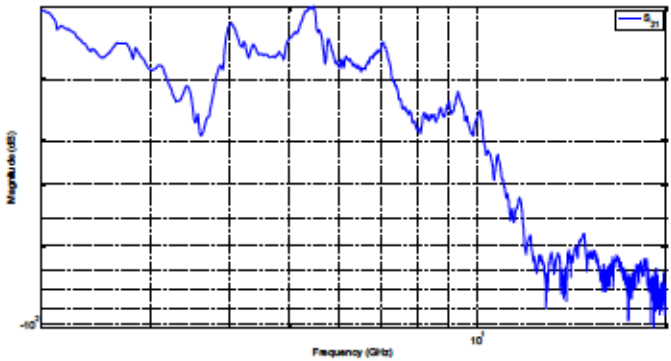

Fig 68. S21 parameter VCSEL#1+Discovery

2- *S11 parameter*

The S11 parameter is presented in this picture:

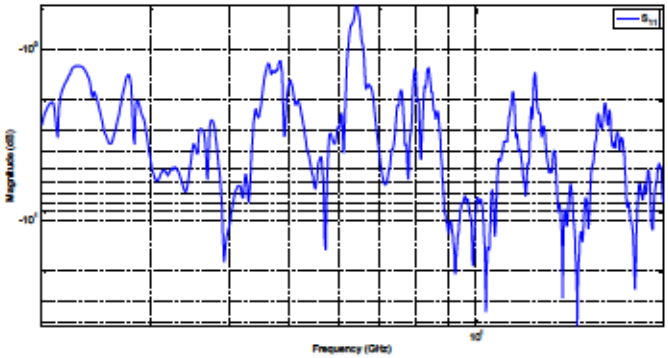

Fig 69. S11 parameter VCSEL#1+Discovery

The previous curve is basically the response of the PCB. The design and fabrication of this board was not easy as we try to

work in a broad radiofrequency bandwidth. The design of it was done carefully. Anyway, this PCB allowed us to work with the VCSEL for one year so far and we have obtained with it very good results as we will see along this document.

Dynamic performance VCSEL#2

1- S21 parameter

In the following image we observe the radiofrequency response of VCSEL#2 and the Discovery photodetector. We see that this curve corresponds to the typical S21 parameter of a laser. So we can conclude, than in this case the PCB is not masking the frequency response of the laser and we can clearly observe the differences between the shape of this curves and the one in Fig 68.

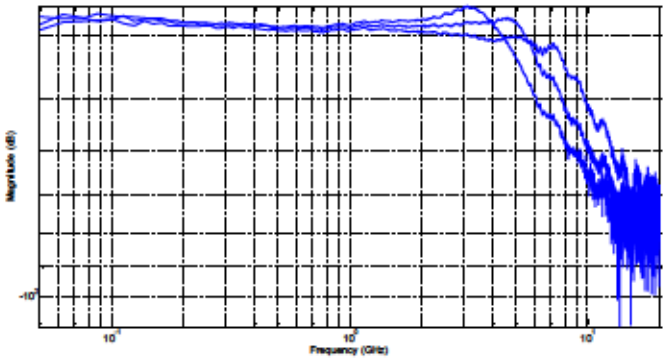

Fig 70. S21 parameter VCSEL#2+Discovery for different bias currents

2- S11 parameter

The S11 parameter is presented in this picture. As we see the S11 parameter is lower in this source than the previous source (VCSEL#1), which will probably imply more power entering the laser.

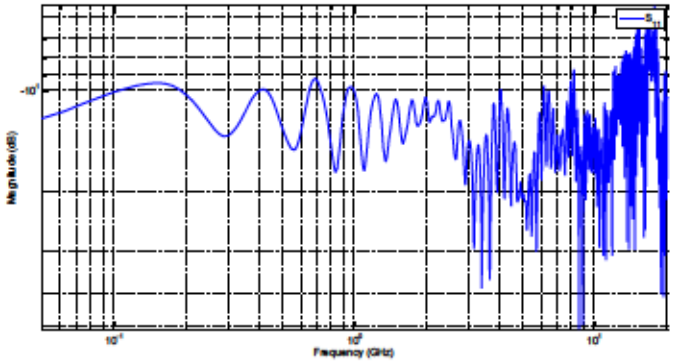

Fig 71. S11 parameter VCSEL#2+Discovery

III. Comparative: DM vs. VCSEL

In this appendix we have checked that the threshold current is much lower in VCSELs than DMs. VCSELs have lower threshold current because of their smaller active region (smaller cavity) [135]. In our samples it changes from around 2.5mA (2.9 for VCSEL#1 and 2.2 for VCEL#2) to 12mA for the DM device.

On the other hand, the slope efficiency is very similar, 0.1mW/mA and 0.12mW/mA in our VCSELs and DMs respectively. This slope efficiency depends on material gain, the internal loses in the cavity (internal quantum efficiency and optical coupling efficiency) and the reflectivity in the mirrors (differential quantum efficiency) [136]. This is a critical point in VCSELs: their cavity is small and therefore they have small round trip gain so they need high reflectivity in the mirrors to increase the photon lifetime and increase the stimulated emission and the slope efficiency. Conversely, this increase in the reflectivity also causes less optical power to be emitted decreasing the slope efficiency. In conclusion, the reflectivity in the mirrors should be carefully selected and this will directly affect the slope efficiency. Anyway, the optical power emitted is much lower in VCSELs than in EELs.

We have seen the wavelength variation with the temperature in each of the samples. Both type of sources change their emitting wavelength 0.1nm/°C. In general, the lasing wavelength depends on the optical length of the cavity (that is related to the refractive index and the length of the active region). Besides, in VCSELs it also depends on the mirrors response [148]. This value of wavelength change with temperature is exactly as expected taking into account several references [68], [152].

Unlike what happened with the temperature, the wavelength variation with bias current is significantly different in each source: it is much higher in VCSELs than in EELs. This is mainly due to the size of the device. VCSEL's cavity is much smaller than DM's and therefore the same current variation implies higher carrier density variation inside the cavity and the same happens with the refractive index variation. As a consequence, the emitted wavelength will vary more in VCSELs than EELs [136].

As conclusion, we can guess that VCSELs will have a good response under GS regime as they present lower threshold current with similar efficiency which will imply a more efficient GS regime. On the other hand, this device is only a prototype laser while the DM is commercial and its packaging has better response which could imply better RF coupling.

Appendix 2. DM-OFC span and teeth variation with the RF Frequency

In this appendix we show two figures that show the tendency of the DM-OFC with the variation in the modulation frequency. We see in Fig 72 that the number of comb teeth decreases continuously as we increase the modulation frequency. However, in Fig 73 the span does not follow the same decrease. This happens because we are decreasing the number of lines but increasing the RF frequency and therefore the distance between teeth: having less teeth we are able to obtain wider combs. We observe that the broadest comb is obtained at 8.3GHz which corresponds to the comb presented in Chapter 5.

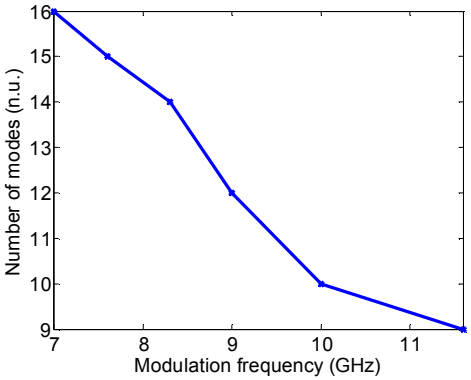

Fig 72. Number of teeth vs RF frequency

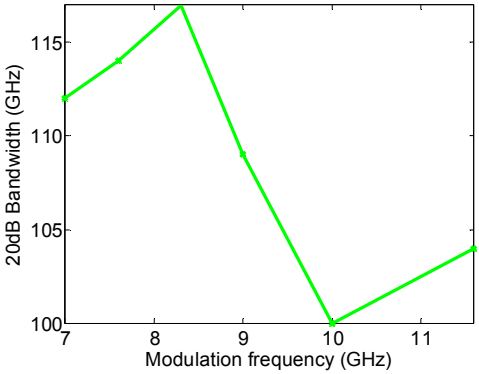

Fig 73. 20dB span vs RF frequency

Appendix 3. VCSEL#1-OFC characterization and chirp

In Chapter 6, we have shown the VCSEL-OFC which is the best comb obtained with the second VCSEL sample. However, before selecting this comb to be the best we have done a detailed study of the VCSEL behaviour under GS in two VCSEL samples. In this appendix we characterize the best comb obtained for the other VCSEL sample, VCSEL#1-OFC. This sample was static and dynamically characterized in Appendix 1. Here we will also include the chirp characterization that was taken only for this VCSEL#1 during my stay in Technische Universität Darmstadt (TUD) during summer 2013.

The set-up used for the VCSEL#1-OFC was shown in Fig 23. VCSEL#1 will be operated maintaining the bias current at 11.4mA and the temperature stabilized at 25ºC. When the GS regime is induced with 15dBm entering the PCB at 5.2GHz, we obtain the broadest comb, which is presented in this image.

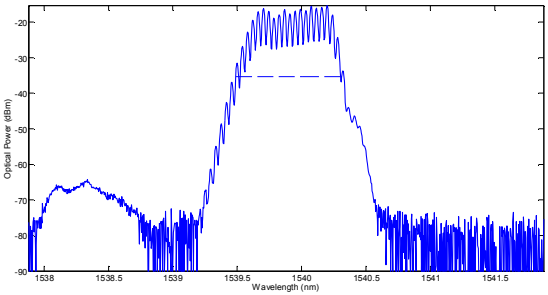

Fig 74. VCSEL#1-OFC (25 ºC, 11.4mA, 5.2GHz, 15dBm) that has 21 teeth in the 20dB span which corresponds to 106GHz

In the image above we observe the resulting comb when optimizing the parameters in order to get the broadest spectrum. We also see a dashed line at -20dB of its maximum, to show the part of the comb that it inside the 20dB span. The VCSEL#1-OFC has 21 teeth in the 20dB optical span that corresponds to 106GHz broad.

The autocorrelation profile that corresponds to this VCSEL#1-OFC is shown in the following figure, where we see that it has a time duration of 67.6ps, Therefore, assuming a profile sech² our pulse has a duration of 41.7ps. This value is above the equipment resolution.

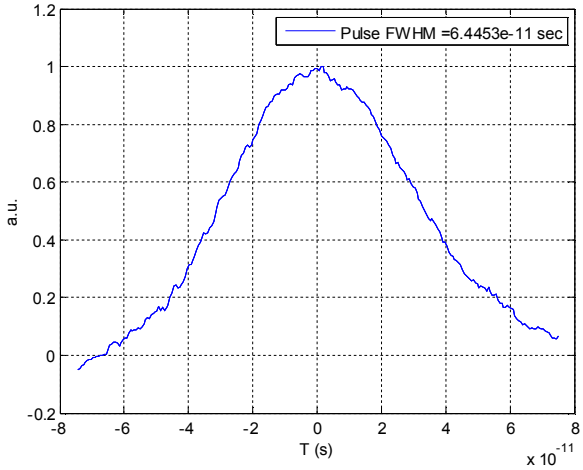

Fig 75. VCSEL#1-OFC: Temporal autocorrelation pulse

The phase noise of the electrical detected signal is shown in the following picture. We see that the phase noise of both the RF source (CW source Agilent and green line) and the detected signal (VCSEL#1-OFC and red line) have the same behaviour along the whole curve. This means that the modes that appear in the GS comb are highly correlated and their remarkable stability is linked to the stability of the CW RF source considered.

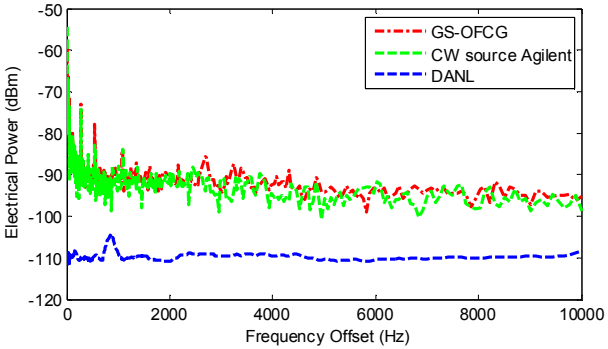

Fig 76. VCSEL#1-OFC: Phase Noise of the electrical detected signal

Chirp measurement

The lasing frequency varies with the current injected in the laser. “A change in carrier density under current injection will lead to a change in the refractive index which will in turn modify the lasing frequency” [136]. The variation of the instantaneous lasing frequency in time is called frequency chirp. The lasing frequency is the following (extracted from the wave equation),

where *M* is an integer, *c* the speed of light, *n* the refractive index and *L* the length of the cavity:

$$f = \frac{M \cdot c}{2nL}$$

Starting from the equation and doing some calculations with the travelling wave equation we reach to the formula of the frequency variation with time [136][153], that is:

$$\delta v(t) = \frac{\beta c}{4\pi}\left(\frac{1}{P_{opt}}\frac{\partial P_{opt}}{\partial t} - \frac{Rsp}{P_{opt}} + kP_{opt}\right)$$

Where P_{opt} is the optical power emitted, R_{sp} is the spontaneous emission rate, *k* is called the adiabatic chirp coefficient and β_c is known as the linewidth enhancement factor. In the equation we see that the frequency variation has three different terms: the second one is due to the spontaneous emission and is usually neglectable as is significantly smaller than the other ones. The third term is called adiabatic chirp and is proportional to the mean power injected, so is also present when the laser is working in steady state conditions. The first term is called transient chirp and is related to the time variation of the logarithm of the optical power [136]. This factor is the most relevant when working in large signal conditions and is the main factor to be considered in our measurements since it increases

notably when entering the GS regime. Therefore, we call chirp the maximum variation of this frequency change [153]:

$$Chirp = \delta v_o = \frac{\beta c}{4\pi}\left(\frac{1}{P_{opt}}\frac{\partial P_{opt}}{\partial t}\right)_{\max}$$

The temporal pulses associated to GS are negatively chirped [70]. In the following image we see the set-up used for these measurements:

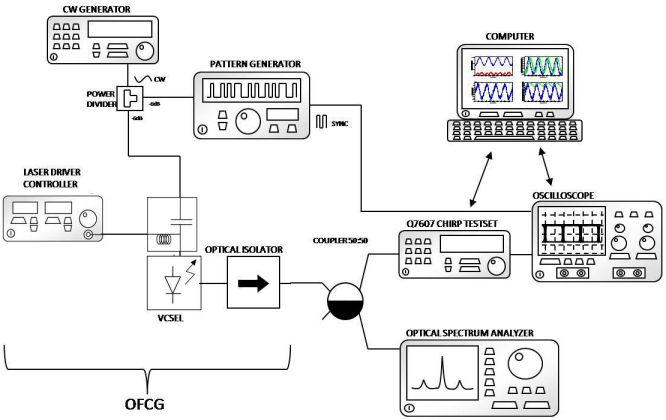

Fig 77. Set-up for the chirp measurement

With this set-up we extract and plot the following information, where we can see the Intensity Modulation of the signal (IM) the Frequency Modulation (FM) the addition and subtraction of them and the frequency variation in time. From this latter

parameter we compute the chirp. In the image we see these results for large signal modulation:

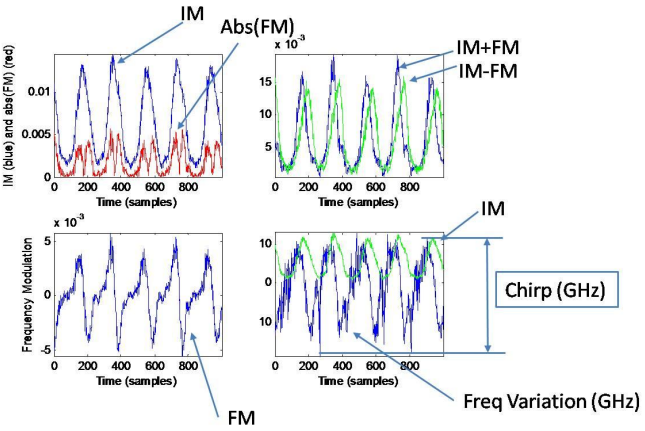

Fig 78. Chirp results with VCSEL#1-OFC (25 ºC, 9mA, 5.2GHz, 15dBm)

It is important to remark that these results were not taken with the same parameters than the comb presented previously (Fig 74), even if it only changes the bias current from 11.4mA to 9mA. This image corresponds to a chirp value of 31.63GHz. Now we are presenting the same results in linear regime (-2dBm RF power), where the chirp is much lower, 12.04GHz.

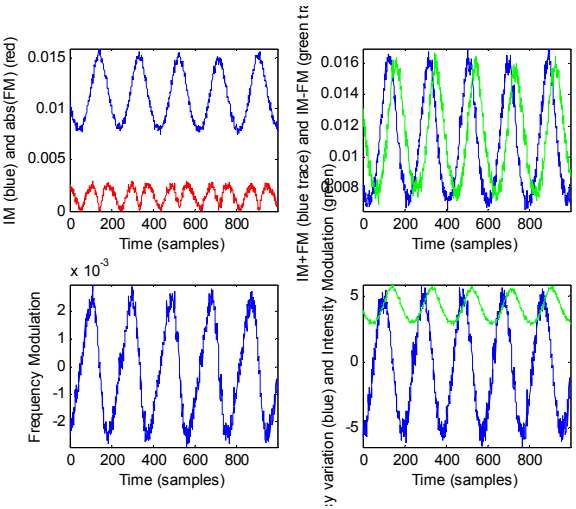

Fig 79. Chirp results with VCSEL#1 in linear regime (25 ºC, 9mA, 5.2GHz, -2dBm)

Comparing the two previous images we see that the adiabatic chirp is presented also when the laser is under linear regime. In this case we obtain a chirp of 12.4GHz, which is quite big compared to typical EEL lasers values [154]. This is because VCSELs have smaller cavity and then the carrier density variation with time is bigger causing bigger chirp values. On the other hand we see how the shape of this frequency variation changes when we enter the GS regime: this is due to the transient chirp that is already dominant than the other terms. A compilation of the chirp values is plotted in the following picture:

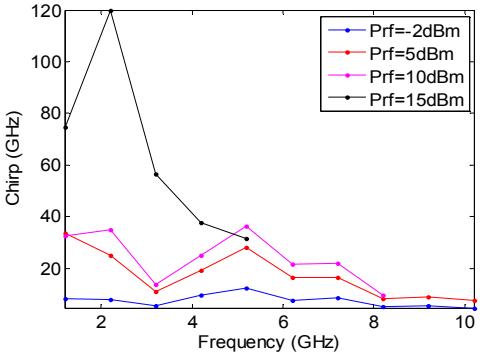

Fig 80. Chirp values for each RF power and RF frequency

In the figure we see the variation of the chirp with RF frequency for different RF powers. We clearly perceive that the chirp decreases with the frequency in a similar way that the S21 parameter does (see Fig 68). Therefore we conclude that the PCB is affecting the measurement and most of the power at high frequencies is not really reaching the laser.

These same results are shown in the table. At -2dBm (blue trace) the laser is working under linear regime so the values of the chirp are much lower in comparison with the other powers. On the other hand we see how it increases with the injected power even if it is affected by the PCB. The highest value, of 120GHz (at 2.2GHz with 15dBm RF power) is quite big in comparison with typical chirp values.

Table I. Different chirp values for each RF power and RF frequency

Chirp (GHz)	P_{RF}=-2dBm	P_{RF}=5dBm	P_{RF}=10dBm	P_{RF}=15dBm
f_{RF}=1.2GHz	8.19	33.68	32.65	74.53
f_{RF}=2.2GHz	7.78	25.15	35.08	120
f_{RF}=3.2GHz	5.65	11.1	13.68	56.37
f_{RF}=4.2GHz	9.5	19.05	24.85	37.8
f_{RF}=5.2GHz	12.4	28.17	36.44	31.63
f_{RF}=6.2GHz	7.5	16.5	21.56	x
f_{RF}=7.2GHz	8.56	16.6	22	x
f_{RF}=8.2GHz	5.25	8.13	9.65	x
f_{RF}=9.2GHz	5.61	8.8	x	x
f_{RF}=10.2GHz	4.65	7.6	x	x

In conclusion, we cannot ensure that these chirp values are the real ones for the VCSEL as the PCB might be interfering, but we can say that are the chirp correspondent to the group VCSEL#1+PCB. Besides, the chirp set-up used cannot measure higher chirp values than 50GHz with our working mode (see Advantest Q7607, whose response has a frequency of 150GHz), so the values above 50GHz might not be valid.

This chirp measurement was taken during my stay in Darmstadt with their set-up and was only taken for this sample (neither for the DM source nor VCSEL #2).

Appendix 4. DM-OFC direct, indirect and combined combs

The same experiment presented with the VCSEL in Chapter 8 comparing the direct, indirect and combined techniques for comb generation was performed for the DM laser source. When the GS regime is induced, the working parameters of the DM are 25 ºC, 61mA, 8.3GHz and 28dBm so the output of the DM is the DM-OFC in Fig 20. In the following figure we compare the combined comb with the sole direct and indirect techniques when using the DM source. Fig 81b (middle line) is the DM-OFC shown in Fig 20 with 15 teeth so 117GHz in the 20dB span. Fig 81c (bottom line) is the indirect comb and Fig 81a (upper line) is the Combined-OFCG. They present 102GHz (13 teeth) and 183GHz (23 teeth) respectively in the 20dB span. Surprisingly, the EO-FOCG in this case is narrower than the sole DM under GS.

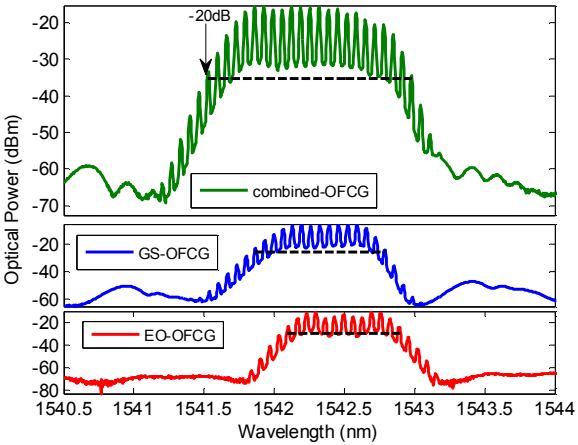

Fig 81. OFCG techniques comparison: GS-OFCG, EO-OFCG and combined-OFCG with the DM

The combined-OFCG offers a comb with an enhanced span that is 70% wider than the comb generated with the sole indirect EO-OFCG and 50% wider than the GS-OFCG. Also, the optical power in each of the optical lines in the comb is similar in both the EO-OFCG and the combined-OFCG. Scaling the EO scheme would permit the generation of a comb with the same width but the power of the optical lines would be significantly smaller and the set-up, more complex and more energy demanding.

Appendix 5. Numerical study of VCSELs under GS

The interactions between light and matter in a laser can be modelled with the Rate Equations that were shown in Chapter 2 (extracted from [37]). These rate equations have been implemented for VCSELs under GS to get an idea of the correspondence between the simulations and the experiments performed. The physical parameters used in these simulations are shown in the following table. Most of them are extracted from [70]. However, it is important to remark that most physical properties of the VCSELs that we use are not available and we do not know whether the values used are similar or relatively different to the real ones. Therefore, we are looking in the simulation for conclusions on the behaviour expected for a generic VCSEL device but not necessarily the exact values. For more information read [21], [58], [59], [65].

The evolution of the comb simulated with changes in the bias current, in the RF power and the RF frequency are presented because these are the parameters that define the Gain Switching working conditions of a given device.

Table II. VCSEL parameters

Parameter	Value	Parameter	Value
Active Volume (cm3)	3.12	**Linewidth enhancement factor, α (-)**	5.9
Confinement factor, Γ (-)	0.02	**Internal quantum efficiency (-)**	0.402
Diferential gain, dG/dn (cm^2)	$1.6*10^{-16}$	**Emitting wavelength, λ (nm)**	1550
Group velocity, v_g (cm/s)	$9.4*10^{9}$	**Refractive index in active region, n (-)**	3.5
Transparency carrier density, No (cm^{-3})	$1.61*10^{18}$	**Threshold current (mA)**	2.9
Carrier Lifetime, τ_N (ns)	1	**Maximum output power (dBm)**	< 1
Photon lifetime, τ_P (ps)	5.5	**RF bandwidth (GHz)**	10
Nonlinear gain compression factor, ε (cm^3)	$1*10^{-17}$	**Beam Profile**	Circular
Spontaneous emission coefficient, β (-)	$1*10^{-5}$		

VCSEL-OFC evolution with the bias current

In the following images we observe the evolution of the generated comb with variations in the bias current. This parameter has been varied normalized to the threshold current from 0.5 to 20 times I_{TH} (the upper limit of this bias current in the simulations is slightly higher than the maximum value stated in the datasheet of our device). f_{RF} has been set to 5GHz and I_{RF} to $10I_{TH}$ in this simulation.

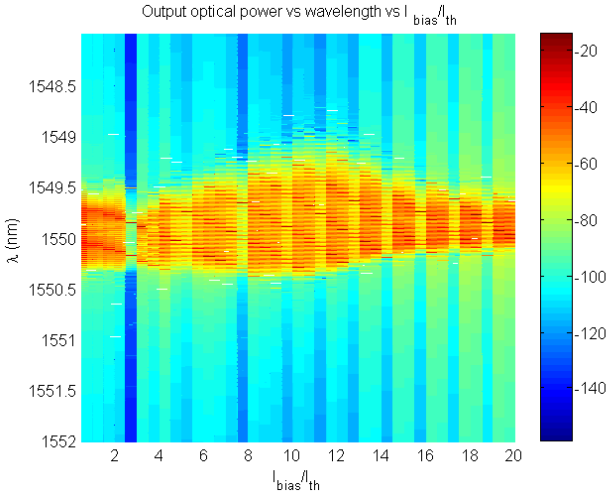

Fig 82. Upper view of the Optical Frequency Comb evolution with the bias current. Ibias varies from 0.5Ith to 20Ith

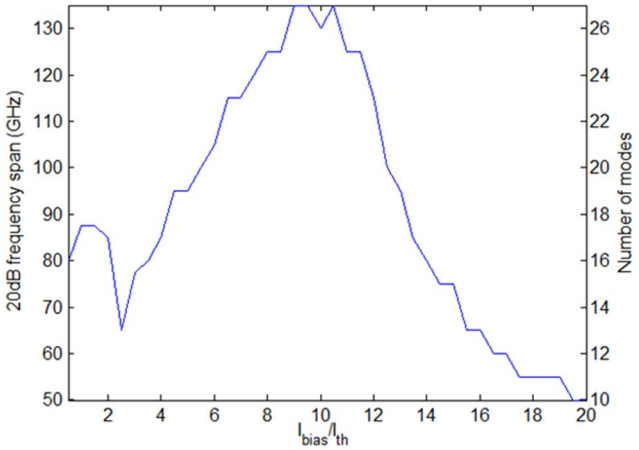

Fig 83. Optical span and number of modes vs. bias current

We see in Fig 83 the optical span in respect to the bias current (I_{BIAS} /I_{TH}) and the number of modes corresponding to this frequency span. We see that a maximum span of 135GHz is obtained when the bias current is around 9.5 times the threshold one. This corresponds to 27 modes inside the 20dB bandwidth. For lower and higher bias the result will be worsened. This would correspond to 19mA in our device. However, we will see that the optimized bias current for the best comb in VCSEL#1 will be 11.4mA.

VCSEL-OFC evolution with the modulation current

In the following images we observe the evolution of the generated comb with variations in the RF current. This parameter has been varied normalized to the threshold current from 0.5 to 20 times I_{TH}. It is important to remark that in practice we cannot increase I_{RF} so much as the VCSEL will be damaged. In this case, f_{RF} is 5GHz and I_{BIAS} is set to 9.5I_{TH} (it was the best result in the previous simulation).

We see in Fig 85 the optical span in respect to the RF current (I_{RF}/I_{TH}). As we can see the optical span increases constantly with the injected current so the higher the current the broader the comb.

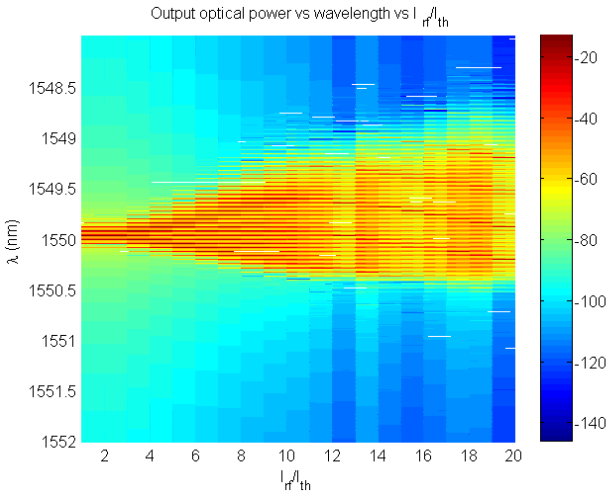

Fig 84. Upper view of the Optical Frequency Comb evolution with the modulation current. This parameter is varied from 0.5Ith to 20Ith

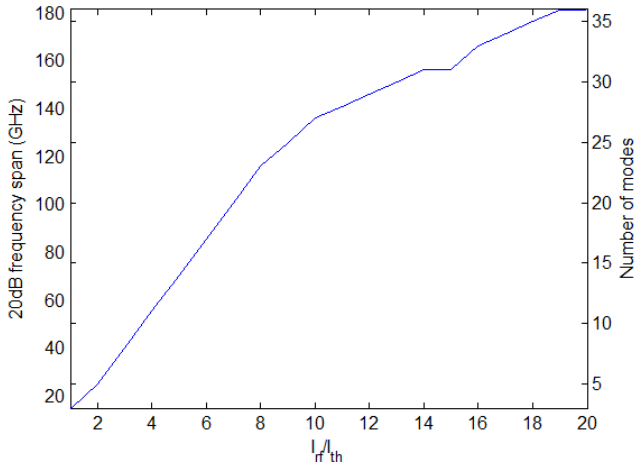

Fig 85. Optical span and number of modes vs. RF current

However, two limits need to be taken into account at this point: on one hand, the maximum power injected in order not to damage the device, on the other hand the double period (DP) behavior of the VCSEL. The increase in the RF power causes the appearance of comb lines separated $f_{RF}/2$ and not only at f_{RF} and rising the injected power even more we can see that other subharmonics come up too. We have already observe this characteristic in the VCSEL in [27]. Therefore in real experiments we select the maximum RF power injected taking into account the appearance of these subharmonics.

VCSEL-OFC evolution with the modulation frequency

In the following image we observe the evolution of the generated comb with variations in the working frequency. The widest span is for frequencies around 4GHz and we observe that the behaviour expected for the VCSEL under GS is to have narrower combs at lower and upper modulation frequencies. We have observed this behaviour in practice but the performance for our VCSELs is optimized around 5-6GHz and therefore that will be the modulation frequency used.

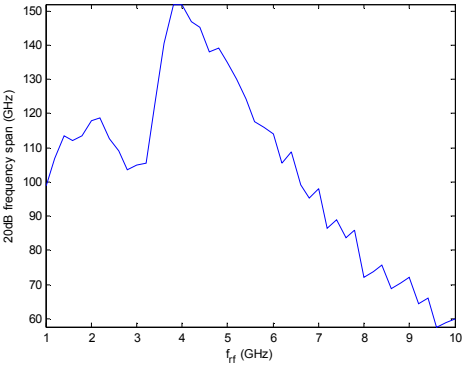

Fig 86. Optical span vs. RF frequency

On the other hand, the number of modes decreases constantly with the RF frequency. This is not always affecting the optical span as there is a tradeoff between the number of modes and the RF frequency because:

$$Optical\_span = \#modes \cdot f_{RF}$$

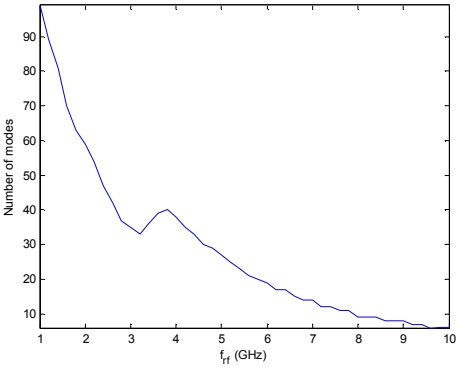

Fig 87. Number of modes vs. RF frequency

References

[1] "The Nobel Prize in Physics 2005." [Online]. Available: http://www.nobelprize.org/nobel_prizes/physics/laureates/2005/. [Accessed: 05-Apr-2016].

[2] F. Zhu, T. Mohamed, J. Strohaber, A. A. Kolomenskii, T. Udem, and H. A. Schuessler, "Real-time dual frequency comb spectroscopy in the near infrared," *Appl. Phys. Lett.*, vol. 102, no. 12, p. 121116, 2013.

[3] P. J. Delfyett, S. Gee, M.-T. Choi, H. Izadpanah, W. Lee, S. Ozharar, F. Quinlan, and T. Yilmaz, "Optical Frequency Combs From Semiconductor Lasers and Applications in Ultrawideband Signal Processing and Communications," *J. Light. Technol.*, vol. 24, no. 7, p. 2701–, Jul. 2006.

[4] A. R. Criado, C. de Dios, G. H. Döhler, S. Preu, S. ; Malzer, S. ; Bauerschmidt, H. ; Lu, A. C. ; Gossard, and P. Acedo, "Ultra-narrow linewidth CW sub-THz generation using GS based OFCG and n-i-pn-i-p superlattice photomi...," *Electron. Lett.*, p. 2, 2012.

[5] S. T. Cundiff and A. M. Weiner, "Optical arbitrary waveform generation," *Nat. Photonics*, vol. 4, no. 11, pp. 760–766, Oct. 2010.

[6] T. Udem, R. Holzwarth, and T. W. Hänsch, "Optical frequency metrology.," *Nature*, vol. 416, no. 6877, pp. 233–7, Mar. 2002.

[7] R. Wu, C. M. Long, D. E. Leaird, and A. M. Weiner, “Directly Generated Gaussian-Shaped Optical Frequency Comb for Microwave Photonic Filtering and Picosecond Pulse Generation,” *IEEE Photonics Technol. Lett.*, vol. 24, no. 17, pp. 1484–1486, Sep. 2012.

[8] Menlo Systems, “Optical Frequency Comb Selection Guide.” [Online]. Available: http://www.menlosystems.com/assets/datasheets/MENLO_CombSelGuide-D-EN_2016-06_3w.pdf. [Accessed: 15-Jun-2016].

[9] J. Ye and S. T. Cundiff, *Femtosecond Optical Frequency Comb: Principle, Operation, and Applications*. Boston: Kluwer Academic Publishers, 2005.

[10] Menlo Systems, “Compact Optical Frequency Comb.” [Online]. Available: http://www.menlosystems.com/assets/datasheets/MENLO_SmartComb-D-EN_2016-02_3w.pdf. [Accessed: 15-Jun-2016].

[11] “Pilot Photonics Optical Wavelength Comb Source.” [Online]. Available: http://www.pilotphotonics.com/PP-OWCS.pdf. [Accessed: 11-Nov-2015].

[12] A. R. Criado, C. de Dios, E. Prior, G. H. Dohler, S. Preu, S. Malzer, H. Lu, A. C. Gossard, and P. Acedo, “Continuous-Wave Sub-THz Photonic Generation With Ultra-Narrow Linewidth, Ultra-High Resolution, Full Frequency Range Coverage and High Long-Term Frequency Stability,” *IEEE Trans. Terahertz Sci. Technol.*, vol. 3, no. 4, pp. 461–471, Jul. 2013.

[13] P. Martin-Mateos, M. Ruiz-Llata, J. Posada-Roman, and P. Acedo, “Dual-Comb Architecture for Fast Spectroscopic Measurements and Spectral Characterization,” *IEEE Photonics Technol. Lett.*, vol. 27, no. 12, pp. 1309–1312, Jun. 2015.

[14] Luzwavelabs, “pulse/P - tunable and compact optical frequency comb.” [Online]. Available: http://luzwavelabs.com/pulsep/. [Accessed: 16-Jun-2016].

[15] Jones, Diddams, Ranka, Stentz, Windeler, Hall, and Cundiff, “Carrier-envelope phase control of femtosecond mode-locked lasers and direct optical frequency synthesis,” *Science*, vol. 288, no. 5466, pp. 635–40, Apr. 2000.

[16] R. Paschotta, “Gain Switching SPIE,” 2016. [Online]. Available:

http://spie.org/publications/fg14_p30-31_gain_switching. [Accessed: 10-May-2016].

[17] T. J. Kippenberg, R. Holzwarth, and S. A. Diddams, "Microresonator-Based Optical Frequency Combs ," *Sci.* , vol. 332 , no. 6029 , pp. 555–559, Apr. 2011.

[18] R. Wu, V. Torres-Company, D. E. Leaird, and A. M. Weiner, "Supercontinuum-based 10-GHz flat-topped optical frequency comb generation," *Opt. Express*, vol. 21, no. 5, p. 6045, Mar. 2013.

[19] V. Torres-Company and A. M. Weiner, "Optical frequency comb technology for ultra-broadband radio-frequency photonics," *Laser Photon. Rev.*, vol. 8, no. 3, pp. 368–393, May 2014.

[20] E. Prior, C. de Dios, A. R. Criado, M. Ortsiefer, P. Meissner, and P. Acedo, "Experimental study of VCSEL-based Optical Frequency Comb Generators," *IEEE Photonics Technol. Lett.*, vol. 26, no. 21, pp. 1–1, Nov. 2014.

[21] L. A. Coldren and S. W. Corzine, *Diode lasers and photonic integrated circuits*. Wiley, 1995.

[22] A. R. Criado, P. Acedo, G. Carpintero, C. de Dios, and K. Yvind, "Observation of phase noise reduction in photonically synthesized sub-THz signals using a passively mode-locked laser diode and highly selective optical filtering," *Opt. Express*, vol. 20, no. 2, p. 1253, Jan. 2012.

[23] A. R. Criado, C. de Dios, P. Acedo, G. Carpintero, and K. Yvind, "Comparison of Monolithic Optical Frequency Comb Generators based on Passively Mode-Locked Lasers for Continuous Wave mm-Wave and sub-THz generation," *J. Light. Technol.*, vol. 30, no. 19, pp. 3133–3141, Jan. 2012.

[24] CLEO Conference 2016, "Topic categories." [Online]. Available: http://www.cleoconference.org/home/submissions/topic-categories/. [Accessed: 16-Jun-2016].

[25] A. Kazemi, "Microresonator--Based Optical Frequency Combs Microresonator-Based Optical Frequency Combs," 2011. [Online]. Available: http://www.optics.unm.edu/sbahae/physics568/studentpapers2011/kazemi.pdf. [Accessed: 16-Jun-2016].

[26] P. P. Vasil'ev, I. H. White, and J. Gowar, *Fast phenomena in semiconductor lasers*, vol. 63. IOP Publishing, 2000.

[27] A. R. Criado, C. de Dios, E. Prior, M. Ortsiefer, P. Meissner, and P. Acedo, "VCSEL-Based Optical Frequency Combs: Toward Efficient Single-Device Comb Generation," *IEEE Photonics Technol. Lett.*, vol. 25, no. 20, pp. 1981–1984, Oct. 2013.

[28] R. Michalzik, *VCSELs*, vol. 166. Springer Berlin Heidelberg, 2013.

[29] "Designing With VCSELs | VCSEL." [Online]. Available: http://myvcsel.com/designing-with-vcsels/. [Accessed: 20-Apr-2016].

[30] E. Kapon and A. Sirbu, "Long-wavelength VCSELs: Power-efficient answer," *Nat. Photonics*, vol. 3, no. 1, pp. 27–29, Jan. 2009.

[31] R. S. Tucker, "Green Optical Communications—Part I: Energy Limitations in Transport," *IEEE J. Sel. Top. Quantum Electron.*, vol. 17, no. 2, pp. 245–260, Mar. 2011.

[32] A. Kasukawa, "VCSEL Technology for Green Optical Interconnects," *IEEE Photonics J.*, vol. 4, no. 2, pp. 642–646, Apr. 2012.

[33] "VCSEL Solutions for Green Photonics from 1.27 µm to 2.3 µm." [Online]. Available: http://www.vertilas.com/sites/default/files/Downloads/vertilas_spectroscopy_v9_0.pdf. [Accessed: 14-Apr-2016].

[34] S. Paul, C. Gierl, J. Cesar, M. Malekizandi, B. Kogel, C. Neumeyr, M. Ortsiefer, and F. Kuppers, "10-Gb/s Direct Modulation of Widely Tunable 1550-nm MEMS VCSEL," *IEEE J. Sel. Top. Quantum Electron.*, vol. 21, no. 6, pp. 436–443, Nov. 2015.

[35] R. Rodes, J. B. Jensen, D. Zibar, C. Neumeyr, E. Roenneberg, J. Rosskopf, M. Ortsiefer, and I. T. Monroy, "All-VCSEL based digital coherent detection link for multi Gbit/s WDM passive optical networks.," *Opt. Express*, vol. 18, no. 24, pp. 24969–74, Nov. 2010.

[36] B. Potsaid, V. Jayaraman, J. G. Fujimoto, J. Jiang, P. J. S. Heim, and A. E. Cable, "MEMS tunable VCSEL light source for ultrahigh speed 60kHz - 1MHz axial scan rate and long range centimeter class OCT imaging," in *SPIE BiOS*, 2012, p. 82130M.

[37] A. Consoli and I. Esquivias, "Pulse shortening of gain switched single

mode semiconductor lasers using a variable delay interferometer.," *Opt. Express*, vol. 20, no. 20, pp. 22481–9, Sep. 2012.

[38] "Luz WaveLabs | THz and Photonics." [Online]. Available: http://luzwavelabs.com/. [Accessed: 11-Apr-2016].

[39] N. US Department of Commerce, "Optical Frequency Combs." [Online]. Available: http://www.nist.gov/public_affairs/releases/frequency_combs.cfm. [Accessed: 05-Jun-2014].

[40] K. Sala, G. Kenney-Wallace, and G. Hall, "CW autocorrelation measurements of picosecond laser pulses," *IEEE J. Quantum Electron.*, vol. 16, no. 9, pp. 990–996, Sep. 1980.

[41] A. Weiner, *Ultrafast Optics*. 2011.

[42] A. R. Criado, "New photonic architectures and devices for generation and detection of sub-THz and THz waves," Carlos III University, Madrid, 2013.

[43] S. A. Diddams, "The evolving optical frequency comb [Invited]," *J. Opt. Soc. Am. B*, vol. 27, no. 11, p. B51, Oct. 2010.

[44] S. Papp, K. Beha, P. Del'Haye, D. Cole, A. Coillet, and S. Diddams, "Self-referencing a CW laser with efficient nonlinear optics," in *Nonlinear Optics*, 2015, p. NTh3A.6.

[45] T. Ideguchi, S. Holzner, B. Bernhardt, G. Guelachvili, N. Picqué, and T. W. Hänsch, "Coherent Raman spectro-imaging with laser frequency combs.," *Nature*, vol. 502, no. 7471, pp. 355–8, Oct. 2013.

[46] T. Udem, "Spectroscopy: Frequency comb benefits," *Nat. Photonics*, vol. 3, no. 2, pp. 82–84, 2009.

[47] V. Durán, S. Tainta, and V. Torres-Company, "Ultrafast electrooptic dual-comb interferometry," *Opt. Express*, vol. 23, no. 23, p. 30557, 2015.

[48] P. Martín-Mateos, B. Jerez, and P. Acedo, "Dual electro-optic optical frequency combs for multiheterodyne molecular dispersion spectroscopy.," *Opt. Express*, vol. 23, no. 16, pp. 21149–58, Aug. 2015.

[49] F. C. Cruz, D. L. Maser, T. Johnson, G. Ycas, A. Klose, F. R. Giorgetta, I.

Coddington, and S. A. Diddams, “Mid-infrared optical frequency combs based on difference frequency generation for molecular spectroscopy.,” *Opt. Express*, vol. 23, no. 20, pp. 26814–24, 2015.

[50] K. F. Lee, N. Granzow, M. A. Schmidt, W. Chang, L. Wang, Q. Coulombier, J. Troles, N. Leindecker, K. L. Vodopyanov, P. G. Schunemann, M. E. Fermann, P. S. J. Russell, and I. Hartl, “Midinfrared frequency combs from coherent supercontinuum in chalcogenide and optical parametric oscillation,” *Opt. Lett.*, vol. 39, no. 7, pp. 2056–2059, 2014.

[51] A. Hugi, G. Villares, S. Blaser, H. C. Liu, and J. Faist, “Mid-infrared frequency comb based on a quantum cascade laser.,” *Nature*, vol. 492, no. 7428, pp. 229–33, 2012.

[52] G. Villares, A. Hugi, S. Blaser, and J. Faist, “Dual-comb spectroscopy based on quantum-cascade-laser frequency combs,” *Nat. Commun.*, vol. 5, p. 5192, Oct. 2014.

[53] C. Zhang, T. Ning, J. Li, L. Pei, C. Li, and S. Ma, “A full-duplex WDM-RoF system based on tunable optical frequency comb generator,” *Opt. Commun.*, vol. 344, pp. 65–70, Jun. 2015.

[54] D. M. Pataca, F. D. Simoes, and M. de Lacerda Rocha, “Optical frequency comb generator for coherent WDM system in Tb/s applications,” in *2011 SBMO/IEEE MTT-S International Microwave and Optoelectronics Conference (IMOC 2011)*, 2011, pp. 30–34.

[55] N. K. Fontaine, R. P. Scott, J. P. Heritage, and S. J. B. Yoo, “Near quantum-limited, single-shot coherent arbitrary optical waveform measurements,” *Opt. Express*, vol. 17, no. 15, p. 12332, Jul. 2009.

[56] E. Bründermann, H.-W. Hübers, and M. F. Kimmitt, *Terahertz Techniques*. Springer, 2012.

[57] E. Prior, M. Ortsiefer, A. R. Criado, P. Meissner, C. de Dios, and P. Acedo, “Continuous wave sub-THz photonic generation with VCSEL-based optical frequency comb,” *Electron. Lett.*, vol. 49, no. 15, pp. 944–945, Jul. 2013.

[58] P. Vasil’ev, *Ultrafast Diode Lasers -Vasil’ev*. Norwood, MA: Artech House, Inc., 1995.

[59] S. O. Kasap, *Optoelectronics and Photonics: Principles and Practices*.

Prentice hall, 2001.

[60] "Encyclopedia of Laser Physics and Technology - surface-emitting semiconductor lasers, VCSEL, VECSEL, HCSEL." [Online]. Available: http://www.rp-photonics.com/surface_emitting_semiconductor_lasers.html. [Accessed: 03-Jun-2014].

[61] N. N. Kanbara Nobuhiko, Noda Ryuuitirou, Yano Tetsuo, Saito Hiroki, Fujimura Naoyuki, "White paper on High speed micromechanically tunable Surface Emitting Laser with Si-MEMS technology | Yokogawa America." [Online]. Available: http://www.yokogawa.com/us/technical-library/white-papers/high-speed-micromechanically-tunable-surface-emitting-laser-with-si-mems-technology.htm. [Accessed: 03-Jun-2014].

[62] "Application Notes | Finisar." [Online]. Available: http://www.finisar.com/products/application-notes. [Accessed: 12-Jun-2014].

[63] "White paper on Discrete Mode Laser diodes with untra narrow linewidth emission." [Online]. Available: http://www.eblanaphotonics.com/downloads/whitepaper200907.pdf. [Accessed: 03-Jun-2014].

[64] "Remembering the laser diode," *Nat. Photonics*, vol. 6, no. 12, pp. 795–795, Nov. 2012.

[65] C. de Dios, "Generación de pulsos cortos mediante diodos láser 'Gain switching': estudio de técnicas de compresión experimental basadas en Lazos Ópticos no Lineales (NOLM)," 2010.

[66] P. Anandarajah, R. Maher, Y. Q. Xu, S. Latkowski, J. O'Carroll, S. G. Murdoch, R. Phelan, J. O'Gorman, and L. P. Barry, "Generation of Coherent Multicarrier Signals by Gain Switching of Discrete Mode Lasers," *IEEE Photonics J.*, vol. 3, no. 1, pp. 112–122, Feb. 2011.

[67] P. Anandarajah, P. Perry, C. Herbert, D. Jones, A. Kaszubowska-Anandarajah, L. P. Barry, B. Kelly, J. O'Carroll, J. O'Gorman, M. Rensing, and R. Phelan, "Discrete mode lasers for communication applications," *IET Optoelectron.*, vol. 3, no. 1, pp. 1–17, Feb. 2009.

[68] J. O'Carroll, R. Phelan, B. Kelly, D. Byrne, L. P. Barry, and J. O'Gorman, "Wide Temperature Range 0 < T < 85 °C Narrow Linewidth Discrete

Mode Laser Diodes for Coherent Communications Applications," in *37th European Conference and Exposition on Optical Communications*, 2011, p. We.10.P1.34.

[69] "Technology | Vertilas." [Online]. Available: http://www.vertilas.com/content/technology. [Accessed: 14-Apr-2016].

[70] A. Consoli, "Short pulse generation from semiconductor lasers: characterization, modeling and applications," E.T.S.I. Telecomunicación (UPM), 2011.

[71] Finisar, "Key Advantages of VCSEL Technology | VCSEL." [Online]. Available: http://myvcsel.com/key-advantages-of-vcsel-technology/. [Accessed: 20-Apr-2016].

[72] L. Raddatz, D. Hardacre, I. H. White, R. V. Penty, D. G. Cunningham, M. R. T. Tan, and S.-Y. Wang, "High bandwidth data transmission in multimode fibre links using subcarrier multiplexing with VCSELs," *Electron. Lett.*, vol. 34, no. 7, p. 686, 1998.

[73] J. Tatum, "VCSEL proliferation," in *Integrated Optoelectronic Devices 2007*, 2007, pp. 648403–648403–7.

[74] C. J. Chang-Hasnain, "Tunable VCSEL," *IEEE J. Sel. Top. Quantum Electron.*, vol. 6, no. 6, pp. 978–987, Nov. 2000.

[75] F. Gruet, A. Al-Samaneh, E. Kroemer, L. Bimboes, D. Miletic, C. Affolderbach, D. Wahl, R. Boudot, G. Mileti, and R. Michalzik, "Metrological characterization of custom-designed 894.6 nm VCSELs for miniature atomic clocks.," *Opt. Express*, vol. 21, no. 5, pp. 5781–92, Mar. 2013.

[76] P. Martin-Mateos, B. Jerez, and P. Acedo, "Heterodyne architecture for tunable laser chirped dispersion spectroscopy using optical processing.," *Opt. Lett.*, vol. 39, no. 9, pp. 2611–3, May 2014.

[77] P. Martín-Mateos and P. Acedo, "Heterodyne phase-sensitive detection for calibration-free molecular dispersion spectroscopy.," *Opt. Express*, vol. 22, no. 12, pp. 15143–53, Jun. 2014.

[78] J. A. Garcia-Souto, P. Martin-Mateos, J. E. Posada, P. Acedo, and D. A. Jackson, "Evaluation of a 1540nm VCSEL for fibre Bragg gratings interrogation in dynamic measurement applications," in *OFS2014*

23rd International Conference on Optical Fiber Sensors, 2014, p. 91573A.

[79] J. Danckaert, B. Nagler, J. Albert, K. Panajotov, I. Veretennicoff, and T. Erneux, "Minimal rate equations describing polarization switching in vertical-cavity surface-emitting lasers," *Opt. Commun.*, vol. 201, no. 1–3, pp. 129–137, Jan. 2002.

[80] "VCSEL Applications | Vertilas." [Online]. Available: http://www.vertilas.com/content/applications. [Accessed: 19-Feb-2016].

[81] D. M. Pataca, P. Gunning, M. L. Rocha, J. K. Lucek, R. Kashyap, K. Smith, D. G. Moodie, R. P. Davey, R. F. Souza, and A. S. Siddiqui, "Gain-Switched DFB Lasers," *Journal of Microwaves, Optoelectronics and Electromagnetic Applications*, 1997. [Online]. Available: http://www.jmoe.org/site-number?id=1&article=230. [Accessed: 26-Jun-2014].

[82] K. Y. Lau, "Short-pulse and high-frequency signal generation in semiconductor lasers," *J. Light. Technol.*, vol. 7, no. 2, pp. 400–419, 1989.

[83] R. Zhou, S. Latkowski, J. O'Carroll, R. Phelan, L. P. Barry, and P. Anandarajah, "40 nm wavelength tunable gain-switched optical comb source.," *Opt. Express*, vol. 19, no. 26, pp. B415–20, Dec. 2011.

[84] P. Anandarajah, K. Shi, J. O'Carroll, A. Kaszubowska, R. Phelan, L. P. Barry, A. D. Ellis, P. Perry, D. Reid, B. Kelly, and J. O'Gorman, "Phase shift keyed systems based on a gain switched laser transmitter," *Opt. Express*, vol. 17, no. 15, p. 12668, Jul. 2009.

[85] P. Anandarajah, A. M. Clarke, C. Guignard, L. Bramerie, L. P. Barry, J. D. Harvey, and J. C. Simon, "System-Performance Analysis of Optimized Gain-Switched Pulse Source Employed in 40- and 80-Gb/s OTDM Systems," *J. Light. Technol.*, vol. 25, no. 6, pp. 1495–1502, Jun. 2007.

[86] T. Pusch, M. Lindemann, N. C. Gerhardt, M. R. Hofmann, and R. Michalzik, "Increasing the Birefringence of VCSELs Beyond 250 GHz," in *The European Conference on Lasers and Electro-Optics*, 2015, p. CB_2_2.

[87] S. Bennett, B. Cai, E. Burr, O. Gough, and A. J. Seeds, "1.8-THz

bandwidth, zero-frequency error, tunable optical comb generator for DWDM applications," *IEEE Photonics Technol. Lett.*, vol. 11, no. 5, pp. 551–553, May 1999.

[88] A. Cerqueira S., J. M. Chavez Boggio, A. A. Rieznik, H. E. Hernandez-Figueroa, H. L. Fragnito, and J. C. Knight, "Highly efficient generation of broadband cascaded four-wave mixing products," *Opt. Express*, vol. 16, no. 4, p. 2816, Feb. 2008.

[89] S. Radic, "Parametric amplification and processing in optical fibers," *Laser & Photonics Review*, 11-Dec-2008. [Online]. Available: http://doi.wiley.com/10.1002/lpor.200810049. [Accessed: 20-Jun-2016].

[90] "EOSpace." [Online]. Available: http://eospace.com/. [Accessed: 20-Jun-2016].

[91] Microscopy Resource Center, "Pockels Cell Modulator." [Online]. Available: http://www.olympusmicro.com/primer/java/pockelscell/index.html. [Accessed: 20-Jun-2016].

[92] M. Bass and Optical Society of America., *Handbook of optics*. McGraw-Hill, 1995.

[93] R. Wu, V. R. Supradeepa, C. M. Long, D. E. Leaird, and A. M. Weiner, "Generation of very flat optical frequency combs from continuous-wave lasers using cascaded intensity and phase modulators driven by tailored radio frequency waveforms.," *Opt. Lett.*, vol. 35, no. 19, pp. 3234–6, Oct. 2010.

[94] S. Ozharar, F. Quinlan, I. Ozdur, S. Gee, and P. J. Delfyett, "Ultraflat Optical Comb Generation by Phase-Only Modulation of Continuous-Wave Light," *IEEE Photonics Technol. Lett.*, vol. 20, no. 1, pp. 36–38, Jan. 2008.

[95] A. J. Metcalf, V. Torres-Company, D. E. Leaird, and A. M. Weiner, "High-Power Broadly Tunable Electrooptic Frequency Comb Generator," *IEEE J. Sel. Top. Quantum Electron.*, vol. 19, no. 6, pp. 231–236, Nov. 2013.

[96] F. Träger, "Springer Handbook of Lasers and Optics," *Springer Handb. Lasers Opt.*, vol. 72, p. 1694, 2007.

[97] G. P. Agrawal, *Nonlinear Fiber Optics*. Academic Press, 2012.

[98] M. Hirano, T. Nakanishi, T. Okuno, and M. Onishi, "Silica-Based Highly Nonlinear Fibers and Their Application," *IEEE J. Sel. Top. Quantum Electron.*, vol. 15, no. 1, pp. 103–113, Jan. 2009.

[99] G. P. Agrawal, "Highly Nonlinear Fibers," in *Applications of Nonlinear Fiber Optics*, 2008, pp. 397–446.

[100] C. de Dios and H. Lamela, "Improvements to Long-Duration Low-Power Gain-Switching Diode Laser Pulses Using a Highly Nonlinear Optical Loop Mirror: Theory and Experiment," *J. Light. Technol.*, vol. 29, no. 5, pp. 700–707, Mar. 2011.

[101] T. Yang, J. Dong, S. Liao, D. Huang, and X. Zhang, "Comparison analysis of optical frequency comb generation with nonlinear effects in highly nonlinear fibers.," *Opt. Express*, vol. 21, no. 7, pp. 8508–20, Apr. 2013.

[102] V. Ataie, E. Myslivets, B. P.-P. Kuo, N. Alic, and S. Radic, "Spectrally Equalized Frequency Comb Generation in Multistage Parametric Mixer With Nonlinear Pulse Shaping," *J. Light. Technol.*, vol. 32, no. 4, pp. 840–846, 2014.

[103] B. P.-P. Kuo, E. Myslivets, N. Alic, and S. Radic, "Wavelength Multicasting via Frequency Comb Generation in a Bandwidth-Enhanced Fiber Optical Parametric Mixer," *J. Light. Technol.*, vol. 29, no. 23, pp. 3515–3522, Dec. 2011.

[104] K. L. Lee, M. P. Fok, S. M. Wan, and C. Shu, "Optically controlled Sagnac loop comb filter," *Opt. Express*, vol. 12, no. 25, p. 6335, Dec. 2004.

[105] C. de Dios and H. Lamela, "Optimum design of NOLM for compression of low power gain-switching pulses," in *Integrated Optoelectronic Devices 2007*, 2007, p. 64681S–64681S–8.

[106] O. Pottiez, R. Paez-Aguirre, H. Santiago-Hernandez, M. Duran-Sanchez, B. Ibarra-Escamilla, E. A. Kuzin, and A. Gonzalez-Garcia, "Characterizing the Statistics of a Bunch of Optical Pulses Using a Nonlinear Optical Loop Mirror," *Math. Probl. Eng.*, vol. 2015, pp. 1–10, 2015.

[107] N. J. Doran and D. Wood, "Nonlinear-optical loop mirror," *Opt. Lett.*, vol. 13, no. 1, p. 56, Jan. 1988.

[108] RP-Photonics, “Fiber Loop Mirrors.” [Online]. Available: https://www.rp-photonics.com/fiber_loop_mirrors.html.

[109] M. E. Fermann, F. Haberl, M. Hofer, and H. Hochreiter, “Nonlinear amplifying loop mirror,” *Opt. Lett.*, vol. 15, no. 13, p. 752, Jul. 1990.

[110] M. P. Fok and C. Shu, “Delay-Asymmetric Nonlinear Loop Mirror,” *Opt. Fiber Commun. Conf. Fiber Opt. Eng. Conf. (2008), Pap. PDP24*, p. PDP24, 2008.

[111] K.-P. Ho and J. M. Kahn, “Optical frequency comb generator using phase modulation in amplified circulating loop,” *IEEE Photonics Technol. Lett.*, vol. 5, no. 6, pp. 721–725, Jun. 1993.

[112] G. P. Agrawal, *Fiber-Optic Communication Systems*. 2012.

[113] Y. S. and H. Rezig, *Advances in Optical Amplifiers*. InTech, 2011.

[114] G. P. Agrawal and N. A. Olsson, “Self-phase modulation and spectral broadening of optical pulses in semiconductor laser amplifiers,” *IEEE J. Quantum Electron.*, vol. 25, no. 11, pp. 2297–2306, 1989.

[115] A. Consoli, A. Valle, L. Pesquera, I. Esquivias, and F. J. Lopez-Hernandez, “Optical Injection-Induced Timing Jitter Reduction in Gain-Switched Single-Mode 1550 nm-VCSELs,” in *Conference on Lasers and Electro-Optics/International Quantum Electronics Conference*, 2009, p. JThE11.

[116] L. Chrostowski and C. J. Chang-Hasnain, “Injection locking of VCSELs,” *IEEE J. Sel. Top. Quantum Electron.*, vol. 9, no. 5, pp. 1386–1393, Sep. 2003.

[117] E. K. Lau and M. C. Wu, “Enhanced Modulation Characteristics of Optical Injection-Locked Lasers: A Tutorial,” *IEEE J. Sel. Top. Quantum Electron.*, vol. 15, no. 3, pp. 618–633, 2009.

[118] J. Ohtsubo, *Semiconductor Lasers*, vol. 111. Berlin, Heidelberg: Springer Berlin Heidelberg, 2013.

[119] D. Parekh, “Optical Injection Locking of Vertical Cavity Surface-Emitting Lasers Digital and Analog Applications,” 2012.

[120] P. J. Delfyett, S. Bhooplapur, N. Hoghooghi, and E. Sarailou, “Injection locked VCSELs for microwave photonic applications in analog RF links

and real time arbitrary waveform generation," in *IEEE Photonics Conference 2012*, 2012, pp. 368–369.

[121] M. Torre, A. Hurtado, A. Quirce, A. Valle, L. Pesquera, and M. Adams, "Polarization Switching in Long-Wavelength VCSELs Subject to Orthogonal Optical Injection," *IEEE J. Quantum Electron.*, vol. 47, no. 1, pp. 92–99, Jan. 2011.

[122] A. Gatto, A. Boletti, P. Boffi, and M. Martinelli, "Adjustable-chirp VCSEL-to-VCSEL injection locking for 10-Gb/s transmission at 1.55 microm.," *Opt. Express*, vol. 17, no. 24, pp. 21748–53, Nov. 2009.

[123] A. Hurtado, I. D. Henning, and M. Adams, "Optical neuron using polarisation switching in a 1550nm-VCSEL.," *Opt. Express*, vol. 18, no. 24, pp. 25170–6, Nov. 2010.

[124] M. Akbulut, S. Bhooplapur, I. Ozdur, J. Davila-Rodriguez, and P. J. Delfyett, "Dynamic line-by-line pulse shaping with GHz update rate.," *Opt. Express*, vol. 18, no. 17, pp. 18284–91, Aug. 2010.

[125] A. Quirce, P. Perez, H. Lin, A. Valle, L. Pesquera, K. Panajotov, and H. Thienpont, "Polarization Switching Regions of Optically Injected Long-Wavelength VCSELs," *IEEE J. Quantum Electron.*, vol. 50, no. 11, pp. 921–928, Nov. 2014.

[126] P. Pérez, A. Quirce, A. Consoli, A. Valle, I. Noriega, L. Pesquera, and I. Esquivias, "Dynamics of long-wavelength VCSELs subject to dual-beam optical injection," in *SPIE Photonics Europe*, 2014, p. 913409.

[127] P. Perez, A. Quirce, A. Valle, A. Consoli, I. Noriega, L. Pesquera, and I. Esquivias, "Photonic Generation of Microwave Signals Using a Single-Mode VCSEL Subject to Dual-Beam Orthogonal Optical Injection," *IEEE Photonics J.*, vol. 7, no. 1, pp. 1–14, Feb. 2015.

[128] A. Hayat, A. Bacou, A. Rissons, and J.-C. Mollier, "Optical Injection-Locking of VCSELs," in *Advances in Optical and Photonic Devices*, InTech, 2010.

[129] T. Okoshi, K. Kikuchi, and A. Nakayama, "Novel method for high resolution measurement of laser output spectrum," *Electron. Lett.*, vol. 16, no. 16, p. 630, Jul. 1980.

[130] D. J. Bradley and G. H. C. New, "Ultrashort pulse measurements," *Proc. IEEE*, vol. 62, no. 3, pp. 313–345, 1974.

[131] C. de Dios and H. Lamela, “Compression and Reshaping of Gain-Switching Low-Quality Pulses Using a Highly Nonlinear Optical Loop Mirror,” *IEEE Photonics Technol. Lett.*, vol. 22, no. 6, pp. 377–379, Mar. 2010.

[132] Eduardo Pérez González, “Caracterización de pulsos de luz láser ultracortos [PFC],” *PFC. Universitat Politècnica de Catalunya. Departament de Teoria del Senyal i Comunicacions*, 2003. [Online]. Available: http://www.icfo.eu/images/publications/MT04-001.pdf. [Accessed: 07-May-2014].

[133] R. Trebino, *Frequency-Resolved Optical Gating: The Measurement of Ultrashort Laser Pulses*. Boston, MA: Springer US, 2000.

[134] L. Cohen, *Time-frequency analysis / Leon Cohen*, no. Accessed from http://nla.gov.au/nla.cat-vn510802. Englewood Cliffs, N.J : Prentice Hall PTR, 1995.

[135] H. E. Li and K. Iga, *Vertical-Cavity Surface-Emitting Laser Devices*, vol. 6. Springer Berlin Heidelberg, 2003.

[136] C. Peucheret, “Direct Current Modulation of Semiconductor Lasers,” 2011. [Online]. Available: http://web-files.ait.dtu.dk/cpeu/download/34130_E2011_CPEU_DML_Sim.pdf. [Accessed: 27-Jan-2016].

[137] E. Prior, C. de Dios, R. Criado, M. Ortsiefer, P. Meissner, and P. Acedo, “1THz span optical frequency comb using VCSELs and off the Shelf expansion techniques,” in *Conference on Lasers and Electro-Optics*, 2016, p. SF2O.3.

[138] E. Prior, C. De Dios, M. Ortsiefer, P. Meissner, and P. Acedo, “Understanding VCSEL-Based Gain Switching Optical Frequency Combs: Experimental Study of Polarization Dynamics,” *J. Light. Technol.*, vol. 33, no. 22, pp. 4572–4579, Nov. 2015.

[139] M. Brunel, J. Thévenin, M. Vallet, J. Thevenin, and M. Vallet, “Dual-polarization frequency comb from a diode-pumped solid-state laser,” in *CLEO: 2013*, 2013, pp. 1–2.

[140] A. D. Shiner, M. Reimer, A. Borowiec, S. O. Gharan, J. Gaudette, P. Mehta, D. Charlton, K. Roberts, and M. O’Sullivan, “Demonstration of an 8-dimensional modulation format with reduced inter-channel nonlinearities in a polarization multiplexed coherent system.,” *Opt.*

Express, vol. 22, no. 17, pp. 20366–74, Aug. 2014.

[141] S. Uvin, S. Keyvaninia, F. Lelarge, G.-H. Duan, B. Kuyken, and G. Roelkens, "Narrow line width frequency comb source based on an injection-locked III–V-on-silicon mode-locked laser," *Opt. Express*, vol. 24, no. 5, p. 5277, Mar. 2016.

[142] P. Gallion, H. Nakajima, G. Debarge, and C. Chabran, "Contribution of spontaneous emission to the linewidth of an injection-locked semiconductor laser," *Electron. Lett.*, vol. 21, no. 14, p. 626, 1985.

[143] H. Dalir and F. Koyama, "Bandwidth enhancement of single-mode VCSEL with lateral optical feedback of slow light," *IEICE Electron. Express*, vol. 8, no. 13, pp. 1075–1081, Jan. 2011.

[144] K. H. Oh, U.-C. Paek, and D. Y. Kim, "Characteristics of a gain switched Fabry-Perot semiconductor laser at 650 nm wavelength," in *Technical Digest. Summaries of papers presented at the Conference on Lasers and Electro-Optics. Postconference Technical Digest (IEEE Cat. No.01CH37170)*, 2001, pp. 194–195.

[145] K. T. Vu, A. Malinowski, M. A. F. Roelens, and D. J. Richardson, "Detailed Comparison of Injection-Seeded and Self-Seeded Performance of a 1060-nm Gain-Switched Fabry–PÉrot Laser Diode," *IEEE J. Quantum Electron.*, vol. 44, no. 7, pp. 645–651, Jul. 2008.

[146] A. Quirce and A. Valle, "High-frequency microwave signal generation using multi-transverse mode VCSELs subject to two-frequency optical injection.," *Opt. Express*, vol. 20, no. 12, pp. 13390–401, Jun. 2012.

[147] S. E. Hashemi, "Relative Intensity Noise (RIN) in High-Speed VCSELs for Short Reach Communication," 2012. [Online]. Available: http://publications.lib.chalmers.se/records/fulltext/156453.pdf. [Accessed: 02-May-2014].

[148] "Modulating VCSELs. App Note. Finisar." [Online]. Available: https://www.finisar.com/sites/default/files/downloads/application_note_modulating_vcsels.pdf. [Accessed: 02-Feb-2016].

[149] B. W. Kögel, "Mikromechanisch weit abstimmbare oberflächenemittierende Laserdioden für Sensoranwendungen," Cuvillier, 2009.

[150] J. E. Bowers, "High speed semiconductor laser design and

performance," *Solid. State. Electron.*, vol. 30, no. 1, pp. 1–11, Jan. 1987.

[151] P. Westbergh, J. S. Gustavsson, B. Kögel, A. Haglund, and A. Larsson, "Impact of Photon Lifetime on High-Speed VCSEL Performance," *IEEE J. Sel. Top. Quantum Electron.*, vol. 17, no. 6, pp. 1603–1613, Nov. 2011.

[152] "VERTILAS - langwellige oberflächenemittierende Laserdioden VCSEL." [Online]. Available: http://www.vertilas.com/produkte_daten_.php. [Accessed: 03-Jun-2014].

[153] G. P. Agrawal, *Semiconductor lasers*. Van Nostrand Reinhold, 1993.

[154] I. Hardcastle, R. A. Saunders, and J. P. King, "Wideband chirp measurement technique for high bit rate sources," *Electron. Lett.*, vol. 30, no. 16, pp. 1336–1338, Aug. 1994.